WA School of Mines: Minerals, Energy and Chemical Engineering

Study the Effects of Nanohybrid Polymers / Polymer Nanocomposites on the Flow Behaviour of Indian Waxy Crude Oil

Rohit Sharma

This thesis is presented for the collaborative Degree of

Doctor of Philosophy

of

Indian Institute of Technology (Indian School of Mines), Dhanbad

and

Curtin University

May 2022

INDIAN INSTITUTE OF TECHNOLOGY
(INDIAN SCHOOL OF MINES) DHANBAD

CERTIFICATE FROM THE SUPERVISOR(S)

This is to certify that the thesis entitled "**Study the effects of nanohybrid polymers/polymer nanocomposites on the flow behaviour of Indian waxy crude oil**" submitted by **Mr. Rohit Sharma** (Ph.D. Registration No. 16DR000194) in fulfilments of the requirements for the award of degree of Doctor of Philosophy, is a bonafide record of the investigations carried out by him, in the Department of Petroleum Engineering, Indian Institute of Technology (Indian School of Mines), Dhanbad and part of the research work has been carried out in the WA School of Mines: Minerals, Energy and Chemical Engineering, Curtin University, Australia under our supervision and guidance. The thesis has fulfilled all the requirements as per the regulations of IIT (ISM), and, in our opinion, has reached the standard needed for submission. The results embodied in this thesis have not been submitted to any other University or Institute for the award of any other degree.

(Dr. Hari Vuthaluru)
Supervisor & Associate Professor
WASM: Minerals, Energy
and Chemical Engineering,
Curtin University, Australia

(Dr. Vikas Mahto)
Supervisor & Professor
Department of Petroleum Engineering
Indian Institute of Technology (ISM),
Dhanbad-826004, Jharkhand, India

(Dr. Ahmed Barifcani)
Co- Supervisor & Associate Professor
WASM: Minerals, Energy
and Chemical Engineering,
Curtin University, Australia

INDIAN INSTITUTE OF TECHNOLOGY (INDIAN SCHOOL OF MINES) DHANBAD

CERTIFICATE FOR CLASSIFIED DATA

This is to certify that the thesis entitled "**Study the Effects of Nanohybrid Polymers/Polymer Nanocomposites on the Flow Behaviour of Indian Waxy Crude Oil**" being submitted to the Indian Institute of Technology (Indian School of Mines), Dhanbad by **Mr. Rohit Sharma** for award of Doctor of Philosophy (Ph.D) Degree in **Petroleum Engineering** does not contains any classified information. This work is original and yet not been submitted to any institution or university for the award of any degree.

(**Dr. Vikas Mahto**)
Supervisor & Professor
Department of Petroleum Engineering
Indian Institute of Technology (ISM),
Dhanbad-826004, Jharkhand, India

(**Rohit Sharma**)
Department of Petroleum Engineering, IIT (ISM), Dhanbad
WA School of Mines: Minerals, Energy and Chemical Engineering
Curtin University, Australia

INDIAN INSTITUTE OF TECHNOLOGY (INDIAN SCHOOL OF MINES) DHANBAD

COPYRIGHT AND CONSENT FORM

To ensure uniformity of treatment among all contributors, other forms may not be substituted for this form, nor may any wording of the form be changed. This form is intended for original material submitted to the IIT (ISM), Dhanbad and must accompany any such material in order to be published by the ISM. Please read the form carefully and keep a copy for your files.

TITLE OF THESIS: STUDY THE EFFECTS OF NANOHYBRID POLYMERS / POLYMER NANOCOMPOSITES ON THE FLOW BEHAVIOUR OF INDIAN WAXY CRUDE OIL

AUTHOR'S NAME & ADDRESS: ROHIT SHARMA,
Department of Petroleum Engineering,
Indian Institute of Technology (ISM),
Dhanbad-826004

COPYRIGHT TRANSFER

1. The undersigned hereby assigns to Indian Institute of Technology (Indian School of Mines), Dhanbad all rights under copyright that may exist in and to: (a) the above Work, including any revised or expanded derivative works submitted to the ISM by the undersigned based on the work; and (b) any associated written or multimedia components or other enhancements accompanying the work.

CONSENT AND RELEASE

2. In the event the undersigned makes a presentation based upon the work at a conference hosted or sponsored in whole or in part by the IIT (ISM) Dhanbad, the undersigned, in consideration for his/her participation in the conference, hereby grants the ISM the unlimited, worldwide, irrevocable permission to use, distribute, publish, license, exhibit, record, digitize, broadcast, reproduce and archive; in any format or medium, whether now known or hereafter developed: (a) his/her presentation and comments at the conference; (b) any written materials or multimedia files used in connection with his/her presentation; and (c) any recorded interviews of him/her (collectively, the "Presentation"). The permission granted includes the transcription and reproduction of the Presentation for inclusion in products sold or distributed by IIT(ISM) Dhanbad and live or recorded broadcast of the Presentation during or after the conference.
3. In connection with the permission granted in Section 2, the undersigned hereby grants IIT (ISM) Dhanbad the unlimited, worldwide, irrevocable right to use his/her name, picture, likeness, voice and biographical information as part of the advertisement, distribution and sale of products incorporating the Work or Presentation, and releases IIT (ISM) Dhanbad from any claim based on right of privacy or publicity.
4. The undersigned hereby warrants that the Work and Presentation (collectively, the "Materials") are original and that he/she is the author of the Materials. To the extent the Materials incorporate text passages, figures, data or other material from the works of others, the undersigned has obtained any necessary permissions. Where necessary, the undersigned has obtained all third party permissions and consents to grant the license above and has provided copies of such permissions and consents to IIT (ISM) Dhanbad.

GENERAL TERMS

* The undersigned represents that he/she has the power and authority to make and execute this assignment.
* The undersigned agrees to indemnify and hold harmless the IIT (ISM) Dhanbad from any damage or expense that may arise in the event of a breach of any of the warranties set forth above.
* In the event the above work is not accepted and published by the IIT (ISM) Dhanbad or is withdrawn by the author(s) before acceptance by the IIT(ISM) Dhanbad, the foregoing copyright transfer shall become null and void and all materials embodying the Work submitted to the IIT(ISM) Dhanbad will be destroyed.
* For jointly authored Works, all joint authors should sign, or one of the authors should sign as authorized agent for the others.

_____
Signature of the Author

INDIAN INSTITUTE OF TECHNOLOGY (INDIAN SCHOOL OF MINES) DHANBAD

CERTIFICATE REGARDING ENGLISH CHECKING

This is to certify that the thesis entitled "**Study the Effects Of Nanohybrid Polymers/Polymer Nanocomposites on the Flow Behaviour of Indian Waxy Crude Oil**" being submitted to the Indian Institute of Technology (Indian School of Mines), Dhanbad by **Mr. Rohit Sharma**, Admission No.: 16DR000194, for the award of Doctor of Philosophy (Ph.D.) Degree has been thoroughly checked for quality of English and logical sequencing of topics.

It is hereby certified that the standard of English is good and that grammar and typos have been thoroughly checked. It is now worthy for evaluation by the panel of examiners.

(Dr. Vikas Mahto)
Supervisor & Professor
Department of Petroleum Engineering
Indian Institute of Technology (ISM),
Dhanbad-826004, Jharkhand, India

(Rohit Sharma)
Department of Petroleum Engineering, IIT (ISM), Dhanbad
WA School of Mines: Minerals, Energy and Chemical Engineering, Curtin University, Australia

(Dr. Hari Vuthaluru)
Supervisor & Associate Professor
WASM: Minerals, Energy
and Chemical Engineering,
Curtin University, Australia

(Dr. Ahmed Barifcani)
Co- Supervisor & Associate Professor
WASM: Minerals, Energy
and Chemical Engineering,
Curtin University, Australia

Acknowledgments

First and foremost, I sincerely thank my supervisor Prof. Vikas Mahto, Department of Petroleum Engineering, IIT (ISM), Dhanbad for his guidance, motivation and visionary approach towards my research work, and his wholehearted support at every stage of my Ph.D. work. I would like to thank the supervisors from my host institute (Curtin University, Australia) A/Prof. Hari Vuthaluru and A/Prof. Ahmed Barifcani for their support to guide me in every aspect of Ph.D. and carry out simulation and modelling research work. Their guidance and technical inputs have helped me to achieve the objectives successfully. I take this opportunity to thank the IIT (ISM), Dhanbad (home institute) for giving me an opportunity to undertake the prestigious Joint Doctoral Programme with Curtin University, Australia, where I was enrolled in Department of Petroleum Engineering, IIT (ISM), Dhanbad and WA School of Mines, Curtin University Australia. This collaboration has helped expand my knowledge, skills, research aptitude and networking with the international research community. I would also like to express my gratitude to IIT (ISM), Dhanbad & Curtin University, Australia for providing me the access to research facilities at both the institutes. Prof. Hari Vuthaluru and Prof. Vikas Mahto have been instrumental in enabling a smooth transition to Joint Doctoral Programme. I express my gratitude to Prof. Rajiv Shekhar, Director, IIT (ISM), Dhanbad, Prof. Ajay Mandal, HOD, Petroleum Engineering Department and Prof. Dheeraj Kumar, IIT (ISM), Dhanbad for their support during my Ph.D. under Joint Doctoral Programme.

I would like to extend special thanks to my colleague Ms. Barasha Deka, whose unfailing support and continuous encouragement has helped me achieve my research objectives and goals, and have always supported me in difficult times. I also like to thank my colleague Dr. Arnab Mandal for his support and sharing his experiences to improve my research work. I owe gratitude to Prof. Chun-Zhu Li for sharing his technical expertise to improve upon my research work strategy. I would also like to thank my Doctoral Scrutiny Committee members of IIT (ISM), Dhanbad and Thesis Committee members of Curtin University, Australia for continuous evaluation of my research work and valuable inputs throughout the journey.

Most importantly, this Ph.D journey would not have progressed without the unending support of my parents, sister and brother. Their patience and continuous backing motivated me to complete my research and this accomplishment is a result of their persistent belief in me.

Date:

Place: (**ROHIT SHARMA**)

Abstract

Wax deposition in crude oil pipelines causes difficulty in handling and results in major obstructions to the flow of crude oil, thus, hampering the routine operations and economy of the transportation project. If the wax deposition is not controlled timely, it may lead to complete pipeline blockage and suspension of the crude oil production and its transportation operations. There are many ways to control the wax deposition, such as chemical, mechanical and thermal methods. The chemical method of wax prevention is considered as one of the economical methods and is widely used in the petroleum industry for improving the flowability of waxy crude oils.

The current research work uses the chemical method to prevent the wax deposition in pipelines, where chemical additives were laboratory synthesized and tested on some Indian waxy crude oils to evaluate them as potential pour point depressants (PPD). Conventional polymeric PPDs have been used for a long time and have shown beneficiation in the crude oil properties. However, they usually demonstrate limited performance improvement and thus, in a quest to produce the additives capable of enhanced beneficiation, the nanocomposite PPDs composed of graphene were developed and tested on waxy crude oils for the first time in this dissertation work. With the recent progress in the science of nanocomposites and considering their remarkable statistics to beneficiate the properties of polymeric compounds, there has been a recent focus on the developing polymeric nanocomposite pour point depressants. This thesis work comprises of synthesizing the polymeric nanocomposites in laboratory conditions, where graphene oxide nanosheets were introduced to the polymeric system. These synthesized polymeric nanocomposites were then tested on the Indian waxy crude oils with the help of several standard tests used in the petroleum industry. A series of polymer nanocomposites were developed in the research works mentioned in this dissertation, where subsequent improvements were made based on the research gaps currently existing in the literatures. These developed nanocomposites were able to improve the flow properties of the crude oil, such as apparent viscosities, gelation point, pour point, and aging effect, and they caused modifications in the morphology of the wax crystals. The performances of the nanocomposites were compared to the conventional polymeric pour point depressants to understand the crude oil beneficiation brought by nanocomposites. Thus, the thesis work has utilized the beneficial properties of graphene in developing novel and efficient

graphene-based nanocomposite pour point depressants. In the later chapters, the thesis illustrates the potential of ionic liquids in preventing flow assurance issues related to wax deposition. The ionic liquids were used to develop PPDs, including a novel class of ionic liquid - graphene nanocomposite PPDs, and this work give encouraging insights into the possible scope of enhancement of the current class of PPDs using ionic liquids. The thesis also details the interactions of the developed nanocomposite and other polymeric additives with the wax crystals in crude oil. Action mechanism of the PPDs are proposed based on the outcomes of pour point tests and microscopic investigations of the changes in wax morphologies after treatment with PPDs. The thesis experimental work is divided into 3 main studies, where studies 1, 2 and 3 details the experimental flow assurance investigations carried out on different crude oils employing PPDs namely, PMMA-GO, P(2-EHA)-GO and PPDR-GO (Also known as IL-GO) respectively. The study 1 illustrated that the pour point of the crude oil (38℃) has been efficiently reduced when treated with nanocomposite additive PMMA-GO, with a maximum depression in pour point of 23 °C using PMMA-1% GO at 1500 ppm, while a 16 °C depression occurred with PMMA-0.5% GO at the same concentration. Thus, PMMA-1% GO exhibited better depression in pour point compared to PMMA-0.5% GO. The performance of the synthesized nanocomposite is also compared to the existing available PPDs in the petroleum industry. The pour points of the crude oil were reduced to 15 °C, 22 °C, 24 °C and 27 ℃ when treated with PMMA-1% GO, PMMA-0.5% GO, Phoenix and PMMA respectively at their respective optimum concentrations, where Phoenix is a commercial PPD and PMMA is a known PPD. Maximum reduction in crude oil viscosity is observed when treated with PMMA-1% GO at temperatures 30℃, 40℃ and 50℃ indicating the best flow improvement among all the other used chemical additives. PMMA-GO reduced the viscosities of the crude oil from 500 cP down to 3 cP (30℃), 2 cP (40℃) and 1 cP (50℃), thus illustrating its role as potential viscosity reducer with reductions about 99.4-99.8%.

In the study 2, a novel nanocomposite P(2-EHA)-GO was synthesized and tested on a highly waxy crude oil (pour point 36℃). The best improvement in pour point was found with the addition of P(2-EHA)-1% GO, producing a 18℃ drop in pour point of crude oil at 750 ppm concentration, while a 15℃ depression was observed in case of P(2-EHA)-0.5% GO and only 12℃ reduction was observed when treated with P(2-EHA) at

the same concentration. This demonstrates the influence of GO nanoparticles in enhancing the flow abilities of existing polymeric additive P(2-EHA). The improvement in the apparent viscosities of crude oil by the additives occur in the following trend; P(2-EHA) < P(2-EHA)-0.5% GO < P(2-EHA)-1% GO. Best beneficiation was observed in case of P(2-EHA)-1% GO, with viscosities dropping down from 1.9 Pa.s (virgin crude oil) to 0.03, 0.02, 0.016 and 0.01 Pa.s at temperatures 10℃, 20℃, 30℃ and 40℃ respectively. The viscosity reductions of the crude oil significantly improved from 95 % with P(2-EHA) (at 100 s-1 shear rate) to 98 % and 99 % with P(2-EHA)-0.5% and P(2-EHA)-1%GO respectively.

In the study 3, novel ionic liquid based additives were laboratory synthesized namely, IL and PPDR-GO to treat the highly waxy and asphaltenic crude oil sample having a pour point of 39℃. The lowest pour point of additive IL treated waxy crude oil was found to be 21℃ at 500 ppm. The synthesized novel nanocomposite PPDR-0.5 %GO also caused a huge pour point reduction from 39℃ to 18℃, i.e. 21℃ reduction at 250 ppm concentration. The synthesized novel nanocomposite PPDR-1%GO produced the greatest reduction in the pour point of the crude oil from 39℃ to 9℃ at 250 ppm concentration only. The additives developed in this work have an added advantage, as they could be doped into the crude oil without prior mixing with any solvents to create fluidity. The additives reduced the crude oil viscosities from 4.1 Pa.s to 0.04 Pa.s - 0.6 Pa.s (IL) and 0.02 Pa.s - 0.2 Pa.s (PPDR-1%GO), thereby demonstrating significant abilities as viscosity reducers and thus, acts as flow improvers for the crude oil. Thus, this study demonstrated highly encouraging results and exhibits that nanoparticles hold immense potential to be utilized in development of pour point depressants and flow improvers. This study is a significant advancement to the efforts of developing nanocomposite additives suitable for flow assurance of crude oils.

Aging tests were performed on crude oil samples treated with and without PPD. These tests are designed in order to evaluate the long term performance of the additives on crude oil flowability. The additive PMMA-GO controlled the significant increases in viscosities of crude oil after 15 days of storage, where the crude oil suffered an increase in viscosities by 16.5 - 37.7%, which is comparatively better than the increase of 40 - 45 % shown in the case of commercial PPD Phoenix treated crude oil. Similarly, in the study 2, aging tests were carried out to test the efficacy of the additive P (2-EHA) on the

Indian crude oil. A 19.8 – 76.7 % increase in viscosities of crude oil was observed in the case of PPD P(2-EHA), while P(2-EHA)-0.5% GO resulted in 22.6 – 49.1 % increase in apparent viscosities, while the PPD P(2-EHA)-1% GO showed the least increase of about 11.4 – 29.8 % over a shear rate range of 0-100 s-1. This test further highlights the beneficiation of the crude oil characteristics upon doping with P(2-EHA)-1% GO and suggest a long term beneficiation effect (until 30 days of pipeline being shutdown) which is advantageous from the perspective of pipeline routine operations. Similarly, in the study 3, aging tests were performed to evaluate the long term performance of the pour point depression of the synthesized additives IL and PPDR-GO on a waxy Indian crude oil. A slight increase in the optimized pour point by 3℃ and 6℃ was observed in additive IL-treated crude oil sample after 15 days and 30 days of storage respectively, while the increase was even limited to 3℃ (pour point reached 12 ℃) in the case of PPDR-1%GO treated crude oil sample after the same storage period. This indicates that PPDR-1%GO exercises better control over the aging tendency and there is limited depreciation in the crude oil properties. This also suggest that the PPDR-1%GO treated oil samples will not experience any major flow assurance issues in terms of longer transportation duration, including during pipeline shutdown and subsequent pipeline restart.

Additionally, simulation studies were carried out for understanding the wax-oil gelation phenomena during flowing conditions of the crude oil in pipelines. The simulation aimed to understand the extent of gelation and wax precipitation under single-phase laminar flow conditions of crude oil, with changes in operating parameters such as flow rate and temperatures (oil and pipeline), where molecular diffusion is considered as the dominant mechanism for precipitation and deposition of wax crystals. The novelty of our work lies in the development and application of these novel nanocomposites in laboratory conditions where graphene oxide nanosheets were introduced to the polymeric/non-polymeric system for the first time for treatment of the waxy crude oils. The incorporation of nanoparticles in the PPD system improves the performance of the conventional PPDs, but along with may involve issues such as poor dispersion of nanoparticles in polymeric/non-polymeric matrix, and this issue can be resolved by functionalization of the nanoparticles. The thesis work illustrates an effective solution for these concerns considering the long-term effectiveness of the PPDs. Thus, the thesis presents a comprehensive treatise for the development, characterization, and application

of nanocomposite PPDs for the waxy and asphaltenic crude oils. A small study in the Appendix section of thesis work is also dedicated to the techno-economic calculations, which estimated the cost incurred to synthesize the different types of PPDs on a laboratory scale. Additionally, the efficiency of the PPDs are calculated in terms of their capability to save the energy consumption in pipeline transportation operations, which illustrates that the nanocomposite PPDs will result in better energy savings in crude oil transportation than conventional polymeric PPDs and several other commercial PPDs.

Table of contents

List of figures

List of tables

List of Symbols

Symbol	Description
L_a	Crystallite size of products
λ_L	Wavelength of Raman Source
λ	Spectral wavelength
I_D	Intensity of Raman D band
I_G :	Intensity of Raman G band
Θ	Braggs Angle
d	Interlayer spacing
W_{cu}	Weight of empty copper tube
W_{wax}	Weight of deposited wax
W_{UT}	Weight of Copper tube with wax deposited in the untreated crude oil
W_T	Weight of Copper tube with wax deposited in the treated crude oil
W_{CO}	Weight of crude oil flowed through pipeline
p	Pressure
ρ	Density
$\vec{v}$	Velocity field
E	Energy
K	Thermal conductivity
T	Temperature
H	Total Enthalpy/energy of the material
h	Sensible enthalpy
L	Latent Heat of Material
$\triangle H$	Latent heat content
h_{ref}	Reference enthalpy
Cp	Specific heat at constant pressure
Z	Liquid fraction
T	Temperature

$T_{solidus}$	Solidus temperature
$T_{liquidus}$	Liquidus temperature
$\triangle H$	Latent heat
$S.G._T$	Specific Gravity at temperature T
S.G.	Specific Gravity
T_{max}	Maximum weight loss temperature
T_i	Temperature at which Initial stage of weight loss begins
T_f	Temperature at which Final stage of weight loss begins
G’	Storage modulus
G”	Loss modulus

Chapter 1

Introduction

1.1. Background

The petroleum industry has been facing several challenges since decades due to wax deposition, such as increased viscosities and pumping pressure, deposition in flowlines, and further gelling of crude oil inside entire flowline. The severity of the problems faced by the operator companies mainly depends on their analysis of the composition of crude oil and the operating conditions and followed practices, as some operations might not experience much difficulties due to wax deposition, while some operations may experience high amount of production losses and downtime, and in severe cases the pipelines and the wells have to be completely plugged and abandoned resulting in huge financial losses. The problem of wax deposition is evident in reservoirs, their transportation to surface and subsequent transfer to surface facilities such as transfer lines, treatment facilities and the oil storage tanks. The problem of wax deposition can be very serious in reservoirs once wax starts to crystalize sufficiently, and in number of cases it led to termination of the oil production through the natural reservoir drives (Modesty Kelechukwu, Said Al-Salim and Saadi, 2013). This wax deposition in reservoirs can be controlled adequately through controlling the choke size but at the cost of lower production rates. Wax deposition can still occur if the flow rates are kept considerably lower, due to cooling of crude oil while being transported through low temperature formations. And if the flow rates are increased, chances of asphaltene deposition are prominent (Becker, 1997).

Once the fluid has reached the surface, maintenance of flow assurance or fluidity of the flow becomes essential. Fluid streams usually experiences wax precipitation during transportation from the reservoir to the surface and some streams may contain abundant wax content which would become serious concern for further transportation to surface facilities. Although techniques such as heating the pipeline by installing line heaters is usually practised but the nature of the precipitated wax crystals would not be altered by heating. Thus, this fluid stream would create wax deposition and gelation issues upon being sent to facilities such as surface facilities and storage tanks. Thus, the problem of

wax deposition started in production stream now manifests itself in the surface facilities (Becker, 1997). Thus, a comprehensive approach must be adopted to ensure flow assurance of crude oils being produced from the reservoir up to the sales point.

1.2 Significance of flow assurance and types of solids deposition

Flow assurance has been a developing idea through the petroleum industry from decades and significant research has been done on it, but still, a significant deal of phenomena is unexplored and requires extensive efforts to be solved. Flow assurance is the ability to produce and transport the crude oil from the reservoir to the sales point without any hindrance to the flow ability and the crude oil should be delivered safely and economically through the production and transportation system.

Flow assurance can be accomplished by looking into some parameters namely, the characteristics of the pipe, the terrain characteristics and the fluid properties. While attention should be focused on important properties such as variation in fluid characteristics including viscosity and fluid rheology and the deposition occurring including solid and organic/inorganic deposition (Al-Safran and Brill, 2017). The different type of depositions usually experienced in the oilfields is exhibited in Figure 1.

Figure 1.1. Different types of solids formed obstructing the flow in pipelines. (Reproduced from (Mullins, 2007) with permission from Springer Nature)

1.3 Waxes and their types

When the crude oil is flowed through onshore or offshore pipelines, wax deposition on pipewalls is a serious problem due to temperature fluctuations. It usually occurs because the temperature of the crude oil is higher in the pipeline, while the surroundings are cooler. Particularly, when the temperature of the crude oil falls below the wax appearance temperature (WAT), the wax crystals starts to precipitate and subsequently deposits on the pipewalls with time (Sharma, Mahto and Vuthaluru, 2019). The flow assurance occurs in multiple places simultaneously such as reservoir, completions, subsea systems, pipelines, host facilities, operations, and export system.

Waxes in the crude oil are of different types such as linear chain, branched chain and cyclic and they appear as solid or liquid at ambient temperature. Waxes can be separated

from the crude oil in laboratories upon cooling them according to standard procedures with the assistance of certain chemicals. The precipitated waxes may be of paraffinic or naphthenic nature based on their carbon number distribution.

The hydrocarbons with carbon number distribution from C_{18}-C_{30} are generally considered as paraffins and the corresponding waxes are termed as macrocrystalline waxes, while those with carbon number distribution from C_{30}-C_{60} are termed as naphthenic hydrocarbons and the resulting waxes are termed as microcrystalline waxes (Bala 2007). Paraffin wax molecules have carbon number greater than 20. Although some authors have found the deposited waxes to have carbon numbers as high as upto C_{92}.

N-paraffins are considered as the primary part of macrocrystalline waxes, results in needle-shaped crystals. While the branched-chain paraffins forms the majority of microcrystalline waxes. Paraffin wax molecules are considered straight chain alkanes containing greater than 15 carbons with minor branching. Waxes containing up to C_{80} iso-paraffin compounds have been reported. Microcrystalline waxes also consists of straight-chain naphthenic and aromatic paraffins. Production and transportation problems are caused by macrocrystalline waxes, while tank bottom sludges are majorly composed of microcrystalline waxes. The waxes deposited during production and transportation of crude oil have been found to mainly comprise of n-paraffins with minor quantities of branched-chain and cyclic paraffins and aromatics (Misra, Baruah and Singh, 1995).

1.4 Problems due to wax deposition in pipeline transportation

Wax deposition can cause huge problems such as reduction in the available pipe diameter and reduced throughput volume, increased pumping pressure, hazard to personnel and pipeline safety. If the wax deposition is not controlled timely, may result in complete pipeline blockage and shutdown of production facilities, thus resulting in serious financial and time losses (Sharma, Mahto and Vuthaluru, 2019).

Wax crystals begin to precipitate out from the crude oil when the temperature falls below wax appearance temperature (WAT) and they continue to precipitate at lower temperatures and crude oil ceases to flow at temperatures below pour point. Pour point is defined as the lowest temperature below which no movement of the fluid occurs. These wax crystals are porous structures having tendency to trap the crude oil, thus causes gelling in pipelines and which grows with time and leads to subsequent wax deposits on the pipe-walls (Sharma, Vuthaluru and Mahto, 2020).

1.5 Methods to prevent wax deposition in pipeline flow

There are several methods to prevent wax deposition such as mechanical, thermal and chemical methods. The mechanical methods involve usage of mechanical devices to reduce or prevent the wax deposition such as different types of pigs and scrapers. Thermal methods involve heating the pipeline to maintain the crude oils above their pour point and WAT. But this method may require large amount of electricity and thus would involve higher costs. While the chemical methods to prevent wax deposition are the most widely followed method such as use of pour point depressants, emulsifiers, asphaltene inhibitors etc. Emulsification is one of the techniques for efficient transportation of crude oils (Sharma *et al.*, 2018) but it requires extensive source of water and electricity which may not always be economically feasible for the project. Also diluting/blending of crude oils with lighter crudes is also one of the methods for crude oil transportation, but the availability and quantity of the diluent is a cause of concern to the operator. Additionally, care should be taken while blending, due to the issues of asphaltene deposition in case of mixing incompatible crude oils. While the usage of pour point depressants requires lesser resources and can be easily added to the crude oil with minimum facilities for their effective transportation.

1.6 Introduction to PPDs and their role in flow assurance

Pour point depressants (PPDs) are chemical additives which are usually doped in very small quantities in crude oil to for its pipeline transportation. The PPDs can be of different types such as polymeric, non-polymeric, polymeric nanocomposites etc. Numerous PPDs have been used throughout the petroleum industry and have successfully contributed to the flow assurance of waxy crude oils. Most of the PPDs used in oilfields are polymeric PPDs. There have been research into the development of polymeric nanocomposites as pour point depressants, where the excellent properties of inorganic products are incorporated into the polymeric base to enhance the effectiveness of polymeric PPDs. Nanoparticles are known to have numerous applications owing to its high surface area, The presence of nanoparticles/nanosheets influences the properties of the polymeric PPDs and possibly leads to improvement in the thermal, mechanical and

electrical properties. (Young *et al.*, 2012; Sharma, Mahto and Vuthaluru, 2019). Silica has been used extensively to prepare the polymeric nanocomposite PPDs, and have yielded good results, but very few works have studied the PPDs based on graphene based polymeric nanocomposites. By looking at the beneficial characteristics of graphene it is imperative to study the modification in the crude oil properties using graphene based polymeric nanocomposites in order to provide new solutions to the flow assurance community.

1.7 Various test to evaluate PPDs including microscopy

A number of tests are conducted to evaluate the efficacy of the PPDs for the crude oils such as pour point determination of crude oil, degree of viscosity reduction, gelation point determination, and microscopic analysis of modification in wax morphology by PPDs, prevention/ delaying the ageing effect in crude oils. The microscopic observation of the effect of PPD on the wax crystals helps to understand the state of wax crystals and determine the mechanism of the PPDs.

1.8 Mechanism of PPDs

The PPDs interact with the wax crystals through the one or more of the following mechanisms.

1.8.1 Nucleation

The polymeric structures are known to assemble as micelle type aggregates possessing crystalline cores and the attached alkyl chains, thus creates nucleation templates for wax precipitation and results in in the formation of smaller sized wax nuclei. These wax nuclei are sterically hindered, that prevents their aggregation and reduced networking and slows the crystal growth and subsequent deposition.

1.8.2 Co-crystallization

The PPDs having alkyl chains can co-crystallize with the wax molecules and prevent their deposition by hindering the extensive interaction among wax molecules. PPDs can also interact while being adsorbed on the surface of the precipitating wax crystals. The co-crystallization phenomena is illustrated through Fig.1.2.

1.8.3 Solubilization

The PPDs can also interact with the soluble wax crystals present in the crude oil at temperatures above WAT. The interaction could occur due to van der Waal forces between wax chains and alkyl part of the PPDs, and this interaction may result in a reduction in the WAT of crude oil.

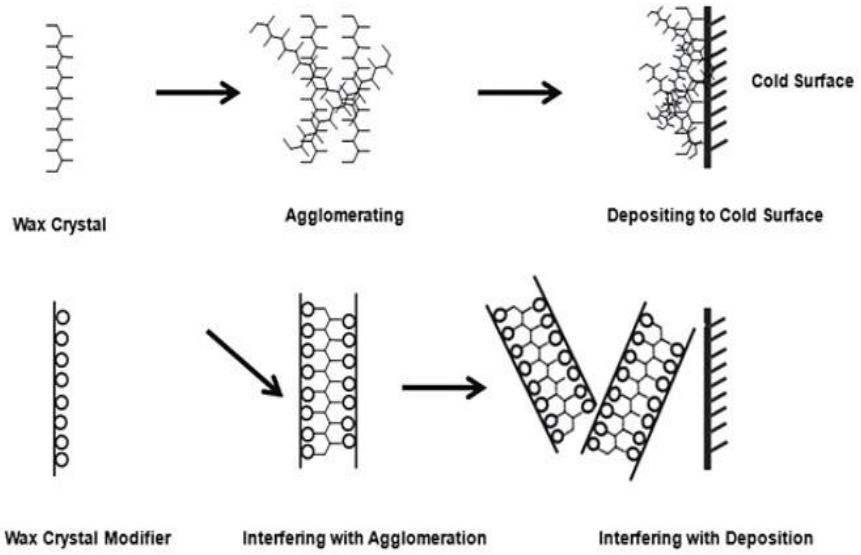

Figure 1.2. Modification in wax crystal network with and without co-crystallization of wax crystal modifier (Reproduced from (Wei, 2015) with permission from Springer Nature). Through co-crystallization, the interaction among waxes alters and their aggregation gets reduced, thus leading to reduced deposition on surfaces

1.9 Process of wax crystallization

As the crude oil cools below WAT, the precipitation of paraffin wax crystal and crystallization occurs to form a crystalline matrix. With crystallization, the gelation phenomena in the crude oil occurs where the oil molecules remain trapped in the porous structures of waxes and the gelation may start from temperatures above the pour point of the crude oil.

At temperatures above the WAT, the waxes remain in a zigzag configuration, which may self-associate to forms wax clusters or may attach to the available surfaces, as the temperature falls below WAT. With continuous precipitation of wax crystals, the equilibrium between dissolved and precipitated/deposited wax gets unbalanced and which results in greater networking and cluster formations of waxes. These precipitated waxes act as nucleation centre for further wax precipitation. Presence of nucleation sites are pre-requisite for stable wax crystals to form, thus nucleation is a regulating factor in formation of paraffin crystals. The crystal growth of waxes becomes spontaneous once nucleation initiates (Sunil Kumar, 2015). Thus, an effective control over nucleation sites could possibly help to control the growth rate of waxes.

1.10 Areas for improvement

The nanocomposite PPDs have been used recently and have found success in improving the flow ability of the crude oil. But the use of nanoparticles also brings some difficulties such as maintaining constant dispersion state of nanoparticles in the polymeric system. Other issues to address include the degradation in the properties of the crude oil with time, which is also known as aging effect in crude oils. The nanocomposite PPD should be able to address these issues in order to serve the real advantage of employing them by the flow assurance community.

1.11 Objectives of research

The thesis primarily aims to understand the synthesis, characterization of the nanocomposite PPDs and their subsequent evaluation to improve the flow characteristics of waxy crude oils. Additionally, focus would be given to understand the CFD approach of the wax deposition process. In order to fulfil the aims, following are the essential objectives of research which would be achieved gradually in the thesis chapters.

(1) To understand the flow assurance of waxy crude oils using chemical methods

(2) To understand the type of crude oil through characterization using standard methods.

(3) To develop nanocomposite pour point depressants and identify their effectiveness for particular waxy crude oils

(4) To characterize the synthesized PPDs using standard analytical techniques to confirm the formation of successful nanocomposites.
(5) To evaluate the beneficiation in the properties with nanocomposite PPDs over conventional polymeric PPDs.
(6) To understand the rheological behaviour of waxy crude oils and their flow improvement in the presence of nanocomposite and conventional polymeric PPDs.
(7) To test the efficiency of the developed PPDs in inhibiting the wax deposition in flowing conditions using cold finger test.
(8) To understand the changes in the wax morphologies of the crude oil treated with PPDs compared to the virgin crude oil.
(9) To develop a robust PPD by addressing the areas for improvement from the previous work on nanocomposite PPDs.
(10) To propose a suitable working mechanism of the nanocomposite PPDs on wax crystals.
(11) To simulate the gelation phenomena of the waxy crude oils through computational fluid dynamics.

1.12 Layout of thesis

Chapter 1 gives a brief introduction to the problems faced during pipeline transportation of crude oil. The major focus of this research work is to improve the flowability of waxy crude oils under low temperature conditions. This chapter provides an overview of the wax deposition issues and the different methods to remediate this issue. It also states the primary objectives of research, and the need for this work, and how this work helped to solve a current research gap in the petroleum industry. This chapter highlights the importance of the possible usages of the graphene-based additives in the petroleum industry and its benefits over conventional polymeric additives currently being used in the petroleum industry.

Chapter 2 provides an exhaustive list of the research works carried out on development and usage of nanocomposite/nanohybrid pour point depressants, and their performances are compared to conventional polymeric pour point depressants. This chapter discusses the methodologies and their results obtained upon using different

nanoparticles by different authors and also identifies the possible research gaps in their application. Also, this chapter explains the various action mechanisms for interaction of PPDs with the wax crystals proposed in the literatures.

Chapter 3 illustrates the methodology of characterizing the crude oils and detailed procedures to evaluate the effectiveness of the additives as pour point depressants and flow improvers. The methodology covers the standard test methods including ASTM standards and other widely followed techniques to evaluate the properties of crude oil, and rheological procedures are described to carry out the experimentation under different experimental conditions to understand the flow behaviour of the crude oils. The methodology also covers the microscopic observation of the wax crystal morphology under different temperature conditions. The experimental section also details the stage wise synthesis procedures of the additives and the characterization details of the synthesized additives. The last portion of the experimental section details the procedures and experimental conditions for evaluation of the synthesized additives including pour point tests, gelation point tests, viscosity determination, tests for evaluating the aging effect. Cold finger tests were performed at later stages of thesis to determine the wax inhibition efficiencies of the laboratory synthesized pour point depressants. To understand the detailed microscopic changes in the wax structures of the PPD-treated crude oil, polarized microscopy was conducted.

Chapter 4 provides the details of flow assurance of a waxy crude oil obtained using a novel class of synthesized polymer nanocomposite poly(methyl methacrylate)-graphene oxide [PMMA-GO], which will constitute the study 1. This chapter mentions the experimental conditions used and the results of characterization of crude oil and characterization of the additive PMMA-GO. Also, the flow improvement of the crude oil using PMMA-GO is discussed in detail and its performance is compared to the conventional polymeric PPD PMMA. Moreover, a possible mechanism for interaction of nanocomposite with wax crystals is proposed based on the microscopic observations. Effect of aging on the crude oil properties is evaluated.

Chapter 5 discusses the flow improvement of an Indian waxy crude oil obtained using a synthesized polymer nanocomposite poly(2-ethylhexylacrylate)-graphene oxide [P(2-EHA)-GO] and a conventional PPD P(2-EHA). The chapter evaluates the characteristic properties of the crude oil tested and the synthesized chemical additives and also details the experimental conditions used and the results obtained from the experimentation. This chapter also explores the detailed aging effects on the analysed crude oil by using these additives over a longer period of time in order to evaluate the efficiency of the synthesized additive. The performance of the P(2-EHA)-GO was compared to a conventional polymeric additive P(2-EHA). The chapter addresses the areas of improvement noted from the previous work.

Chapter 6 illustrates the evaluation of a novel kind of laboratory synthesized ionic liquid-graphene oxide nanocomposites on an Indian waxy crude oil. The work also details the evaluation of a novel ionic liquid PPD and the performances of the two synthesized PPDs are compared and discussed in detail. The experimental conditions for the experiment and the results obtained from the experimentation are discussed. Also, this kind of additive has a different type of interaction mechanism with wax as well as asphaltenes present in the crude oil, differently than previously developed polymer nanocomposites. Efforts were given to improve the dispersion state of the additive and cold finger tests was performed to evaluate the wax inhibition efficiency of the synthesized nanocomposite. The purpose of this work is to develop a highly effective PPD which could provide enormous beneficiation in crude oil properties and improve upon the important areas of concern experienced in previous works.

Chapter 7 provides the modelling and simulation aspects of the wax deposition in the pipeline transportation of waxy crude oil under different operating conditions using computational fluid dynamics. A new approach is adopted to simulate the gelation phenomena of the crude oil under laminar flow conditions in a pipeline flow.

Chapter 8 This chapter illustrates the summary and conclusion of the Ph.D. research work and also discusses the limitation and future scope of the work. Important conclusion derived from this research work are mentioned below.

1. The crude oil characterized were of waxy nature with medium API gravity.
2. The polymer nanocomposites synthesized in the laboratory were successfully evaluated as potential pour point depressants for the waxy crude oils.
3. The performances of the nanocomposite PPDs were found to be significantly better than the conventional polymeric PPDs.
4. The research works apart from evaluating the nanocomposite PPDs, also revealed new type of action/ working mechanism of these PPDs on the wax crystals in crude oil.
5. The research work was able to identify and develop a novel class of PPDs ionic liquid graphene oxide nanocomposite PPD, which performed best among all the additives developed and was also able to address the important areas of concern usually experienced with practical application of nanocomposite PPDs.
6. The simulation work on the wax oil gelation phenomena provided insights into the changes in gelation under different flowing conditions in the pipeline.

Chapter 2
Literature review

2.1 Background

With the continuous demand for improvement in the material properties, a lot of focus has been concentrated on the nanotechnology. The developments in nanotechnology have provided immense improvement in the material science. The dispersion of nanoparticles into the polymeric matrices leads to development of composite materials and often improves the properties such as thermal and electrical conductivity, mechanical strength, crystallization temperature and others. Nanoparticles possess large surface area to volume ratio, which helps to increase their interactions with polymer matrix. Properties of materials can change drastically upon when brought under nanoscale limits. The definition of nanoparticles is not exact and varies depending upon particular application. In general, the particles falling in the range 1-100 nm are termed as nanoparticles, but sometimes the size may also go as high as 1 μm. The nanoparticles possess great properties like for example the materials which are opaque under normal conditions (larger size) may turn in to transparent when being converted into nanosize dimensions (Šupová, Martynková and Barabaszová, 2011)

2.2 Introduction to nanocomposites

Polymer nanocomposites have emerged as new class of materials with plethora of applications in various sectors. Polymer nanocomposites in general are a mixture of at least two or more materials, where the primary phase is polymeric matrix and the dispersed phase should be nanomaterials (at least one dimension less than 100 nm).

The proper dispersion of nanofillers in the polymers is an important criterion in order to extract maximum benefits of the polymer nanocomposite. Three major types of polymer nanocomposites can be formed based on the degree of dispersion of nanomaterials. They are microcomposites (conventional), intercalated and exfoliated composites. When the dispersion of the nanomaterials is poor in the polymeric matrix, they result in microcomposites and their characteristics may be similar to traditional composites usually formed. When the polymer chains are arranged/intercalated in

between the nanomaterials (usually nanosheets) in a regular manner, they result in intercalated nanocomposites. When the nanomaterials are homogeneously dispersed in a polymer matrix, resulting in a uniform distribution they are termed as exfoliated nanocomposites, and these type of nanocomposites possess the highest contact area between the nanomaterials and polymer matrix which could be beneficial for application purposes (Dantas de Oliveira and Augusto Gonçalves Beatrice, 2018).

2.3 Current applications of nanoparticles in the petroleum industry

The use of nanoparticles in the flow assurance of the crude oil has brought tremendous advantages. Authors Anto and co-workers (Anto *et al.*, 2020) illustrated that the usage of silica and alumina nanoparticles on crude oils led to improvement in the rheological properties such as apparent viscosities and viscoelastic development. The nanoparticles were able to reduce the apparent viscosities of the two crude oils. The nanoparticles were shown to adsorb on the crude oil. Both nanoparticles showed varied effects when tested with different experiments. The reduction in apparent viscosities was attributed to the adsorption of nanoparticles on asphaltenes and thus minimizing the viscoelastic network formed by asphaltenes. A higher reduction in viscosities of two crude oils were obtained using silica nanoparticles compared to alumina nanoparticles (both silica and alumina were doped 0.3 wt.%). While the alumina nanoparticles were able to create a higher reduction in the viscoelastic parameters G' and G" at higher temperatures (55℃), while silica nanoparticles were more effective in reducing these viscoelastic parameters at lower temperatures (upto 40℃).

The nanoparticles are known to have higher specific surface area, thermal stability and other properties compared to the other particles. The nanoparticles have been used in the oilfield for numerous applications such as in flow assurance, enhancing the drilling fluid formulation in shale reservoirs, improving the chemical formulation for matrix acidizing through use of double emulsions. They also find use in nanofiltration technique to remove the organic deposits from the natural gas condensates in order to increase its commercial value, and can also assist in purification of produced water from the organic deposits so that it can be recycled for multiple surface operations or for harmless disposal in environment. They find use in the development of better elastomers for usage in well completion equipments, by incorporating nanoparticles into the conventional polymeric system generally used to develop elastomers. They are also used in developing smart

coatings in pipelines in order to serve multiple purposes such as reducing corrosion, abrasion and scaling and providing warnings in advance for any development of corrosion activity. Recently, focus is given to superparamagnetic nanoparticles which have the ability to generate heat when put under magnetic field oscillation of particular frequencies. These superparamagnetic nanoparticles can be used to develop nanopaint on the inner walls of the pipeline, which would heat up and melt the layers of waxes and asphaltenes nearby (Ko and Huh, 2019).

The addition of nanoparticles such as silica in the drilling mud was found to be effective in reducing the seepage of drilling fluid water into the nano-size pores of the shale formations, which is otherwise difficult to control, in general, in the case of water-based drilling muds. The nanoparticles are assumed to occupy these nanopores to obstruct the seepage of water.

The benefits of nanoparticles can be utilized in development of low weight and high strength alloys that can be used for well completion equipments such as tubings and casings. Another benefit that can be extracted with nanoscience is via coating the inner walls of tubings in order to achieve multiple benefits simultaneously including curtailed corrosion and abrasion, reduced pressure loss and lesser scale or organic deposition.
Improvements in the well cementing quality can be made in the following areas such as cement viscosifier, improving setting time and density control of cement, self-healing of cement micro-cracks. The nanoparticles such as silica owing to higher surface area decreases the duration for hydration of cement, thereby beneficiating the cementing operations in low temperature conditions of deepwater oil and gas projects (Ko and Huh, 2019).

Nanoparticles also find use in the hydraulic fracturing of the reservoir. They can be used to resolve problems such as reduced viscosity hampering the pressure gradient required to fracture the formation and also to maintain the higher viscosity to avoid leakage of fluid into the adjacent matrix. Additionally, this fracturing fluid must possess characteristics ensuring its removal from fractures in order to provide a clean and safe passage for the inflow of hydrocarbons and water. Another area for improvement in the employment of hydraulic fracturing is a consistent and massive source of water requirement, which would be subsequently disposed. Thus, to avoid this problem, CO_2 foam-based fracture fluid is developed nowadays as a substitute to conventional

fracturing fluids, and one of the works used silica nanoparticles to maintain consistent salinity of CO2 foam fluids and were able to contain the water volume fraction down to as low as 2 %.

The formation of oil-in-water emulsion has been a continuous problem in produced oil for decades, and a lot of research efforts are given for demulsification. However, the expensive nature of treatment and complexity of the processes have usually forced the researchers to look for a viable and easy alternative for demulsification. Recently, major research has been initiated into the utilization of functionalized nanoparticles having the ability to adsorb on the water-oil interface and destabilize the emulsions. Under the presence of a magnetic field, compounds such as magnetic carbon nanotubes can remove the entrapped oil from the produced water through adsorption on the interface of oil and water and subsequently pulling nanoparticle attached droplets out of water. In one of the works, the superparamagnetic nanoparticles were also able to segregate the oil droplets from the produced water up to 99.9 %, where the nanoparticles being positively charged attached themselves to negatively charged oil droplets (Ko and Huh, 2019).

Nanoparticles also find an essential role in improving the sensing applications of reservoir properties. The nanoparticles can be sent into the downhole to extract information about the reservoir fluid properties and to estimate the injected fluid, connate water, and hydrocarbons. Three types of procedures were followed to extract such information.

(1) Incorporating specific nanoparticles in the injection fluid to be carried downhole, which would record the information that can be extracted once they reach the surface.

(2) Sending the nanoparticle mixed injection fluid downhole for operations such as in enhanced oil recovery operations and remotely tracing their location and flow dynamics.

(3) Sending and positioning sensing devices incorporating nanoparticles in downhole to trace the properties near wellbore (Ko and Huh, 2019).

2.4 Graphene based nanocomposites

Although nanoparticles have proven their potential in different applications owing to its enhanced structural features, yet the major concern is to develop materials possessing superior physicochemical properties that are more suitable in the field of

nanoscience. Regarding this aspect, discovery of graphene based nanocomposites finds substantial application in nanoscience technology, thus contributing to significant developments in technology (Kuilla *et al.*, 2010). Graphene based polymer nanocomposites is an important frontier of research in material science owing to its numerous applications and interesting properties (Kim, Abdala and MacOsko, 2010). Graphene has played a significant role in the development of polymer nanocomposites due to its high specific surface area and its excellent thermal, electrical and mechanical properties owing to its unique monolayer structure comprising of hexagonal array of carbon atoms with sp^2 hybridization forming sigma bonds with three nearest neighbours in the layer (Tang *et al.*, 2012). But the solubility of graphene in both aqueous and non-aqueous phase is a serious issue to its application. Often, it is converted to GO which is then functionalized through various methods to improve its solubility and dispersion in different matrices (Al-Sabagh *et al.*, 2016). GO, an oxidized form of graphene is an important material for the development of polymer nanocomposites due to presence of oxygenated functionalities such as hydroxyl, epoxide, carbonyl and carboxyl groups on its basal planes and around periphery. These oxygenated functional groups act as possible sites for polymerization (A. Kumar *et al.*, 2016).

The development of graphene oxide (GO) went through a remarkable journey involving years of research started in year 1859 when the synthesis of GO was first reported by Brodie (Benjamin, 1859) by adding potassium chlorate and nitric acid to the graphite slurry. Later, Staudenmaier in 1898 (Staudenmaier, 1898), refined Brodies' work through usage of nitric acid, sulfuric acid (conc.) and the chlorate was added in several batches during the reaction procedure. Thus, a production of highly oxidized GO in a single vessel was obtained by this slight modification in the procedure by Staudenmaier. Nearly half a century later, in 1958, Hummers developed a method where the oxidation of graphite was performed with $KMnO_4$ and $NaNO_3$ in concentrated H_2SO_4. (Marcano et al., 2010). Several authors have also reported other modifications in these GO synthesis procedures along time.

Similarly, the structure of GO has been debated since years, where its several versions have been reported with time. Its possible structures have been demonstrated by eminent researchers including Thiele, Hoffman and Rudolf, Ruess, Scholz and Boehm, Nakajima and Matuso, Lerf and Klinowski, Szabo-Dekany and Dimie–Alemany–Tour.

Among all the GO models demonstrated by several researchers, Lerf and Klinowski model (Lerf *et al.*, 1998) has been widely accepted, especially for moderate oxidized samples of GO (Sun, 2019). The Figure 1 demonstrates several GO models proposed by the above-mentioned eminent scientists.

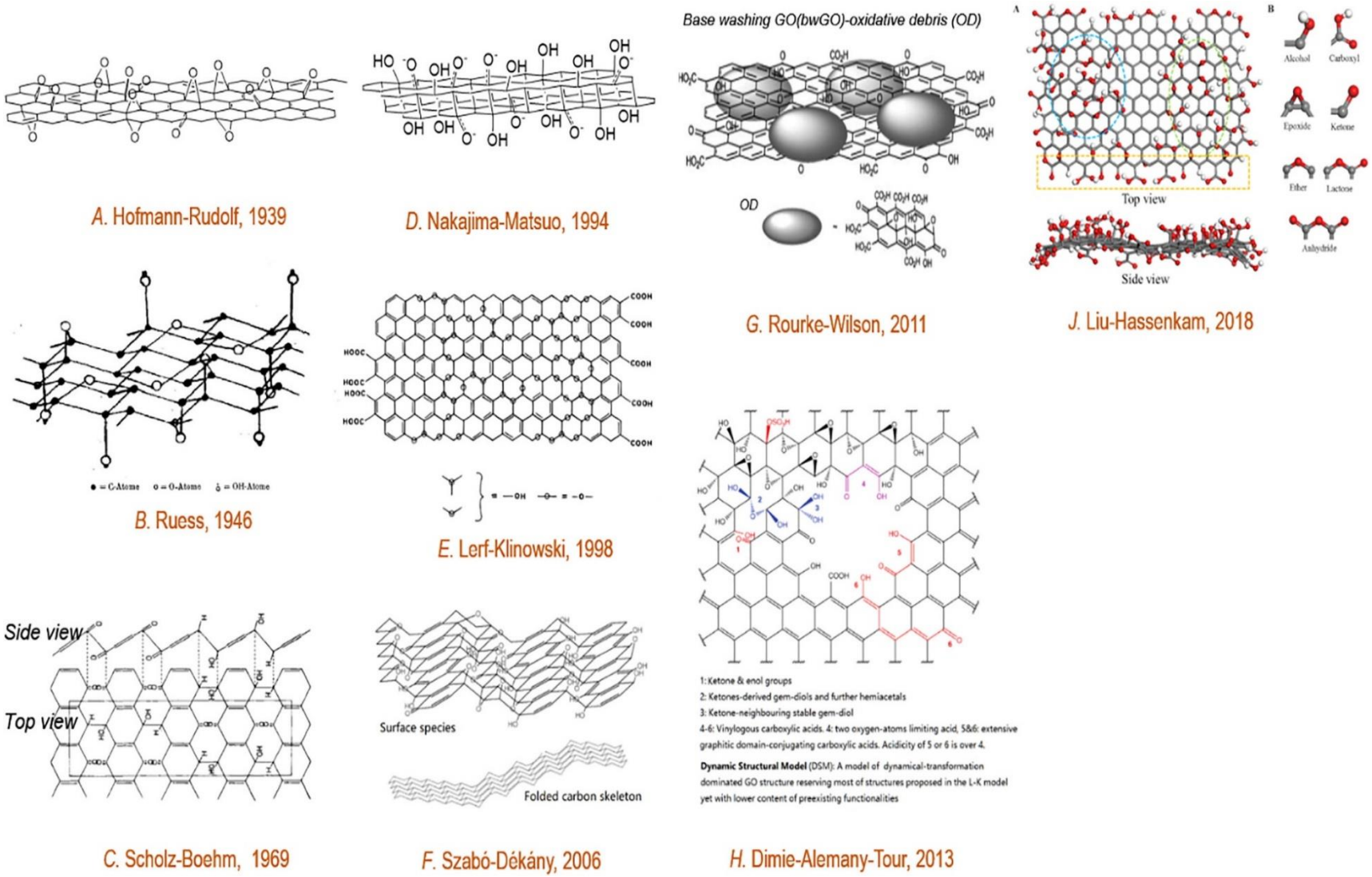

Figure 2.1. List of possible theoretical models of graphene oxide. Reproduced from (Sun, 2019) with permission from Elsevier.

2.5 Pour point depressants

2.5.1 Polymeric PPDs

Polymers are extensively used in modern world due to its low cost and simple process of manufacturing, rendering immense use in oilfield applications. One of the major uses of polymers is development of polymeric additives for oilfield operations and transportation purposes. Conventional polymeric PPDs are usually synthesized using homo and co-polymers of different monomers. Their interaction with crude oil molecules involves surface adsorption, nucleation and co-crystallization mechanisms, thereby altering the wax crystal growth and morphology. In order to understand the development and effect of polymeric PPDs on the flowability of oil, Table 1 lists several important works on the development of polymeric PPDs and their application in improving the flow properties of crude/model oil.

Table 2.1. List of research works on development of polymeric pour point depressants with their beneficiation details on crude/model oils.

Authors (Year)	PPD composition	Beneficiation Details
(Yang *et al.*, 2018)	Poly (octadecyl acrylate) [POA]	POA was doped in a 10 wt.% model waxy oil. POA was able to modify the wax morphology and resulted in the heterogenous wax distribution. POA reduced the total wax deposit mass .
(Yao et al. 2016)	Poly (octadecyl acrylate-vinyl acetate). [POA-VA], VA molar fraction between 0-50 mol. %.	POA-25 % VA causes the most compact wax morphology and shows the highest reduction in WAT, pour point (13°C - 22°C) and viscosity of crude oil. VA being the polar moiety in the PPD, modifies the wax crystallization ability.
(Deka *et al.*, 2018)	Triethanolamine was polymerized to form its trimer (TTEA) and then	TTEA di-oleate caused a 17°C reduction in the pour point of the crude oil. WAT was reduced by 1.8 °C and the WPT

	esterified with oleic acid to form tri-triethanolamine di oleate (TTEA di-oleate)	decreased by 5.5 °C. Reduction in the apparent viscosities up to 91% was recorded.
(Deka, Sharma and Mahto, 2020)	Polymeric PPDs**:** poly (n-dodecyl linoleate –co-succinic anhydride) {MALN} and poly (n-dodecyl ricinoleate –co-succinic anhydride) {MARC}	Pour point reduction of a waxy crude oil by 20°C and 22°C respectively by MALN and MARC PPDs. Huge reduction in the viscosities were observed, MARC showed better results. Gelation points of crude oil were reduced heavily by 11°C and 15°C by MALN and MARC respectively. The wax inhibition capacities of the MALN was determined to 41.8% - 51.32%, while for MARC it was 48% - 63.9%.
(Soni and Bharambe, 2006)	Polymeric diesters of oleic acid series and methacrylic acid series, prepared by esterification of the copolymers of alkyl oleate/methacrylate and maleic anhydride.	Flow improvement through maximum pour point reduction of crude oil by 6°C and 9°C by methacrylic acid diesters and oleic acid diesters. The viscosity reduction is observed from 75 cPs down to 12 cPs with methacrylic acid diesters and a higher reduction from 75 cPs down to 4 cPs with oleic acid diesters.
(Deshmukh and Bharambe, 2008)	Poly(n-alkyl acrylates co-N-hexadecylmalmeimide), prepared by reaction of anyhride copolymers with hexadecylamine	The pour point reduction of the crude oil was observed to between 6-27°C by the additives and the highest reduction is observed with additive having C-14 carbon group. While the viscosity reduction of the crude oil occurred from 0.09 Pa.s (24°C) and 0.03 Pa.s (27°C) to 0.01127 Pa.s (24°C) and 0.11 Pa.s (27°C) with the additive with containing C-14 group. The yield stress

(Al-Sabagh *et al.*, 2013)	Poly(n-alkyl oleate co-succinic anhydride)	Maximum pour point reduction of crude oil occurs by 12°C. Dynamic viscosity of the crude oil reduces from 7.28 - 358 mPa.s. down to 5.92 - 97 mPa.s. at 5000 ppm of additive concentration.

2.5.2 Nanocomposite/ Nanohybrid PPDs

To improve the flow performance of conventional polymeric PPDs, one of the methods is to introduce inorganic particles/sheets into the polymer matrix to form polymer nanocomposites, thereby resulting in a significant improvement in mechanical, thermal and electrical properties [7,8]. Significant research is initiated into the development of polymer/inorganic nanocomposites or nano-hybrid materials. Previously, nanocomposite PPDs have been developed and have shown significant reduction in pour point of crude oil and improved rheological characteristics. One type of nanohybrid pour point depressant was prepared based on organically modified nano-SiO_2 in ethylene and vinyl acetate (EVA) and its effect was evaluated on the cold flow properties of a model waxy oil (25 wt. % paraffin content). Vinyl acetate (VA) content in EVA affected the interaction between modified nanoparticles and EVA. Therefore, an optimized 32% VA in EVA was used to provide the best flow improvement for model waxy oil at 500 ppm nanohybrid concentration. There was a significant pour point reduction from 34°C up to 5°C. The possible mechanism behind such drastic improvement is that, nanohybrid PPD acted as nucleation centers to promote wax crystallization, which leads to the formation of compact sized wax crystals and thereby causing weaker wax network structure (Jing *et al.*, 2017). Another nanocomposite namely NPPD, based on montmorillonite (MMT) and EVA was applied on a waxy crude oil (wax content= 30.9%) and it exhibited improved flowability. NPPD when doped in the crude oil, showed substantial pour point reduction of 14°C and viscosity reduction up to 87.4% at minimal dosage around 50 ppm. The action mechanism for this reduction is that EVA co-crystallizes with paraffin chains and modifies the shape and size of wax crystals, while the nanoparticles provided heterogeneous nucleation sites for deposition of wax crystals. The nanoparticles also caused the charging of wax molecules resulting in a substantial electrostatic repulsion (He

et al., 2016). Important works of several authors on nanocomposite/nanohybrid PPDs have been listed in the Table 2, where the beneficiation caused by the PPDs on crude oil/ model oil have been elaborated.

Table 2.2. List of research works on development and application of nanocomposite PPDs

Authors (Year)	PPD composition	Beneficiation Details
(Yao *et al.*, 2017)	Poly(octadecyl acrylate) - polyhedral oligomeric silsesquioxane [POA-POSS] nanocomposite PPDs	Lowered the yield stress, gelation point, pour point, and apparent viscosities of the crude oil. Reduction in the pour point by 5°C and gelation point of crude oil by 1.8°C and reduction in the viscosities by about 46 %. Modifies the wax crystallization habit and helps in accumulation of the wax precipitated crystals. These crystals reduces the solid-liquid interfacial interaction and thus, improves the rheology.
(Sharma, Mahto and Vuthaluru, 2019)	Nanocomposite PPD: Poly(methyl methacrylate)-modified graphene oxide [PMMA-GO], with GO concentrations varying between 0.5 - 1% GO.	PMMA-GO was synthesized in the laboratory and evaluated on an Indian waxy crude oil (pour point = 38°C). The nanocomposite additive resulted in a maximum pour point reduction of 23°C and up to 99.99% reduction in the apparent viscosities of crude oil. The yield stress values reduced from 60 Pa to 0.1 Pa. The additive controlled the aging tendency of the crude oils. The performance of PMMA-GO was compared to a conventional PPDs: PMMA and Phoenix and it was found to be

		superior to the conventional ones. Long term stability of the nanocomposite treated crude oil was better than conventional ones.
(Sharma *et al.*, 2019)	Nanocomposite PPD: Poly(2-ethyl hexyl acrylate)-graphene oxide [P(2-EHA)-GO], GO concentrations were varied between 0.5-2 wt.%.	P(2-EHA)-GO was laboratory synthesized and evaluated on an Indian waxy crude oil (pour point= 36°C). The additive resulted in an enormous beneficiation in the flow properties of crude oil with the maximum pour point depression achieved about 18°C and the gelation point depression was recorded to be around 17.8°C. Improvement in the flow viscosities was observed greatly with viscosities falling from 1.9 Pa.s (crude oil) to 0.01-0.03 Pa.s (additive treated crude oil). The performance of P(2-EHA)-1% GO was compared to a conventional additive P(2-EHA) and found to superior to the latter. The aging tendency in the crude oils was significantly reduced as the pour points increased not more than 3°C and 6° after 15 and 30 days of sample storage respectively in the case of P(2-EHA)-1%GO.
(Huang *et al.*, 2018)	EVA/montmorillonite nanocomposite	The nanocomposite PPD resulted in reduction of the viscosities of a model waxy oil by the order of 10^2. The yield stresses of the model oil reduces by nearly the order of 10^1. A nucleation and co-crystallization mechanism was proposed for the interaction of nanocomposite with the wax crystals.
(Li *et al.*, 2018)	EVA/montmorillonite nanohybrids	Maximum reduction in the pour point of about 32°C and the viscosity reduction of about 10^2 of a model waxy oil was observed.

		Performance was compared to the conventional additive EVA and was found to be better in terms of pour point evaluation and rheology.
(Yao *et al.*, 2016)	Poly(octadecyl) acrylate /clay nanocomposite	A maximum reduction of pour point of a waxy crude oil was found to be 12°C. While the reduction in gelation point occurred up to 5.8°C.
(Sharma et al., 2020)	Nanocomposite PPD: poly(methyl methacrylate) – modified graphene oxide [PMMA-GO]	The PMMA-GO nanocomposite was evaluated on a waxy crude oil in terms of pour point, gelation and enduring thermal conditioning, shear conditioning and aging effect. PMMA-GO reduced the pour by maximum of 23 °C and the gelation point by 24°C indicating excellent effectiveness. The PMMA-GO excellently reduced the thermal conditioning effect in crude oil through controlling the change in its pour point at different re-heating temperatures of crude oil. The crude oil suffered higher with conventional PPD PMMA (with 3°C increase in optimum pour point). Also, the PMMA-GO controlled the changes in gelation points better when cooled at different rates. Effect of aging was well controlled in crude oil when treated with PMMA-GO, with surge in the viscosities falling between 16 % - 34 % and the optimum pour point increases by only 2°C.
(Jing *et al.*, 2017)	EVA/modified nano-SiO_2 nanohybrid PPD	Pour point was reduced up to 5°C, while the viscosity reductions of nanohybrid-treated

		model waxy oils are slightly better than pure EVA and nano-SiO_2 treated model oils.
(Yang, Paso, *et al.*, 2015)	POA/nanosilica nanohybrid	Gelation point was reduced by 6°C for the model waxy oil system when treated with nanohybrid
(Wang *et al.*, 2011)	NPPD nanohybrid PPD and EVA PPDs	The pour point was decreased by 14°C with NPPD, while only 7.5°C depression in pour point was observed with EVA PPD. The apparent viscosities decreased by around 87.4% with NPPD compared to 84.7% by EVA PPDs initially, while after 10 days the viscosity reduction with NPPD (85.9%) was better than with EVA (78.1%)
(He *et al.*, 2016)	Montmorillonite/EVA nanocomposite	Pour point reduces by 10°C and the apparent viscosities of waxy crude oil get reduced by 82.1% up to 308 mPa.s. upon treatment with nanocomposite

2.6 Precipitation of wax crystals

In the virgin crude oil, there is abundance of wax crystals in smaller sizes, which create significant interfacial areas between liquid-solids. This enormous interfacial area promotes extensive wax-wax interactions, leading to high wax networking, resulting in substantial wax precipitation. In addition, there are solvation layers reported to be present around the precipitated waxes, indicating the presence of liquid oils on the interface of wax crystals constituting the solvation layers. The large interfacial area among wax crystals creates high wax-wax networking and enormous amount of solvation layers, resulting in an increased volume fraction on the wax crystals and the trapped oil volume fraction. These reasons contribute to a waxy nature of crude oil with significant gelation characteristics (Yao, Li, Yang, Zhang, *et al.*, 2016).

The PPDs are added to the crude oil in order to break this wax-wax interactions and the networking capacity of the wax crystals and reduce their deposition. Usually, the conventional polymeric pour point depressants possess in general, alkyl structures (non-polar part) which can co-crystallize with the waxes and prevent their deposition. A section of the PPDs possesses polar constituents in its composition, in order to improve their efficacy on crude oil. These polar PPD constituents gets attached to the surface of wax crystals, thereby, covering the surface and disrupting the normal formation of solvation layers, and there is also increase in the interaction among polar constituents on wax surfaces. Both of these reasons lead to creation of large wax flocs and results in a smaller interfacial area between wax crystals and oil. This reduced interfacial area also leads to decreased gelling characteristics in crude oil and reduced wax networking.

The reason for including polar part in the PPD composition may also be attributed to control the asphaltenes aggregation behaviour and the benefits it offers to control the wax deposition. The polar part of the PPD attaches themselves to the asphaltenes to from PPD-asphaltene clusters and they behave as nucleation sites for precipitation of wax crystals, thereby leading to an altered wax morphology and a reduced wax precipitation.

The nanocomposite PPD when doped into the crude oil, provides nucleation templates for wax precipitation leading to formation of larger and more compact wax flocs, thereby resulting in a less density of wax crystals and gelling due to their poor networking and lesser oil entrapment. This leads to degraded structural strength and yield stresses in the crude oils, thereby making the crude oil flow easier (Yao, Li, Yang, Zhang, *et al.*, 2016). The nanocomposite PPDs can also control the dispersion state of the conventional polymeric structures of the PPDs, which would improve the working efficacy of the conventional PPDs.

2.7 Action mechanism of nanocomposites on wax crystals

Various theories have been proposed regarding action mechanism of polymer nanocomposites on wax crystals. Mechanism of polymer nanocomposites and its comparison with conventional ones in mechanism and modifying wax crystal morphology.

Different authors have varied ideas regarding the wax deposition process and the role of nanocomposite PPDs in modifying the wax crystal morphology and their flow improvement

2.7.1 Co-crystallization and nucleation

Another research by Al-Sabagh and co-workers (Al-Sabagah et al., 2019), developed a nanohybrid based on montmorillonite [MMT] and poly(octadecyl acrylate) [POA] and stated that the presence of MMT layers attached to the polymeric chains of conventional flow improver POA, provides nucleation sites for precipitation of wax crystals. This leads to alteration of wax morphology, where the wax crystals adsorb on the surface of polymer nanohybrid and thus, the interaction among wax crystals reduces significantly. Moreover, the MMT layers are known to have acid sites, to which the hydrocarbon molecules get attached, and this would lead to less occlusion of oil in the porous structures of waxes and therefore, less gelation characteristics would be present. Additionally, the oxygen atoms present in the clay surface can provide charges to the wax crystals deposited over nanohybrid surface and can create electrostatic repulsion among wax crystals leading to improved flowability of the waxy crude oils.

2.7.2 Electrostatic charging

Another type of action mechanism for delayed and less wax deposition in nanocomposite beneficiated crude oil can be explained by the electrostatic charging of wax particles and consequent repulsion between them, where the nanosheets in the oil medium act as nucleation sites for the wax crystals to get adsorbed on them, subsequently the polarity is generated on nanosheets due to presence of oxygen or other functionalities (based on PPD composition) on them. Thus, a repulsive force acts amongst the charged wax crystals in nanocomposite beneficiated crude oil (Agaev *et al.*, 1981; He *et al.*, 2016). The electrostatic repulsion leads to less gelation of the wax particles and results in a loose wax crystal network, and therefore leads to significant reduction in yield stress. The above mechanism is now explained in detailed below.

According to the studies done by Agaev et.al, 1980 and Cunzhe et.al, 2016, the determination of electro kinetic potential of crude oil showed that wax crystals were positively charged. The charging of wax particles was attributed to the presence of electrical double layer on the surface of the dispersed wax particles. Electro kinetic potential values remained very small in case of virgin crude oil and the small amount of charges were due to presence of polar groups in asphaltenes and metal ions. Very high electro kinetic potential values were reported in the case of crude oils beneficiated with

additives (nanoparticle based PPD) compared to untreated raw crude oil. As illustrated in the plot of total energy curves of wax crystals, the large energy barrier gap between nanocomposite beneficiated and virgin crude oil sample can be attributed to higher EDL repulsion occurring in nanocomposite beneficiated crude oil (Agaev *et al.*, 1981; He *et al.*, 2016).

Thus, the above stated theory confirms a new type of the action mechanism, where a delayed and less wax deposition in nanocomposite beneficiated, crude oil would be observed, which may be attributed to the increased electrostatic charging of wax particles and consequent repulsion between them. The nanoparticles/nanosheets in the oil medium would act as nucleation sites for the wax crystals to get adsorbed on it. Polarity is generated on nanoparticles/sheets due to presence of polar functional groups present (based on PPD composition) on them, which gets transferred to the wax crystals adhered to nanoparticles/nanosheets. Thus, a larger repulsive force would act amongst the charged wax crystals in nanocomposite beneficiated crude oil. The electrostatic repulsion leads to less gelation of the wax particles and would result in a loose wax crystal network, and therefore leads to significant reduction in yield stress.

2.8 Areas to improve in nanocomposite PPDs

2.8.1 Dispersion ability

The dispersion of nanoparticles/nanosheets in the polymeric matrix is an essential criterion for its effectiveness for long term. Several authors have stated the problem of poor dispersion of the nanoparticles in nanocomposites and it affects their performance on crude oil.

In general, the nanoparticles have poor dispersion in the polymeric/non-polymeric matrix. Dispersion of nanoparticles can be enhanced by its surface modification through functionalization with vinylic groups, octadecyl trimethyl ammonium chloride. Through surface modification the solubility/dispersion can be enhanced to a great extent, which would help the nanoparticles to participate in further reactions such as in-situ polymerization of chemical additives etc. (Sharma, Mahto and Vuthaluru, 2019).

2.8.2 Low dosage application

The improvement in the flow properties of the crude oil has been observed with nanocomposites/nanohybrid over conventional pour point depressants. But their quantity

requirement for producing the optimum results have been in general found to be higher, which would increase the load on cost-economics of the project. Moreover, high requirement of the additives creates additional burden on the storage capacity of the manufacturing plant, further increasing the handling costs. Also, enormous quantities of the chemical additives pose serious risk to the safety of the handling personnel's. Therefore, it is essential to control the quantities of the chemical additives required for the operation, and it could be achieved by optimizing the synthesis process of the polymeric/non-polymeric nanocomposites, resulting in a cost economic PPD/ and or flow improver.

2.8.3 Enhanced pour point depression

Pour point depression is one of the major criteria for judging the efficiency of an effective PPD. Other criteria could also include the capacity of the chemical additive to supress the gelation points of the crude oil, reduce the wax appearance temperature (WAT), wax precipitation temperature and others. There is a continuous research being carried out to develop a cost-effective PPD having capacity for significant pour point depression for waxy crude oils.

2.8.4 Aging effect

Aging is an important criterion to judge the efficacy of the used chemical additives for its long-term efficacy. The PPDs in general, show good effect on the pour point depression initially, but their performance tends to degrade with time. The chemical additives are added into the crude oil, which is transported for several days, or weeks and it is expected that the additive maintains its initial performance or at least the degradation in its properties is not substantial that would defeat its purpose. It has been observed with the nanocomposites, that their initial performance is encouraging, but their performance is not very effective for long durations. Therefore, the research works on development of nanocomposites should bear in mind about this important issue.

2.8.5 Eliminating the need of hydrocarbon solvent for PPDs

The pour depressants used in the petroleum industry are significantly viscous in nature and in general, there is a requirement to mix them with a hydrocarbon solvent such as toluene, xylene and others, before adding in crude oil. The addition of solvent reduces the viscous nature of the PPD and helps in proper mixing with the crude oil. Also, many

nanocomposite/nanohybrid PPDs developed remain in the stated of solid powder, and they need to be mixed with solvent before being doped into the crude oil. The requirement of solvent increases the projects costs and also require additional storage capabilities and needs to be handed safely.

Therefore, the focus should be given to develop PPD products in such a fluidic state which can be doped directly into the crude oil without needing any solvent. This would significantly improve the project economics

2.9 Effect of operating conditions on the effectiveness of the chemical additives

2.9.1 Continuous shearing during pipeline transportation - cold finger method

Apart from the laboratory tests such as pour point test and gelation tests, one of the tests to validate the efficacy of the selected wax inhibitor/PPD under flowing conditions is the cold finger test. During pipeline transportation for longer distances, the waxy crude oil undergoes continuous shear force and as well as variation in ambient temperatures. Thus, validating a particular wax inhibitor/PPD through cold finger test gives additional confidence in selection of a robust flow improver more suited to pipeline transportation application.

According to the research work by Jennings and co-workers (Jennings and Weisfenning, 2005) the efficiency of the wax inhibitors was found to increase with surge in shear rate. Similar findings were observed by Tinsley and co-workers (Tinsley et al. 2007) for the wax inhibitors on wax deposition from model oils. But the effect of shear force was found to have different results upon changes in temperatures, especially below WAT. Above WAT, the efficacy of the PPDs was found to be less affected with change in shear, but their efficacy tends to decrease with the shearing at temperatures below WAT (Yang, Zhao, *et al.*, 2015). This indicates that shearing surely affects the performance of the chemical additives on crude oil/model oil and the effect of shearing on the efficacy of the polymeric additives cannot be stated directly and requires comparison with the data from other evaluation tests such as pour point tests and gelation tests.

2.9.2 Thermal conditioning

Changes in the surrounding ambient temperatures affects the pipeline temperature profile, which subsequently alters the dynamics of crude oil flow in pipeline through phenomenon such as molecular diffusion, leading to precipitation and deposition of

waxes along the pipeline length. Temperatures usually fluctuate during pipeline transportation during day cycle and changes in location wise weather, increasing or decreasing during the entire flow. Pour point of the crude oils can change in such conditions due to repeated thermal heating and cooling process, and therefore it is necessary for a particular PPD to have capacity to control such fluctuations in the properties of the crude oil and maintain a steady flow throughout. The gelation properties of the crude oil could also be tested under different cooling rates similar to those experienced in pipeline operations, this would help to develop PPDs appropriate enough to control the gelation tendency in crude oils with changes in temperature during transportation. (Sharma, Rohit ; Mahto, Vikas; Vuthaluru, Hari ; Li, 2020).

2.9.3 Aging/Storage

The beneficiation caused by the PPDs/flow improvers for a particular crude oil usually tends to supress with time and the crude oil depending on its composition, operating pressures/temperatures and duration of pipeline transport may face significant flow assurance challenges including shutdown of pipeline. Thus, the developed chemical additives should be tested for its capabilities to control the aging tendency in crude oil for significant duration, at least for total duration of pipeline transport and keeping safety margins (Sharma, Rohit ; Mahto, Vikas; Vuthaluru, Hari ; Li, 2020).

2.9.4 Pumping pressure

If the prime movers/ pumps can maintain sufficient pressure throughout the entire pipeline length, then it is possible to avoid the usage of chemical additives at all, or atleast the requirement of the additives would be optimal.

2.10 Preparation techniques of nanocomposites

The synthesis process should be adopted considering the advantages and disadvantages of each and every process. Nanocomposites can be synthesized mostly by the following preparation methods (Khan, Hamadneh and Khan, 2016)

2.10.1 In-situ polymerization

In situ polymerization is the most widely used method and it involves intrusion of the low-molecular weight monomer solution among the nanofillers/nanosheets, resulting in enlargement of nanofiller size/interlayer spacing among nanosheets [35]. The

polymerization can be performed using either of radiation, heat, initiator diffusion or by organic initiator. The monomer is then polymerized among interlayers resulting in exfoliated or intercalated nanocomposites.

2.10.2 Melt blending

Melt blending involves the formation of a viscous polymer solution by melting the polymer and subsequently nanofillers are incorporated into polymer solution under high shear force together with high temperature diffusion.

2.10.3 Melt intercalation

Melt intercalation is a method that involves mixing the nanofillers into the polymer matrix at molten temperature where the mixture of nanofibers and polymer are annealed either under shear or statically. This method is compatible with contemporary industrial methods, including injection molding and extrusion and it permits the usage of polymers, which are not suitable for solution intercalation or in situ polymerization techniques.

2.10.4 Sol-Gel method

The sol-gel method involves states, sol and gel. Sol is a colloidal suspension of solid nanoparticles suspension in monomer solution and the interconnecting network formed among phases, results in a three-dimensional gel [35]. In this method, a colloidal suspension of solid nanoparticles (sol) is formed by dispersion of nanoparticles in the monomer matrix, they form interconnecting network between phases (gel) by polymerization reactions and subsequently the hydrolysis procedure is performed. The polymer nanoparticle gel network covers the entire liquid [35]. The polymer provides nucleation sites and promotes the growth of layered crystals. As the crystals grow, the polymer gets inserted among layers, resulting in a nanocomposite.

2.10.5 Solution blending

In this method, dispersion of the nanoparticles in solvent and the polymer dispersion is done in a co-solvent. The solvent evaporation could be performed in order to recover the resulting nanocomposites from solvent (Khan, Hamadneh and Khan, 2016).

2.11 Effect of asphaltenes on wax morphology and the action mechanism of the PPDs

Already there is no universal agreement over a common action mechanism for PPDs. To add to the complexity of these chemical additives over wax crystals, the presence of natural polar components in crude oil also play a possible role in the precipitation and deposition of the waxes. These polar components includes primarily asphaltenes, then resins and naphthenic acids and others**.** The structure of asphaltenes contain both polar and non-polar structures. The non-polar part of the asphaltene .i.e. the alkyl part is similar to the wax structure, and it could co-precipitate with the waxes and affect its morphology and networking tendency and thus can control its precipitation and deposition tendency.

But the results of studies performed to evaluate and understand the impact/effect of asphaltenes over the wax structures in crude oil has not yielded strong unidirectional results based on which straightforward generalized theory/models could be developed and owing to different composition of individual crude oils, experiments need to be specifically carried out for the particular crude oil. Literatures suggest that the presence of asphaltenes either helps to increase or decrease the pour points of crude oil or bear no effect at all. These findings could be extended to other properties such as WAT and rheology. But still due to structural similarities among asphaltenes and waxes, their synergistic co-precipitation has been reported in literatures, which leads to several theories about their interactions (Ariza-Leon, E. et al. 2014).

In one of the studies by Machado and Lucas it was stated that the asphaltenes could potentially mimic the characteristics of the PPDs, which may be attributed to the amphiphilic nature of the asphaltenes having polar aromatic rings and non-polar aliphatic chains which could possibly co-crystallize with the alkyl part of the wax structures. Additionally, the solubility of asphaltenes in crude oil adds advantage to them acting as likely PPDs. Thus, asphaltenes could either precipitate simultaneously with waxes or acts as PPD in order to alter the aggregation of wax crystals, which results in poor gel strength of crude oil, thus, improving the flowability of crude oils (Venkatesan *et al.*, 2003).

The simultaneous presence of waxes and asphaltenes has been reported from almost all streams of petroleum industry i.e. from upstream (oil wells), to midstream (pipeline transportation) and further to downstream (refinery operations). Their presence has been reported through fouling studies, which revealed paraffinic crude oil have

problems of asphaltene precipitation. The sediments recovered from the storage tanks have also revealed that deposited material consisted of asphaltenes and wax compositions together (Carbognani *et al.*, 2000; Rogel *et al.*, 2016).

Most of the studies related to asphaltene-wax interactions have been carried out by testing on synthetic fluids i.e. model oils which mimic the crude oil compositionally. These kinds of studies are essential to understand the individual effect of each component on crude oil properties, but in order to develop a generalized theory/models on asphaltene-wax interactions, the results generated from these studies needs to be validated on raw crude oils. Therefore, emphasis must be laid on understanding the interactions among different components of crude oil, which would further help to develop deeper understanding of action mechanism of the newer laboratory synthesized PPD/flow improvers/wax inhibitors and also for conventional additives currently in use in petroleum industry.

2.12 Overview on wax deposition mechanisms during pipeline transportation of crude oil

There are few theories that have been proposed explaining the details of mechanism of wax deposition in crude oils namely Brownian diffusion, molecular diffusion, shear dispersion and gravity settling. These mechanisms have been developed on the basis of sound experiments conducted by several scientists. But still, there is a lack of universal consensus over any fully accepted particular wax deposition mechanism. Molecular diffusion of wax particles from the bulk crude oil is the preferably accepted mechanism among them. The molecular diffusion is initiated due to the development of a thermal gradient between the temperature of bulk fluid and the fluid at the pipe-walls. One of the prominent works on wax deposition models (Singh *et al.*, 2000) stated that the formation of incipient thin wax- oil gel developed at beginning is responsible for the following wax precipitation and deposition process. During pipeline transportation, at lower ambient temperatures, wax precipitation is prominent in fluids adjacent to the pipewall, developing a concentration gradient in the crude oils, and the wax molecules starts to migrate from the bulk oil towards the lower temperature oil at walls. At this point, the hydrocarbons with carbon number higher than the critical carbon number begins to precipitate and migrate towards lower carbon hydrocarbons, leading to the initial development of wax networking at walls. These wax crystals being porous in nature tends

to capture enormous quantity of oil, in range 90-95 %. Due to this porous and liquid entrapment characteristics of wax crystals, a gel structure forms at the pipewalls and it forms the initial stage of wax deposition, comprises a mixture of different carbon numbers. After this gel formation stage, there would probably be the diffusion of carbon compounds towards pipewall as we discussed above. Subsequently, the diffusion of high carbon numbers continue in gel deposits and results in increased thickness of the wax-oil gel deposit. There would be decrease in the thermal gradient between bulk oil and oil-gel deposit as the diffusion continues, and it would lead to reduction in the growth of wax thickness (Sharma, Vuthaluru and Mahto, 2020). The Fig. 2 exhibits the temperature profile of the oil flow in a pipeline, where the bulk oil temperature is higher than the pipewall temperature, leading to a negative radial temperature gradient, and therefore, the molecular diffusion process leads to development of wax deposits at the wall.

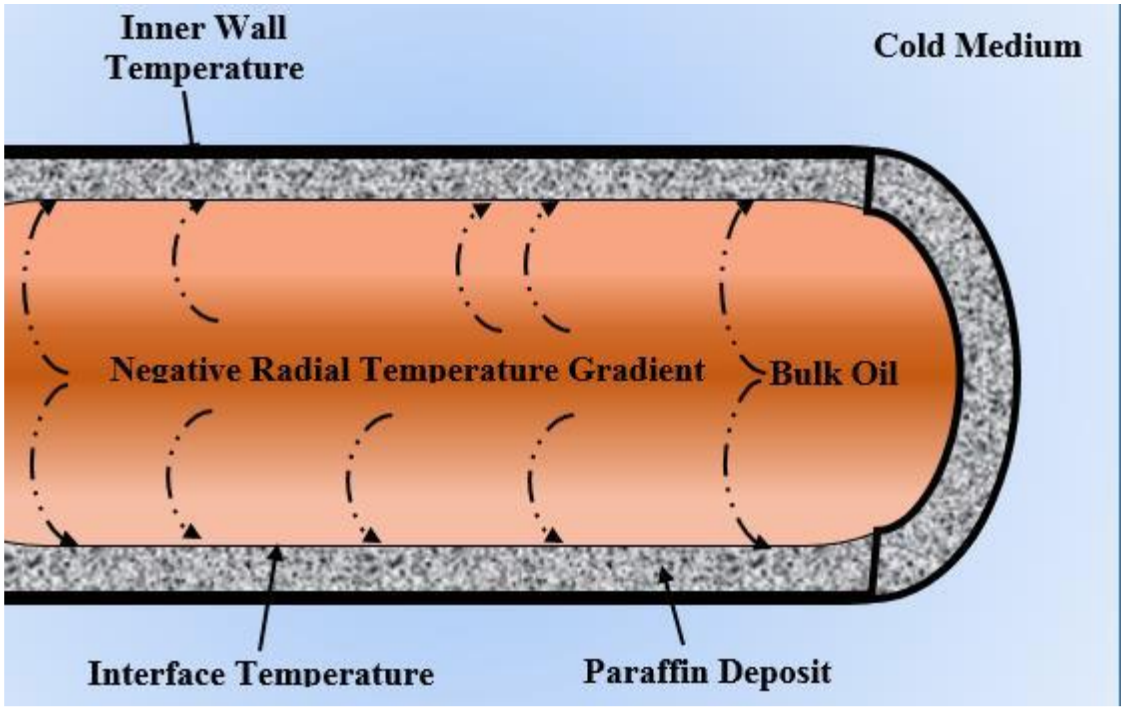

Figure 2.2. Schematic of the temperature profile of oil flow in a pipeline [Reproduced from (Dubey, 2016) with permission from ProQuest Dissertations]

Wax deposition studies have been conducted with the assistance of a large number of cold finger and flow loop experiments carried out on crude oil individually without the

addition of wax inhibitors/pour point depressants. The reason may be attributed to the complex chemistry involved between additives and crude oil in static as well as flowing conditions, where their interactions would be affected with change in operating conditions in pipeline transportation process. There are only a few comprehensive studies regarding evaluation of the efficacy of the chemical additives on crude oil, one of them was performed using maleic anhydride copolymers to investigate the wax deposition in a Caspian Sea condensate (wax content = 9.5 wt.%) under different temperature differentials between bulk oil and pipeline (Dubey, 2016) .

This thesis work would gradually focus on this aspect where the chemical additives synthesized in the laboratory would be tested on crude oil firstly using industry standard tests as well as cold finger tests would be performed for some additives in order to develop a good understanding of inhibitor performance and developing a robust flow improver suitable for efficient pipeline transportation of crude oil.

2.13 Conclusions

1. Wax prevention is essential for flow assurance of waxy crude oils and can save billions of dollars for the project, which would otherwise be spent on project non-productive time by resulting issues such as wax removal, lesser hydrocarbon throughput, pipeline shutdown, well shutdown and host of other issues including safety hazards.
2. A lot of experimental work has been performed on conventional PPDs on waxy crude oils, and there is a need for improvement in their properties to develop more robust PPDs. To address this issue, the development of nanocomposite PPDs seems to be a promising class of chemical additives.
3. There is a need of PPDs which are cost effective, low dosage, better dispersion characteristics in solvents, better long term stability and improved performance under flowing and static conditions.
4. Nanoparticles have exhibited tremendous applications in petroleum industry, and thus, there potential should be analyzed in the development of chemical additives for flow improvement for pipeline transportation of crude oils.
5. Graphenes have excellent surface and chemical properties, and its potential could be utilized to develop introductory studies on nanocomposite pour point depressants.

6. Literatures suggest the role of asphaltenes in affecting the wax deposition process during pipeline transportation, this should be emphasized while designing and selection of PPDs for crude oils.
7. There is lack of universal agreement over uniform working mechanism of PPDs over wax crystals, and there is a need for designing better experimental strategies using chemical additives to define their exact working mechanism.
8. Pipeline operating conditions affect the efficacy of the pour point depressants for waxy crude oils and should be incorporated to the list of tests for selection of the PPDs for any particular crude oil.
9. The simulation of wax deposition and gelation computationally using computational fluid dynamics would help to further develop our understanding from experimental findings and previous literatures.

Chapter 3
Methodology

3.1 Introduction

This chapter covers the experimental details for all the experimental research works performed in this thesis. The experimental studies are carved into three major parts according to synthesis and application of three different type of nanocomposite additives tested on different Indian crude oils. Most of the experimental procedures and operating conditions of the analytical equipment's used in all the experimental works are comprehensively mentioned in this chapter and any specific changes in the testing parameters for individual synthesized products not mentioned in this chapter would be listed in the respective chapters discussed subsequently, detailing the results obtained upon application of the synthesized additives on crude oils. The study 1, study 2 and study 3 corresponds to the research performed for synthesis, characterization and evaluation of PMMA-GO nanocomposite, P(2-EHA)-GO nanocomposite and PPDR-GO nanocomposite respectively. The methodology for the simulation work mentioned in Chapter 7 would be discussed there itself and is not discussed in this chapter.

3.2 Procurement of materials

3.2.1 Materials used for Study 1 (PMMA-GO nanocomposite)

Crude oil sample used under the present study was collected from western Indian oilfields. Graphite powder (G), methyl methacrylate, benzoyl peroxide, n-heptane was purchased from Loba Chemie Pvt. Ltd. (Mumbai, India). Potassium permanganate, sulphuric acid (98% concentrated), hydrochloric acid (35.4% concentrated), methanol, acetone, 1,4 dioxane, sodium chloride, hydrogen peroxide (30%) and acrylonitrile (99%) were purchased from Rankem Avantor Performance Materials (New Delhi, India), n-decane, toluene, sodium dodecyl sulfate and silica from Merck Specialities Pvt. Ltd. (Mumbai, India), acetonitrile, chloroform and n-pentane were purchased from Rankem RFCL limited (New Delhi, India), n-hexane was purchased from Nice Chemicals Pvt Ltd. (Kerala, India). Distilled water used in the research work was collected from Merck Millipore setup. The commercial PPD Phoenix was obtained from a chemical supplier.

3.2.2 Materials used for Study 2 (P(2-EHA)-GO nanocomposite)

The waxy crude oil sample for analyses was gathered from an Indian oilfield. Graphite powder (G), n-heptane, 2-ethylhexyl acrylate (99%), isopropyl alcohol and benzoyl peroxide were procured from Loba Chemie Private Limited (Mumbai, India). Sodium chloride, hydrogen peroxide, methanol, potassium permanganate, n-pentane, acetonitrile, hydrochloric acid (35.4% conc.), 1,4-dioxane, acetone, hydrogen peroxide (30%), chloroform, and sulphuric acid (98% conc.) and acrylonitrile (99%) were procured from Rankem Avantor Performance Materials (New Delhi, India). Silica gel, n-hexane, and toluene were acquired from Merck Specialities Private Limited (Mumbai, India).

3.2.3. Materials Used for Study 3 (Ionic Liquid and PPDR-GO nanocomposite)

The waxy crude oil sample (WCO) used for testing in this research work has been obtained from a Western Indian oilfield. Chemicals used in the synthesis process and characterization of the crude oil including 1-chlorooctane (98 %) and 1-methylimidazole (98 %), were purchased from Avra Synthesis Pvt. Ltd. While ethyl acetate, acrylonitrile (99 %), 1,4-dioxan, sulphuric acid (98 %), hydrochloric acid (35.4 %), potassium permanganate, n-pentane, acetonitrile (99 %), hydrogen peroxide (30 %), sodium chloride, methanol and acetone were acquired from Rankem Avantor Performance Materials (New Delhi, India). N-hexane, toluene and silica gel were purchased from Merck Specialites Pvt. Ltd (Mumbai, India). N-heptane and graphite powder were obtained from Loba Chemie Pvt. Ltd (Mumbai, India). The distilled water was collected regularly from the Merck Millipore Setup.

3.3 Determination of physio-chemical properties of crude oils

3.3.1 Basic Sediment & Water determination

Determination of water and sediments content in crude oil was performed with the help of Dean and Stark setup using ASTM D95-13e1 method. A mixture of 100 mL of toluene and crude oil (1:1) was heated gradually in flask attached with Dean and Stark apparatus (ASTM D95-13e1, 2013). The vapor was collected in receiver, the amount of water collected was calculated from subtracting the amount of toluene used from the 100 mL mixture. The crude oils collected in all the three studies 1, 2 and 3 are non-contaminated and were collected directly from Group Gathering Stations and wellheads at the surface.

3.3.2 Pour point determination

Pour point of crude oil was determined as per standard ASTM D97-17a method (ASTM D97-17a, 2017). The crude oil was preheated to create fluidity and transferred in a test tube with cork and thermometer arrangement which was placed in pour point apparatus, in which the tube was surrounded by an ice bath. The test tube was pulled out for every 3 °C change in temperature to check the movement of crude oil. The temperature at which crude oil ceases to flow is called pour point temperature.

3.3.3 Wax content determination

Modified Universal Oil Products 46-64 method was adopted for wax content determination in crude oil samples. 2 g raw crude oil is dispersed in 40 ml n-pentane and stirred for 0.5 hour on a magnetic stirrer. Add, 120 ml of acetone to the mixture and freeze the mixture for 24 hours at .−30°C. The mixture is removed from freezer after set duration and is filtered using Whatman filter paper (No.934 AH) and then washed with solvent hexane. Hexane dissolve the waxes, leaving the aromatic asphaltenes as precipitates. The hexane solution is removed and then is left to evaporate, leaving the dried solid wax, which is then weighted to calculate the percentage of wax fraction in crude oil (Burger, Perkins and Striegler, 1981; Coto *et al.*, 2008; Deka *et al.*, 2018).

3.3.4 Density and API gravity determination of crude oils

Density of crude oil was determined using Bingham pycnometer using distilled water as the reference liquid with the standard method ASTM D1480-15 and API gravity was calculated based on the equations (1)-(3) (ASTM D1480-15, 2010).

$$\text{Specific gravity [S. G (@60℃)]} = \left(\frac{\text{Density of crude oil (@60℃)}}{\text{Density of water}}\right) \text{……..} \quad (3.1)$$

Specific gravity of crude oil at particular temperature can be related to a reference temperature specific gravity (S.G. @15℃) using the following equation:

$$\text{S. G}_{\text{T}} = \text{S. G}_{15} - [5.93 * 10^{-4} * (\text{T} - 15)] \text{……...} \quad (3.2)$$

Where $S.G_T$ = Specific gravity of crude oil at T℃

and $S.G_{15}$ = Specific gravity of crude oil at 15℃

This is an empirical equation to determine specific gravity of crude oil taken from API standards (Wright, 2014) and it remains valid for all crude oils. Based on specific gravity, the API gravity of oil sample can be calculated with the help of following equation:

$$^{0}\text{API} = \left(\frac{141.5}{\text{S.G}_{15}}\right) - 131.5 \quad \text{..... (3.3)}$$

3.3.5 Determination of Saturates, Aromatics, Resin and Asphaltene

The amount of saturates, aromatics, resins, and asphaltenes (SARA) present in the crude oil were determined using a column chromatography method as per the experimental procedures outlined by Deka et al. and others (Deka *et al.*, 2018; Sharma *et al.*, 2018; Mandal *et al.*, 2019; Sharma, Mahto and Vuthaluru, 2019). Crude oil is a mixture of hydrocarbons comprising of different components with different chemical and physical properties. The crude oil primarily consists of four main fractions namely Saturate, Aromatic, Resin, and Asphaltene (SARA). In the SARA fractionation, asphaltenes is removed firstly using hexane or heptane solvent prior to separation of crude oil into saturates, aromatics, and resins by liquid chromatography technique (Miller, 1982; Speight, 2006).

Asphaltene precipitation is performed with n-heptane (crude oil is dispersed into heptane in 1:30 w/v). This dispersion is pre-heated for 2-3 hours interval and subsequently cooled under ambient temperature conditions for 3-4 hours duration. The dispersion is filtered using a glass microfiber Whatman filter (No. 934) placed on top of Buchner Funnel attached to a glass filtration flask and vacuum pump. The filtrate collected in the funnel is termed maltene, which would be used to extract the asphaltenes by washing with toluene. The column-chromatography technique has been followed to extract the rest of SARA fractions from crude oil. A silica-gel bed (50 g) is developed in the chromatography column, which is slightly wetted with solvent heptane initially, before passing the maltene mixture through it. 100 mL of heptane is passed through the silica gel bed saturated with maltene mixture in order to elute the saturate components, and then

100 ml toluene is passed to elute the aromatics. To elute the resins, a mixture of solvents were passed through the silica gel bed in the following four sequential steps:

(1) 100 ml methanol-toluene mixture (1:1),

(2) 100 ml chloroform- methanol mixture (1:1),

(3) 100 ml chloroform and lastly,

(4) 100 ml acetonitrile.

Elutes of different components were collected in individual flasks and weighted (Jha *et al.*, 2014). This methodology has been used for SARA analysis and wax content determination by some authors (Deka *et al.*, 2018; Sharma, Mahto and Vuthaluru, 2019) The SARA analysis and the wax content analysis of every crude oil were repeated thrice, and the averaged results were reported in the results section.

3.3.6 Determination of wax appearance temperature (WAT)

The WAT of the crude oil was calculated from rheology according to the deviation observed in the Arrhenius relation between the viscosity of the crude oil sample and temperature (Paso, Silset, Sørland, Gonçalves, *et al.*, 2009; Sharma, Mahto and Vuthaluru, 2019).

3.3.7 FTIR of crude oil

FTIR analysis was performed using Perkin Elmer spectrophotometer in the range 4000 cm^{-1}- 400 cm^{-1} to identify the functional groups present in crude oil.

3.4 Synthesis procedure of chemical additives

3.4.1 Synthesis of graphene oxide

Graphene oxide was synthesized from graphite using the improved Hummers Method (Mahato et al., 2016). This method avoids the use of $NaNO_3$ in reaction scheme so as to avoid the release of toxic gases such as such as NO_2 and N_2O4 during the GO synthesis which is a major advantage of this method. Also, the residual ions (Na+ and NO_3 −) formed during synthesis and purification would get carried into the waste-water and become difficult to remove (Chen *et al.*, 2013). 1 g graphite flakes were added to a flask containing 23 mL concentrated H_2SO_4 and the mixture was stirred at low temperature (~5°C) for 30 min to create a homogeneous system. Subsequently 3 g

$KMnO_4$ was introduced into the mixture gradually under continuous stirring. The system was then heated at 50 °C for 2 h. Then, 70 mL distilled water was added moderately and the temperature of the system was then raised to 98 °C for 20 min. Again, 70 mL of distilled water and 5 mL H_2O_2 (30%) was added in it. Finally, the reaction mixture was washed with distilled water repeatedly till pH reaches to around 6.5–6.99. The three-dimensional framework of laboratory synthesized GO is depicted in Fig. 3.1. The color of the supernatant from the GO washing changes gradually from dark yellow thick gel type (Fig 3.2(a)) to pale yellow lesser viscous fluid (Fig 3.2(b)), and finally turns into transparent liquid as the pH approached near 7. The pH of the GO supernatant gradually increases and approaches 7 with subsequent washing, indicating removal of the excess unreacted acidic content from the final GO product.

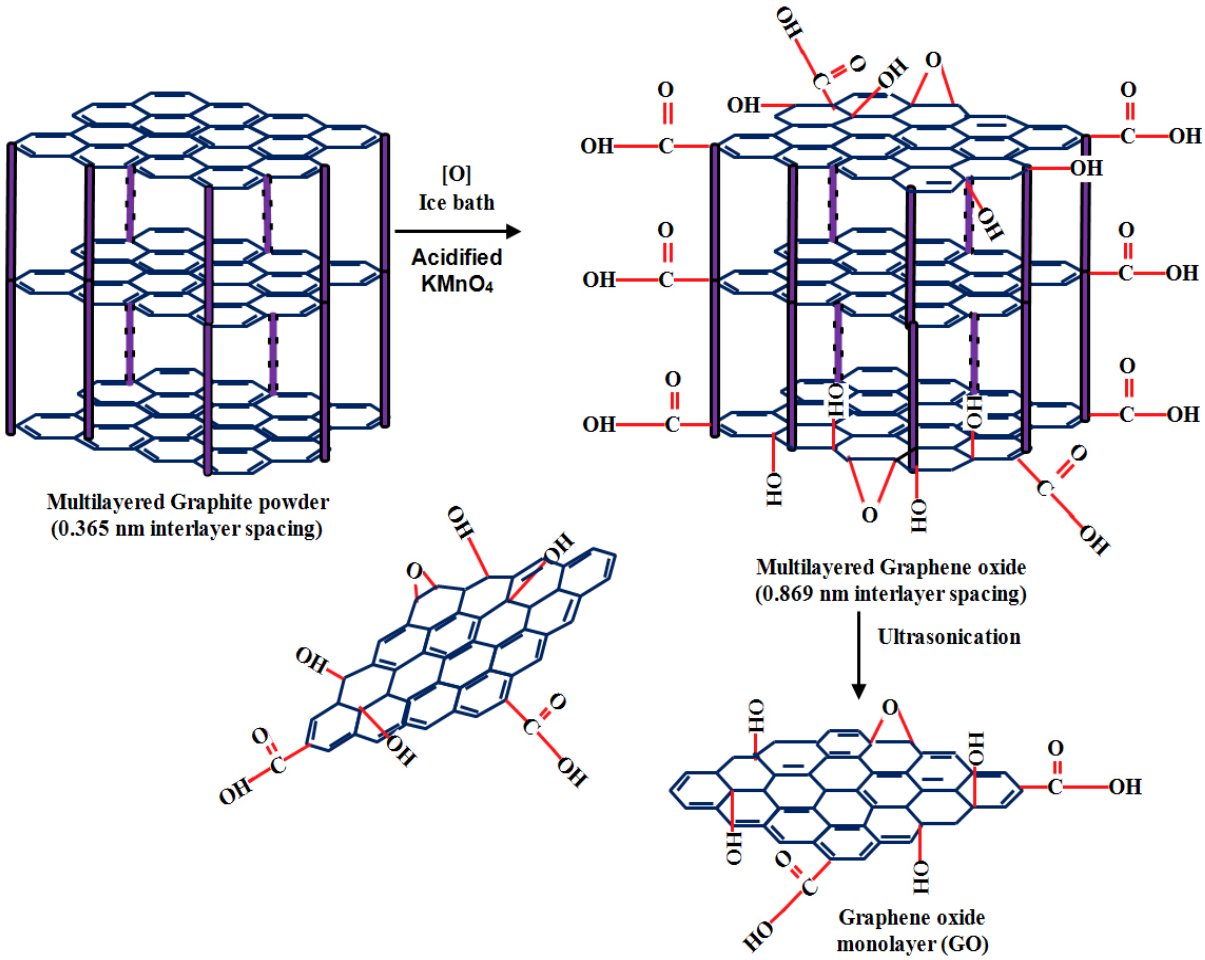

Figure 3.1. Schematic three-dimensional diagram of synthesized multilayered graphene oxide (GO). Reproduced from (Sharma, Mahto and Vuthaluru, 2019) **with permission from Elsevier.**

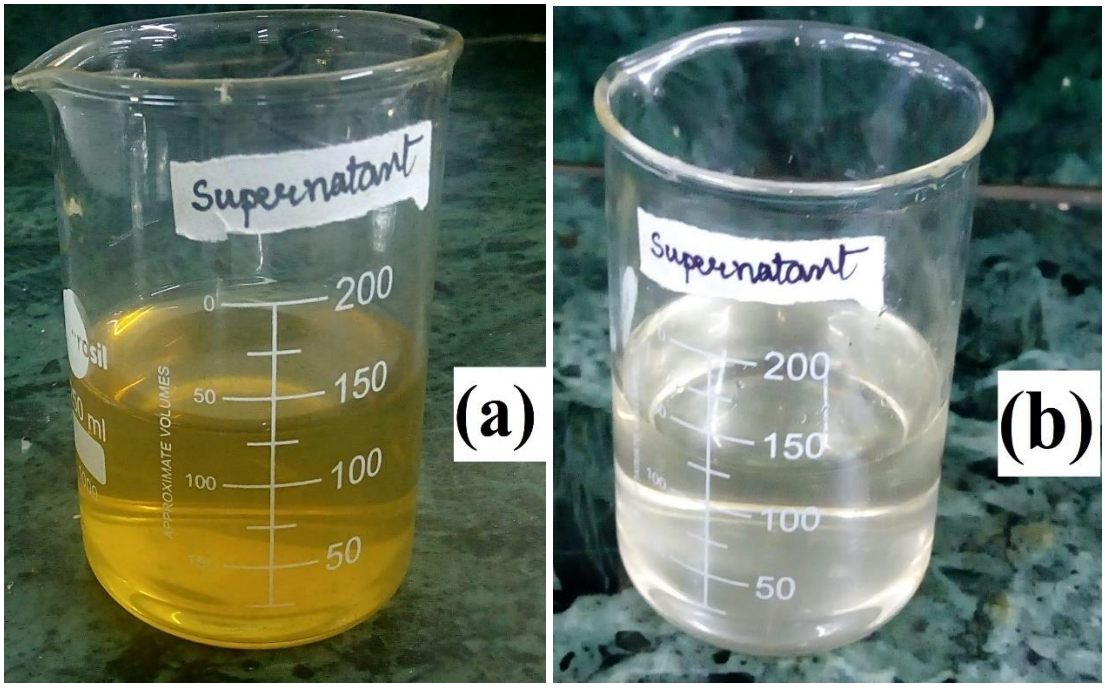

Figure 3.2. GO supernatant during its washing process, (a) dark yellow color at initial washing stages when its acidic (b) near transparent solution at later stages when its pH approaches near pH=7

3.4.2 Synthesis of vinyl graphene oxide (VGO)

Introduction of vinyl group on GO is necessary for it to participate in polymerization and formation of nanocomposite PPD. Vinyl graphene oxide was synthesized using Pinners reaction and its reaction mechanism is shown in Fig. 3.3 and its schematic three dimensional structure is shown in Fig. 3.4. Functionalization of GO through Pinners reaction facilitates the attachment of vinyl moieties to the GO platelets and thereby improves its solubility (Mcgrail, Rodier and Pentzer, 2014). Alcohol moieties of the platelets react with the vinylic nitrile group of the acrylonitrile to yield VGO. Firstly, in a 100 mL flask, GO (1.46 g) was introduced into a 50 mL water/1,4-dioxan solvent mixture (3:1 v/v proportion) and suspension was acidified with 0.5M HCl to create acidic medium for reaction to propagate. The suspension was then sonicated for 1 min for effective dispersion of GO. Subsequently acrylonitrile monomer (50 mL) was added under vigorous stirring to the suspension of GO and the stirring was continued for 3 h at room temperature leading to an esterification reaction. The reaction was terminated by addition of 5 wt. % NaCl that helps in accumulation of particles at the water/organic

interface and the resulting particle layer was separated by filtration and washed continuously with 9:1 distilled water-dioxane mixture to remove traces of acidity and unreacted acrylonitrile monomers. Acrylonitrile monomers reacted with graphene oxide sheets in an acidic environment to form an imino-substituted GO sheets which further hydrolysed to complete the esterification reaction and a vinyl group substituted GO product was obtained. The catalyst HCl gets separated after the completion of this process with release of a small amount of ammonia gas [17].

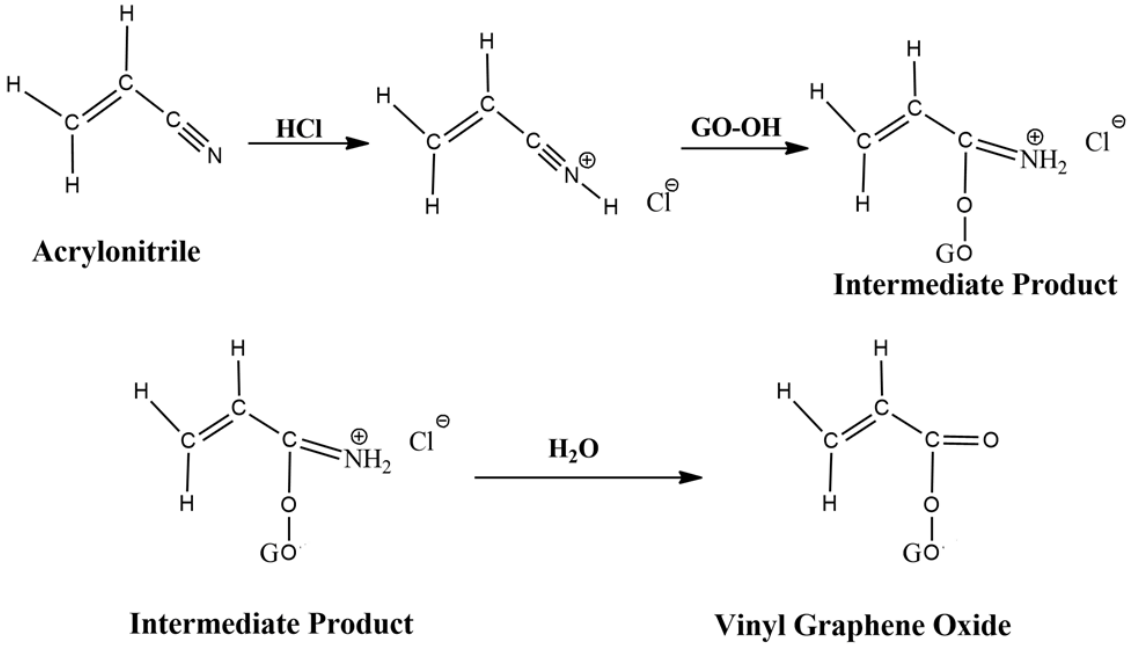

Figure 3.3. Schematic diagram of chemical reaction representing the formation of vinyl graphene oxide (VGO). Reproduced from (Sharma, Mahto and Vuthaluru, 2019) **with permission from Elsevier.**

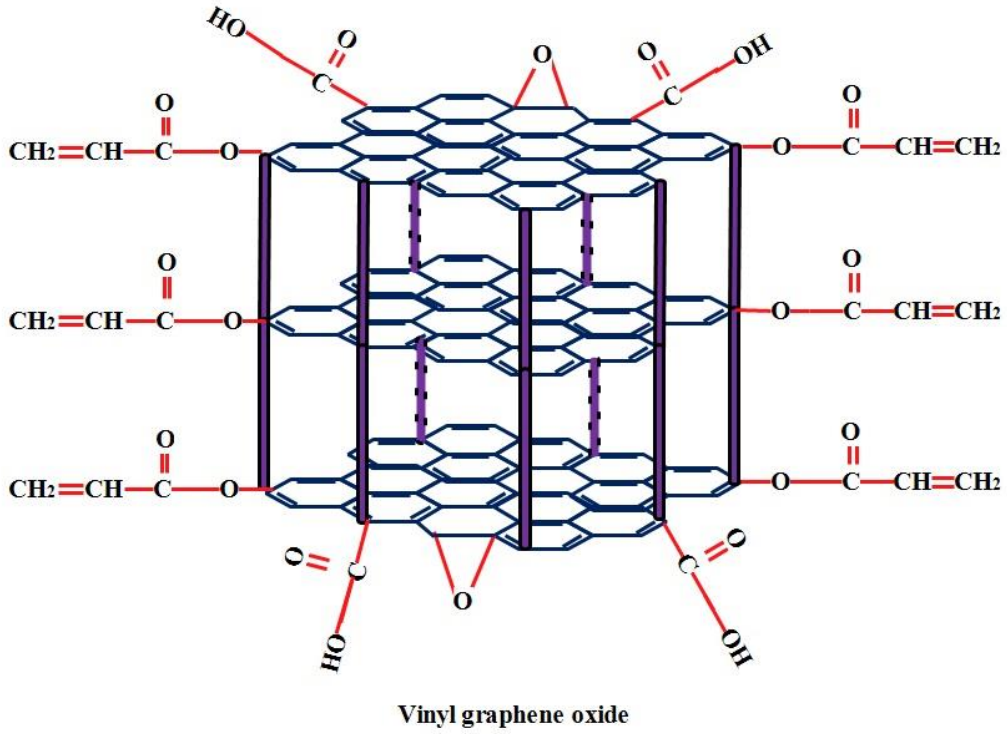

Figure 3.4. Schematic three-dimensional diagram of synthesized Vinyl Graphene Oxide (VGO). Reproduced from (Sharma, Mahto and Vuthaluru, 2019) **with permission from Elsevier.**

3.4.3 Synthesis of polymer nanocomposite PMMA-GO

Different amounts of VGO (0.05 g & 0.1 g) were added to 15 mL toluene and the suspension was sonicated for 50 min at low temperature (~5°C) in a nitrogen environment to create a good GO dispersion in toluene solution. MMA monomers (dispersed in toluene, 40 wt. %) were added to the prepared VGO mixture to form 0.5%, 1% GO to PMMA mixtures. The mixture was then sonicated at ~5 °C under nitrogen environment to create uniform dispersed solution. The mixture was then heated in a 100 mL flask and Benzoyl Peroxide initiator was added (0.03 g in 1 mL toluene) to the dispersed solution as the temperature reaches 75 °C and the temperature was maintained for 30 min, afterwards, the temperature was decreased to 55 °C and was maintained for another 6 h. Precipitation was initiated by addition of 50 mL methanol to the reaction mixture, and the precipitated product obtained was PMMA-GO nanocomposite. The resulting product was dried at 65 °C in a petri dish to get thin film of PMMA-GO.

3.4.4 Synthesis of polymer nanocomposite P(2-EHA)-GO

Synthesis of Polymerizable Vinyl Graphene Oxide. The Pinners reaction was used to synthesize vinyl graphene oxide (VGO) following the reaction scheme of Sharma et al. and others (Mcgrail, Rodier and Pentzer, 2014; Sharma, Mahto and Vuthaluru, 2019). GO (1.46 g) was dispersed within a 50 mL solvent mixture of water/1,4-dioxane (3:1 v/v), and then, a 0.5 M HCl solution was introduced to the mixture, which acted as a catalyst. The esterification reaction was performed by adding 50 mL of acrylonitrile monomers to the GO dispersed mixture, which was subsequently washed with a solvent mixture of water/dioxane (9:1 v/v). Acrylonitrile monomers reacted with hydroxyl groups of GO sheets to develop an imino-substituted GO intermediate product, which subsequently hydrolyzed, thereby concluding the esterification reaction to result in vinyl groups attached to GO (Sharma, Mahto and Vuthaluru, 2019).

3.4.5 Synthesis of ionic liquid- graphene oxide nanocomposite

The synthesis procedure of the nanocomposite PPDR-GO involves simultaneous synthesis of an ionic liquid chemical additive [(OMIM) Cl]. The procedures are detailed as follows.

3.4.5.1 Synthesis of ionic liquid 1-octyl 3-methylimidazolium chloride [(OMIM) Cl]

11.9 g 1-chloro-octane is mixed with 8.2 g 1-methylimidazle in a three neck round bottom flask with reflux condenser under nitrogen atmosphere and is kept at 70^{o}C for 48 hours. The completion of the reaction results in the formation of two phases. The top layer is considered the unreacted material and is removed by decantation, followed by washing with ethyl actetate thrice. The remaining solvent was evaporated by heating at 70℃ and further the product is vacuum distilled in vacuum oven at 80℃. The final product obtained is ionic liquid [(OMIM) Cl]. This synthesized ionic liquid would be abbreviated as IL throughout this research work, for the sake of simplicity during repeated mentioning of this product.

3.4.5.2 Synthesis of 1-octyl 3-methylimidazolium chloride-graphene oxide nanocomposite PPDR-GO

The final reaction step comprises of in-situ polymerization reaction where the synthesized ionic liquid IL was polymerized with prepared vinyl graphene oxide to form the nanocomposites poly(1-octyl 3-methyl imidazolium chloride)-graphene oxide {P[(OMIM) Cl]-1% GO}(Sharma et al., 2020) .

The ionic liquid [(OMIM) Cl] was dispersed in toluene 40 wt.% and mixed with 0.05 g, 0.1 g, 1.5 g and 2 g VGO (dispersed in 20 mL toluene) individually. The mixture was subsequently sonicated at low temperatures near 5℃ under a nitrogen environment for proper homogenization, afterwards heated to 75 ℃ and an initiator benzyl peroxide was added (0.05 g in 2 mL toluene) for polymerization. The mixture temperature was maintained at 75℃ for half an hour, subsequently decreased to 55℃ for the next 6 hours to complete the polymerization reaction. The mixture resulting from polymerization was then washed with 50 mL methanol, and the precipitate formed was collected and further vacuum dried to obtain resultant product P[(OMIM) Cl]- 0.5 % GO, P[(OMIM) Cl]- 1 % GO, P[(OMIM) Cl]- 1.5 % GO, P[(OMIM) Cl]- 2 % GO. These nanocomposites would be abbreviated as PIL – 0.5 % GO, PIL - 1 % GO, PIL – 1.5 % GO, PIL - 2 % GO respectively throughout this research work for the sake of simplicity while repeated usage of these terms.

3.4.6 Synthesis of poly(n-methyl butylacrylate)-graphene oxide nanocomposites

n-methyl butylacrylate (nMBA monomers) (dispersed in toluene, 40 wt.%) were added to the prepared VGO mixture to form 0.5 wt% , 1 wt% GO to nMBA. The mixture was then sonicated at ~5 °C under nitrogen environment to create uniform dispersed solution. The mixture was then heated in a 100 mL flask and BOP initiator was added (0.03g in 1 mL toluene) to the dispersed solution as the temperature reaches 75 °C and is maintained for half an hour, afterwards the temperature is reduced to 55°C and is maintained for another 6 hour. Precipitation is done by addition of 50 mL methanol to the reaction mixture, and the precipitated product obtained is PnMBA-GO nanocomposite. The resulting product is dried at 75°C in a petri dish to get PnMBA-GO.

3.5 Characterization methodology of the synthesized additives

3.5.1 FTIR spectroscopy

FTIR of the graphite derivatives and polymeric samples was performed using Perkin Elmer Spectrum Two FT-IR spectrometer (US), (wavenumber range 4000–400 cm^{-1}) to identify the functional groups present in them.

3.5.2 Raman Spectroscopy

Raman Spectroscopy of graphite derivatives was done using LabRAM HR Evolution Raman microscopes (Horiba Jobin Yvon) with a laser wavelength of 632.8 nm and power of 17mw.

In the case of study involving the ionic liquid additive and its nanocomposite, Raman spectroscopy of the graphite, GO, VGO and PPDR-1%GO was performed using LABRAM HR Evolution Raman microscope (HORIBA Jobin Yvon) using laser power laser wavelength 532 nm and 17 mW.

3.5.3 ^{1}H NMR spectroscopy

Solution-state ^{1}H NMR spectra of the additives IL and PIL-1% GO was acquired with a solution-state NMR Spectrometer (Make: JEOL, Model: ECZ 500, Frequency: 500 MHz). The additive samples were initially dispersed in solvent $CDCl_3$ for preparation of NMR spectroscopy.

3.5.4 XRD spectroscopy

The X-ray diffraction (XRD) analyses of graphite, GO, VGO, and nanocomposites were performed on a PANalytical X'pert powder X-ray diffractometer, employing Cu Kα radiation (λ = 1.542 Å) and the range of Braggs angle (2θ) was 5°-80°.

3.5.5 UV-visible spectroscopy

UV-visible spectroscopy of graphite derivatives dissolved in respective solvents was performed using UV-Vis-NIR spectrophotometer (Agilent Carry 5000). In the study of P(2-EHA)-GO nanocomposite, the UV-visible spectra of the graphite, VGO, and nanocomposites were acquired by sonicating them in a THF solution.

3.5.6 FE-SEM

The field emission scanning electron microscopy (FE-SEM) imaging of GO, VGO, PMMA-1% GO and P(2-EHA)-1% GO was taken with a FE-SEM Supra 55 setup (Carl Zeiss, Germany). It was done in order to gain understanding of surface morphological modification of the samples after synthesis.

3.5.7 Thermal analysis

Thermogravimetric-derivative thermogravimetric analyses (TGA-DTG) of GO and nanocomposites were performed using a NETZSCH STA 449 F3 Jupiter model (made in Germany), and the software used was Proteus. The analyses were carried out with approximately 15 mg of samples with an operating temperature range of 24°C - 600 °C in the presence of a nitrogen atmosphere with an operating pressure of 9.81 bar and heating rate of 10 °C/min.

3.6 Evaluation techniques for the chemical additives on the crude oil

Pour point, viscosity, gelation point measurements and microscopic imaging of nanocomposite beneficiated crude oil

For the purpose of measuring pour point of treated crude oil, the chemical additives were either doped in the crude oil directly or were pre-dissolved 10 wt.% in xylene (to improve their fluidity). Similar procedure was followed for the measurement of rheological properties of treated crude oil.

3.6.1 Operating conditions for Study 1

Rheological measurements of virgin crude oil and treated crude oil were performed at any temperatures between 10℃ - 50℃ at their optimum concentration (at which the pour point is the lowest) using Bohlin Gemini 2 rheometer (Malvern Instruments, UK) with various chemical additives. A standardized rheology protocol was adopted to explicitly measure the apparent viscosity of the untreated and treated crude oil. The rheometer was operated under controlled shear rate conditions. A concentric cylindrical geometry was employed for the rheological measurements and the crude oil samples to be tested were placed in a sealed container. The crude oil was loaded into the cylindrical geometry and was pre-sheared within the shear rate range (0-500 s^{-1}) consisting of 20 step intervals of 20 s duration each. The rheological plots were then recorded with the shear rate being increased during the measurements in range 0-500 s^{-1} at 10 step intervals of 20s duration each and the apparent viscosity values were calculated. The measurements were repeated twice and the results obtained were averaged to improve the reliability and accuracy of obtained results (Paso, 2014).

The gelation points of the virgin and additive treated crude oil were determined by using rheometric method (Yang, Paso, *et al.*, 2015). Considering the experimental temperature range of 70-10°C, firstly the crude oil sample was maintained at 70°C for 5 min and cooled to 60°C at a cooling rate of 10°C/min. Subsequently, the oil sample was cooled at rate 0.5°C/min and sheared under a controlled shear stress of 0.1 Pa. The change in shear rate with drop in temperature is observed. Plot of shear rate versus experimental temperature indicates a distinctive point on the curves that show the clear break in the pattern of shear rate on decreasing temperature, which is denoted as the gelation temperature.

The wax structures of the crude oil samples with and without addition of additives were analyzed under a polarized microscope OLYMPUS BX51-P. The WCO samples were pre-heated to 60℃ for 30 minutes to dissolve the wax crystals and create fluidity, and subsequently a drop of the crude oil sample was placed carefully on the glass microslide and enveloped by coverslip. The measurements were taken at ambient temperatures (30℃).

3.6.2 Operating conditions for Study 2

Additive-beneficiated crude oil samples were tested for their pour points where the additive were mixed in 10 wt. % xylene prior to doping it in crude oil to create improved fluidity of viscous polymeric nanocomposites. The beneficiation effect caused due to xylene has been adjusted from the pour point results (as it caused an average reduction of 2°C in the pour point of crude oil as obtained from the blank pour point measurements of virgin crude oil (VC) doped with xylene itself). The rheological characteristics of crude oil doped with PPDs (diluted in 10 wt. % xylene) were measured on a rheometer Bohlin Gemini 2 (Malvern instruments, UK). The measurements were performed at every 10 °C interval in the temperature range of 10°C - 40°C, and all of the chemical additives were doped at their optimized pour point concentrations for testing. Rheological experiments (viscosity-shear rate) were performed on the basis of a common rheology protocol as outlined here. The crude oil samples were initially preheated to create fluidity and then were loaded into a 10 mL concentric cylindrical vessel that was then sealed for performing the experiment. The rheometer was employed under controlled shear rate conditions (0-100 s^{-1}), and the viscosity measurements were taken in 10 step intervals, with an interval duration of 20 s. Rheological plots of apparent viscosities against the shear rate were obtained. The experiments were performed thrice, and the percentage error bar for the measurements was reported.

The determination of the gelation point of crude oil samples was performed using the following rheometric method. Temperature sweep tests under oscillatory mode for the PPD-beneficiated samples of crude oil were performed to study the viscoelastic parameters G' (storage modulus or elastic modulus) and G (loss modulus or viscous modulus) under decreasing temperatures. The samples were first heated to 60 °C and maintained at this temperature for 10 min, and the samples were then cooled at a rate 0.5 °C/min down to 10°C. The oscillation frequency of measurements was kept constant at 1Hz. An extremely low shear strain amplitude of 0.0005 ensured that the wax crystal network structure remained undamaged by the applied shear rate during cooling (Yang, Li and Wang, 2013).

In order to visualize the effects of nanocomposite PPDs on the wax network structure of crude oil, a polarized optical microscopy study of the PPD-treated crude oil was carried out using an Olympus BX51P microscope. For analyses, PPDs were doped

in a crude oil sample at their optimum concentrations (at which the pour point of the sample is lowest, which would be evaluated based on pour point tests), and all of the analyses were performed at ambient temperature (29 ℃).

3.6.3 Operating conditions for Study 3

The rheological behaviour of WCO doped with additives was determined on a rheometer (Bohlin Gemini 2, Malvern Instruments, UK). The WCO samples were tested at temperatures 30℃, 40℃ and 50℃ and their apparent viscosities were recorded against shear rate. A standard rheology protocol was followed to perform the experiments and record the results, and the protocol is outlined in the following discussion.

Initial pre-heating of the WCO samples to 60℃ for 30 minutes was performed in order to dissolve the wax crystals substantially. The optimized pour point concentrations (based on the lowest pour point) of the chemical additives were doped in crude oil for testing. 10 mL of the WCO samples were charged and sealed into a concentric cylindrical vessel for experimentation (cup and bob setup). A controlled shear rate mode (40−100 s^{-1}) of the rheometer was selected, and the readings of viscosities were recorded in 50 step intervals, and the average interval duration was 3 s to understand the viscosity changes at smaller intervals. The experimentation would produce rheological curve of apparent viscosities versus the shear rates.

The gelation points of the WCO and the additive-treated WCO samples were determined using the oscillatory mode of rheometer (model: Bohlin Gemini 2, Malvern Instruments, UK), using temperature sweep tests. The aim of this experiment is to determine the variation in viscoelastic parameters G' (storage modulus/elastic modulus) as well as G" (loss modulus/viscous modulus) against a range of temperatures (60 ℃ - 10 ℃). Temperatures were kept in range (60 ℃ -10 ℃). Samples were pre-heated to high temperature (60℃) for 25 - 30 minutes to dissolve the wax crystals and create fluidity. Samples were then cooled down to 10℃ at a cooling rate of 0.5℃/min. A fixed oscillation frequency of 1 Hz was kept in the experimentation and a small strain amplitude of 0.0005 ensures a minimal shearing effect on the wax structure in crude oil during experimentation (Sharma *et al.*, 2019). For the experiment, the optimum concentrations (based on the lowest pour point recorded) of the additives were selected for doping in WCO.

The wax structural morphology of the crude oil samples with and without addition of additives were analyzed under a polarized microscope OLYMPUS BX51-P. The WCO

samples were pre-heated to 60℃ for 30 minutes to dissolve the wax crystals and create fluidity, and subsequently a drop of the WCO sample was placed carefully on the glass microslide and enveloped by coverslip. The optimized concentrations of the additives were used for the experiment. The samples were then tested using polarized light microscope under ambient temperature conditions (25℃), while the sample demonstrating the better beneficiation was observed at different temperatures (15℃, 25℃ and 35℃) in order to understand the transition of wax morphology with change in temperatures.

Chapter 4

Evaluation of poly(methyl methacrylate) - graphene oxide nanocomposite as novel pour point depressant

4.1 Introduction

Poly(methyl methacrylate)-Graphene oxide (PMMA-GO) polymer nanocomposite reported in this thesis chapter is a laboratory synthesized material using in situ free radical polymerization technique.

Polymers are extensively used in the modern world due to its low cost of manufacturing, rendering immense use in oilfield applications. One of the major uses of the polymer is development of polymeric additives for use in oilfield operations and transportation purposes. Their interaction with crude oil involves surface adsorption, nucleation and co-crystallization mechanisms, thereby altering the wax crystal growth and morphology. The alkyl acrylate based PPDs have been reported previously to improve the pour point of the crude oil significantly (Kazantsev *et al.*, 2021). This work has focused to improve the performance of the acrylate based PPD through the formation of acylate based graphene polymer nanocomposites Other considerable areas to improve in PMMA is its low thermal and mechanical stability (Tiwari *et al.*, 2017). Thermal and mechanical stability of polymer PMMA could be improved by addition of nanoparticles to maintain the beneficiation in flow properties of PPD treated crude oil. During pipeline transportation, degradation in thermal properties of PPDs would result in inferior beneficiation effect in crude oil. Mechanical stability of nanocomposite indicates the improvement in viscoelastic properties with increase in temperature such as storage modulus and loss modulus which are related to gelation temperature determination of crude oil samples. As determination of gelation temperature is essential for pipeline restart flow studies, so mechanical property enhancement by addition of nanoparticle to the polymer matrix is a positive factor in flow assurance studies. Formation of PMMA-GO polymer nanocomposite improves these imperfections of PMMA and as a PPD yields significantly improved performance highlighting its usefulness for transportation purposes**.** Current work aims to develop and investigate the effectiveness of laboratory synthesized polymer

nanocomposite PMMA-GO in improving the flow ability of Indian waxy crude oil. (Sharma, Mahto and Vuthaluru, 2019). Nanocomposite is subjected to several analytical techniques and its results are discussed including the comparison of their effectiveness in improving pour point depression effect and rheological properties with a commercially available PPD including long term application of synthesized nanocomposite[1]

---

[1] ***This chapter is a slightly modified version of my research publication titled "Synthesis of PMMA/modified graphene oxide nanocomposite pour point depressant and its effect on the flow properties of Indian waxy crude oil" published in Fuel (2019), 235, 1245-1259 and it has been reproduced here with the permission of copyright holder.***

4.2 Characterization results of crude oil

4.2.1 Determination of physico-chemical properties

The physico-chemical properties of the crude oil are listed in Table 4.1. The crude oil sample is medium heavy as its API gravity lies in the range 22.3–31.1. Amount of waxes in the crude oil studied was 14 wt. % which indicates the waxy nature of crude oil. The wax content of the crude oil studied was determined following modified UOP 46-64 method, which was reported by several researchers (Burger, Perkins and Striegler, 1981; Coto *et al.*, 2008; Deka *et al.*, 2018). Pour point of the crude oil obtained was very high which might be attributed to the high amount of wax present in it. Emulsified water in the crude oil appeared to be about 10 vol. % as obtained from Dean & Stark method using toluene as solvent carrier liquid (ASTM D 95-13, 2014). Presence of emulsified water can decrease the performance efficiency of polymeric additives on application in crude oil and may lead to deviated results in the crude oil characteristic properties determination. There lies the importance of removing water from crude oil before performing any experiments. Fraction of major components present in crude oil as obtained from SARA analysis is shown in Table 4.2. Crude oil is primarily rich in saturates with moderate amount of aromatic and resin content, while asphaltene content is found to be low in crude oil indicating lesser chance of asphaltic deposition. Resin-asphaltene ratio being higher indicates the presence of sufficient amount of resins to prevent asphaltenes from precipitation. Asphaltene stability can be indicated by resin is to asphaltene ratio based on the theory that resins tend to surround the asphaltene and thus preventing their deposition. Resins are known to decrease the intermolecular π-π and hydrogen bonding capabilities among asphaltene monomers, and thus prevents their aggregation behaviour (Bardon *et al.*, 1996).

Table 4.1. Physico-chemical properties of untreated Indian crude oil

Parameters	Method	Observed Values
Water content (vol. %)	ASTM D95-13e1	10
Pour point (°C)	ASTM D97-17a	38
Specific Gravity (@15°C)	ASTM D1480-15	0.885
API gravity (°)	ASTM D1480-15	28.387
Wax content (wt. %)	Modified UOP 46-64	14
WAT (°C)	Viscosity-Temperature	53

Table 4.2 SARA analysis of crude oil (in wt. %)

Saturate	Asphaltene	Aromatic	Resin	Resin-Asphaltene
66	1.5	12	15.5	10.33

When temperature of crude oil falls below wax appearance temperature (WAT), wax molecules starts to precipitate out from crude oil. WAT determination helps in identification of temperatures below which the wax precipitation would start, understanding the possible changes in crude oil rheological behaviour, and most importantly in wax prevention and deposition strategies.

4.2.2 WAT determination

Apparent viscosity values obtained from the rheometric measurements at range of experimental temperatures are utilized to calculate the WAT of crude oil and the methodology followed for determination is based on the Arrhenius relation of viscosity measurement. Shear rate of 10 s^{-1} is used for the measurement. The rheological measurements of the crude oil were performed at temperatures starting from 70°C and cooling it up to 1°C at a rate of 1°C/min, and the experiments are performed at constant shear rate of 10 s^{-1} (Paso, *et al.*, 2009).

Apparent viscosities of crude oil appears to be following the Arrhenius relation of viscosity measurement at higher experimental temperatures. Following non-Arrhenius methodology of WAT determination, as observed form the plot there is a noticeable deviation from Arrhenius relation starting at temperature 51.2°C (324.35 K). Afterwards a rapid nonlinear increase in viscosity at lower temperatures is observed from the Fig 4.1. Therefore, the wax appearance temperature of the crude oil analyzed is 51.2°C (Paso, *et al.*, 2009).

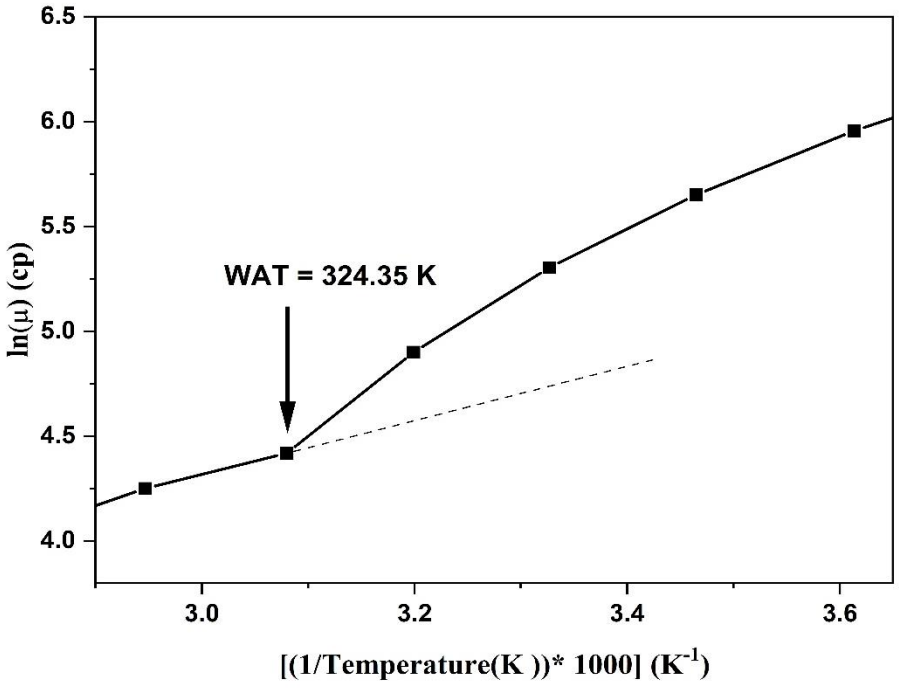

Figure 4.1. Rheometric measurements depicting non-Arrhenius methodology of calculating WAT of crude oil at constant shear rate 10 s-1 in the temperature range (274-343 K)

4.2.3 FTIR spectroscopic analysis of crude oil

The crude oil FTIR spectra shown in Fig. 4.2., exhibits peaks at 2920 cm^{-1} and 2839 cm^{-1} occurs corresponding to symmetrical and assymetrical C-H stretching vibrations in saturated hydrocarbons containing methylene groups. Peak at 1606 cm^{-1} appears owing to C=C stretching band vibrations in aromatic rings. Sharp peaks are observed at 1457 cm^{-1} and 1375 cm^{-1} corresponding to asymmetrical and symmetrical C-

H bending vibrations within a methyl group. FTIR peak at 720 cm^{-1} indicates methylene group rocking vibrations in which all the methylene groups vibrate in same phase observed in straight chain alkanes containing about 7 and higher carbon atoms indicates the wax molecules in crude oil. Peak at 809 cm^{-1} corresponds to out of plane C-H bending in polynuclear aromatics suggesting the possible presence of asphaltenes (Silverstein et al, 2014; Wilt et al., 1998).

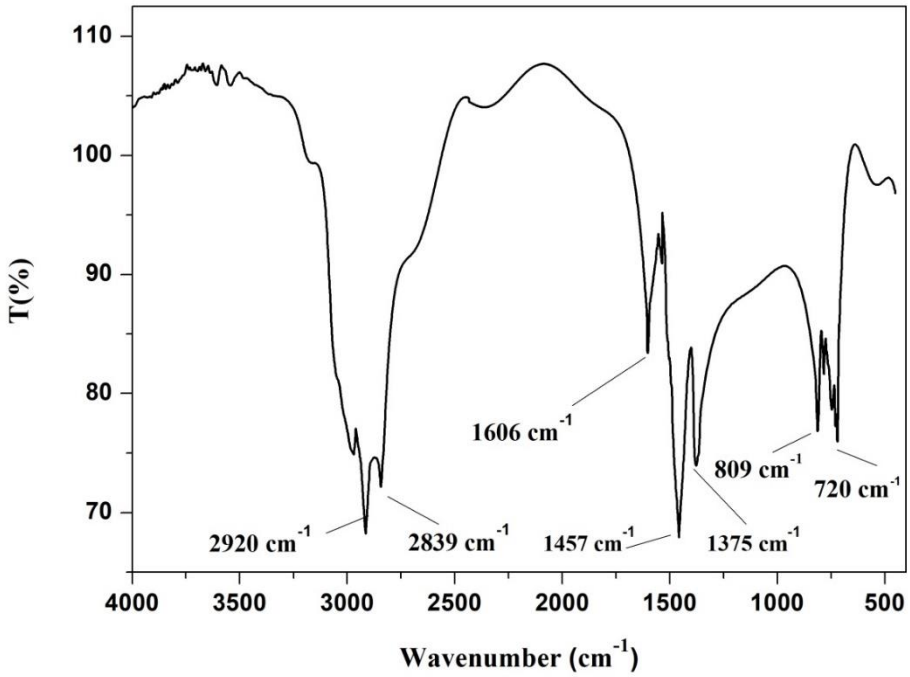

Figure 4.2. FTIR spectroscopy of virgin crude oil

4.3 Characterization details of the chemical additives

4.3.1 FTIR spectra of additives

Presence of functional groups in graphite and its derivatives is depicted in Fig. 4.3. GO displays more intense frequency bands. Frequency bands at around 1050 cm^{-1} appears due to C-O functional group stretching vibrations. Peak at around 1630 cm^{-1} is observed due to presence of unreacted graphite (-C=C-). Peak at 1724 cm^{-1} is due to carbonyl group stretching (C=O) while peak at around 1260 cm^{-1} is due to (-C-O-C-)

group stretching vibrations (Khan et al., 2015; Marcano et al., 2010.). The broad frequency band at 3398 cm^{-1} can be attributed to stretching mode of hydroxyl groups present in large amount (Paredes *et al.*, 2008). These peaks indicate presence of functional groups such as carbonyl, hydroxyl, carboxylic, and epoxy groups in laboratory synthesized GO, conforming the successful formation of GO from graphite. Observing the FTIR spectra of VGO, as a result of Pinner reaction, vinyl group is grafted on graphene oxide which is indicated by prominent intensity band near 1400 cm^{-1}, while the intensity of rest of the bands has been suppressed. The peaks at 1397 cm^{-1} and 1246 cm^{-1} corresponds to O-H bending and C-O stretching vibrations present within the carboxylic acids. The bands at 3398 cm^{-1} is decreased due to participation of hydroxyl groups in esterification reaction between GO and vinyl group of acrylonitrile monomers. Peak at around 1730 cm^{-1} is due to esterification reaction. Peak at 1626 cm^{-1} may be due to skeletal vibration band of unoxidized graphene or stretching vibration mode of O-H groups (Stankovich *et al.*, 2006). The FTIR analysis results provide evidence of the presence of different type of oxygen functionalities on graphite. Covalent bonding exists in vinyl graphene oxide (VGO), as the unsaturation (C=C) present in acrylonitrile reacts with graphene oxide to form an ester linkage in VGO and the same can be observed from FTIR analysis.

FTIR spectrum of PMMA-1% GO is depicted in Fig. 4.3. It reveals two prominent peaks at 2924 cm^{-1} and 2850 cm^{-1} owing to symmetrical and asymmetrical C-H stretching vibrations respectively. These peaks also indicate the insertion of polymer (PMMA) in between GO sheets. Peak at 1730 cm^{-1} in VGO FTIR spectrum is shifted to 1720 cm^{-1} in PMMA-1% GO which corresponds to C=O stretching (attributed to esterification reaction in VGO preparation). Other major peaks correspond to stretching vibrations due to PMMA which appears at around 2900 cm^{-1}, 1400 cm^{-1}, 1250 cm^{-1}. Hydrogen bonding is present in the nanocomposite that exist between carbonyl group (C=O) of PMMA and carboxylic group (COOH) group in vinyl graphene oxide (GO)**.** The presence of hydrogen bonding is confirmed through FTIR analysis exhibited in Fig. 4.3. Hydroxyl bond peak observed at 3398 cm^{-1} in VGO got shifted by 10 cm^{-1} towards higher wave number to 3408 cm^{-1} in PMMA-1% GO where a sharp peak is observed.

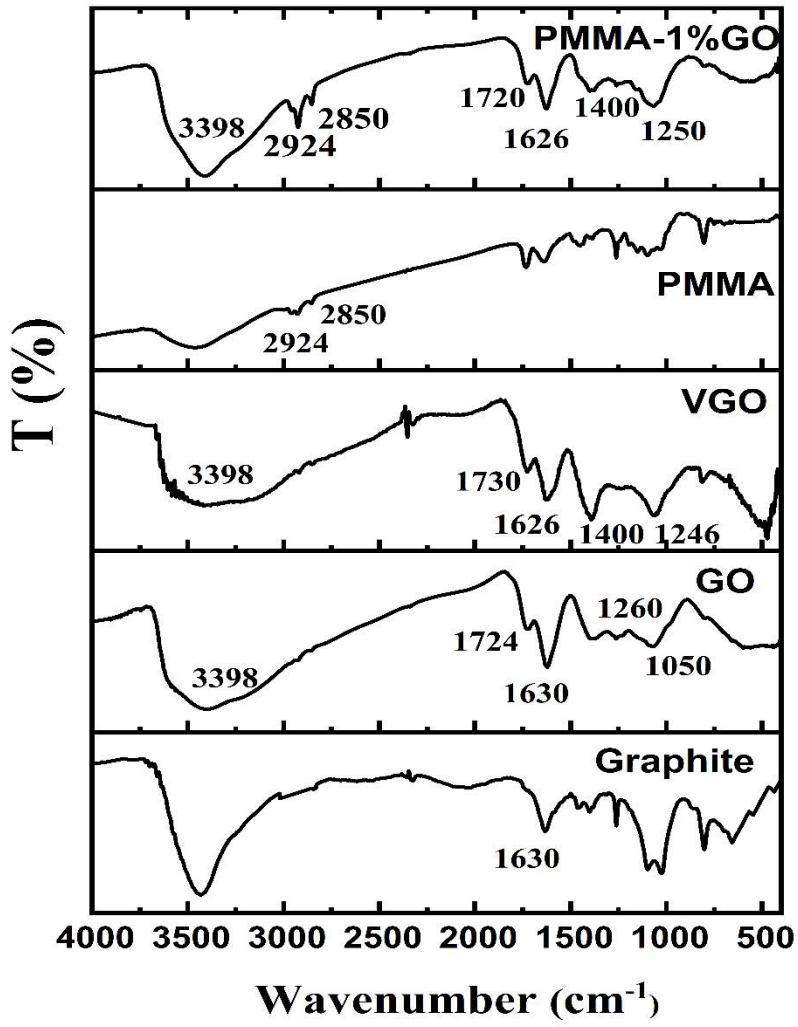

Figure 4.3. FTIR spectroscopy plot of (a) Graphite, GO & VGO, PMMA & PMMA-1% GO

4.3.2 Raman spectra of additives

To further substantiate the formation and functionalization of graphene oxide and also the formation of nanocomposite, Raman spectroscopic analysis of the samples was performed. Raman spectroscopy investigates the molecular vibration within atoms and molecules. It is a means to investigate the morphological features of graphene based materials (Veerapandian *et al.*, 2012). The Raman spectra of Graphite, GO, VGO,

PMMA-1% GO is depicted in the Fig. 4.4 (a)-(b). G band and D band are the most prominent ones. Generally, the characteristic D and G band peaks are observed at around 1340 cm^{-1} and 1580 cm^{-1} respectively (Yang *et al.*, 2009; Jorio, 2012). On the similar lines in the synthesized GO as depicted in Fig. 4.4 (a), D band is observed at 1336 cm^{-1} and G band at 1586 cm^{-1}, while VGO exhibits D band at 1330 cm^{-1} and the G band at 1582 cm^{-1}. In graphite G band is evidently prominent than D band indicating larger presence of sp^2 hybridized structures. Intensity and shape of D and G band changes considerably in graphene oxide compared to graphite**.** In GO and VGO, intensity and the line width of D band becomes higher than G band. Presence of a strong D band in both GO and VGO confirms the defects produced on carbon basal planes of graphite flakes due to attachment of various functional groups. A typical band at 2720 cm^{-1} in graphite, designated as 2D band (second order characteristic of D band) is observed based on which comprehensive information regarding stacking number of graphene sheets could be deduced. 2D band features diminishes in case of GO and VGO Raman plots attributable to large disorder due to defects induced on the sp^2 hybridized hexagonal sheet of the carbon in GO. The defects have been caused due to the treatment of carbon sp^2 structures with strong chemicals.

Ratio of intensity of the D band (I_D) to intensity of the G band (I_G) increases sequentially with reaction steps. I_D/I_G for graphene oxide is 1.167 which becomes 1.194 for vinyl graphene oxide, which further increases to 1.27 for PMMA-1% GO as calculated from Fig. 4.4 (b). Increasing I_D/I_G ratio indicates increase in defect density with more number of sp^2 carbons participating in chemical reaction and forming sp^3 clusters. I_D/I_G of VGO is higher attributed to reduction of GO due to introduction of vinyl groups reducing the density of oxygenated groups. In the preparation of nanocomposite, further increase in defect density is observed due to more number of sp^2 carbons undergoing treatment with chemicals leading to further increased I_D/I_G ratio (Hu *et al.*, 2014). Raman spectra of PMMA-1% GO nanocomposite as observed from Fig. 7(b) shows major peaks at 1736 cm^{-1} (carbonyl group stretching), 1330 cm^{-1} (C-H deformation), 1456 cm^{-1} (C-H bending), 850 cm^{-1} (aliphatic ether group stretching), 819 cm^{-1} (CH_3 rocking). Size of crystallinity (L_a) of GO and nanocomposite was calculated using the following equation:

$$L_a\,(\mathrm{nm}) = 2.4 \times (10)^{-10}\,(\mathrm{nm})^{-3} \times \lambda_L{}^4\,(\mathrm{nm})^4 \times (I_D/I_G) \quad \ldots\ldots\ldots\ldots\ldots\ldots (4.1)$$

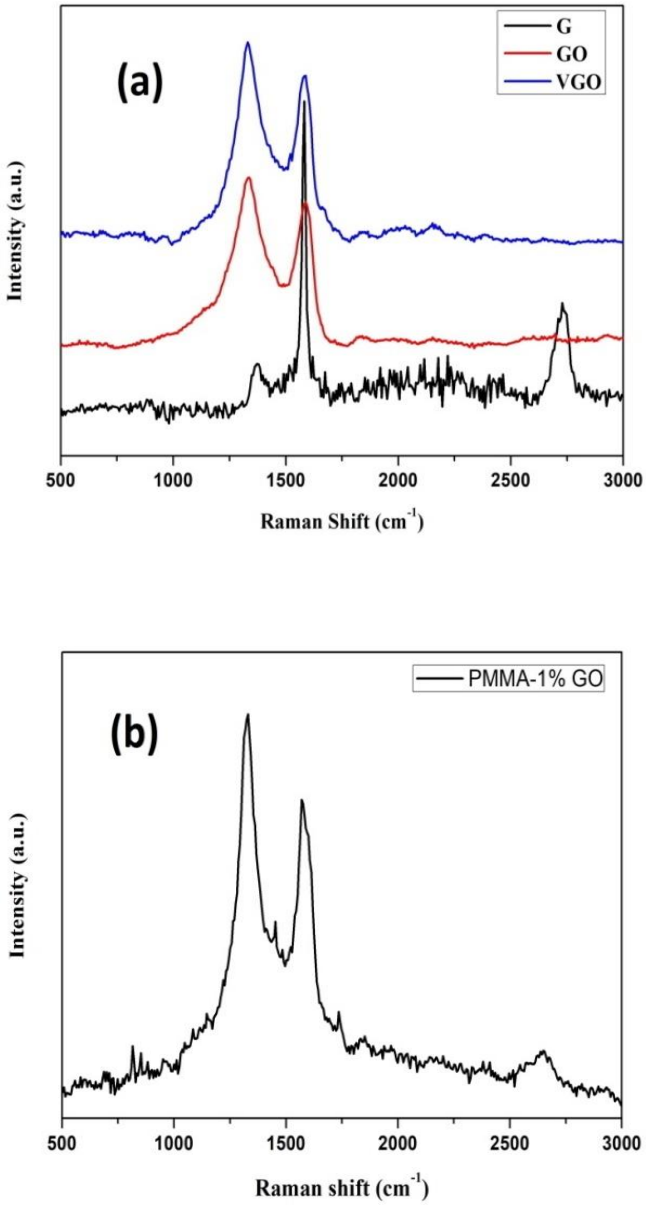

Figure 4.4 Raman spectra of (a). Graphite (G) and its oxides and (b). PMMA-1% GO nanocomposite. G and D bands become smaller and larger respectively with chemical reactions occurring on the graphitic structure of PMMA-1% GO, indicating generation of chemical defects due to chemical reactions.

Where λ_L is the wavelength of laser source (nm) used in the Raman measurement and I_D and I_G are the Raman intensities of D and G peaks respectively. The values

obtained through the equation are 44.91 nm for GO and 45.95 nm for VGO which suggest that crystallite size of VGO increased due to treatment with chemicals during Pinners reaction and crystallite size of PMMA-GO further increases to be 48.87 nm.

4.3.3 XRD Spectra

XRD analysis is carried out to get an insight about the XRD pattern of G, GO, VGO and PMMA-1% GO and their XRD plots are depicted in Fig 4.5. It is a well-known information that graphite powder shows an interlayer spacing around 0.3658 nm (observed at $2\theta = 26.48°$) (Zhang *et al.*, 2009) which could be calculated using Braggs equation ($n\lambda = 2d\sin\theta$)**.** The disappearance of the peak at $2\theta = 26.48°$ and advent of peak at $2\theta = 10.18°$ indicates that laboratory synthesized product GO is completely oxidized (Du *et al.*, 2010; Venugopal *et al.*, 2012). Interlayer spacing of GO has been increased to 0.869 nm (corresponding to a strong peak observed at $2\theta = 10.18°$). This increase in interlayer spacing and corresponding decrease in Bragg's angle is attributed to attachment of hydroxyl, carbonyl and epoxy groups at graphite surfaces and edges. Further expansion in d spacing of VGO is observed which becomes 1.279 nm (corresponding to a strong peak observed at $2\theta = 6.91°$) which confirms the incorporation of vinyl ester groups on GO structure. The peak further shifts to lower Bragg's angle in nanocomposite PMMA-1%GO.

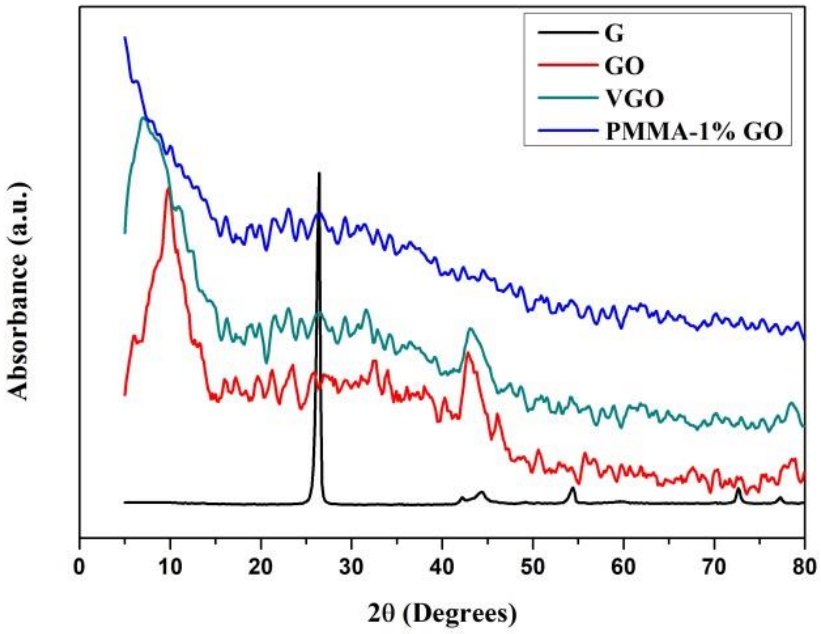

Figure 4.5. XRD plots of Graphite (G), GO, VGO and PMMA-1% GO. A decrease in Braggs angle of PMMA-1%GO corresponds to an increased interlayer spacing.

4.3.4 UV-visible spectra

Aqueous dispersion of GO appears to be light brown in color as observed from Fig. 4.6, indicating complete oxidation of graphite (Chen *et al.*, 2014), while VGO appears to be black in color probably due to esterification reaction leading to inclusion of vinyl group on GO sheets. UV-visible spectroscopy also assist in confirming the grafting of PMMA on GO. Variation in absorbance of prepared dispersed solutions with respect to wavelength recorded in the UV-visible spectrophotometer has been illustrated in Fig. 4.7. Graphite shows no significant absorption peaks in the wavelength range from 200 to 700 nm, rather some abrupt small peaks are found all over the wavelength range (Mahato et al., 2016). GO shows two major peaks centered at 230 nm and 300 nm. The absorption band centered at 230 nm is attributed to $\Pi \rightarrow \Pi^*$transition of aromatic C-C bonds while a less intense absorption band appears at 305 nm corresponding to $n \rightarrow \Pi^*$ transition caused by stretching mode of C=O bonds (Lai *et al.*, 2013; Singh *et al.*, 2015). Significant absorption peaks observed in PMMA is 280 nm due to $n \rightarrow \Pi^*$transition of C=O groups. Characteristic absorption peaks observed in PMMA-GO are 230 and 290 nm. In PMMA -GO, the peak observed at 230 nm corresponds to $\Pi \rightarrow \Pi^*$ transition of aromatic C-C

bonds owing to the inherited characteristics of GO. Other major peak observed at 290 nm corresponds to $n \rightarrow \Pi^*$ transition of carbonyl groups due to the acquired characteristics of PMMA as this peak gets blue shifted by 10 nm. This observed absorption spectra confirms the formation of nanocomposite.

Figure 4.6. A dispersion of GO and VGO in distilled water, qualitatively illustrates a homogeneous and well dispersion of the nanoparticles in water, and also demonstrates the color variation of GO and VGO samples.

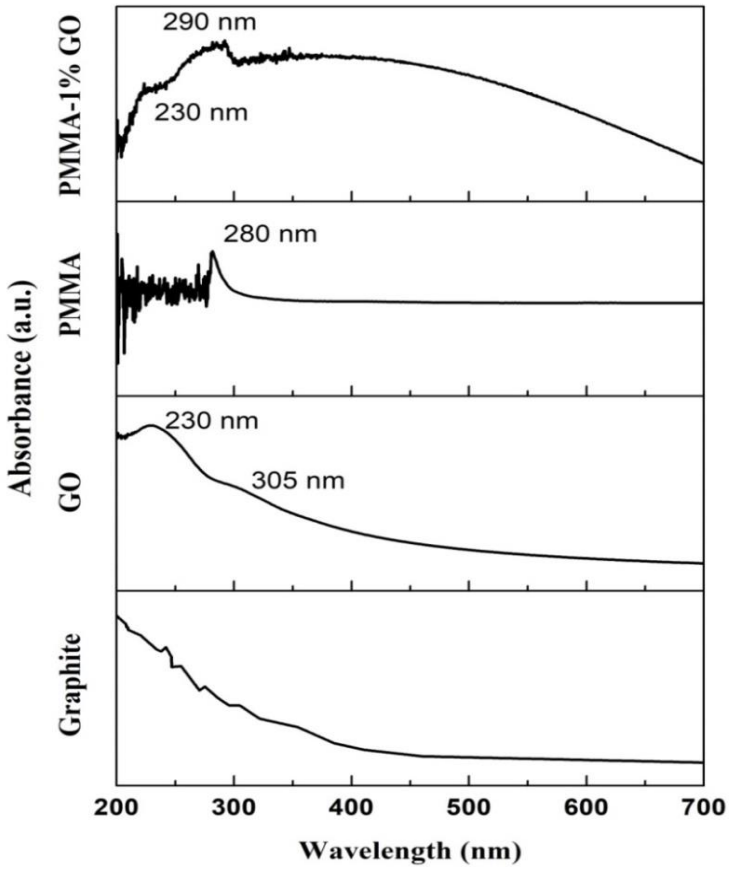

Figure 4.7. UV- visible absorption spectra of Graphite (G), Graphene oxide (GO) and additives

4.3.5 FE-SEM

To understand the surface morphology of polymer grafted nanocomposite and to examine the dispersion degree of GO onto polymer matrix, FE-SEM imaging analysis is performed as depicted in Fig. 4.8 (a)-(d). The FE-SEM imaging of graphene oxide as observed in Fig. 4.8 (a) reveals the presence of distinct thin layer structure. There are a number of layers overlapping each other leaving spaces for organic moieties to get entrapped in between through electrostatic interactions (Mahato et al., 2016). Observing the Fig. 4.8 (b) of VGO, it can be seen that some moieties have been attached to the sheet

structure of GO, this indicates the probable entrapment of vinyl groups on GO sheets. It can be deduced from Fig. 4.8 (c) & (d) that the GO was firmly attached to the polymer framework as GO agglomerates are clearly seen to be densely distributed on polymer PMMA base. Mean platelet size was analyzed from FE-SEM images. GO was synthesized with a mean platelet size of 4.191 μm while that of Vinyl-GO is found to be 2.832 μm. This reduction in the platelet size is attributed to the esterification reaction. The nanocomposite agglomerate size is found be ~ 300 nm, indicating successful in situ polymerization of PMMA on GO sheets.

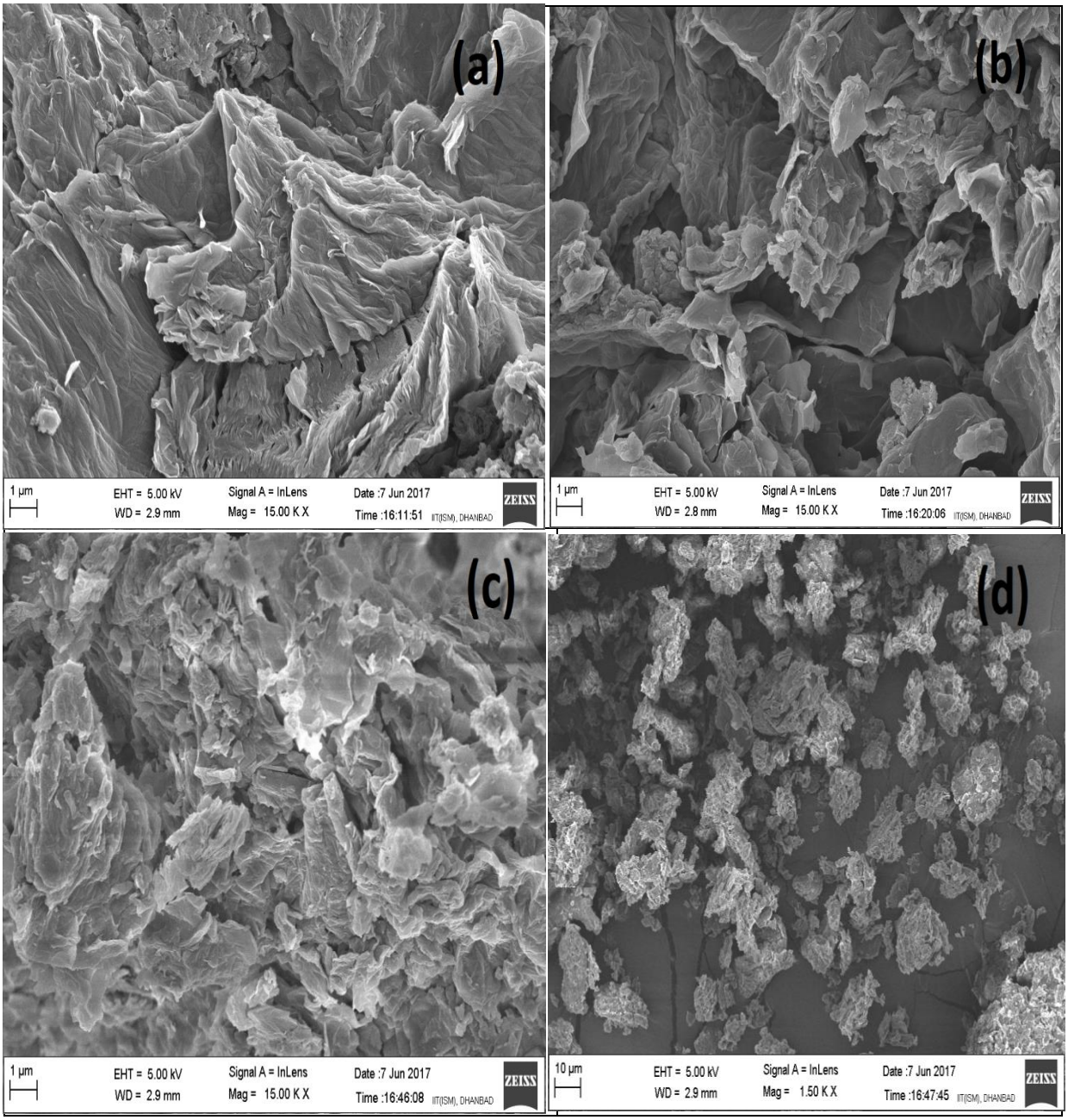

Figure 4.8. FE-SEM images of (a) Graphene oxide (mag. 15 K X); (b) Vinyl Graphene oxide (mag. 15 K X); (c) PMMA-1% GO (mag. 15 K X) & (d) PMMA-1% GO (mag. 1.5 K X)

4.3.6 Thermal Analysis

Thermal properties of the synthesized samples were evaluated using Thermogravimetric analysis (TGA) under a nitrogen atmosphere as exhibited in Fig. 4.9. TGA is the study of weight loss that changes of a specimen as a function of temperature. PMMA formed by free radical polymerization contain weak links formed as a consequence of termination by disproportionation or combination. Although, the temperatures usually experienced in the oilfield operations/PPD applications lies well below 100°C, but the TGA measurements were performed over a broad temperature range (0-800°C) to gain understanding about the thermal stability of the products. Thermal stability of PMMA formed by free radical polymerization is discussed in detail. The outset of degradation in PMMA starts near 140°C due to scissions of those chains incorporating head to head linkages formed as a result of termination by combination (Chong *et al.*, 2006)**.** The second outset of degradation occurs in two stages, one at 200°C and other at 270°C. This degradation is initiated by scissions at unsaturated ends resulting from termination by disproportionation. The last step of degradation initiates near 400°C due to arbitrary scissions within the PMMA chain (Ferriol, Gentilhomme and Cochez, 2003).

GO start to lose weight gradually from initial temperatures itself and a rapid mass loss is observed in temperature range 150-200°C leading to 40 wt.% mass loss up to 200°C. This mass loss results due to release of water molecules and COOH molecules trapped on GO sheets. Thereafter, very less thermal degradation is observed till 375°C after which another significant weight loss (~10 wt.%) occurs up to 425 °C which is due to loss of epoxy and hydroxyl groups present in GO. From there onward very less thermal degradation (~5 wt.%) up to 800°C is observed in GO indicating excellent resistance to heating and greater stability at higher temperatures This mass loss is a result of degradation of more stable oxygen functionalities. Therefore, incorporating GO sheets into the polymer matrix would lead to enhancement in thermal stability of nanocomposite. As evident from the TGA plot of the nanocomposites in Fig 12, PMMA-1% GO undergoes significant weight loss in three stages. (1) In first stage, significant thermal degradation initiates at 140°C and continues up to 190°C. This degradation is attributed to scissions of chains containing head to head linkages. (2) In second stage, degradation

occurs continuously and involves significant mass loss up to 485°C and this might be attributed to chain scissions at unsaturated ends. A major mass loss in PMMA occurs up to 400°C, while almost equivalent mass loss occurs up to 450°C in PMMA-0.5% GO and up to 485°C in PMMA-1% GO. This observation indicates that on increasing the content of GO in polymer chains, there is a shift in mass degradation towards higher temperatures and the thermal stability of nanocomposite increases. (3) Subsequently in the last stage, lesser thermal degradation is observed in PMMA-1% GO after 500°C and up to 800°C. The reduced weight loss in PMMA-GO may be attributed to very slow thermal degradation of more carbonaceous materials present in them. Residual mass obtained in case of PMMA-1% GO is slightly higher than PMMA-0.5% GO at 800°C. These results from TGA indicate that the synthesized nanocomposite possesses superior thermal stability compared to polymer PMMA.

PMMA-1% GO suffered around 96 % mass loss at 800°C indicating improved thermal stability of the nanocomposite as compared to polymer PMMA which suffered almost same amount of weight loss at 400°C itself. This might be attributed to incorporated GO sheets causing resistance to thermal degradation. Also, PMMA-0.5 % GO experiences nearly 97 % weight loss at 800°C, while PMMA suffered 98% weight loss at the same temperature. From weight loss curve, real concentration of GO was obtained in PMMA-1% GO and was found to be nearly 1 wt. %, while it was found to be 0.5 wt. % in PMMA-0.5% GO.

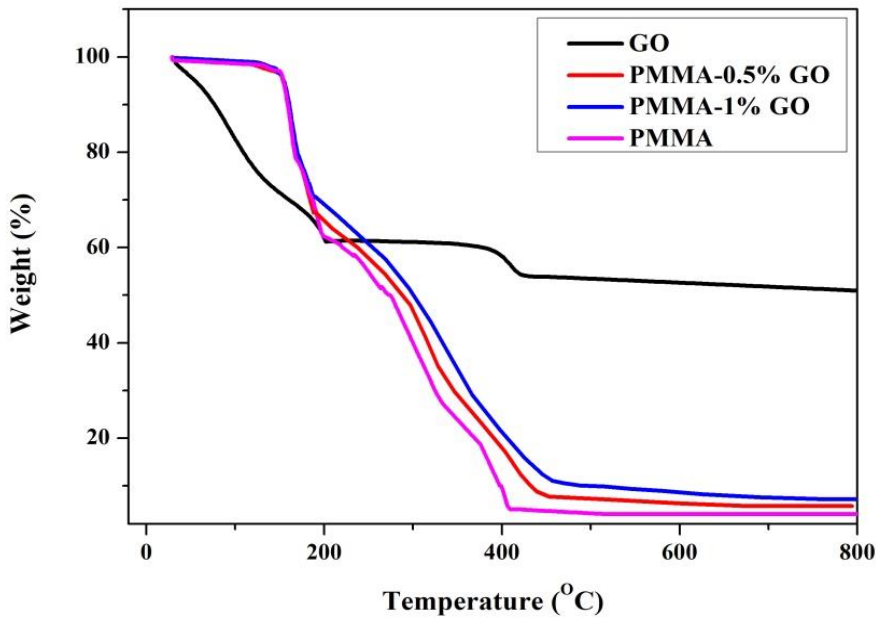

Figure 4.9. TGA plot of GO, PMMA, PMMA-0.5% GO and PMMA-1% GO

DTG is the numerical derivative of TGA plot which illustrate the temperatures at which significant mass loss occurs. As observed from the Fig. 4.10, initial significant thermal degradation of polymer and nanocomposite occurs at a similar range 140-190°C (i.e. the DTG peak is near about the same) during which PMMA experienced the highest mass loss. During the second stage of degradation, the difference in the mass loss between PMMA and nanocomposites can be observed from the DTG plot which shows presence of enormous number of abrupt peaks in PMMA compared to nanocomposites and indicates higher mass loss in PMMA. This observation was also evident from the TGA plot of PMMA and nanocomposite. Subsequently, very less degradation is observed up to 800°C in all samples.

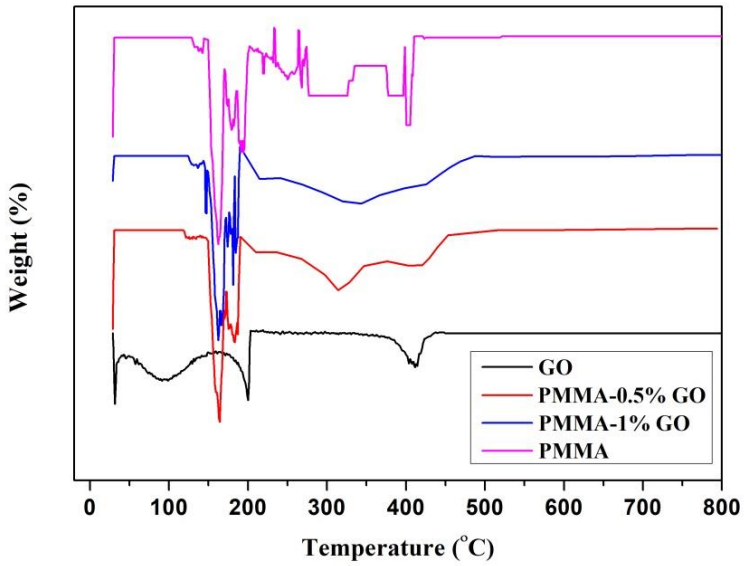

Figure 4.10. DTG plot of GO, PMMA, PMMA-0.5% GO, PMMA-1% GO

4.4 Evaluation of the synthesized additives

Improvement in the flow properties of the crude oil was evaluated through pour point determination and rheology (the viscometry mode and sweep tests under oscillatory mode) for determining the modifications in apparent viscosities and gelling tendency of crude oil for both virgin and PPD-treated crude oils samples. The aging effect evaluates with long term flow efficacy of the crude oil treated with synthesized additives.

4.4.1 Pour point depression

Pour Point of the untreated crude oil was found to be 38°C. Depression in pour point of various additives treated crude oil is mentioned in Table 4.4. Pour point of the crude oil has been efficiently reduced when treated with PMMA-GO as the major depression in pour point observed was 23°C using PMMA-1% GO at 1500 ppm, while 16°C depression occurred with PMMA-0.5% GO at the same concentration. 14°C pour point depression was observed in case of Phoenix at 1250 ppm while only 11 °C depression was observed with PMMA at the same concentration. 15°C, 22°C, 24°C, 27°C was found to be the pour point of crude oil when treated with PMMA-1% GO, PMMA-0.5% GO, Phoenix and PMMA respectively at their respective optimum concentration.

Optimum concentration of PMMA-1% GO and PMMA-0.5% GO was 1500 ppm while for PMMA and Phoenix was observed to be 1250 ppm. There occurs a sudden increase in crude oil pour point values above the optimum concentration of PPD, resulting from inclusion of extra concentration of additives which gets suspended and causes gelling in crude oil, thereby making the fluid flow heavier. There is significant improvement in the pour point depression of crude oil treated with polymer nanocomposite compared to commerical PPD. This can be explained on the basis of change in wax crystal morphology induced by nanocomposites (Khidr, Doheim and El-Shamy, 2015). Reduction in pour point brought by PMMA might be due to PMMA modifying the wax crystal morphology by co-crystallizing with wax molecules. In nanocomposite beneficiated crude oil, the primary motive of the nanocomposite is to provide nucleation sites with interfaces that acts as regular shaped templates on which wax molecules can easily precipitate and retain a compact form with change in their shape (Yang, Paso, *et al.*, 2015). The action mechanism for reduced wax deposition in nanocomposite beneficiated crude oil can be explained on the account of GO nanosheets in the oil medium acting as nucleation sites for the wax crystals to get precipitated on it, due to which the wax crystals takes a compact form and therefore avoids forming interlocking wax network (Yao, Li, Yang, Sjöblom, *et al.*, 2016; Yao, Li, Yang, Zhang, *et al.*, 2016; Yang *et al.*, 2017; Yao *et al.*, 2018). This leads to less gelation among the wax crystals, resulting in a loose wax crystal network, and therefore causes significant reduction in yield stress. Thus, PMMA-1% GO exhibited better flowability and depression in pour point compared to PMMA- 0.5% GO.

Table 4.3 Pour point of crude oil treated with different additives (°C)

Concentration (ppm)	Phoenix	PMMA (10 wt.% xylene)	PMMA-0.5%GO (10 wt.% xylene)	PMMA-1% GO (10 wt.% xylene)
0	38	38	38	38
250	36	36	35	35
500	33	33	33	32
750	30	31	30	28
1000	27	28	27	25
1250	24	27	26	21
1500	26	28	22	15
1750	29	30	25	19

4.4.2 Effect on apparent viscosities

Based on the pour point determination of the additives, the optimum concentration would be added to the crude oils for rheological testing in order to evaluate their performance in improving the rheology of crude oil.

The flow behavior of the raw crude oil and the crude oil treated with different additives is studied over a broad shear rate range 0-500 s^{-1} as observed in rheology plots depicted in Fig. 4.11 (a)-(c). A non-Newtonian and a shear-thinning flow behavior is noticed for both the virgin as well as treated crude oil samples over the examined shear rates. Viscosity of crude oil decreases with rise in temperatures. As observed from the rheology plots, maximum reduction in viscosity occurs in crude oil treated with PMMA-1% GO at all temperatures 30, 40, 50°C indicating the best flow improvement among all other used chemical additives. The viscosity value of crude oil at 30°C decreases significantly from 500 cP of virgin crude oil up to 3 cP (99.4% viscosity reduction) in case of crude oil treated with PMMA-1% GO, 10 cP (in case of PMMA-0.5 % GO), 35 cP (Phoenix), 45 cP (PMMA). At 40°C, viscosity drops from 460 cP of virgin crude oil up to 2 cP for crude oil treated with PMMA-1% GO (99.6% reduction), to 6 cP (PMMA-1% GO), 25 cP (Phoenix), 40 cP (PMMA). At 50°C, viscosity reduction occurs from 390 cP of virgin crude oil to around 1 cP (99.8% reduction) when crude oil is treated with PMMA-1% GO, 5 cP (PMMA-0.5% GO), 20 cP (Phoenix), 40 cP (PMMA). The viscosity values

from these rheology plots indicates that there is significant flow improvement as enormous reduction in viscosity is observed for crude oil treated with polymer nanocomposites and the reduction efficiency increases with increased GO content in nanocomposite, among which PMMA-1% GO providing comparatively better results than others.

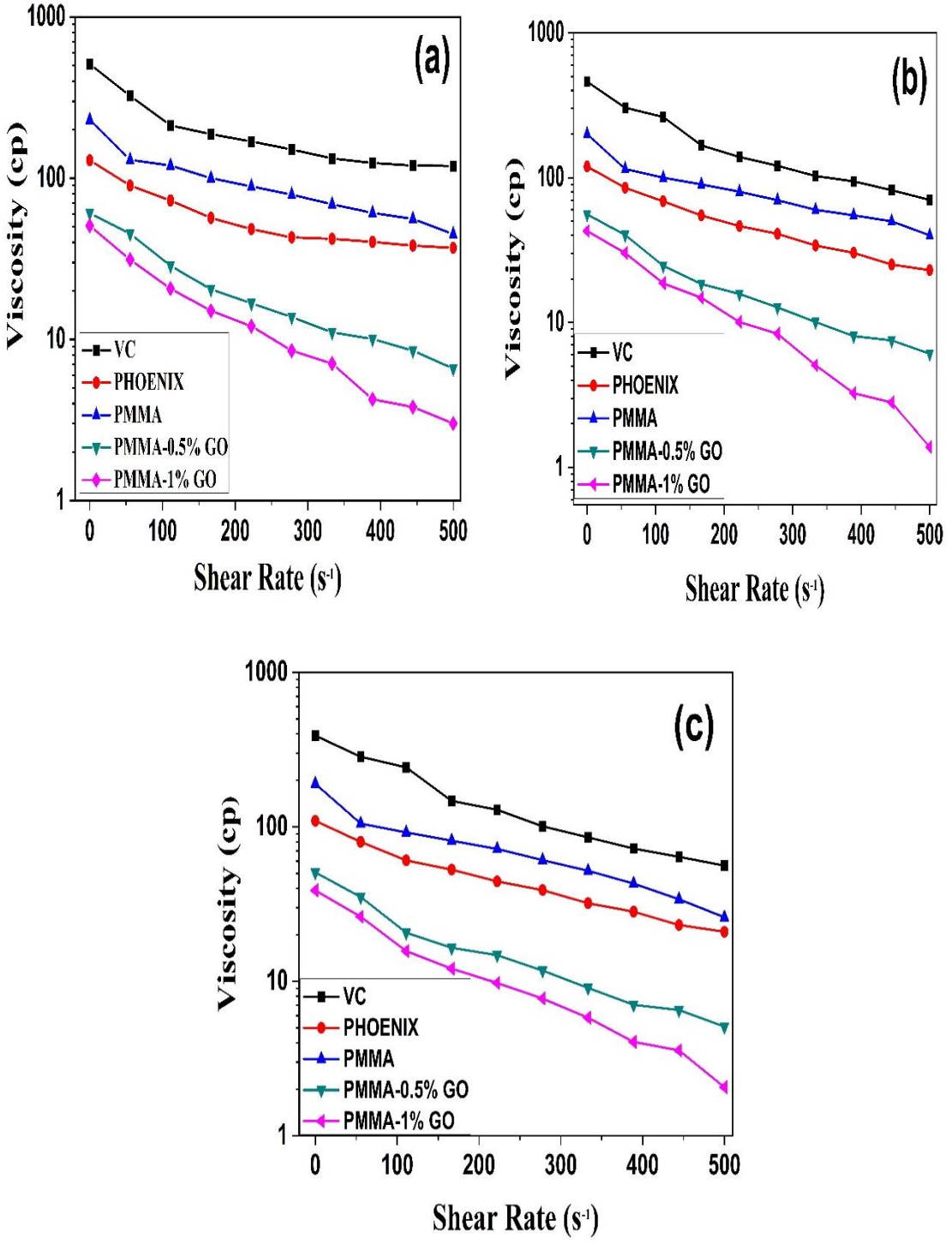

Figure 4.11. Rheological plots of virgin crude (VC) oil and crude oil treated with various additives at 1500 ppm at temperatures (a) 30°C; (b) 40°C and (c) 50°C

4.4.3 Aging effect

As observed from rheology plots as shown in Fig. 4.12 (a)-(c), the crude oil treated with various PPDs post 15 days retain its non-Newtonian shear thinning behavior, but the most important observation is that apparent viscosity of Phoenix treated crude oil increases significantly compared to PMMA-GO treated crude as can be observed from the Table 5. Long term stability (after 15 days) of the crude oil treated with polymer nanocomposites was much better compared to commercial PPD after the same time period, where the increase in apparent viscosity varies from 16.5% - 32.92% in case of PMMA-1%GO treated crude oil under a temperature range of 30-50°C, whereas the apparent viscosity varies from 28% - 37.74% in case of PMMA-0.5% GO treated crude oil, which was much better than the performance of Phoenix where apparent viscosity values rises by 40.175% - 44.93% in temperature range 30-50°C. This observation indicates that PMMA-GO treated crude oil exhibits excellent stability even after 15 days of treatment compared to rapid rheological degradation occurring in Phoenix treated crude oil. This nanocomposite PPD would yield significantly beneficial results upon its application in the petroleum industry**.**

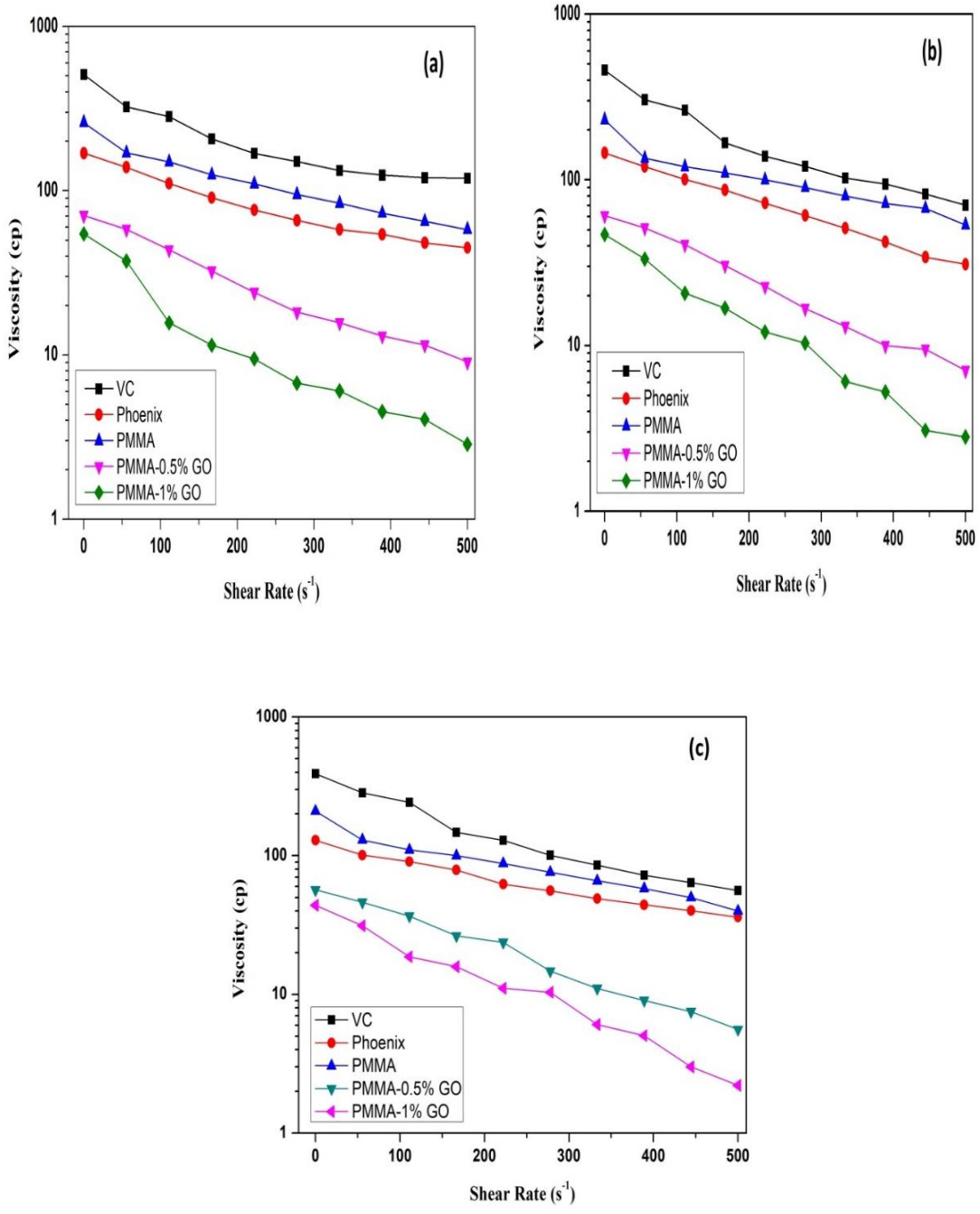

Figure 4.12. Post 15 days rheological plot of virgin crude oil (VC) and the crude oil treated with various additives at (a) 30°C; (b) 40°C; (c) 50°C at 1500 ppm

Table 4.4. Increase in apparent viscosity of crude oil treated with various additives at different temperatures post 15 days of treatment

Crude beneficiated with additives	Temperature (°C)		
	30	40	50
Phoenix	44.93 %	41.2 %	40.17 %
PMMA-0.5% GO	37.74 %	33.9 %	28 %
PMMA-1% GO	32.92 %	34.3%	16.5 %

4.4.4 Effect on gelation tendency and yield stress of crude oil

The gelation points of the virgin and additive treated crude oil were determined by using rheometric method (Yang, Paso, *et al.*, 2015). Considering the experimental temperature range of 70-10°C, firstly the crude oil sample was maintained at 70°C for 5 min and cooled to 60°C at a cooling rate of 10°C/min. Subsequently, the oil sample was cooled at rate 0.5°C/min and sheared under a controlled shear stress of 0.1 Pa. The change in shear rate with drop in temperature is observed. Plot of shear rate versus experimental temperature indicates a distinctive point on the curves that show the clear break in the pattern of shear rate on decreasing temperature, which is denoted as the gelation temperature.

For better understanding of deposition of waxy crude oils under flowing conditions in pipelines, knowledge of gelation temperature is necessary. Pour point determination method helps in understanding only the static gelation of waxy crude oils while gelation temperature helps to measure the outset of gelation under static and fluid flowing conditions (Venkatesan *et al.*, 2002). As observed from the Fig. 4.13 there is a distinct break from the decreasing pattern in the shearing curve of virgin crude oil at 41°C, this temperature is denoted as gelation point of the sample crude oil. There is a reduction in gelation point observed in nanocomposite treated crude oil samples, with values obtained as 25°C in PMMA-0.5%GO treated crude oil (1500 ppm) while lowest gelation point of about 17°C is observed for PMMA-1% GO treated crude oil (1500 ppm). This reduction in gelation points may be attributed to the change in wax crystal network induced by nanocomposite PPDs.

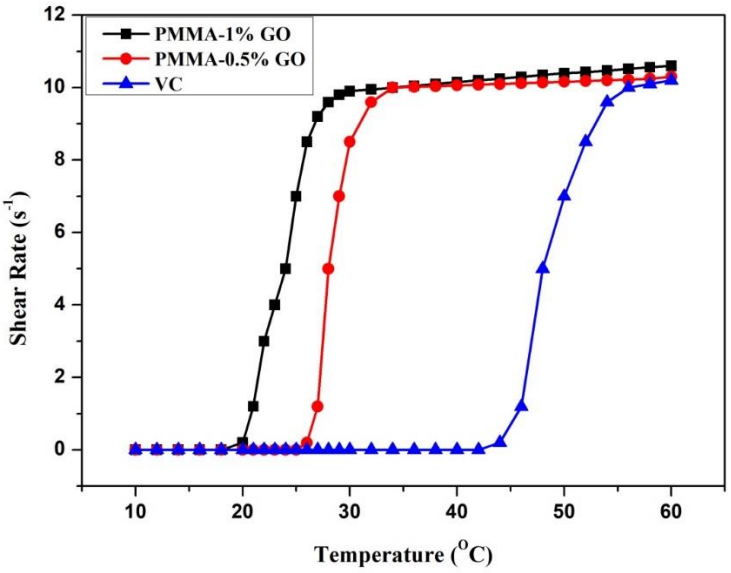

Figure 4.13. Effect of nanocomposite additives PMMA-0.5%, 1% GO at 1500 ppm concentration on the gel strength of virgin crude oil (VC)

Yield stress is a fluid parameter below which the fluid flow would remain inactive. Lower yield stress values in crude oil would create lesser clearance pressure drop in oil pipeline, although other factors such as pipeline length, diameter and fluid density may also play an important role in calculating pressure drop. As observed from Fig. 4.14, the yield stress observed in the virgin crude oil (VC) is about 60 Pa which gets reduced to around 10 Pa in PMMA-0.5% GO (1500 ppm) treated crude oil sample, while lowest yield stress of about 0.1 Pa is observed in case of PMMA-1% GO (1500 ppm) treated crude oil. It is evident from this experiment that nanocomposite PPDs have significantly

decreased the gel strength of wax crystal networks and thus could be used as an effective flow improvers for pipeline transportation of waxy crude oils (Yang, *et al.*, 2015). .

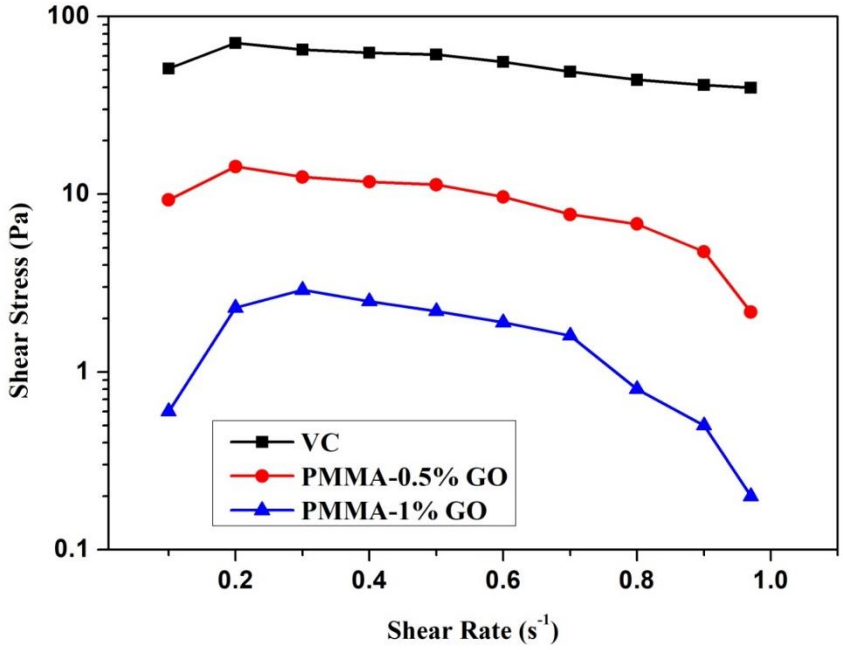

Figure 4.14. Effect of nanocomposite additives PMMA-0.5%, 1% GO on yield stress of virgin crude oil (VC) at temperature 17°C.

4.4.5 Microscopic analysis of wax crystals morphology

As observed from the microscopic images in Fig. 4.15 (a)–(d), in the virgin crude oil, wax molecules are abundant and smaller and form a dense and interconnected wax crystal network. Upon addition of Phoenix PPD, interlocking between wax crystals slightly reduces as they co-crystallizes with polymer chains and takes more compact form. Moreover, upon treatment with PMMA-0.5% GO there is a significant reduction in amount of dispersed wax molecules as they gets precipitated upon various nucleation centers provided by GO sheets. Similarly, in case of PMMA-1% GO treated crude oil, fine wax crystals completely disappears and the wax crystal network breaks down comprehensively as can be seen in the Fig. 4.15(d). This can be explained on the account that PMMA chains co-crystallizes with wax molecules and get precipitated on GO nucleation sites, and thus reduces the dispersed wax crystals, thereby, resulting in a much compact disconnected structure. Therefore, the wax crystals would not create hindrance in flowability of crude oil and ultimately would help in improvement of its rheological properties (Yao, Li, Yang, Sjöblom, *et al.*, 2016).

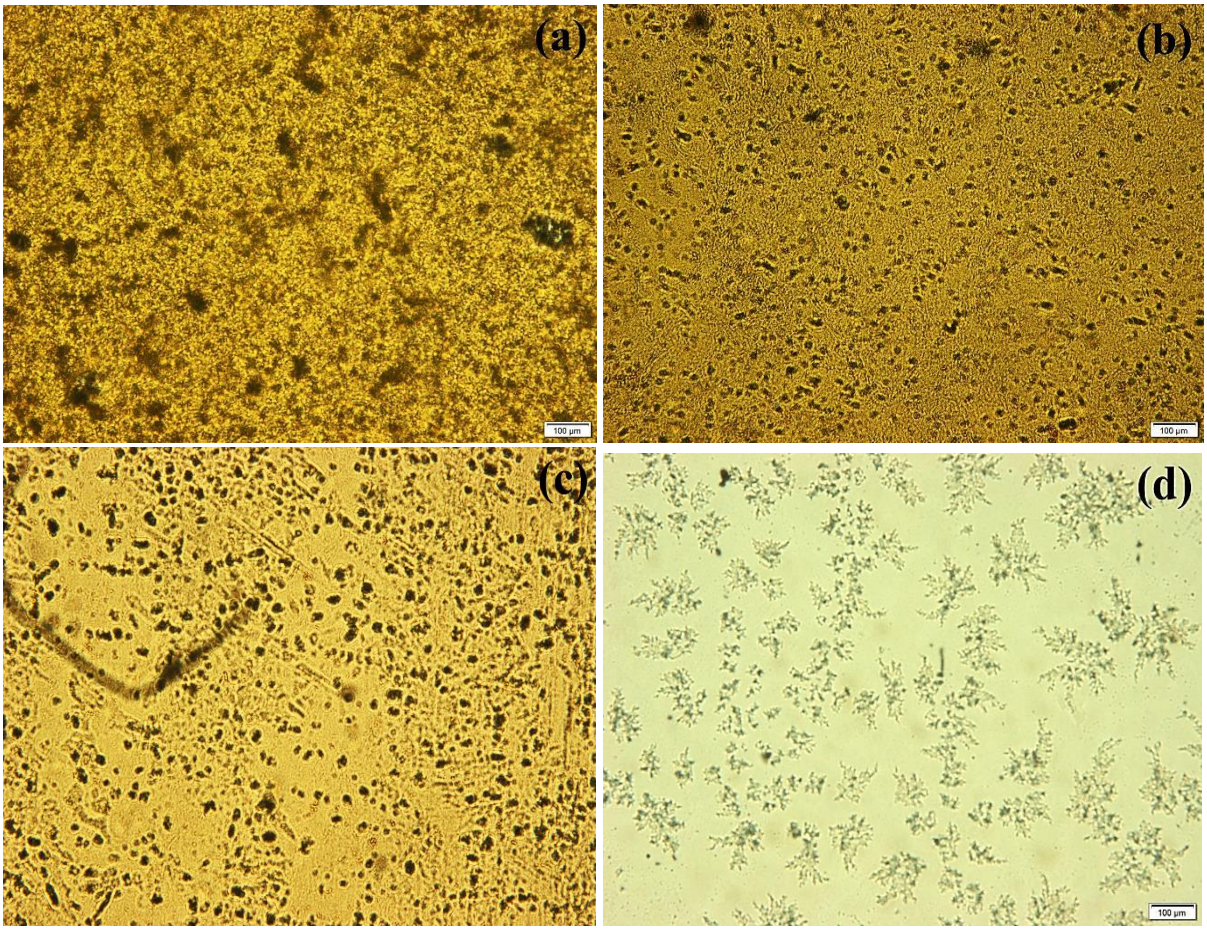

Figure 4.15. Polarized microscopic images at 100 µm magnification of (a) Virgin crude, and crude oil samples beneficiated with the following PPDs (b) Phoenix, (c) PMMA-0.5% GO and (d) PMMA-1% GO

4.5 Conclusions

The polymer nanocomposite was successfully synthesized in laboratory, characterized and evaluated as pour point depressant for Indian waxy crude oil. Significant depression in pour point about 23 °C and the improved rheological properties of crude oil was observed as the apparent viscosity values fall to as low as 1 cP (about 99.8% viscosity reduction) for PMMA-1% GO treated crude at 1500 ppm. Nanocomposite has shown to significantly decrease the gelation point and the gel strength of the wax crystal network of crude oil and the reduction in wax gel network in PMMA-GO beneficiated crude was clearly substantiated by polarized microscopic analysis.

Spectroscopic studies such as FTIR, UV-visible and Raman analysis confirmed the formation of nanocomposite. Action mechanism for reduced wax deposition in synthesized polymer nanocomposite treated crude oil is explained on the basis of GO sheets in nanocomposites acting as nucleation templates for precipitation of wax crystals, leading to development of wax crystals in a compact form, thereby preventing the overlap between wax crystals and the formation of volume spanning wax network. As a result, improved flow properties of treated crude oil were observed. The results obtained from the current research work are of practical significance and valuable to petroleum industries in establishing assured flow properties of waxy crude oil in pipelines. Also, optimizing the amount of synthesized additives in crude oil as discussed in the research work will lead to economic benefit of the petroleum industry.

Chapter 5

Evaluation of poly (2-ethyl hexyl acrylate) - graphene oxide as novel nanocomposite pour point depressant

5.1 Introduction

This chapter would detail the results obtained from the experimentation performed on an Indian waxy crude oil using chemical additives: conventional additive poly(2-ethyl hexyl acrylate) [P(2-EHA)] and a novel polymer nanocomposite poly(2-ethylhexyl acrylate)-graphene oxide [P(2-EHA)-GO]. The performances of these two additives are compared and the results present an interesting outlook on the performance of nanocomposite additives on waxy crude oils over the conventional polymeric additives currently in use by the petroleum industry. This chapter illustrates the working of the chemical additives used for the treatment of the crude oil and the changes they bring in the morphological structure of waxes (Fig 5.1), and also differences in the mechanisms of these type of additives on the networking of wax crystals are analyzed. This work significantly enhances our understanding towards working and development of nanocomposite additives, and also focuses on the role of graphene oxide in flow assurance of crude oils. This work would also address the research gap from previous chapter, where the beneficiation effect of the synthesized chemical additive on the crude oil, could be extended over a longer period of time (aging effect) from 15 days (in the case of PMMA-GO) to 30 days (P(2-EHA)-GO), that would be extremely important in preventing any deposition issue in the case of pipeline flow as well as shutdown for extended periods of time. The characterization techniques of the chemical additive also produces extensive data sufficient to develop similar kind of polymeric and polymer nanocomposite additives. [2]

[2] ***This chapter is a slightly modified version of my research publication titled "Investigation into the Flow Assurance of Waxy Crude Oil by Application of Graphene-Based Novel Nanocomposite Pour Point Depressants." published in Energy & Fuels (2019), 33(12), 12330-12345 and it has been reproduced here with the permission of copyright holder.***

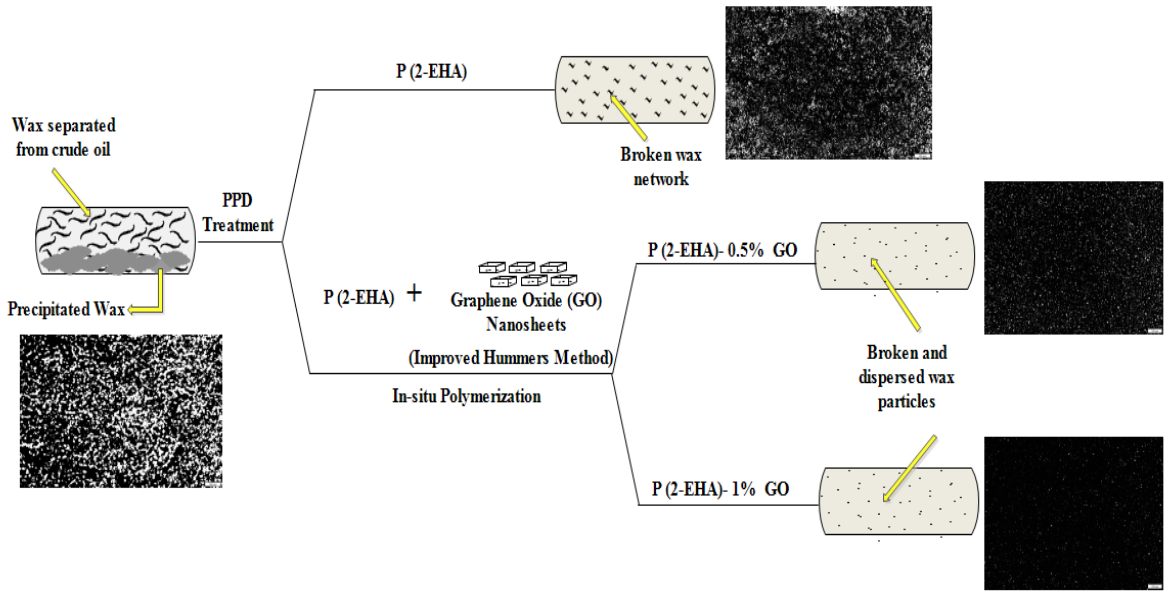

Fig 5.1. Improvement in the properties of the crude oil treated with chemical additives: P(2-EHA) and P(2-EHA)-1%GO, illustrated through morphological modification of wax crystals.

5.2 Characterization of crude oil

5.2.1 Determination of physico-chemical properties

Table 5.1 lists the physico-chemical characteristics of the selected crude oil. Crude oil contain 12 wt. % of wax, indicating a high wax crude. Its pour point was found to be 36°C, which is typically high and it may be possibly attributed to the high wax content. API gravity lies in the range 22.3-31.1° which implies that the crude oil is medium in nature. In general, if the API gravity lies in the range 22.3-31.1°, it implies that the crude oil is medium in nature. The crude oil used in this study is a medium crude oil with an API gravity of 27.4º. Results of the SARA analysis of the crude oil are as listed in the Table 5.1, reveals that saturates are in majority and aromatic and resin are in moderate quantity, while the crude oil contain very less asphaltene, indicating minimal chances of asphaltic deposition. Resin-asphaltene proportion is quite high, indicating that asphaltenes are well stabilized by resins in the crude oil and presents nominal chances of asphaltic deposition. The amount of saturates, aromatics, resins and asphaltenes (SARA)

present in crude oil were determined based on the solubility of each component in particular organic solvents.

Table 5.1. Characteristics of the virgin crude oil studied

Properties	Measured Values	Properties	Measured Values
Water content (vol. %)	5		
Pour point (°C)	36	Saturate (wt. %)	61
Specific Gravity (15°C)	0.89	Asphaltene (wt. %)	1
API gravity (°)	27.4	Aromatic (wt. %)	10
Wax content (wt. %)	12	Resin (wt. %)	12
WAT	50.2 °C	Resin/Asphaltene (wt. % / wt. %)	12

5.2.2 WAT determination

WAT of crude oil is calculated from the plot of Arrhenius relation of viscosity with temperature as shown in Fig. 5.2. WAT of the crude oil as determined from the non-Arrhenius methodology was found to be 50.2°C (323.12 K). At 323.12 K we can see a break from Arrhenius relation of viscosity and temperature indicating appearance of the WAT. This suggests that the crude oil has significant wax deposition problems starting from high temperatures The WAT calculation technique is illustrated through WAT plot (Fig. 5.1) This method to determine WAT of crude oil was discussed by Sharma et al. (Sharma, Mahto and Vuthaluru, 2019) and Paso et al. (Paso *et al.*, 2009).

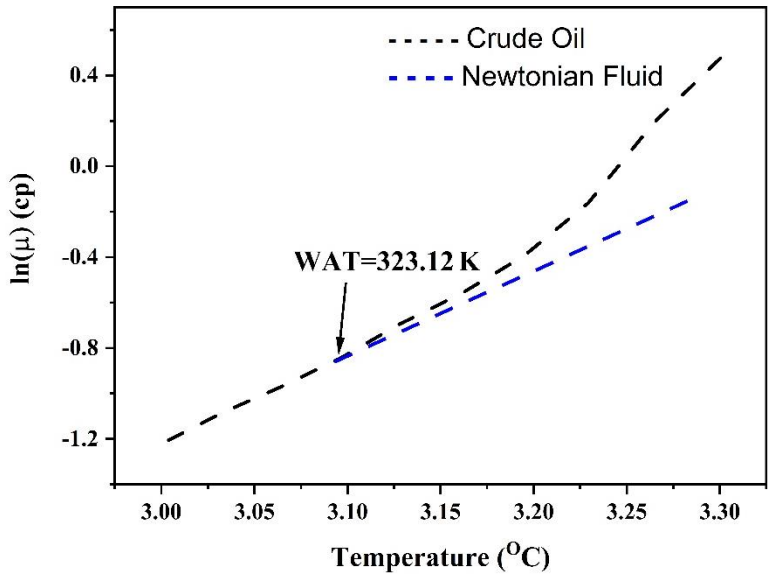

Figure 5.2. Determination of Wax appearance temperature (WAT) of crude oil at constant shear rate 10 s^{-1} using Non-Arrhenius Methodology in the temperature range (273 - 333 K)

5.3 Characterization of graphitic compounds and polymer nanocomposites

5.3.1 FTIR spectroscopy

The FTIR spectrum of graphite as observed from Fig. 5.3 (a) exhibited a peculiar peak at 1630 cm^{-1} attributable to C=C group vibrations (stretching). The information provided in this analysis is of qualitative nature. In graphite, FTIR peak observed at around 3400 cm^{-1} appears due to the entrapment of moisture from environment in graphite during sample preparation. The FTIR spectral analysis of GO (Fig. 5.3 (b)) revealed peaks at 1065 cm^{-1} and 1245 cm^{-1} corresponding to C-O-C symmetric and asymmetric vibrations (stretching) occurring in epoxy groups. Also, the peak observed at 1370 cm^{-1} is attributable to C-O stretching vibrations occurring in COOH groups. Moreover, the peak at 1626 cm^{-1} appears owing to stretching vibrations occurring in un-oxidized sp^2 carbons (Tiwari *et al.*, 2017). A broad peak at 3398 cm^{-1} corresponds to presence of hydroxyl group introduced on graphene sheets post oxidation of graphite to graphene oxide.

GO is functionalized to obtain VGO. FTIR spectrum of VGO (Fig. 5.3 (c)) exhibited peaks of functional groups. The peaks appearing at 1065 cm^{-1}, 1245 cm^{-1}, 1626

cm^{-1} and 3398 cm^{-1} are attributable to the inherited characteristic of GO. Appearance of a new peak at 1405 cm^{-1} corresponds to asymmetric bending vibrations occurring in C-H bond of the vinyl groups, and the presence of this peak confirms the vinyl esterification process in VGO (Silverstein et al., 2014). The peak at 1722 cm^{-1} is attributed to C=O stretching vibrations, which are particular characteristics of esters.

The FTIR of base polymer P(2-EHA) exhibited peaks at 720 cm^{-1} , 1170 cm^{-1} and 1460 cm^{-1} in Fig. 5.3(d) which are attributable to the bending vibrations observed in C-H bonds of methylene groups. Appearance of a strong peak at 1730 cm^{-1} is attributed to C=O stretching vibrations, usually observed in esters. Also, the peak observed at 2860 cm^{-1} indicates symmetrical C-H stretching vibrations occurring in methylene groups while the C-H stretching vibrations also occurs in methyl groups demonstrated by a nearby peak at 2965 cm^{-1}.

In the FTIR spectra of P(2-EHA)-1% GO as illustrated in Fig. 5.3 (e), the notable peaks observed at 720 cm^{-1}, 1170 cm^{-1}, 1460 cm^{-1}, 2860 cm^{-1} and 2930 cm^{-1} are characteristics of methylene group vibrations while the peak at 2961 cm^{-1} indicates methyl group stretching, these peaks can be attributed to characteristics acquired from the polymer P(2-EHA). While the characteristics of graphitic material in nanocomposite can be observed from the following FTIR peaks. The peak observed at 1390 cm^{-1} occurs due to peak shifting from 1400 cm^{-1} (in VGO) which corresponds to the bending vibrations in vinyl group of the synthesized nanocomposite. Moreover, the presence of unsaturated carbon skeleton in the P(2-EHA)-GO is indicated by C=C asymmetric stretching vibrations occurring in conjugated groups at 1631 cm^{-1}, possibly inherited from the GO. The presence of carbonyl group in the nanocomposite is demonstrated through a sharp intense peak at 1730 cm^{-1} which might have been inherited from either GO or P(2-EHA) (Silverstein et al., 2014). It could be understood from the above FTIR discussion that the nanocomposite possesses comprehensive characteristics of base constituents. The peak corresponding to the presence of hydroxyl groups shifts from 3398 cm^{-1} in GO, VGO to a sharper peak at 3440 cm^{-1} in P(2-EHA)-1% GO. This shift is possibly attributed to the presence of hydrogen bonding between the carbonyl group (C=O) of P(2-EHA) and COOH group of VGO. Thus, hydrogen bonding possibly exists between the VGO sheets and the polymer P(2-EHA) in the nanocomposite (Tiwari *et al.*, 2017; Sharma, Mahto and Vuthaluru, 2019) .

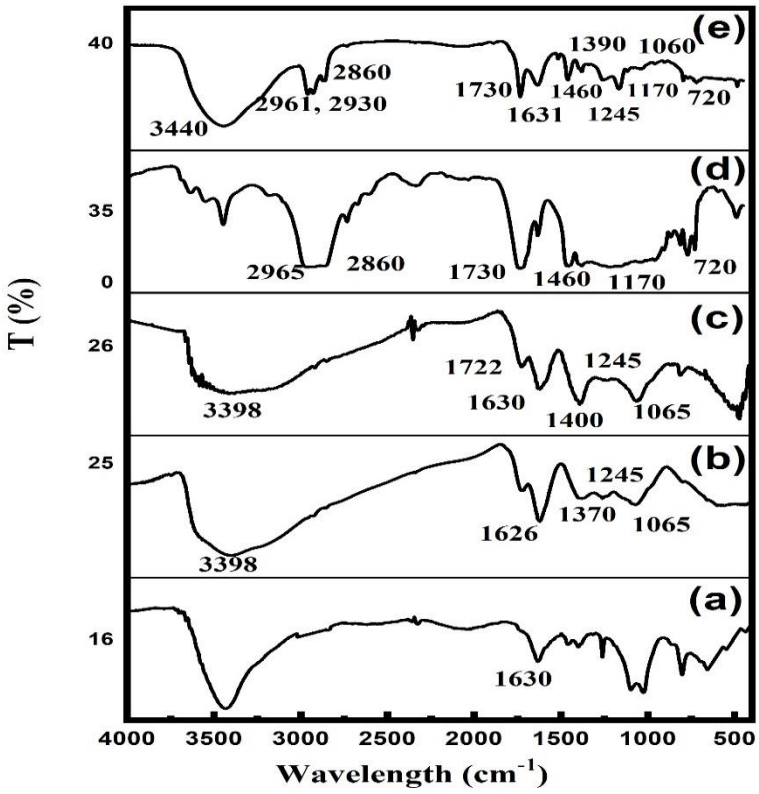

Figure 5.3. FTIR spectra of (a) Graphite, (b) GO, (c) VGO, (d) P(2-EHA) and (d) P(2-EHA)-1% GO nanocomposite

5.3.2 Raman analysis

The Raman spectra of graphite, GO and VGO is shown in Fig. 5.4 (a). For carbonaceous materials G and D band are important characteristics. Graphite exhibited a strong G band at 1584 cm^{-1} indicating a large presence of sp^2 hybridized carbon structure while a smaller D band is found at 1370 cm^{-1}. The analysis presented here is of qualitative nature. The intensity ratio of D and G bands is an indispensable parameter to understand graphitic structures (Li, Hayashi and Li, 2006). More evident in the Raman spectra of GO and VGO, elevation in the intensity ratio of D band to G band was detected in synthesized products. Ratio of intensity of D band (I_D) to G band (I_G) was found to be 0.15 (graphite), which increased to 1.16 (GO), which ultimately increased to 1.19 (VGO). This rise in intensity ratio (I_D/I_G) may be attributed to the increase in defect density in GO and VGO owing to carbon atoms participating in the reaction, thereby increasing the density of sp^3 carbons. These defects may be categorized as foreign adatom defects where

foreign atoms (other than carbon) are introduced and bonded to adjacent carbon atom (on the surface of graphene sheets in this case) due to the chemical treatments (such as oxidation), thereby oxygen functionalities get attached in case of GO and additional vinyl groups attach in case of VGO, thus the sp^2 carbons get converted to sp^3 carbon domains (Banhart, Kotakoski and Krasheninnikov, 2011; Tian *et al.*, 2017). Crystallinity size of products was determined with the following equation

$$L_a\ (nm) = 2.4 \times (10)^{-10}\ (nm)^{-3} \times {\lambda_L}^4\ (nm)^4 \times (I_D/I_G) \quad \text{.....(5.1)}$$

here λ_L is the wavelength of laser source (nm) utilized in the Raman analysis and I_G and I_D are the intensity of G and D bands respectively. The crystallite size of GO was determined to be 44.6 nm and 45.8 nm for VGO which indicates that crystallite size of VGO increased due to chemical treatment occurring in Pinners reaction, and crystallite size of P(2-EHA)-1% GO was determined to be slightly increased to 46 nm during polymerization (based on I_D/I_G = 1.194) [12].

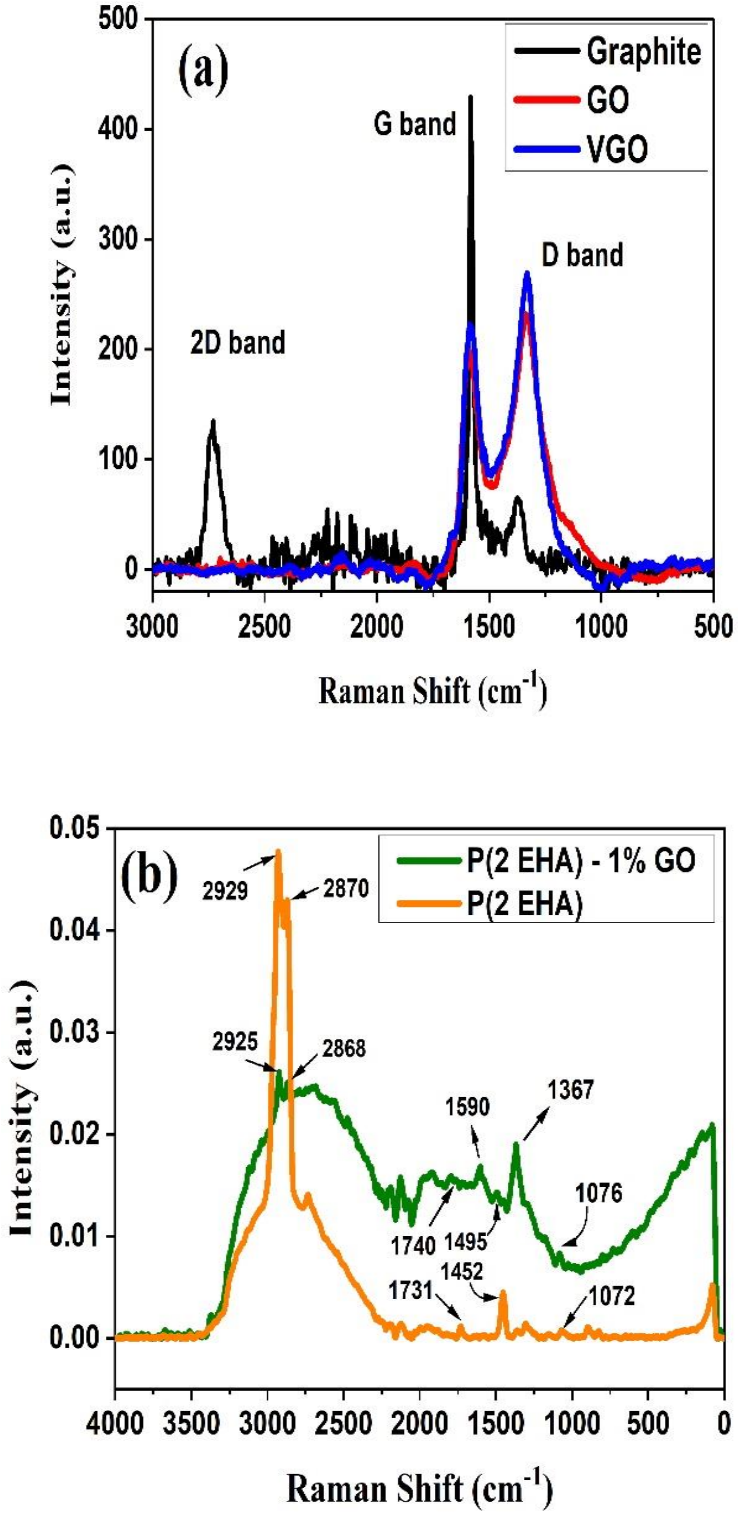

Figure 5.4. Raman spectroscopy of (a) Graphite, GO & VGO, (b) P(2-EHA) & P(2-EHA-1%GO).

In graphite, a Raman band designated as 2D band appeared at 2730 cm^{-1} and this band characteristics attenuated in GO and VGO. This is because of large disorder created owing to defects being generated on the sp^2 carbon containing GO sheet and these defects resulted from the chemical treatment of carbon sp^2 structures. Previous research works (Xu and Cheng, 2013) have shown that the intensity of a D band was observed to be proportional to the concentration of defects generated on the sp^2 carbon structures, while the intensity of 2D band was inversely proportional to these defects. Thus, the intensity of 2D band diminishes and its broadening occurs during sequential preparation steps of P(2-EHA)-GO, intensity being the highest in graphite and the lowest in P(2-EHA)-GO. Observing the Raman spectroscopic plots of graphite, GO and VGO, it can be concluded that graphite was successfully oxidized to graphene oxide**.**

The Raman spectrum of P(2-EHA) exhibited several peaks attributed to the functional groups present in a polymeric material as can be seen from Fig. 5.4 (b). A weak Raman peak at 1072 cm^{-1} corresponds to the O-C-C band of esters of primary alcohol. The peak observed at 1452 cm^{-1} corresponds to asymmetric bending vibrations observed in methyl groups. The peak at 1731 cm^{-1} appeared owing to C=O bond present in the ester group of P(2-EHA). The Raman peaks at 2870 cm^{-1} and 2929 cm^{-1} appeared owing to symmetric and asymmetric C-H vibrations (stretching) exhibited by methyl groups respectively.

The Raman spectrum of P(2-EHA)-1%GO [Fig. 5.4 (b)] exhibited a number of new peaks corresponding to the in-situ polymerization of monomer in presence of GO nanosheets. The Raman spectrum of P(2-EHA)-GO exhibited peaks at 1076 cm^{-1} (O-C-C band, esters), 1740 cm^{-1} (C=O bond, esters), 2868 cm^{-1} and 2925 cm^{-1} (C-H stretching, methylene), which is attributed to characteristics inherited from polymer P(2-EHA) in nanocomposite. Peak at 1495 cm^{-1} corresponds to C=C stretching usually observed in aromatic structures. Peak at 1367 cm^{-1} corresponds to D band while peak at 1590 cm^{-1} corresponds to G band. D band was observed to be intense than G band, indicating possible chemical treatment of carbon skeleton and reduction in the sp^2 hybridization in the nanocomposite. These peaks confirmed the presence of graphitic structure in nanocomposite. Peak at 1740 cm^{-1} corresponds to C=O group of synthesized ester formed post the esterification reaction. Peaks observed at 2868 cm^{-1} and 2925 cm^{-1} are

attributable to symmetric and the asymmetric stretching vibrations of methylene groups (Silverstein et al., 2014). From the Raman analysis of graphite and its derivatives, detailed information of functional groups present were obtained and it helped to characterize the synthesized nanocomposite.

5.3.3 NMR spectroscopic analysis

^{13}C NMR spectroscopy of graphene oxide (GO) was performed. In GO, major ^{13}C NMR peaks were observed in Fig. 5.5 (a) at 59.67 ppm corresponding to the epoxy groups (C-O-C) and the peak at 69.436 ppm corresponds to hydroxyl groups (-OH). The peak at 129.179 ppm is attributed to the unsaturated sp^2 hybridized carbon (C=C) present in the aromatic rings of GO. These double bonds can be conjugated or isolated in the aromatic structure (Feng et al., 2012). The peaks at 165.062 ppm and 193.6 ppm corresponds to the presence of COOH group. In vinyl graphene oxide (VGO), the major ^{13}C NMR peaks in Fig. 5.5 (b) at 59.96 ppm, 69.398 ppm, 129.358 ppm and 191.539 ppm were observed due to the characteristics acquired from GO. The peak at 165.062 ppm in GO (due to COOH groups) got shifted to 170.997 ppm in VGO owing to the formation of an ester (functional group R-COOR) during the Pinners reaction in VGO (Silverstein et al., 2014; Feng et al., 2012).

For further understanding of the chemical structure of P(2-EHA), ^1H NMR spectroscopy was performed as shown in Fig. 5.5 (c). ^1H NMR peaks at 0.882, 0.896 ppm chemical shift corresponds to methyl groups ($-CH_3$) in P(2-EHA). While the peaks at 1.280 -1.379 ppm chemical shift corresponds to the methylene ($-CH_2$) groups in P(2-EHA). ^1H peaks in the range 1.5 - 2.5 ppm and 4.034 - 4.079 ppm are attributed to the presence of ester groups in the polymer P(2-EHA). While the peaks at 3.9 ppm corresponds to the pendant methylene protons. ^1H peaks at 5.53, 5.58 ppm indicates the presence of some unreacted alkene left from the polymerization process and the peak at 7.26 ppm is attributed to the solvent $CDCl_3$ used for dispersing the polymer for the NMR analysis. A sharp singlet at 7.26 ppm indicating the presence of residual protons in solvent $CDCl_3$, has been removed from the NMR spectra for convenience. Thus, a comprehensive spectroscopic study of the polymer nanocomposite revealed the possible chemical structures present in it and improved our understanding about it (Silverstein et al., 2014).

Fig. 5.5 (d) illustrates the ^1H NMR spectra of nanocomposite P(2-EHA)-1% GO, where the peaks in chemical shift range 0.87 - 0.89 ppm corresponds to methyl proton

(functional group -CH_3) present in the polymer P(2-EHA). Strong NMR peaks in chemical shift range 1.27 - 1.4 ppm appeared due to the methylene protons present in the P(2-EHA), indicating the substantial presence of alkanes in the nanocomposite. The peaks in range 1.56 - 1.61 ppm are attributed to methine protons (functional group =CH-) of an ester group, confirming the esterification reaction of VGO. Also, the singlet appearing at 2.28 ppm is attributed to the presence of epoxy groups on the VGO sheets. Also, the peaks in range 3.9 - 3.96 ppm corresponds to methylene protons (functional group =CH_2) present in the polymer. While, the peaks in range 4.06 - 4.08 ppm are attributed to methylene protons in an ester group present in the polymer. The peaks in range 5.52 - 5.82 ppm corresponds to vinylic groups, which were present in VGO sheets. The peaks in the chemical shift range 6.09 - 6.15 ppm are attributed to alkenes present in unreacted monomer 2-EHA. Moreover, the two doublets observed at 6.36, 6.37 ppm and 6.40, 6.41 ppm are attributed to the presence of aromatic system in P(2-EHA)-GO and also, the peaks in range 7.51 – 8.21 indicates towards presence of aromatic system (mainly phenyl functional group) in the nanocomposite. A sharp singlet at 7.26 ppm indicating the presence of residual protons in solvent $CDCl_3$, has been removed from the NMR spectra for convenience. Thus, a comprehensive spectroscopic study of the polymer nanocomposite revealed the possible chemical structures present in it and improved our understanding about it (Silverstein et al., 2014).

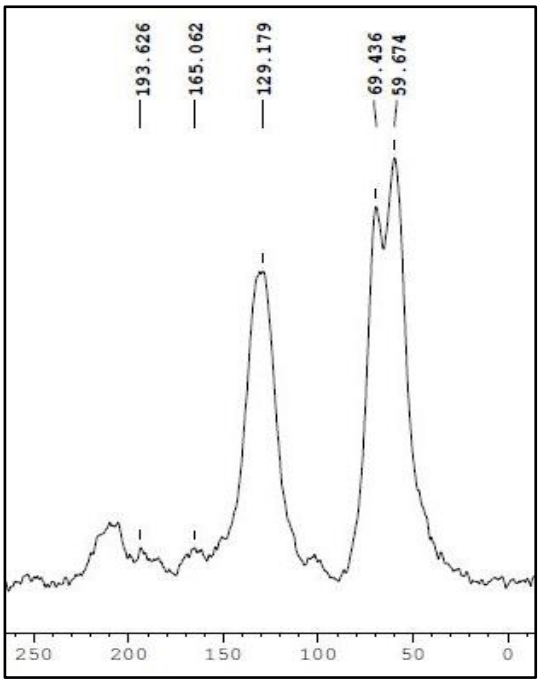

Figure 5.5 (a). ^{13}C NMR of GO

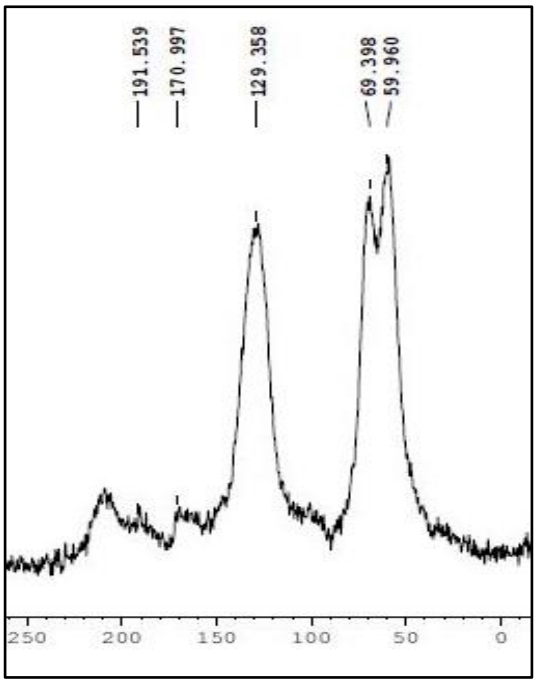

Figure 5.5 (b). ^{13}C NMR of VGO

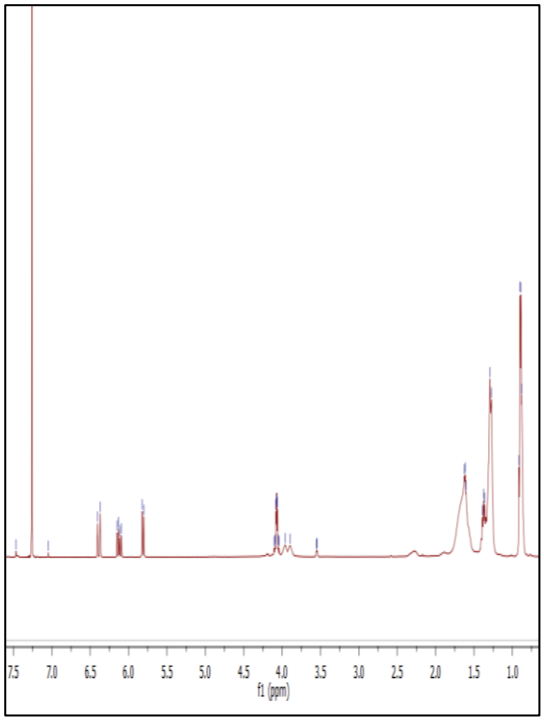

Figure 5.5(c). ^{1}H NMR of P(2-EHA)

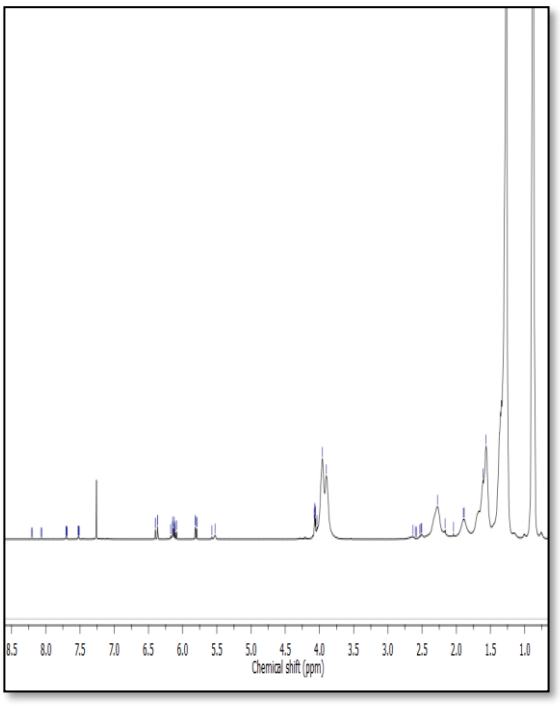

Figure 5. 5(d).^{1}H NMR of P(2-EHA)-1%GO

5.3.4 XRD analysis

As observed from the Fig. 5.6, graphite exhibited a characteristic peak at 2θ = 26.5°, which corresponds to an interlayer spacing of 3.36 A° (calculated based on Bragg's equation nλ= 2dSinθ) (Zhang *et al.*, 2009). GO showed a major peak at 2θ = 10.3°, corresponding to an interlayer spacing of 8.58 A° (Venugopal *et al.*, 2012). This substantial increase in interlayer spacing signifies that graphite was successfully oxidized to GO. This increase in spacing may be attributed to the incorporation of hydroxyl, epoxy and carboxyl functional groups on graphene oxide sheets on its surfaces and at edges. A subsequent reduction in Bragg's angle and a corresponding increment in interlayer spacing was obtained in VGO. Interlayer spacing in VGO was found to be further enlarged to 12.45 A° corresponding to Braggs' angle 2θ = 7.1°, which confirms the incorporation of vinylic esters in it. The nanocomposite exhibited two significant peaks, the broader peak at 2θ = 19.362° and a small peak at 2θ = 6.353° corresponding to the polymer P(2-EHA), which occupies majority of the polymer nanocomposite. Moreover, interlayer spacing of nanocomposite increased to 13.9 A° (corresponding to 2θ = 19.362°) indicating that VGO sheets were properly embedded in the polymer matrix. Thus, the XRD experiment helped to gain understanding about the structural changes in the nanocomposite.

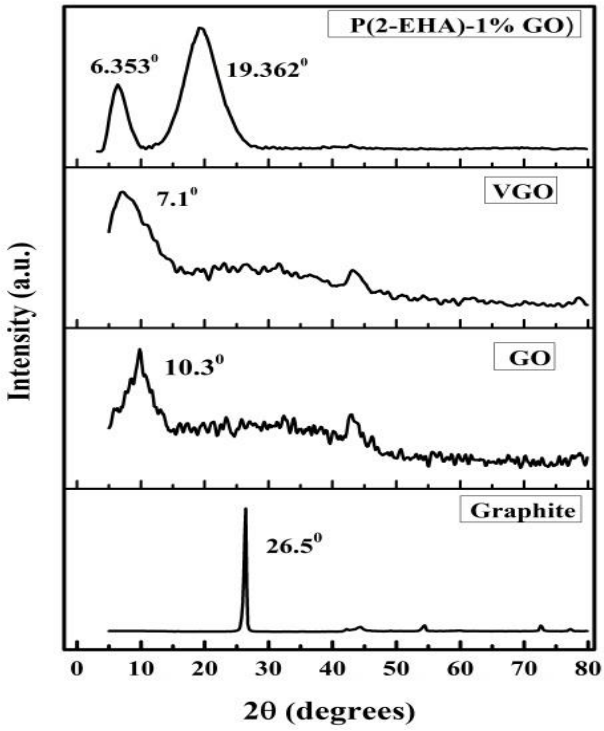

Figure 5.6. XRD plot of Graphite, GO, VGO and P(2-EHA)-1% GO

5.3.5 UV - visible spectroscopy of chemical additives

This technique aids in confirming and understanding the formation of nanocomposites. Graphite, GO, P(2-EHA) and P(2-EHA)-1% GO were initially mixed in Tetrahydrofuran (THF) and then sonicated for two minutes to get them properly dispersed before the measurements are performed with the UV-visible spectrophotometer. The UV-visible absorption spectra of the dispersed chemicals can be observed from Fig. 5.7 and the dispersion of samples in THF is exhibited in Fig. 5.8. Absorbance of the prepared solutions were measured over a wavelength range of 200-700 nm. Graphite exhibits a major absorption peak at 240 nm, which is attributed to the $\Pi \rightarrow \Pi^*$ transition of aromatic C=C bonds**.** Two major peaks are observed in absorption spectra of GO at 230 nm and 305 nm. The absorption peak at 230 nm is attributed to characteristic $\Pi \rightarrow \Pi^*$ transition of aromatic C=C bonds, while a small absorption peak at 305 nm corresponds to $n \rightarrow \Pi^*$ transition owing to the stretching mode of carbonyl groups in GO. In P(2-EHA), absorption peaks are recorded at 232 nm and 276 nm. In the nanocomposite P(2-EHA)-

1% GO, the peak at 232 nm appearing due to $\Pi \rightarrow \Pi^*$ transition get redshifted to 234 nm. The absorption peaks at 233 nm and 276 nm in nanocomposite are attributed to the characteristics of P(2-EHA) in nanocomposite, while a new peak appearing at 314 nm in nanocomposite is a result of red shifting of the peak at 305 nm (present in GO), which is attributed to $n \rightarrow \Pi^*$ transition owing to the stretching mode of C=O bonds in GO. Thus, from the observations it can be concluded that UV-visible spectroscopy helped to understand the formation of nanocomposite.

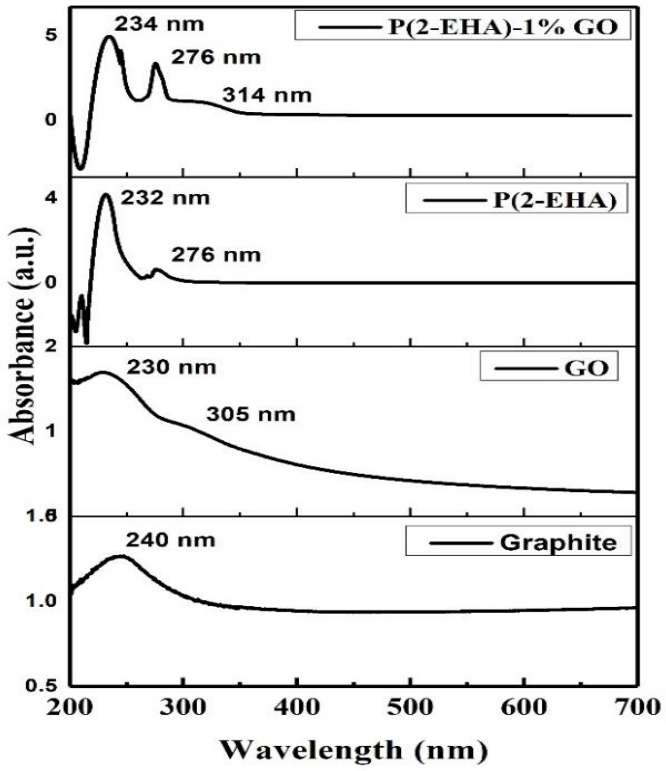

Figure 5.7. UV-visible spectroscopic plot of Graphite, GO, P(2-EHA) and P(2-EHA)-1% GO

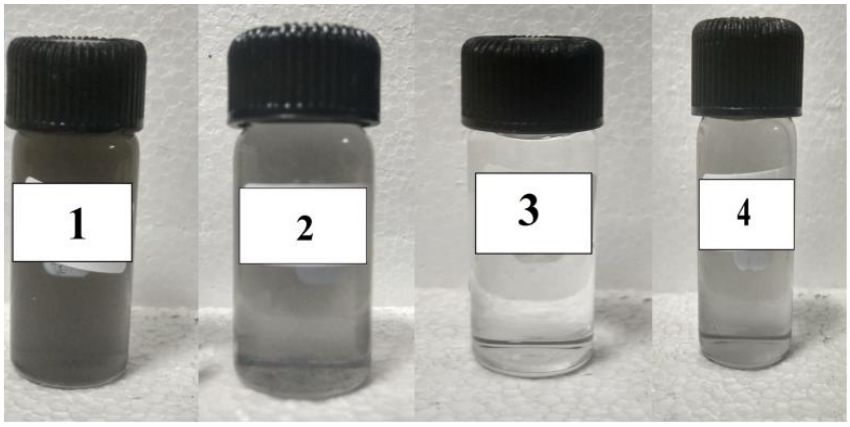

Figure 5.8. Images of dissolution of (1) Graphite, (2) GO, (3) P(2-EHA) and (4) P(2-EHA)-1% GO in THF solvent

5.3.6 FE-SEM analysis

The modifications in the surface morphology of GO and nanocomposites were understood by conducting FE-SEM imaging analysis exhibited in Fig. 5.9 (a)-(d). FE-SEM images of graphene oxide [Fig. 5.9 (a)] illustrates a characteristic sheet type structure. The sheet structure appears somewhat disordered owing to the residence of oxygenated functionalities on the edges and surfaces of graphene oxide (Bhawal *et al.*, 2016). FE-SEM images of vinyl graphene oxide as observed in Fig. 5.9 (b) reveals a slight modification in the sheet structure exhibiting wrinkles and crumpled structure possibly owing to introduction of vinyl functional groups over the GO sheets. FE-SEM images of P(2-EHA)-1% GO [Fig. 5.9 (c) & 5.9 (d)] exhibits the VGO sheets being firmly embedded within the gelled polymer P(2-EHA) resulting in a glutinous structure which resembles a lesser wrinkled nanocomposite. Specifically, VGO appeared to be well dispersed in P(2-EHA) matrix as observed from Fig. 5.9 (c) & 5.9 (d), indicating occurrence of an intense grafting of polymer P(2-EHA) on VGO sheets resulting in formation of P(2-EHA)-1% GO nanocomposite.

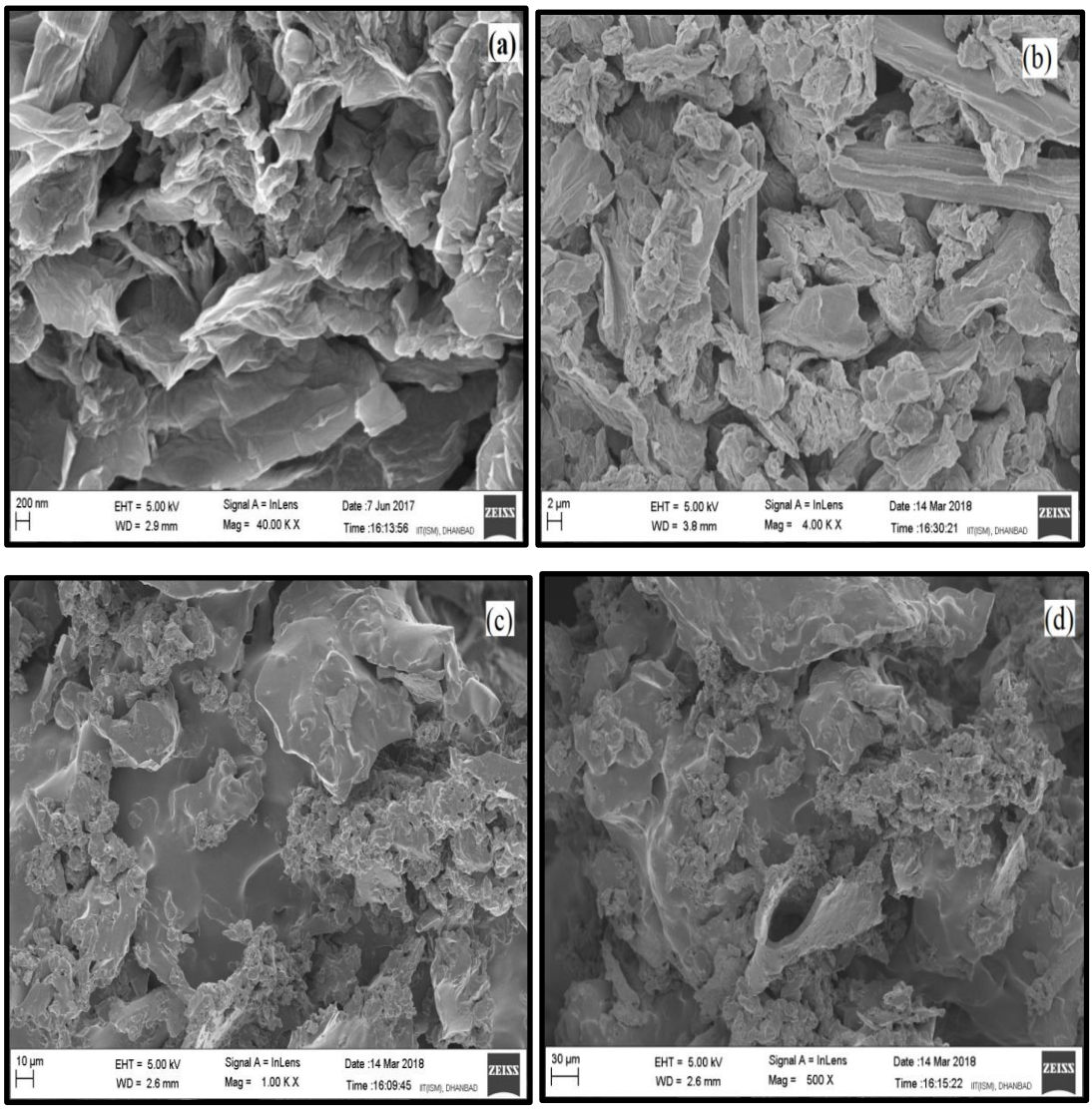

Figure 5.9. FE-SEM images (a) GO, (b) VGO, (c) & (d) P(2-EHA)-1% GO

5.3.7 Thermal Analysis

Thermal characteristics of the synthesized products were studied and compared using thermogravimetric analysis (TGA) in a nitrogen atmosphere. A broad temperature range in the experiments was used to study the detailed thermal characteristics of the polymeric additives, although these temperatures used are relatively higher than that prevalent in oilfield operations/petroleum industry. The recorded TGA curves are exhibited in Fig. 5.10 (a). P(2-EHA) was formed by the free radical polymerization technique and the major degradation stages of P(2-EHA) would be discussed in this section. Polymeric structure of P(2-EHA) starts to gradually degrade from 125℃ owing

to the cleavage of polymeric chains possessing head to head linkages which were formed by termination by combination mechanism. Further, the significant degradation commences at 270℃ attributable to cleavage of chains at unsaturated ends formed from termination by disproportionation mechanism. Lastly, another mass degradation starts at 430℃ owing to the random chain breakages in P(2-EHA) matrix (Sharma, Mahto and Vuthaluru, 2019).

Stage-wise weight loss was experienced by GO as it was heated over a temperature range (25 °C - 600°C) and the loss occurred moderately initiating from room-temperature itself. The first stage of thermal degradation in GO lasted up to 100°C, accounting for 11 wt. % mass loss, which might be attributed to the release of water molecules trapped between GO sheets upon the initial heat treatment. The second stage of degradation continued up to 240°C and resulted in a significant 29 wt. % loss, which might be accounted to the possible loss of less stable oxygen functionalities such as hydroxyl, COOH and epoxy groups. Subsequently, a gradual thermal degradation continued till 600°C which accounted for another notable weight loss (~ 15 wt. %), this could be a result of decomposition of more stable functional groups including carbonyl and esters present on the GO sheets (Hou *et al.*, 2018). This thermogram of GO highlights its excellent thermal resistance tendency till higher temperatures. Therefore, the thermal stability of the nanocomposite would be significantly beneficiated upon inclusion of GO sheets into the polymer system.

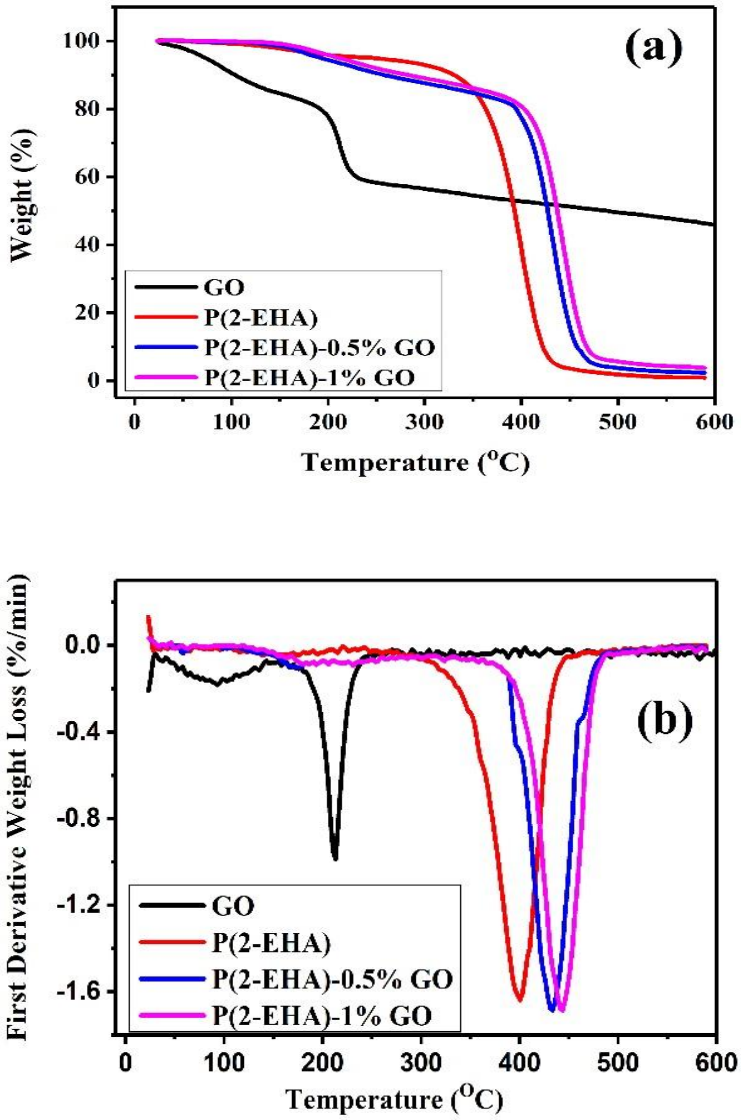

Figure 5.10. TGA (a) and DTG (b) of GO and chemical additives

The thermal stability profile of the nanocomposite P(2-EHA)-1% GO as illustrated through DTG, which is displayed in Fig. 5.10 (b), was observed to be better than the base polymer P(2-EHA). At temperatures up to 150°C, both the polymers and nanocomposite have similar thermal characteristics. Maximum weight loss temperature (T_{max}) appears at 400°C for P(2-EHA). Incorporation of 0.5 wt.% GO in polymer system resulted in shift of T_{max} to 430°C, while the addition of 1 wt.% GO resulted in T_{max} to 450°C, indicating the improvement in thermal properties of nanocomposites due to addition of GO sheets as compared to base polymer. This increase in the thermal

resistance of nanocomposite at high temperatures might be attributed to the excellent thermal characteristics of GO sheets being embedded in the nanocomposite.

As observed in the TGA and DTG plots of pour point depressants, there are overlapping decomposition processes of P(2-EHA), and especially the P(2-EHA)-0.5% GO and P(2-EHA)-1% GO. In this case, DTG helped to identify their T_{max} and moreover, clearly exhibits the gradual shift in T_{max} of different PPDs with temperature, which was not so clear in their TGA plots. DTG peak height at any temperature gives the rate of mass loss, which indicated that the weight losses in nanocomposites occurred faster but at higher temperatures than P(2-EHA). Also, the area under the DTG peak is directly proportional to the weight loss, the DTG peak of P(2-EHA) is broader than nanocomposites, indicating greater mass loss occurs at lower temperatures compared to nanocomposites. T_i is nearly the same around 140℃ for the P(2-EHA), P(2-EHA)-0.5% GO and P(2-EHA)-1% GO. T_f is around 450℃ and 490℃ for P(2-EHA) and nanocomposites respectively, suggesting the superior thermal characteristics of nanocomposites. Thus, TGA and DTG of additives helped to gain a comprehensive understanding about their thermal stabilities.

5.4 Evaluation of the synthesized additives

5.4.1 Pour point depression

Pour point of the virgin crude oil sample was observed to be 36°C. Reductions in the pour point of crude oil treated with different chemical additives are illustrated in Fig. 5.11. The best improvement in pour point was found with addition of P(2-EHA)-1% GO, producing a 18°C drop in pour point of crude oil at 750 ppm concentration, while 15°C depression is observed in case of P(2-EHA)-0.5% GO and only 12°C reduction was observed when treated with P(2-EHA) at the same concentration. Upon increasing the GO content, the beneficiation effect of nanocomposite PPD is improved. The pour point of the treated crude oil is found to increase above the PPD optimized concentration due to suspension of additional quantity of doped additives, subsequently leading to increased gelling in crude oil and greater difficulty in flow ability of crude oil (Sharma, Mahto and Vuthaluru, 2019). Depression in the pour point caused by P(2-EHA) additive could be attributed to co-crystallization of its polymeric chains with the wax crystals, thereby

reducing the wax precipitation tendency. The action mechanism of polymer nanocomposites on crude oil is different, where an enhanced depression in pour point might be attributed to the role of GO sheets in nanocomposites posing as heterogeneous nucleation sites with interfaces, upon which wax crystals gets precipitated and co-crystallizes with the polymeric chains. This mechanism results in the development of fine wax crystals which remains dispersed in crude oil and avoiding formation of an interconnected wax crystal network, and in this way nanocomposite PPD weakens the wax structures, enhancing the flow ability of crude oil.

The possible interaction of nanocomposites and P(2-EHA) with wax crystals is illustrated in the Fig. 5.12. As shown in this figure, GO sheets act as nucleation templates for wax precipitation where the polymer chains attached to GO sheets binds well with wax molecular chains, thereby reduces the possible interactions among wax crystals and the development of a dense wax network. This mechanism leads to an enhanced pour point depression in nanocomposite PPD-treated crude oil. Moreover, this enhancement in the flow ability of crude oil could be further substantiated by understanding the modifications in the wax network morphology upon interaction with nanocomposites, which was visualized through their polarized microscopic observations, where a dispersed and disassociated wax structure was observed as discussed later in the current article. Therefore, several disassociated nucleation templates with polymer co-crystallized wax molecules deposited on them would be present in the crude oil system, leading to a uniform dispersion of wax crystals and reduced networking between them.

While in the case of polymer P(2-EHA), the wax crystals co-crystallize with the P(2-EHA) chains and in this way reduces the interaction among wax crystals leading to improvement in arrangement of wax molecular structure. This mechanism keeps the wax molecules in a dispersed state but in a less regular arrangement than the nanocomposite PPDs, due to absence of nanosheets, resulting in reduced inhibition to wax networking.

Pour points of crude oil samples treated with polymeric nanocomposites containing 1.5 wt.% GO and 2 wt.% GO were also tested, but the results indicated substantially higher values of optimum pour points of 27°C and 30°C respectively. The reason for this unusual result may be attributed to the presence of excessive nucleation sites (due to greater quantity of GO sheets), leading to an increased wax precipitation and subsequent agglomeration of wax crystals, possibly due to attractive forces between wax

crystals overcoming their co-crystallization tendency (between wax crystals and polymer chains on GO sheets). Therefore, nanocomposites containing only 0.5 wt.% GO and 1 wt.% GO were considered for further evaluation tests as PPDs in the current article.

Moreover, the pour points of the crude oils were also determined with the addition of GO and VGO alone to check the possible influence of nanosheets individually, where GO and VGO (dispersed in xylene) were doped in concentration ranging from 250-1500 ppm in crude oil. This test was conducted in order to check the possible influence of nanoparticles alone on the flow improvement of crude oil. The results showed that there is no change in pour point of the crude oil upon doping GO and VGO only. Thus, it can be concluded that the nanoparticles alone have no influence on the flow ability of crude oil, rather it improves beneficiation of polymer PPD when formed a polymer nanocomposite.

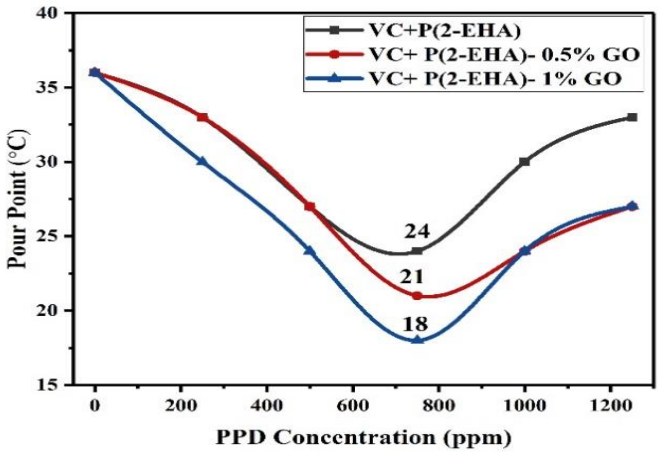

Figure 5.11. Pour point reduction of virgin crude oil (VC) with additives

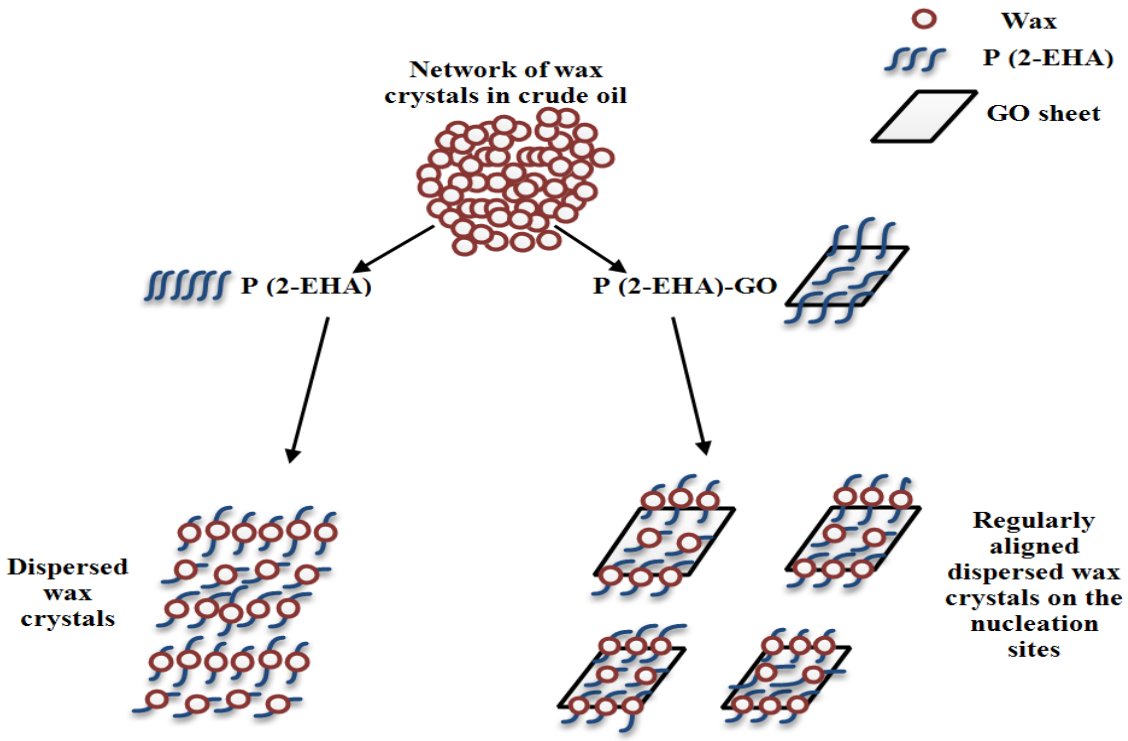

Figure 5.12. Schematic diagram representing possible interaction of P(2-EHA) and polymer nanocomposite P(2-EHA)-GO with the wax crystals in crude oil

5.4.2 Effect on apparent viscosities

Apart from the restart flow studies of crude oil, in order to analyze the dynamic flow characteristics of PPD-treated crude oil samples in pipelines, flow curves of virgin as well as additive-treated crude oil were studied over temperature range 10 - 40°C and shear rates between 0 - 100 s^{-1}, as is represented in Fig. 5.13 (a)-(d), where the measurements were performed with optimized concentrations of additives doped in crude oil. The apparent viscosities of the additive-treated crude oils decrease with increasing shear rate (i.e. shear thinning behavior) and their viscosities also decrease with increase in temperature. The figures indicate that improvement in the apparent viscosity curves of additive–treated crude oils occur in the following trend; P(2-EHA) < P(2-EHA)-0.5% GO < P(2-EHA)-1% GO. Best beneficiation was observed in case of P(2-EHA)-1% GO, with viscosities dropping down from 1.9 Pa.s (virgin crude oil) to 0.03, 0.02, 0.016 and 0.01

Pa.s at temperatures 10, 20, 30 and 40°C respectively. The rheological experiments were performed thrice and the deviation in the recorded values were reported in the form of percentage error bar.

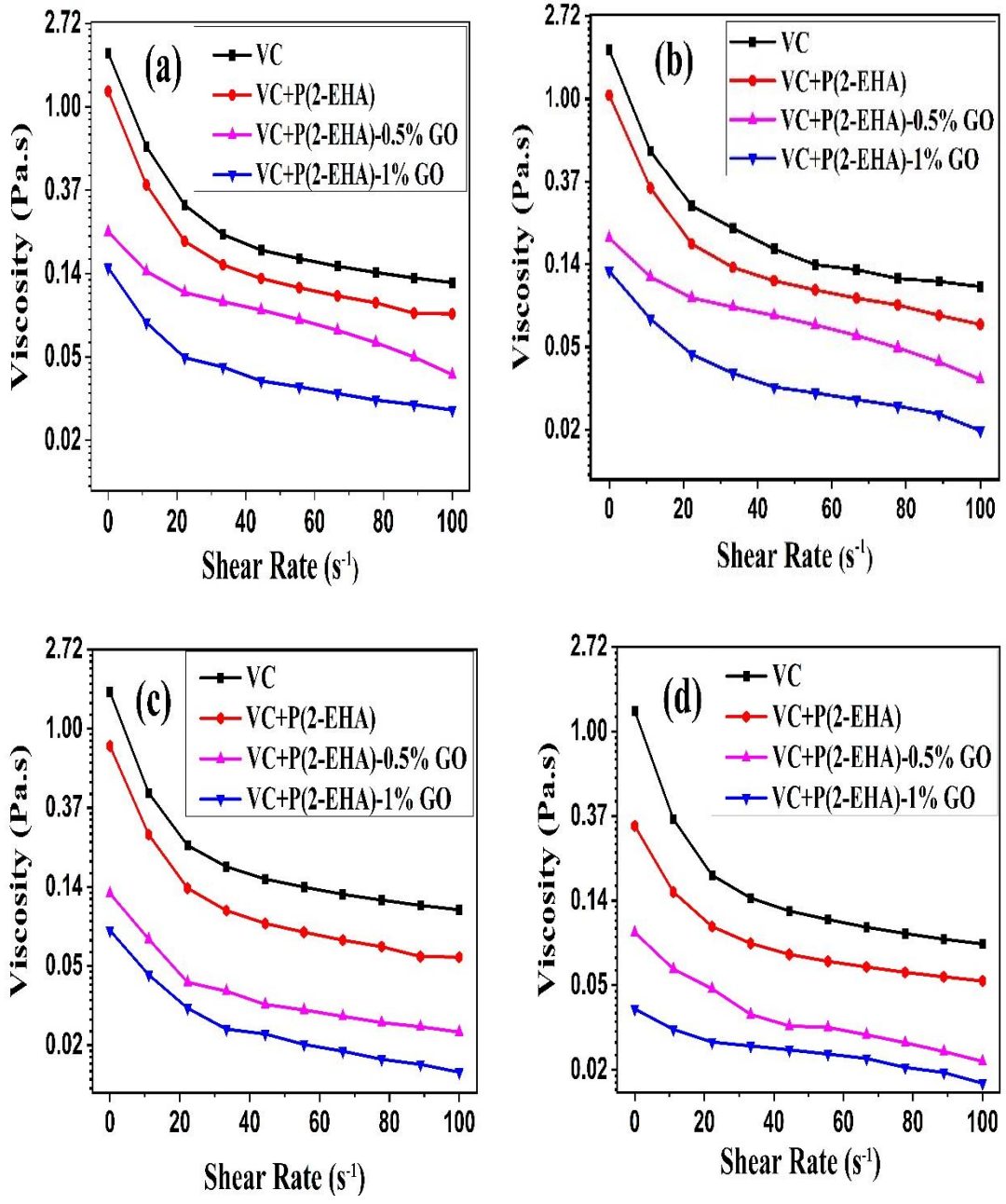

Figure 5.13. Viscosity-shear rate flow curves of virgin crude oil (VC) and the synthesized PPDs treated crude oil samples at different experimental temperatures (a) 10°C, (b) 20°C, (c) 30°C and (d) 40°C

Moreover, Table 5.2. demonstrates the apparent viscosity reduction of PPD-treated crude oils (at its optimum concentration-750 ppm) in terms of percentage change at a shear rate 100 s^{-1}. These reduced viscosities indicates easy flow ability of crude oil through pipelines and highlights that nanocomposite PPDs work well under a set of different pipeline temperatures, and where P(2-EHA)-1% GO was the most effective pour point depressant among all the additives. This improvement in the long term flow properties may be attributed to the presence of GO sheets in the crude oil system, which possibly modifies the wax crystals morphology and their networking capacity.

Table 5.2. Percentage reduction in the apparent viscosities of crude oil upon treatment with different chemical additives in temperature range (10 - 40° C), calculated at the shear rate 100 s^{-1}

Crude oil beneficiated with	Temperature (°C)			
	10	20	30	40
P(2-EHA)	95.6 %	96.4 %	96.4 %	96 %
P(2-EHA)-0.5% GO	97.9 %	98.1 %	98.6 %	98.4 %
P(2-EHA)-1% GO	98.4 %	98.8 %	98.9 %	99.2 %

5.4.3 Aging effect/long term flow characteristics of PPD-treated crude oil

For this rheological test the PPDs were doped at their determined optimized concentrations (i.e.750 ppm). The additive-treated crude oil samples were stored for a particular number of days before performing the rheological tests. As observed from the Fig. 5.14 (a)-(d), there were increases in the apparent viscosities of the PPD-treated crude oils after 15 days and 30 days of storage, measured at temperatures 10^{o}C and 40^{o}C. A lower temperature 10^{o}C was selected to exhibit rheological characteristics far below the pour point and gelation point of samples, while a higher temperature 40^{o}C was chosen to observe changes in viscosities near the pour point and the gelation point of virgin crude oil. Also, measurements at shear rates 10 s^{-1}, 50 s^{-1} and 100 s^{-1} would provide a comprehensive understanding of the flow behavior of samples under different shear conditions, usually encountered in a pipeline flow. PPD P(2-EHA) resulted in a 19.8 – 76.7 % increase in viscosities of crude oil , while P(2-EHA)-0.5% GO resulted in 22.6 –

49.1 % increase in apparent viscosities, while the PPD P(2-EHA)-1% GO showed the least increase of about 11.4 – 29.8 % over a shear rate range of 0-100 s^{-1}. This test further highlights the beneficiation of the crude oil characteristics upon doping with P(2-EHA)-1% GO and suggest a long term beneficiation effect (until 30 days of pipeline being shutdown) which is advantageous from the perspective of pipeline routine operations. The measured data indicates that at low temperatures, the surge in apparent viscosities recorded was higher than at 40°C, because at low temperatures there is a decrease in co-crystallization tendency of waxes with the polymeric structures, resulting in wax precipitation and gelling of crude oil (Borthakur *et al.*, 1995).

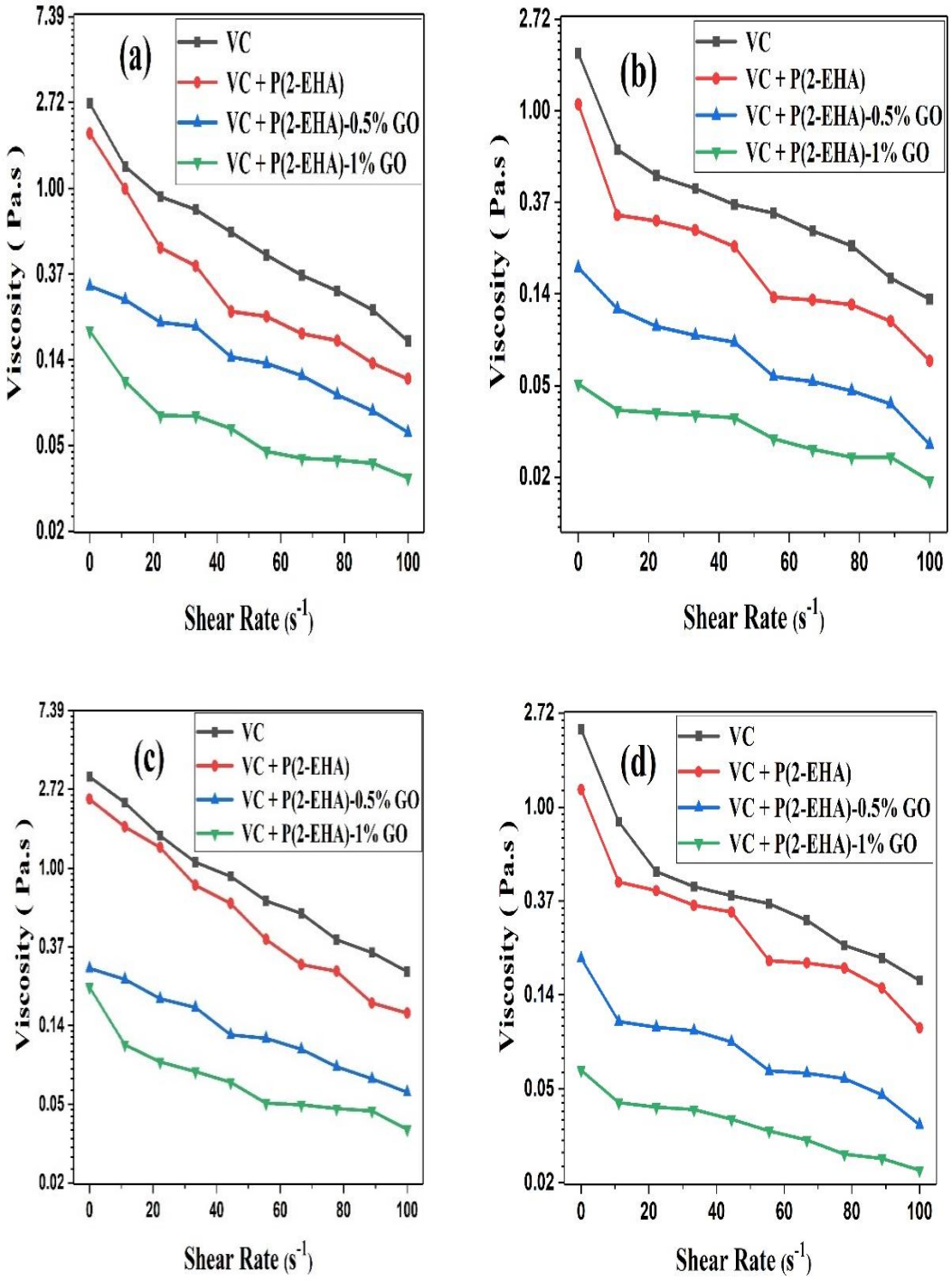

Figure 5.14. Rheograms of treated crude oil samples after (a) 15 days at 10°C, (b) 15 days at 40°C, (c) 30 days at 10°C, and (d) 30 days at 40°C

Moreover, it can be seen from the Fig. 5.13 (a)-(d), that the non-Newtonian characteristics and shear thinning flow behavior was exhibited by all the PPD-treated crude oils samples even after 15 and 30 days of storage. Also, the significant degradation in rheology of P(2-EHA)-doped crude oil with viscosities surging upto 77% (from the original viscosities at initial day) upon its long term storage, indicates that although P(2-EHA) proved to be a good PPD for waxy crude oil, but with time its performance gets limited. On a similar line, although P(2-EHA)-0.5% GO previously resulted in a notable pour point reduction but the treated crude oil rheological characteristics degrades on long term storage (upto 49% increased viscosity from original is observed with P(2-EHA)-0.5% GO), nevertheless its performance was much better than PPD P(2-EHA), emphasizing the importance of GO sheets in polymeric system in order to improve the flow characteristics. With P(2-EHA)-1% GO, a maximum viscosity increase of 29% was observed, which is quite lower than the other PPDs used. With all the PPDs, rheological characteristics after 30 days degraded more compared with that of post 15 days, which indicates a greater wax precipitation during this period, ultimately increases gelation tendency of crude oil. Also it is to be noted that at low and medium shear rates i.e. 10 s^{-1} and 50 s^{-1} respectively, the increase in viscosity observed was greater than at higher shear rate 100 s^{-1}, indicating a better performance of these PPDs at higher shear rates. These rheograms also hints towards the improved flow performance of crude oil with nanocomposite PPDs even when encountered with low shear rates in pipelines. The long term stability of crude oil doped with P(2-EHA)-1% GO was found to be the best among all the additives tested, with the increase in viscosity being limited to under 30% for all the shear rates at both low (10°C) and high (40°C) temperatures.

Moreover, the Table 5.3 shows that the pour point of PPD treated-samples suffers degradation with storage time. P(2-EHA)-treated crude oil experiences increment in pour point of about 6°C & 9°C, same increments were observed with P(2-EHA)-0.5% GO, while the least surge was observed with P(2-EHA)-1% GO of 3°C & 6°C on 15 and 30 days of storage respectively. With increase in the GO content from 0.5 to 1 wt. % in the PPD, there is a significant improvement in the long-term rheological characteristics of crude oils as the percentage increase in viscosities are controlled substantially with the passage of time (at a broad range of shear rate and under different set of temperature conditions) and also the degradation in pour points are controlled with storage time. This

improvement might be attributed to the increased density of GO sheets in nanocomposite PPD, which through its nucleation mechanism, hindered the tendency of waxy crystals to interlock and expand its presence in crude oil during the pipeline shutdown, and thus would provide better flow characteristics upon restart application of pipeline.

P(2-EHA)-1% GO treated crude oils have exhibited better flow characteristics after 15 and 30 days of storage compared to the previously synthesized nanocomposite PPD PMMA-1% GO (Sharma, Mahto and Vuthaluru, 2019) which suffered upto 34.3% increase in apparent viscosity at 40°C (after 15 days), while only 11.4 % – 27.8 % surge (observed after 15 days) and an increase of 25.6 % - 29.8 % (after 30 days) in the case of P(2-EHA)-1% GO was observed. This improved performance of P(2-EHA)-1% GO compared to PMMA-1% GO might be attributed to the high molecular weight P(2-EHA) chains co-crystallizing better with the wax crystals for a longer duration, avoiding wax precipitation and thereby providing improved crude oil flow characteristics for greater time. Also, the improvement in the pour point of crude oils having low asphaltene content is better when treated with high molecular weight chemical additives (Taraneh *et al.*, 2008) such as with P(2-EHA) on the Indian waxy crude oil in this research work. This improvement may also be linked to the changes in morphological behavior of wax crystals when treated with P(2-EHA)-1% GO (completely dispersed in oil) compared to with PMMA-1% GO where the wax crystals became more compact in shape and less in density (remains still dispersed but in small amounts).

Table 5.3. Aging in the PPD-treated crude oils

PPD	Pour point (°C)	
	15 days	30 days
P(2-EHA)	30	33
P(2-EHA)-0.5% GO	27	30
P(2-EHA)-1% GO	21	24

5.4.4 Effect on gelation tendency of crude oil

Gelation point (GP) is considered to be the temperature where loss modulus (G") equals storage modulus (G') (Yang, Li and Wang, 2013). At temperatures below the gelation point (GP), solid like characteristics of the crude oil dominates, possibly due to precipitation of wax molecules in system and therefore storage modulus overcomes loss modulus at these temperatures. Similarly, at temperatures above the GP, there is more of liquid like characteristics, possibly due to major wax particles are still in dissolved state and thus G'' remains higher than G' (Venkatesan *et al.*, 2002). As observed from the Fig. 5.15 (a), GP of the untreated crude oil was determined as 39.8°C, which indicates that the crude oil is prone to gelling from high temperatures itself. While the GP of P(2-EHA) treated crude oil was found to be 29°C [Fig. 5.15 (b)], GP of P(2-EHA)-0.5% GO treated crude oil was 25°C (Fig. 5.15(c)) and GP of P(2-EHA)-1% GO doped crude oil was 22°C [Fig. 5.15 (d)]. There was a significant reduction about 17.8°C in GP of crude oil upon treatment with P(2-EHA)-1% GO. This reduction of GP brought by addition of nanocomposite PPDs indicates significant enhancement waxy crude oil in terms of restart flow ability.

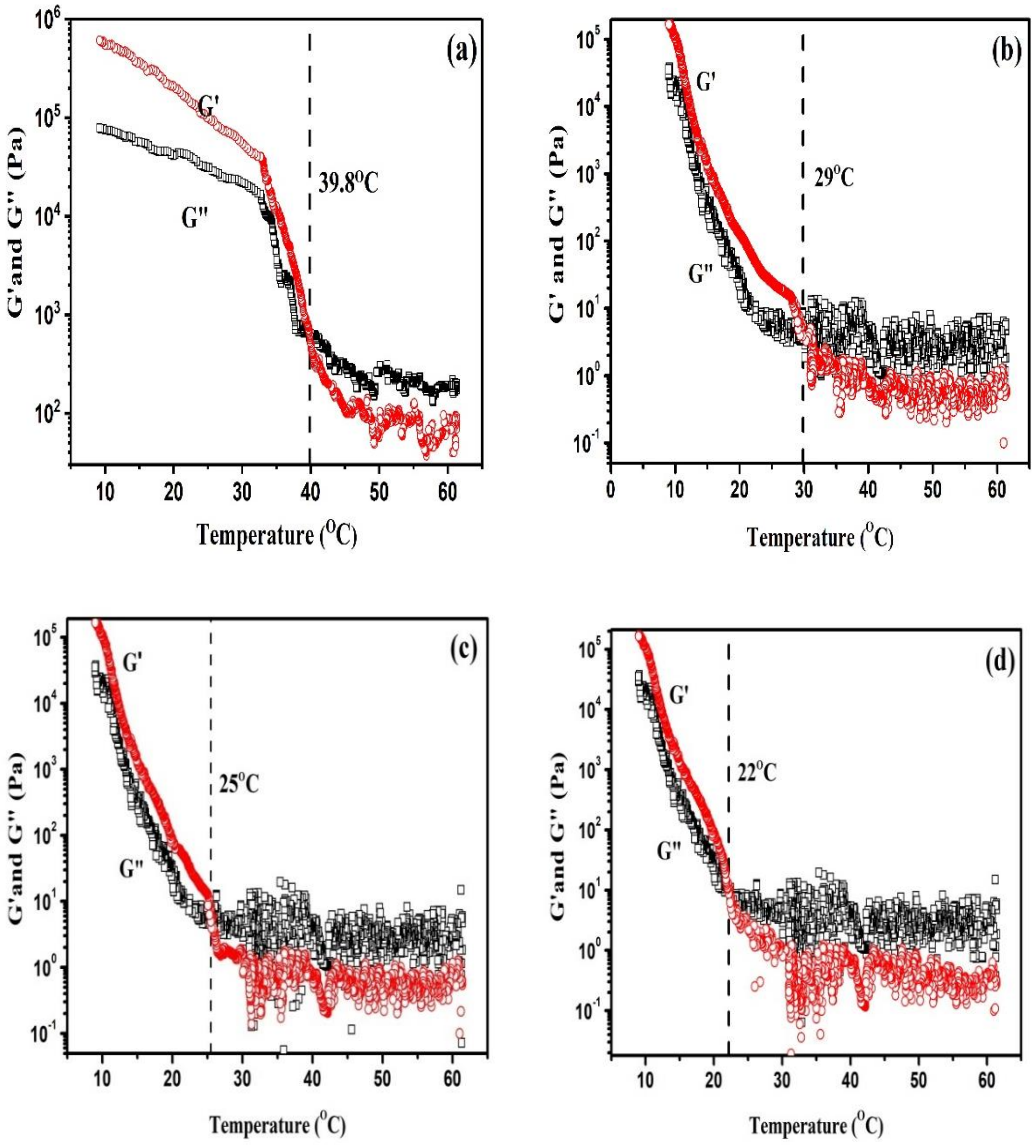

Figure 5.15. Determination of Gelation point from rheometric measurements based on loss modulus (G") and storage modulus (G') for (a) Raw crude oil; and for the crude oil samples doped with following PPDs (b) P(2-EHA), (c) P(2-EHA)-0.5% GO, (d) P(2-EHA)-1%GO

Fig. 5.16 exhibits a graphical comparison of beneficiation in pour point and the gelation point of crude oil upon treatment with different chemical additives (at their optimum concentrations). It can be concluded from the bar chart that additive P(2-EHA)-1% GO was found to be the most effective PPD for the analyzed crude oil.

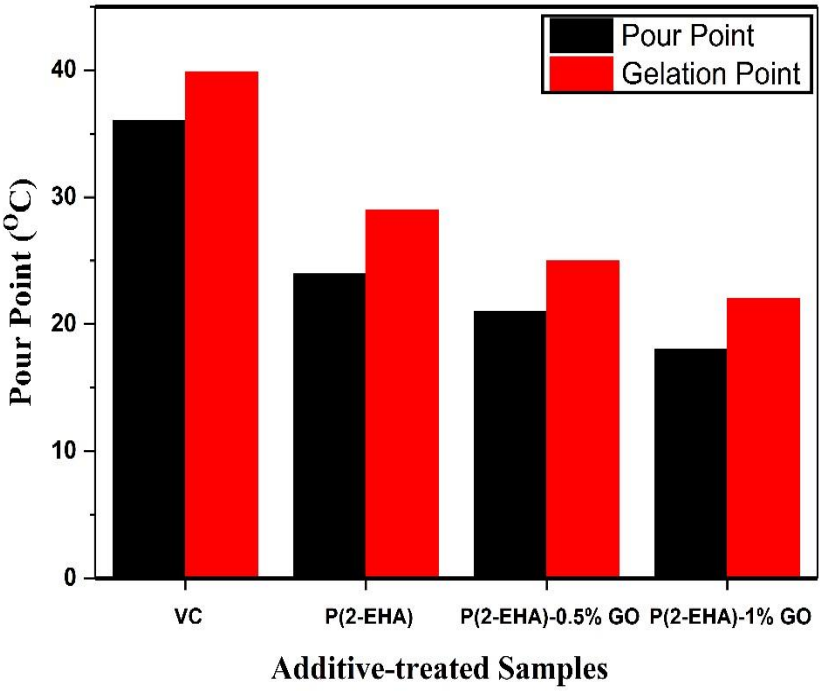

Figure 5.16. Comparison of the beneficiation of pour point and gelation point of crude oil samples treated with different additives (at their optimum concentrations of 750 ppm)

5.4.5 Microscopic analysis of wax crystal morphology

Polarized microscopic imaging of the raw and crude oil treated with nanocomposite PPD are exhibited in Fig. 5.17 (a)-(d). All the additives were doped at their optimum concentrations (750 ppm) in the crude oil samples. In polarization microscopy, the wax crystals appear as bright spots on the black background of crude oil (Ronningsen *et al.*, 1991). As observed from Fig. 5.17 (a), at 19°C a dense and interconnected wax network structure was present in the virgin crude oil. This wax network deteriorates to some extent upon treatment with PPD P(2-EHA) as seen in Fig. 5.17(b). The action mechanism leading to this reduction may be attributed to the co-crystallization of long alkyl chains in P(2-EHA) with wax molecules, which reduces their precipitation tendency and results in reduced wax aggregation in the sample. As observed from Fig. 5.17 (c), P(2-EHA)-0.5% GO has significantly modified the wax crystal morphology; the wax network appeared substantially less interlocked as the wax

molecules have become smaller and seems to be in much dispersed state, possibly avoiding networking. Wax network volume further diminishes and wax crystals seemed to be in much dispersed form when doped with P(2-EHA)-1% GO (Fig. 5.17 (d)). The possible action mechanism of nanocomposites behind this reduced wax crystal density is explained as following: The high surface area bearing GO-sheets acts as nucleation sites/templates upon which wax crystals tend to precipitate, thus improving the co-crystallization capability of polymeric chains (attached on the surfaces of GO sheets) with the wax crystals, keeping the wax molecules in a highly dispersed state and avoids their precipitation. Increased percentage of GO content in P(2-EHA)-1% GO provides more nucleation sites and higher surface area, therefore trapping more wax and providing greater interaction between polymeric chains and wax crystals, thereby showing improved dispersion of wax crystals in crude oil than P(2-EHA)-0.5% GO.

As the temperature is increased to 29℃ and 39℃, we can observe a decrease in the wax crystal density in the Figs. 5.18 (a)-(d) and Figs. 5.19 (a)-(d) respectively, as the solubility of wax crystals in crude oil increases with temperature, and the nanocomposite PPDs exhibits the best improvement, as the density of wax crystals in Figs 5.18 (c)-(d) and Fig 5.19 (c)-(d) reduces substantially, with P(2-EHA)-1% GO improving the wax morphology the most. At temperatures above and below the pour point of all the PPD-treated crude oils, we can observe significant improvement in the wax morphology of nanocomposite treated crude oils. Thus, it was observed from the microscopic analysis that the introduction of GO sheets in the polymer system modified the wax morphology and thereby helped to improve the flowability of the high pour point waxy crude oil. This analysis helps to substantiate the improvements reported in the pour point, flow behaviour and the restart flow ability of nanocomposite PPD-treated crude oils by exhibiting the reduction in abundance and interlocking of wax crystals. Thus, microscopic analysis confirms that the PPD modified the wax crystal network and their precipitation tendency.

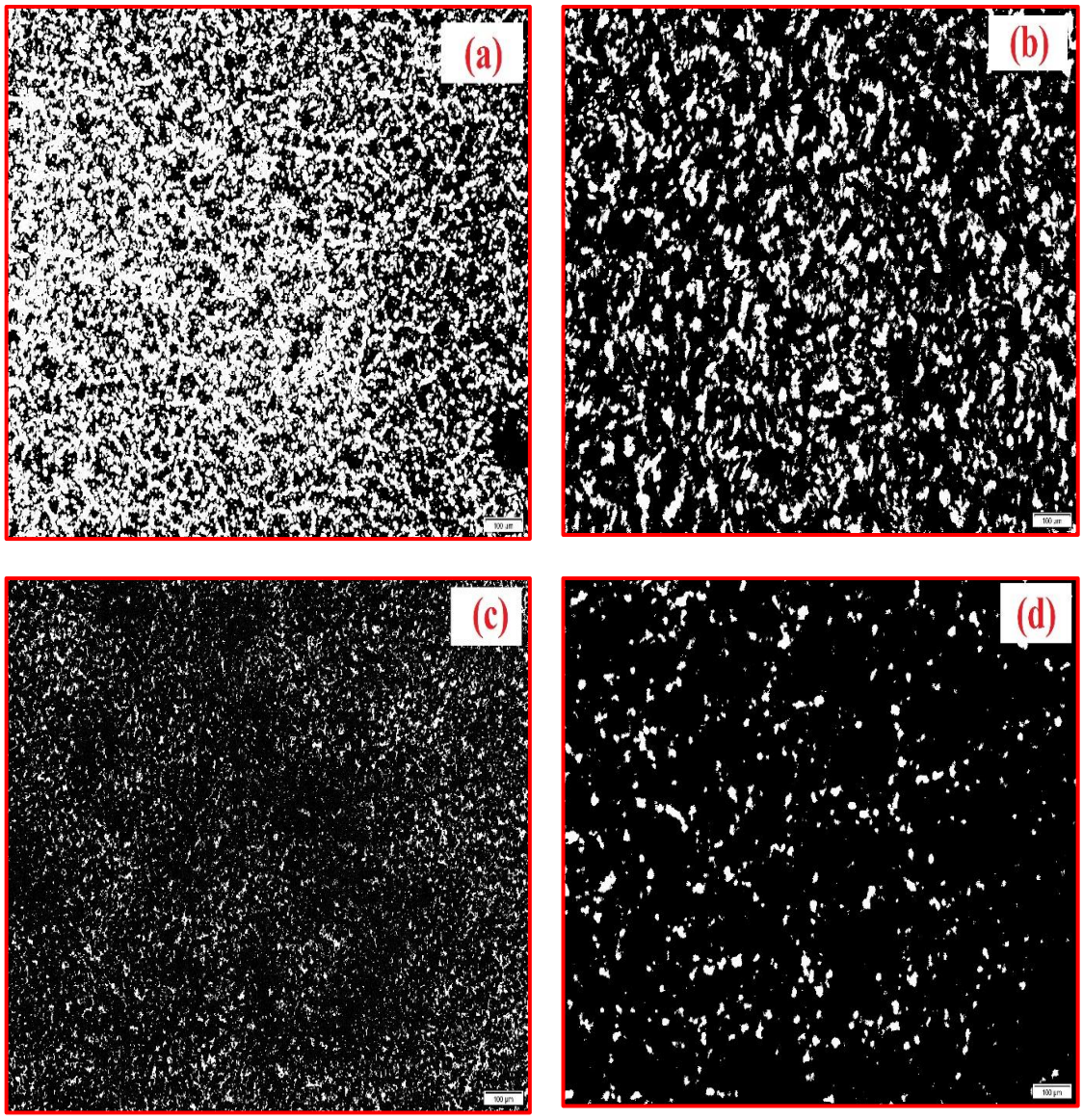

Figure 5.17. Polarized microscopic images at temperature 19°C illustrating wax crystal morphology of (a) Virgin crude oil, and the beneficiation effect of the PPDs on the wax structure of crude oil treated with (b) P(2-EHA) (c) P(2-EHA)-0.5% GO and (d) P(2-EHA)-1% GO

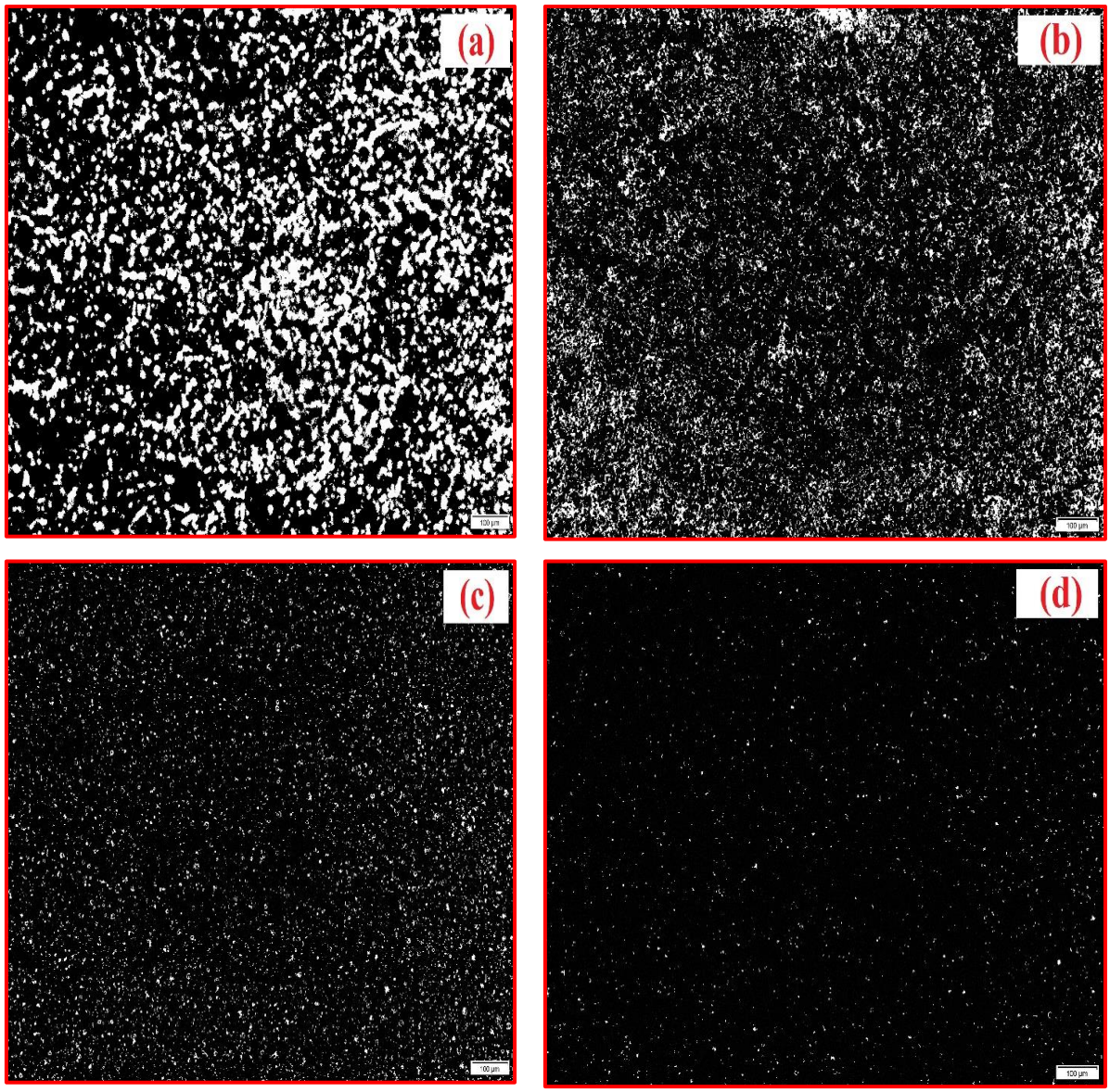

Figure 5.18. Polarized microscopic images at temperature 29°C illustrating wax crystal morphology of (a) Virgin crude oil, and the beneficiation effect of the PPDs on the wax structure of crude oil treated with (b) P(2-EHA) (c) P(2-EHA)-0.5% GO and (d) P(2-EHA)-1% GO

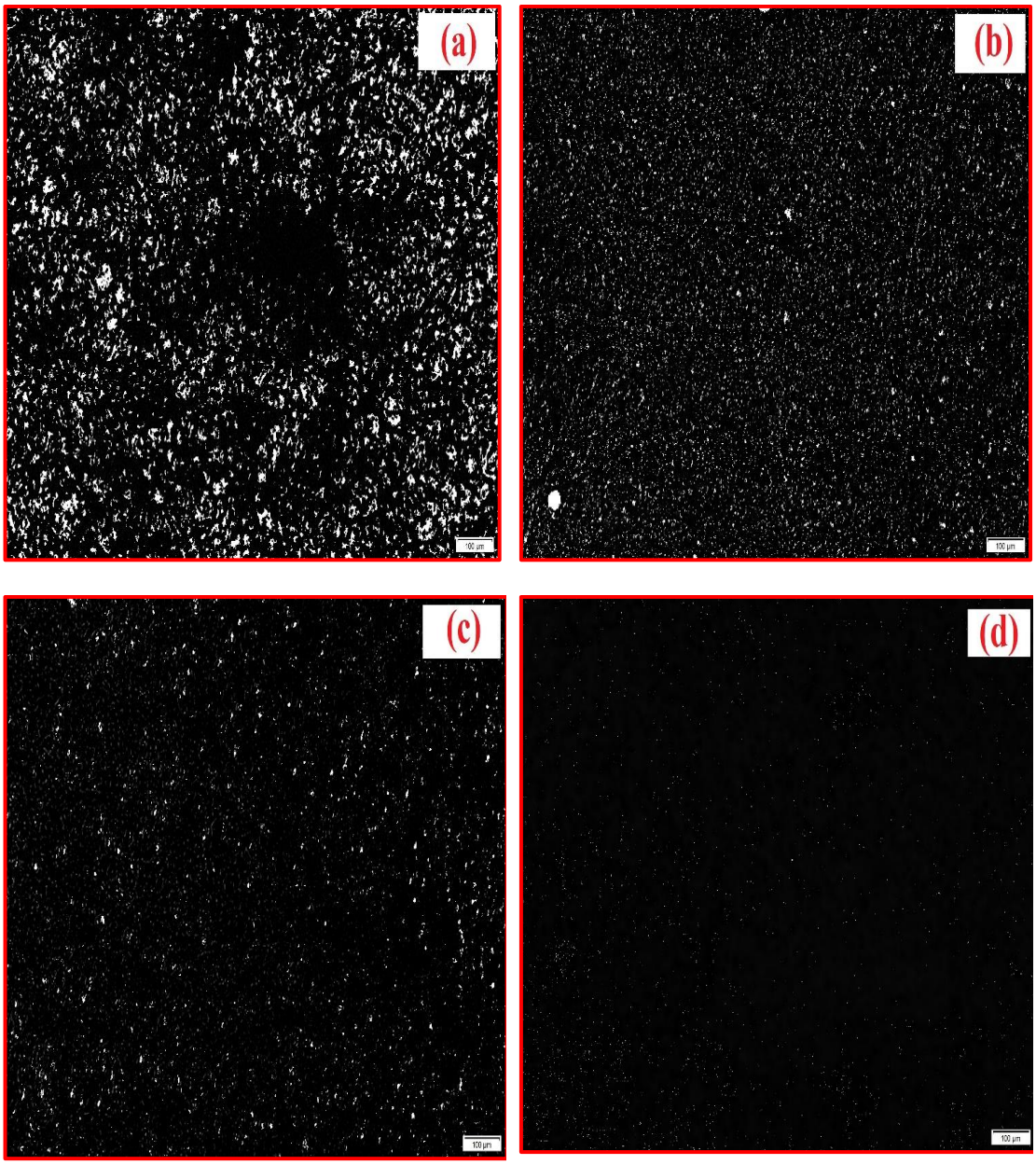

Figure 5.19. Polarized microscopic images at temperature 39°C illustrating wax crystal morphology of (a) Virgin crude oil and the beneficiation effect of the PPDs on the wax structure of crude oil treated with (b) P(2-EHA) (c) P(2-EHA)-0.5% GO and (d) P(2-EHA)-1% GO

5.5 Effect of solvents on hydrogen bonding in nanocomposite

As indicated by the FTIR analyses, presence of hydrogen bonding is observed between GO and polymer in P(2-EHA)-1% GO. A schematic representing possible hydrogen bonding is shown in Fig. 5.20. The nanocomposite PPDs P(2-EHA)-1% GO and P(2-EHA)-0.5% GO have shown beneficiation in the flow properties of crude oil which indicates that the synthesized PPD has retained its form and characteristics intact

even when doped in crude oil. Still, to understand that the hydrogen bonding in the nanocomposite remains intact when doped in crude oil, the following experiments were carried out. The nanocomposite PPDs were tested to understand their strength of hydrogen bonding by dispersing them into the following alcohols (10 wt. %); isopropyl alcohol and methanol individually, and the tests were also performed by dispersing PPDs in water (10 wt. %) as well. It was observed from the dispersion tests (PPD in alcohol and water) that there was no visible physical separations, as no aggregation of nanoparticles were observed physically, and neither the polymer was seen to separate out from the nanocomposite system. Subsequently, the prepared PPD-solvent dispersed systems then were doped into the crude oil, and the pour point tests were carried out similarly as performed before (with ASTM D97-17b method). The pour point reduction pattern observed here was more or less same in comparison with the previous pour point reduction results obtained without the dispersion of alcohol and water solvents. The only difference was that an additional pour point reduction upto 4°C was observed when PPD-in-alcohol system was doped in crude oil, which was due to the effect of alcohol alone (checked by performing blank experiments with doping alcohol alone in crude oil), and it was adjusted (reduced) from the experimental results. Upon addition of PPD-in-water system, there were no differences observed in the pattern of pour point reduction of crude oil, and the results were same as obtained with PPD alone. These results indicates that the hydrogen bonding in the polymer nanocomposite remains intact and sufficiently strong (where the GO sheets hold the polymeric chains strongly enough) to prevent any physical or chemical degradation of polymer nanocomposite system in the crude oil, in the presence of other chemicals bearing tendency to form intermolecular hydrogen bonding with either polymer or GO (which would have reduced the bonding between P(2-EHA) and GO). This observation and results would be beneficial for its transportation in pipelines and was also substantiated from the results of experiments for PPD evaluation.

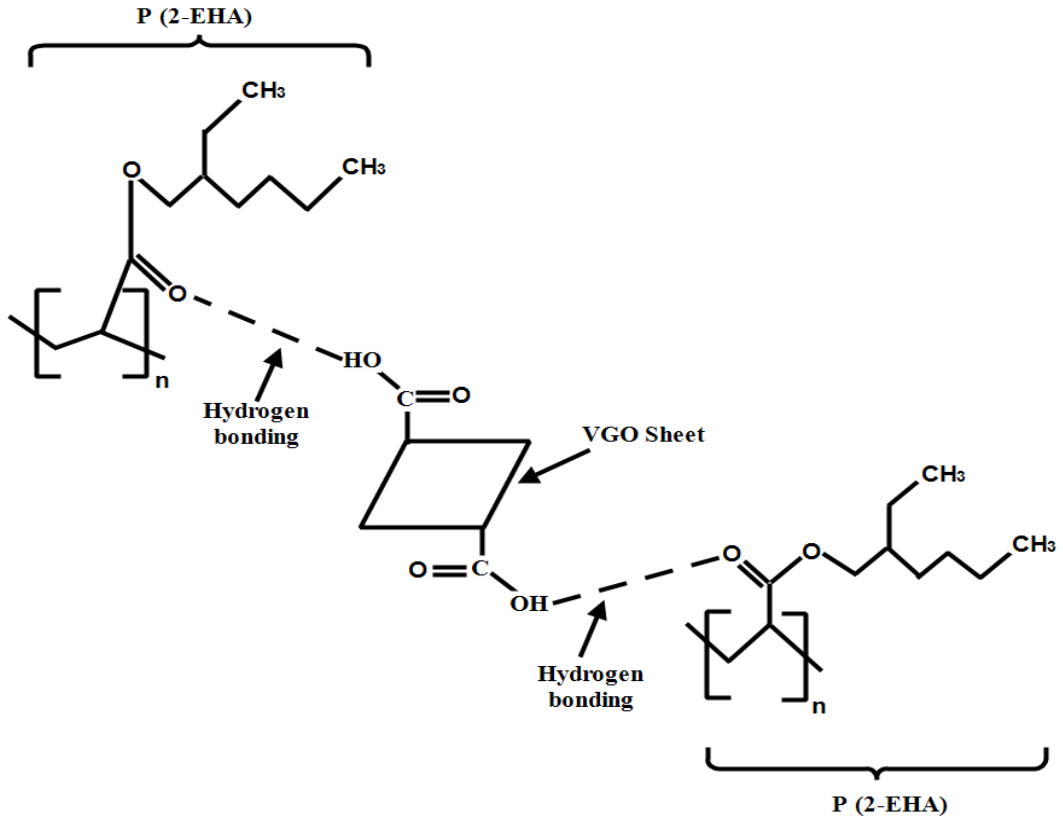

Figure 5.20. Schematic exhibiting possible presence of hydrogen bonding between polymer P(2-EHA) and VGO in the nanocomposite P(2-EHA)-GO

5.6. Conclusions

A successful synthesis of novel polymer nanocomposite P(2-EHA)-GO was performed in laboratory and its characteristics were found to be better than graphene oxide and polymeric PPD P(2-EHA). Subsequently, it was evaluated as a potential pour point depressant for an Indian waxy crude oil, where P(2-EHA)-1% GO showed better beneficiation effect than polymeric PPD P(2-EHA) alone. P(2-EHA)-1% GO exhibited excellent pour point depression with maximum reduction upto 18°C at its optimum concentration (750 ppm) in crude oil. It also imparted excellent restart flow ability in crude oils as it reduced the gelation points of virgin crude oil by 17.8°C [while only 10.8°C reduction with P(2-EHA)], and also it caused upto 99 % reduction in crude oil apparent viscosities in comparison to 96% viscosity reduction with P(2-EHA), indicating that a significantly beneficiated flow performance was produced with nanocomposite PPD and the improvement may be attributed to the modified-beneficiation mechanism for waxy crude oils, created due to the involvement of graphenes in PPD-action

mechanism in nanocomposite PPDs. This was substantiated with microscopic studies, which revealed that the nanocomposite PPD keeps the wax crystals dispersed in the crude oil using a nucleation and co-crystallization mechanism, thus avoiding their precipitation.

Long-term stability tests of the P(2-EHA)-GO-treated crude oil samples indicated that presence of GO helped in the improved flow performance and pour point depression over a long duration of 30 days, and based on the results it was evaluated as a better flow improver than previously developed PMMA-GO polymer nanocomposites. Overall, the nanocomposite P(2-EHA)-1% GO was found to be the most effective PPD with simultaneous improvements in the restart flow ability of an Indian waxy crude oil significantly.

This research work highlights that graphene substrates could be potentially applied to develop numerous products for flow assurance techniques in petroleum industry. The extensive characterization of the nanocomposite performed in this research work would also be of great assistance for the development of further such GO PPD products. Based on the favorable results obtained, it is understood that the graphene based polymeric nanocomposites distinguishes itself as an important class of PPDs, which can yield significant benefits for the flow assurance problems, by reducing the wax deposition and gelation tendency usually encountered in pipeline flow of waxy crude oil.

Chapter 6

Evaluation of ionic liquid and its graphene oxide nanocomposite as novel pour point depressants

6.1 Introduction

Wax deposition in pipelines transporting crude oil is a serious problem as wax tends to precipitate under low temperature conditions observed during pipeline flow. The current chapter embarks on the development of novel nanocomposite pour point depressant (PPD) for waxy crude oils. Two additives were synthesized in the laboratory: 1-octyl 3-methylimidazolium chloride [(OMIM)Cl], and a novel class of nanocomposite PPD: PPDR-GO. These additives were tested on an Indian waxy crude oil and proved to be acting as PPDs and flow improvers. Pour point reduction occurred from 39℃ to 21℃ with [(OMIM)Cl], while the depression occurred from 39℃ up to 9℃ with nanocomposite PPDR-1%GO, suggesting significant improvement in the flow ability of the crude oil as illustrated in Fig 6.1. The PPDs also induced reduction in the apparent viscosities of crude oil significantly, especially by PPDR-1%GO. Apart from the pour point and viscosity tests, the effectiveness of the additives were tested by cold finger, gelation point and aging tests and they produced encouraging set of results. The characterization of the two PPDs performed using spectroscopic analytical techniques FTIR, Proton NMR, XRD and Raman helped identifying the presence of different components and confirm their structure. The purpose of this work is to develop new pour point depressants which are highly effective for providing flow assurance of waxy crude oils. This research also aimed at improving the synthesized PPDs in important areas such as improving dispersion of VGO nanosheets in nanocomposite matrix, enhanced pour point depression ability, low dosage requirement of PPDs, eliminating the need of solvent for PPDs.

Overall, this work emphasizes on the characterization, evaluation and development of synthesized chemical additives as novel pour point depressants for waxy crudes: 1-octyl 3-methylimidazolium chloride [(OMIM) Cl] and the nanocomposite {PPDR – GO}, where an ionic liquid is synthesized and tested as a novel pour point depressant, and also it is being used for the first time to develop an ionic liquid-graphene-

based novel nanocomposite pour point depressant. The performances of the additives are also compared in this chapter. This chapter provides insights into the possible interactions of wax crystals with ionic liquid and graphene oxide sheets, thus, a new working mechanism of the synthesized pour point depressants on wax crystals is proposed, that explains the possible role of ionic liquids, graphene oxide and asphaltenes in the affecting the wax networking and precipitation tendency.[3]

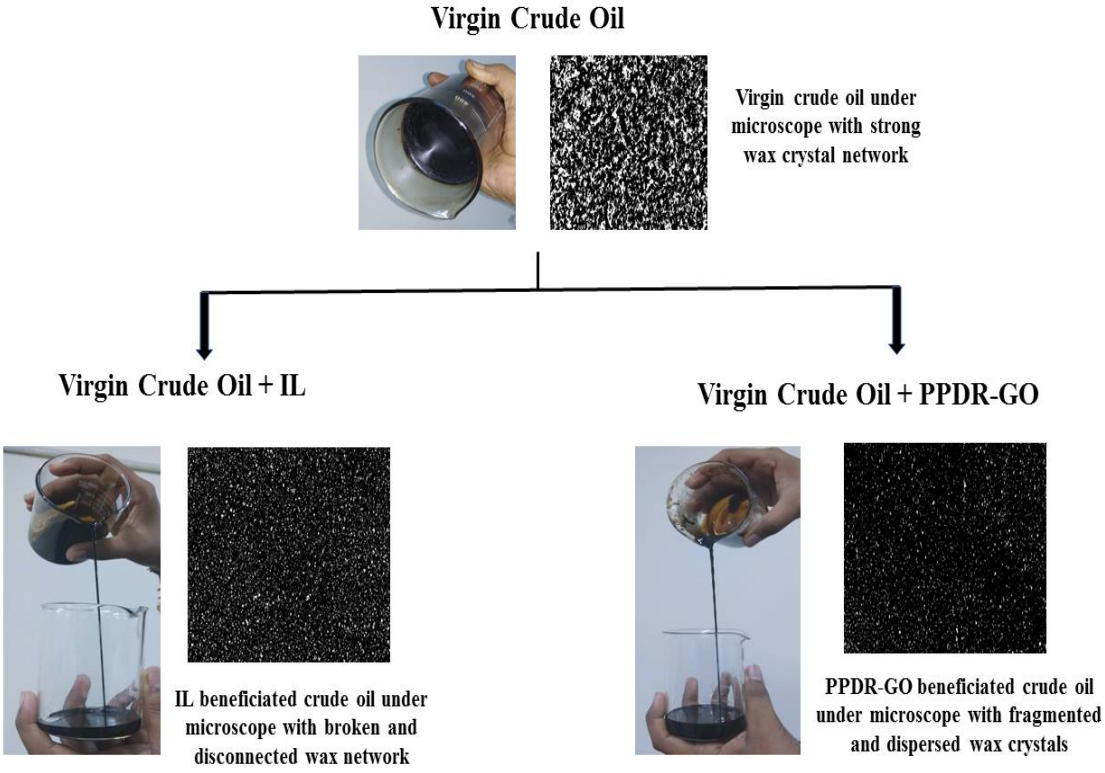

Figure 6.1. Improvement in the flow ability of the waxy crude oil upon treatment with IL and PPDR-GO chemical additives.

[3] ***This chapter is a slightly modified version of my research publication titled "Experimental investigation into the development and evaluation of ionic liquid and its graphene oxide nanocomposite as novel pour point depressants for waxy crude oil" published in Journal of Petroleum Science and Engineering (2022), 208, 109691 and has been reproduced here with the permission of copyright holder.***

6.2 Advanced experimentation technique - Cold Finger Test

In this work, an additional test was carried out to evaluate the efficacy of the developed additives.

The improvement in the flow ability of the WCO treated with synthesized additives was evaluated using a laboratory designed cold finger setup. This setup would simulate the field conditions of the crude oil transportation pipeline. The cold finger setup consists of the following components: a temperature-controlled hot-water bath, a temperature-controlled cooling bath, copper tube of particular dimensions, a crude oil container and a peristaltic pump. The specifications of these components are mentioned as follows: copper tube (diameter = 0.20 inch and tube length = 13 ft), hot water bath (Temperature = 55 ℃ (constant)), whereas the cooling bath was adjusted to three varying temperatures for different experiments (20 ℃, 25 ℃ and 30 ℃), the peristaltic pump (Brand = Electrolab, motor type = stepper, motor torque = 10 kg, model = PP 201V, head type = engineering plastic).

Usually, several tests are performed to evaluate the performance of the synthesized additive as potential pour point depressant and flow improver for different crude oils. These tests includes pour point tests, gelation point tests, viscosity tests, aging tests and microscopic tests. Apart from these standard tests designed to evaluate a chemical additive as the flow improver, the additive is further analysed for its capability to prevent the precipitation and deposition of waxes during the dynamic conditions i.e. flow of crude oil in pipelines. The Cold Finger tests are designed to test this capability of the additive/flow improver by varying different operating parameters such as flow rate, temperature and pressure. This test hold high importance in the pipeline flow of hydrocarbons as it tests the flow improvement ability of the additive.

***Operating principle of the cold finger setup is described below*:**

The operating principle of this test is also detailed in the work of Deka et al. (Deka, Sharma and Mahto, 2020). The schematic of the cold finger setup is illustrated in Fig. 6.2. The WCO in the hot-water bath was maintained at 55℃, which is above the WAT of WCO, ensuring that majority of the wax crystals remains in a dissolved state. This high temperature WCO (in hot bath) represents the temperature of the crude oil kept at the pumping station, which would then be pumped into a 13 ft long copper tube

(representing the oil pipeline), and the flow then passes through the cold-water bath set at temperatures 20 ℃, 25 ℃ or 30 ℃ (for different set of experiments), which actually represents the surface temperature/pipeline wall temperature under ambient conditions. The oil then re-circulates between hot and cold-water baths, simulating the flow conditions of oil in pipelines under different temperature conditions. The flow rate of the oil was kept constant at 400 ml/min and 800 mL of crude oil (WCO) was used in the experiment. The experiment was run continuously for 3 hours. After the experimental run and the weight measurements were completed, the copper tubes were flushed with diesel in order to dissolve and remove the deposit left on pipe walls, and then the pipes were left to dry for 12 hours. Subsequently, cleaning was completed by flushing the tube with acetone several times.

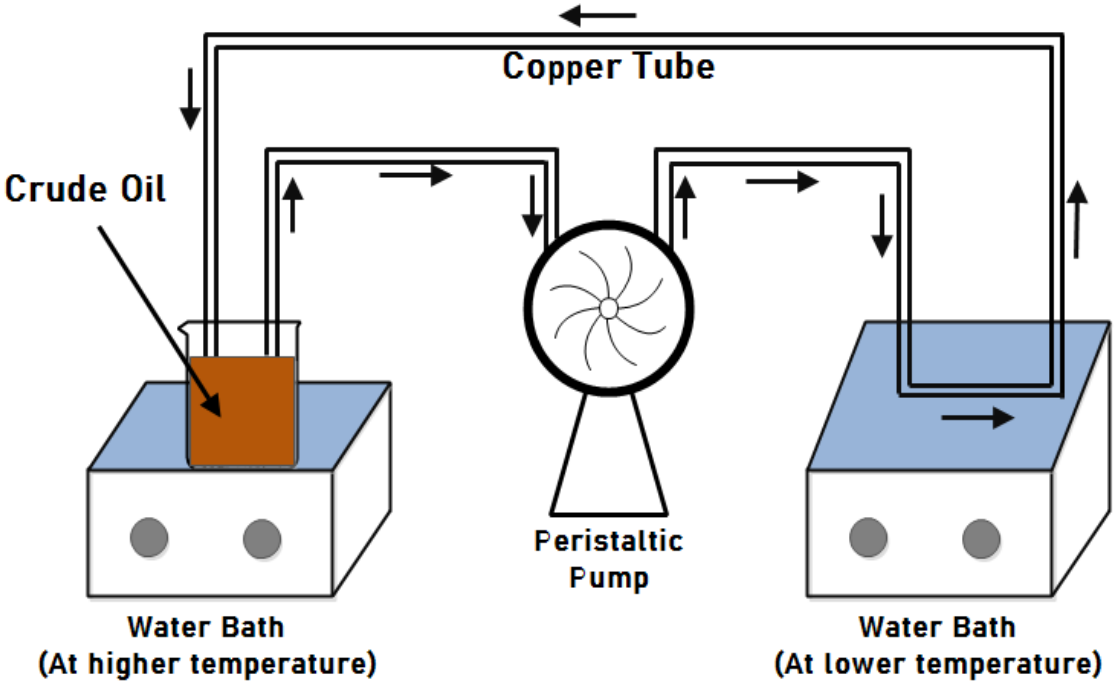

Figure. 6.2. Illustration of the cold finger setup to determine the wax deposition

6.3 Characterization of crude oil

6.3.1 Determination of physico-chemical properties

The crude oil (WCO) was characterized using standard ASTM methods and the results are summarized in Table 6.1. It is evident from the results that pour point of the WCO is very high (39°C), indicating possible flowability issues during low temperatures,

especially during winter seasons. Wax content of the crude oil is significant (17.5 wt.%) and may lead to wax network build-up in the pipelines. The API gravity (27.13°) suggests the WCO is a medium oil by nature. The crude oil contain asphaltene content of 1.5 wt. %. The results of pour point and wax content indicates that the crude oil studied is extremely waxy in nature. The water content was found to be in negligible amount.

6.3.2 WAT determination

WAT of the WCO is 52℃, determined using the non-Arrhenius methodology via the viscosity-temperature plot as mentioned by Paso and co-workers (Paso, K. *et al.*, 2009) and in our previous works (Sharma *et al.*, 2019).

Table 6.1. Characterization of the crude oil (WCO)

Properties	Methods	Observed Values
Pour point (℃)	ASTM D97-17b	39
Water content (vol. %)	ASTM D95-13 (using Dean & Stark setup)	nil
Wax content (wt.%)	Modified UOP 46-64	17.5
Specific Gravity (15℃)	ASTM D1480-15 (using Bingham Pycnometer)	0.892
API Gravity (º)	ASTM D1480-15	27.13
WAT (℃)	Viscosity-Temperature Curve	52
Asphaltene (wt. %)		1.5

6.4 Characterization of synthesized additives

6.4.1 Fourier Transform Infrared (FTIR) spectroscopy

Detailed FTIR interpretation of graphite, graphene oxide and vinyl graphene oxide is mentioned in detail in our previous works (Sharma *et al.*, 2019; Sharma, Mahto and Vuthaluru, 2019). The FTIR spectra of IL and PPDR-1%GO are exhibited in the Fig. 6.3 and their FTIR peaks are listed and described in Table 6.2. The peaks of IL representing the imidazole group are indicated at 620 cm^{-1}, 760 cm^{-1}, 856 cm^{-1}, 1167 cm^{-}

[1], 1461 cm^{-1}, 1569 cm^{-1}, 1634 cm^{-1}, 3078 cm^{-1} and 3144 cm^{-1}. While the peaks at 1108 cm^{-1}, 2855 cm^{-1}, 2925 cm^{-1} are attributed to the existence of alkyl groups in the IL.

In the nanocomposite PPDR-1% GO, the FTIR peaks observed at 619 cm^{-1}, 753 cm^{-1}, 834 cm^{-1}, 1167 cm^{-1}, 1461 cm^{-1}, 1569 cm^{-1}, 1635 cm^{-1}, 3094 cm^{-1} and 3143 cm^{-1} are attributable to the characteristics inherited from the IL. The FTIR peak at 1027 cm^{-1} indicates presence of C-O-C group, which may be attributed to VGO sheets in the nanocomposite system. Similarly, the peak in PPDR-1%GO at 1425 cm^{-1} is attributed to the existence of vinyl groups of VGO, thus confirming the vinyl esterification process (confirming the transformation of GO into VGO). Thus, this FTIR analysis helped to confirm the formation of the IL and its nanocomposite PPDR-1%GO.

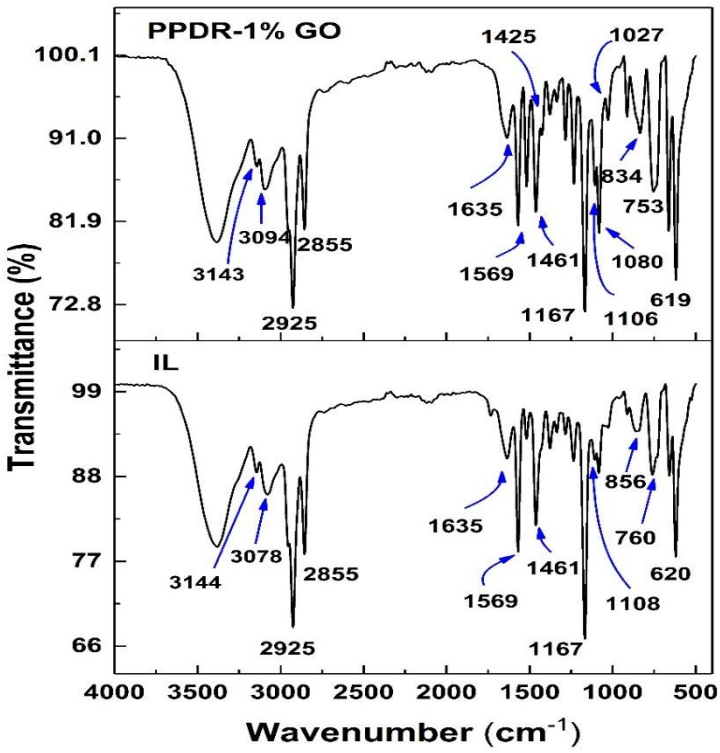

Figure 6.3. FTIR spectroscopic analysis of additives, IL and PPDR-1%GO nanocomposite

Table 6.2. Peak interpretation from FTIR spectra

Peak Position (cm^{-1})		Description
IL	PPDR-1% GO	
620	619	C-N-C bending vibrations in Imidazole (Rajkumar and Ranga Rao, 2008) / C-N stretching vibrations (Dharaskar *et al.*, 2016)
760	753	Out-of-plane imidazole C-H bending (Rajkumar and Ranga Rao, 2008) / C-N stretching vibration (Dharaskar *et al.*, 2016)
856	834	In-plane imidazole ring bending vibrations
	1027	C-O-C stretching in VGO , epoxy group
	1080	C-O-C stretching in VGO, epoxy group (Sharma *et al.*, 2019)
1108	1106	In-plane bending vibrations due to methyl groups (Rajkumar and Ranga Rao, 2008)
1167	1167	Imidazole H-C-C and H-C-N bending/ In-plane bending vibrations due to methyl groups (Dharaskar *et al.*, 2016)
	1425	asymmetric bending vibrations occurring in C-H bond of the vinyl groups, confirms the vinyl esterification process in VGO (Sharma *et al.*, 2019)
1461	1461	C=N stretching in imidazole (Dharaskar *et al.*, 2016)
1569	1569	C-N ring stretching in Imidazole (Lyu *et al.*, 2017)
1634	1635	Ring C=C stretching in imidazole
2855	2855	Symmetric Aliphatic C-H stretching vibrations
2925	2925	Asymmetric Aliphatic C-H stretching vibrations (Silverstein et al., 2014)
3078	3094	Aromatic C-H stretch (in imidazole)
3144	3143	Imidazole C-H stretch (Rajkumar and Ranga Rao, 2008)

6.4.2 Raman Analysis

To increase our understanding towards the formation of graphene oxide and its derivatives, Raman spectroscopy was conducted. Through the FTIR analysis, the type of

functional groups present in the graphitic products were identified comprehensively, and the Raman spectra would characterize the synthesized graphitic derivatives in terms of two most prominent bands for carbonaceous compounds .i.e. D and G bands. The Fig. 6.4 illustrates the Raman spectra of graphite, GO, VGO and PPDR. The D band and G band of graphite appears at 1375 cm^{-1} and 1579 cm^{-1}. These bands appears to be shifted to 1349 cm^{-1} and 1593 cm^{-1} in GO respectively. While in VGO, the D band appears at 1342 cm^{-1} and the G band at 1609 cm^{-1}. The PPDR-1%GO exhibits D band at 1342 cm^{-1} and the G band at 1573 cm^{-1}. The G band peak is of substantially higher intensity than D band in the Raman spectra of graphite. The ratio of intensities of D (I_D) and G bands (I_G) .i.e. (I_D/I_G) is determined to be 0.18 for graphite indicating strong presence of sp^2 carbon network, while the I_D/I_G ratio increased to 0.93 in the case of GO indicating substantial formation of defects in the sp^2 carbon framework of graphitic structure, owing to attachment of oxygen functionalities such as hydroxides, epoxides and carboxylic groups on the carbon basal planes. The I_D/I_G further increased to 0.94 in the case of VGO, indicating further chemical treatment of GO with acrylonitrile to result in attachment of vinyl functional groups. The final product PPDR-1%GO possesses the highest I_D/I_G of 0.95 among all products, which may be attributed to the incorporation of IL among VGO sheets. The crystallite size of the products was calculated based on the following equation

$$L_a\,(\mathrm{nm}) = 2.4 \times (10)^{-10}\,(\mathrm{nm})^{-3} \times \lambda_L{}^4\,(\mathrm{nm})^4 \times (I_D/I_G) \quad \text{.....(6.1)}$$

The crystallite size of GO was determined based on the equation 6.1 (Sharma *et al.*, 2019) to be 17.8 nm, which increased to 18.1 nm in VGO due to the chemical treatment of GO with acrylonitrile during synthesis process. The crystallite size of PPDR-1%GO was found to further increase to about 18.3 nm suggesting the incorporation of IL among VGO sheets. Thus, the Raman spectra detailed the characterization of the products synthesized in this work comprehensively.

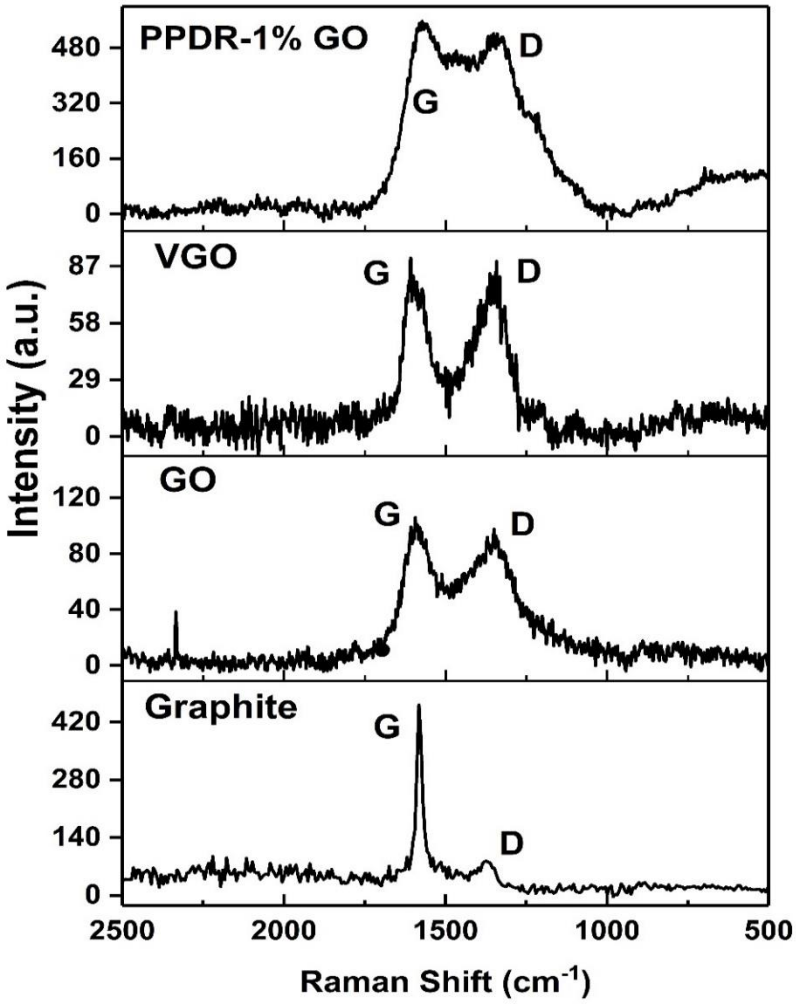

Figure 6.4. Raman spectra of graphite, GO, VGO and PPDR-1%GO, with G and D Raman bands marked.

6.4.3 ^{1}H NMR spectral analysis of nanocomposite

To complement the detailed characterization information of the PPDR-1%GO acquired from the FTIR, ^{1}H NMR spectroscopic analysis was performed and shown in Fig. 6.5. The major peaks in the spectra are listed in Table 6.3 with detailed description. The ^{1}H NMR peaks at 1.05, 1.07 - 1.527, 3.924 and 4.32 ppm chemical shift represent the presence of alkyl part in the PPDR-GO nanocomposite (Silverstein et al., 2014). The peaks at 5.46, 7.112, 7.502 - 7.749 ppm chemical shift represents the vinyl groups in the nanocomposite (Sharma *et al.*, 2019). While the peaks at 7.112, 7.23 - 7.258 and 10.683

ppm chemical shift represent the presence of imidazole ring in the ^{1}H NMR spectra (Lyu *et al.*, 2017). Thus, through the NMR characterization of the PPDR-1%GO, the presence of major functional groups is identified and confirmed, and it confirms the successful formation of the nanocomposite PPDR-1% GO from its raw ingredients.

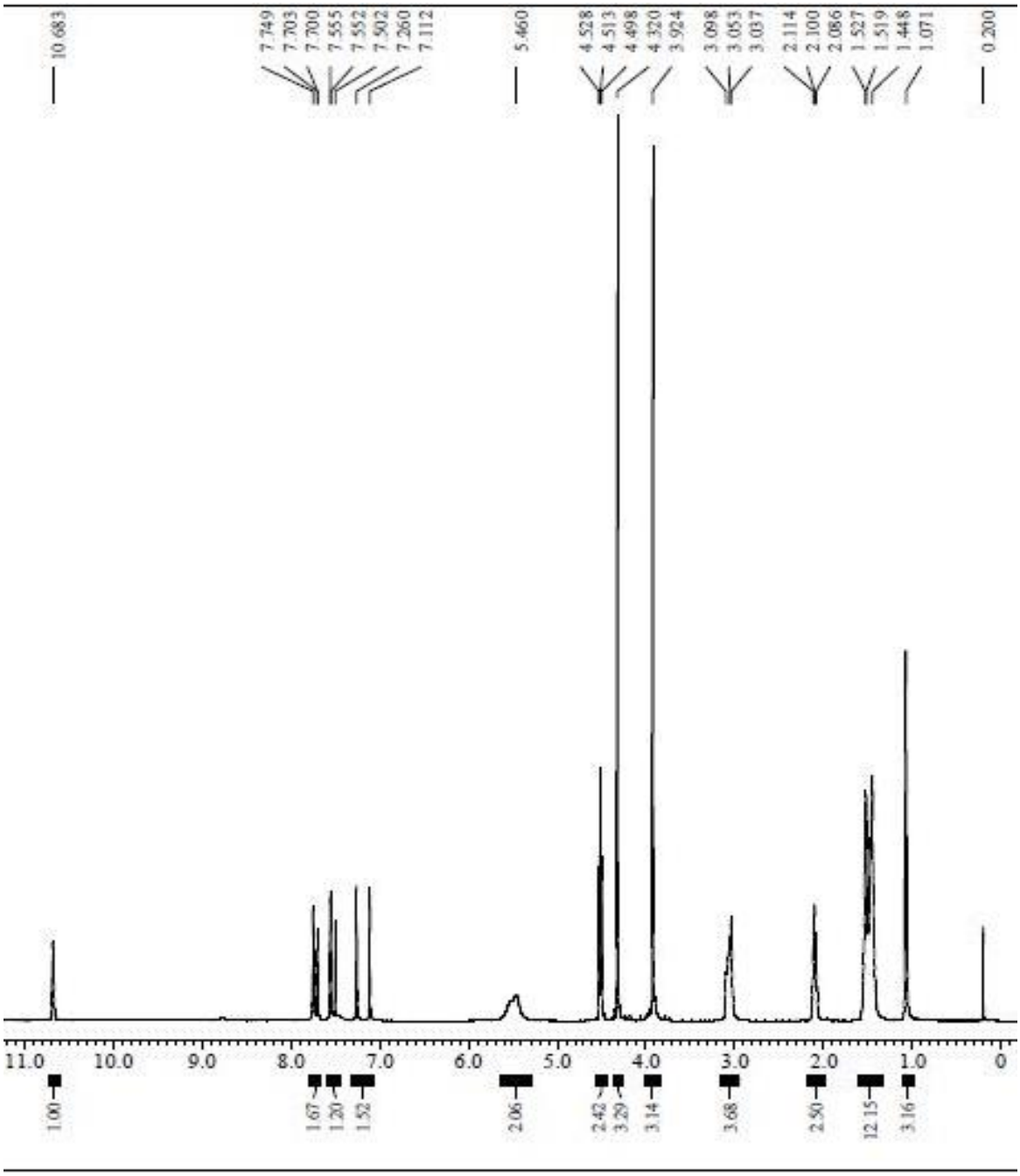

Figure 6.5. ^{1}H NMR spectra of nanocomposite PPDR-1%GO

Table 6.3. 1H NMR interpretation of PPDR-1%GO nanocomposite

Peak (ppm)	Description
1.05	Presence of terminal methyl protons on the alkyl chain of the ionic liquid
1.07-1.527	Cumulative effect of the methylene protons of the octyl chains of the ionic liquid
2.071-2.129	Methine proton of VGO
3.924	Methyl protons attached on the side of imidazole and may also be due to methine proton of VGO
4.32	Methylene proton on the junction of imidazole and alkyl chain of ionic liquid
5.46	Indicates presence of vinyl group protons attached to ester of VGO group
7.112	Presence of vinyl protons attached to the ester group of VGO & Presence of methine proton in the imidazole group
7.23- 7.258	Methine proton in the imidazole ring of ionic liquid
7.26	Residual protons in deuterated chloroform
7.502-7.749	Due to protons on the conjugated aromatic fused rings of VGO
10.683	Presence of a methine proton attached between nitrogen groups in imidazole ring of ionic liquid

6.4.4 XRD Analysis

The XRD spectra of graphite (Fig. 6.6) exhibits a characteristic peak at diffraction angle 2Θ = 26.5°, corresponding to an interlayer spacing of 3.36 A° , which agrees with the previous literatures (Sharma *et al.,* 2019; Sharma, Mahto and Vuthaluru, 2019). The interlayer spacing of the products was calculated from the Braggs equation $n\lambda = 2d\sin\Theta$. The XRD spectra of GO reveals a sharp peak at 2Θ =10.3°, which corresponds to an interlayer spacing of 8.58 A°, which is in agreement with previous works. This substantial increase in the interlayer spacing indicates the exfoliation of graphitic sheets and the formation of GO from graphite owing to attachment of functionalities such as COOH, OH and C-O-C groups on the graphitic sheets at edges and surfaces. The XRD of PPDR-

1%GO illustrates two major peaks, one peak at 2Θ = 7.1° attributed to the VGO component in the PPDR-1%GO, while the other broader peak at 2Θ = 20.9° corresponds to its ionic liquid component [(OMIM)Cl], indicating amorphous nature of the ionic liquid. The interlayer spacing among the VGO sheets in PPDR-1%GO was found to further increase to 12.45 A° (corresponding to 2Θ = 7.1°), which suggest that the [(OMIM)Cl] was properly intercalated in between the VGO sheets and it constitutes majority of the PPDR-1%GO. The XRD spectra successfully characterized the graphitic derivatives and helped to understand the structural changes in the products.

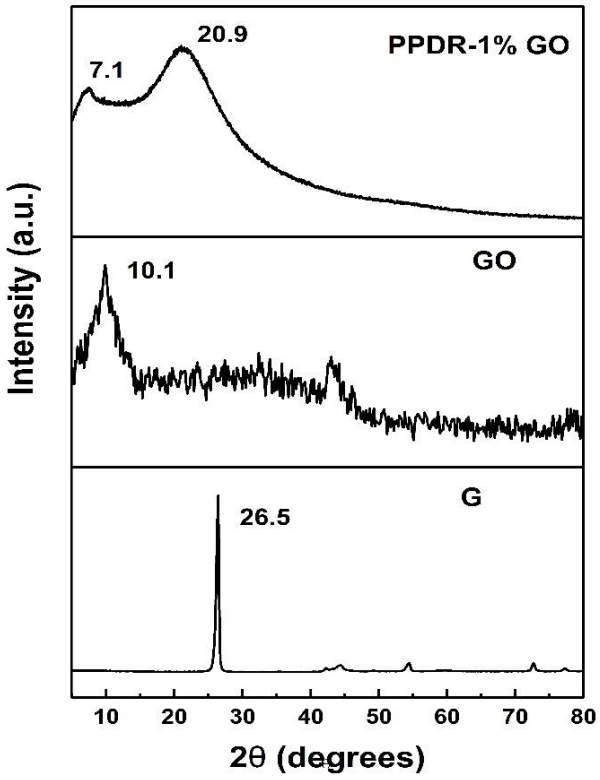

Figure 6.6. XRD spectral analysis of G, GO and PPDR-1%GO

6.4.5 Dispersion stability of additives

The nanocomposite PPDR-1%GO is shown in the Fig. 6.7 (a), illustrates a black coloured homogeneous dispersion where the VGO nanosheets are effectively dispersed in the base ionic liquid system and showed no settling for a long time, which suggest that the ionic liquid holds the VGO sheets well, and this also indicates that they will remain stable for sufficient duration before being doped into the crude oil. The Fig. 6.7 (b)

illustrates the additive IL, which is a yellowish coloured clear solution, which also appears to be quite stable and homogeneous. Thus, the additives developed in this research addressed on one of the areas for improvement for nanocomposites where dispersion of nanosheets would not become a concern in long term storage.

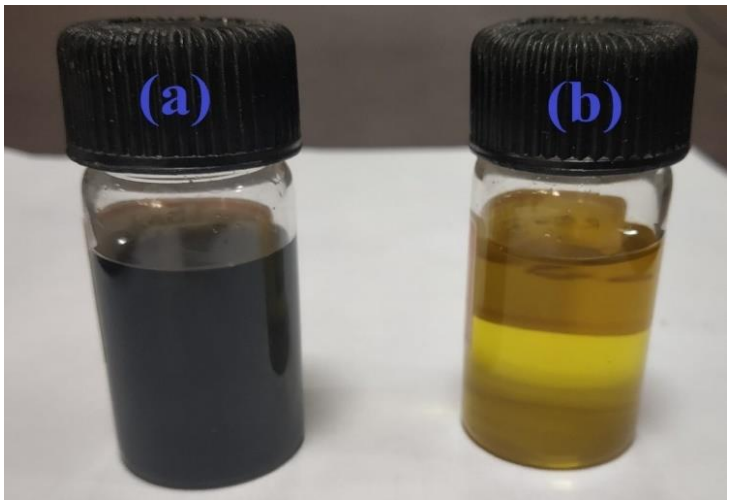

Figure 6.7. Samples of the synthesized additives (a) PPDR - 1 %GO & (b) IL

6.5. Evaluation of the synthesized additives as flow improvers

6.5.1 Pour point determination

The pour point results of the virgin WCO and the additive-treated WCO samples were determined using standard ASTM D97-17b and the results are presented in Table 6.4, where it is clearly evident that the IL and nanocomposites reduced the pour point of WCO appreciably and are surely capable of functioning as PPDs. The PPDs were doped into the WCO without being prior dispersed in any solvent.

Table 6.4. Pour point of the crude oil (WCO) at different concentrations of ionic liquid IL and nanocomposite PPDR-0.5 % GO and PPDR-1% GO

Concentration (ppm)	Pour point (℃)		
	IL	PPDR-0.5%GO	PPDR-1%GO
0	39	39	39
100	36	30	27
250	27	15	9
500	21	18	12
750	24	21	15

The lowest pour point of additive IL-treated WCO sample was found to be 21℃ at 500 ppm. Upon further increasing its concentration the pour point rises. Therefore, 500 ppm is considered as the optimum concentration of the additive IL. The synthesized novel nanocomposite PPDR-0.5 %GO also caused a huge pour point reduction from 39℃ to 18℃, i.e. 21℃ reduction at 250 ppm optimum concentration. The synthesized novel nanocomposite PPDR-1%GO showed best reduction in the pour point of the WCO from 39℃ to 9℃ at 250 ppm concentration only, and the pour point rises with its increasing concentrations (Sharma et al., 2020). Therefore, 250 ppm is considered as the optimum concentration of PPDR-0.5% GO and PPDR-1%GO for WCO. The pour point of the crude oil rises after addition of the optimized concentration of the PPD and it may be attributed to the suspension of extra quantities of the PPD leading to increased gelling and difficulty in the flowability (Sharma, Mahto and Vuthaluru, 2019). This increase in pour point might also possibly be attributed to the additional PPD quantities making the doped fluid bulkier, lesser soluble and less effective (Deka *et al.*, 2018). All the additives reduced the pour point significantly, therefore they are termed as pour point depressants for the Indian WCO. The PPDR - GO PPDs causes a huge reduction in the pour point at a very low concentration (low dosage PPDs), thus can possibly improve the economics of the flow assurance project. The higher value of optimized concentrations of PPDs would require stocking of larger quantities of the chemical, which would put additional burden on storage facilities and increase operating expenditure to maintain them.

It was observed that the pour point reduction was significantly beneficiated with PPDR-GO compared to the IL additive. This improvement maybe possibly attributed to the influence of VGO sheets in the PPDR-GO, where the VGO sheets act as nucleation sites over which wax crystals gets adsorbed. Also, the reduction in pour point by 30℃ is a substantial improvement, indicating the PPDR-GO nanocomposite possesses the ability to improve the crude oil flow characteristics during pipeline transportation at different temperature seasons where the temperature drops to lower levels.

The additives developed in this work have an advantage, as they could be doped into the crude oil without the help of any solvents to create fluidity. The PPDs IL, PPDR-0.5 %GO and PPDR-1 %GO remains in a very fluid state, which could be doped alone into the crude oil without the need of any solvent to cause beneficiation, which is an essential advancement from the learnings of the previously developed several PPDs

including PMMA-GO and P(2-EHA)-GO (Sharma *et al.*, 2019; Sharma, Mahto and Vuthaluru, 2019), where they needed to be dispersed into a hydrocarbon solvent such as xylene to prepare a fluidic and dopable sample of PPD. Moreover, the pour point reduction achieved using PPDR-1% GO (30℃) is significantly higher compared to the developments made in the previous works (i.e. PMMA-GO (23℃) and P(2-EHA)-GO [18℃]). Therefore, these PPDs were able to address the areas of concern listed from the previous works (Sharma *et al.*, 2019; Sharma, Mahto and Vuthaluru, 2019) comprehensively.

The pour point tests of the WCO were also conducted with higher GO concentrated nanocomposites (> 1 wt.% GO), but their effects were less promising compared to PPDR-0.5%GO and PPDR-1%GO. The optimum pour point of WCO samples observed were .i.e., 18℃ and 21℃ with PPDR - 1.5%GO and PPDR - 2%GO respectively at 250 ppm respectively and a surge in the values were observed at higher dosages. These synthesized nanocomposites provides higher values of optimum pour points comparatively and thus, would not be considered for further evaluation in this research work. Based on the pour point results, since PPDR-1%GO showed the best performance among the nanocomposites, thus, only PPDR-1% GO would be considered among the nanocomposites, along with IL for further evaluation in this research work.

The improvement in the pour point depression by the PPDs lies in their action mechanism to interact with the wax crystals of the crude oil. Describing the action mechanism of ionic liquids in brief, they prevent the asphaltene flocculation, which in turn prevents wax networking & deposition. Additionally, their alkyl part interacts with the waxes & co-crystallizes to prevent their precipitation. The detailed mechanism is explained in the following discussion below.

Asphaltenes are known to interact with the waxes in crude oil through the alkyl chains attached on the periphery of their aromatic rings and affect the wax precipitation. Asphaltenes could also participate in the wax precipitation stages and thus modify the wax crystallization style, its deposition and thus the flow ability of the waxy crude oils (Li, Mao, Shi, *et al.*, 2018). Thus, it could be inferred that the asphaltenes play a possible role in preventing wax deposition. Ionic liquids are learned to reduce asphaltene aggregation and precipitation, through interaction among respective polar constituents via electrostatic interactions (Hu and Guo, 2005), while the non-polar component of ionic

liquids could interact with the wax structure of the crude oil. Preventing the asphaltenes precipitation and aggregation would make them available to bind with the waxes and thus reduces wax-wax interactions and networking, and subsequent deposition. Moreover, the alkyl component of ionic liquid IL could also co-crystallize with the alkyl chains of the waxes and co-crystallizes with them. Thus, IL additive reduces the potential of wax deposition with the assistance of asphaltenes and breaks the tendency of wax networking.

In the case of PPDR-GO nanocomposites, the VGO sheets provide the nucleation sites for wax precipitation, where the wax crystals would precipitate and grow in a restricted and localized way and avoids networking, and therefore would result in discrete and dispersed waxes. This reduced wax networking assists the working and efficacy of ionic liquid component in nanocomposite, which would then co-crystallize with these precipitated waxes easily and would produce an enhanced modification in the wax morphology. Thus, the presence of VGO sheets provides additional nucleation mechanism in addition to the co-crystallization feature of the ionic liquid with wax crystals. Due to this synergistic effect of VGO sheets and IL, efficacy of the nanocomposite was better than the additive IL which was substantiated through the experimental results of pour point determination and other evaluation techniques.

6.5.2 Influence of the additives on the apparent viscosities

The rheological experiments helped to comprehend the flow behaviour of the PPD-treated WCO samples for different shear rates and at different temperatures, representing the crude oil flow in pipelines. The rheological data curves obtained from the experimentation are illustrated in the viscosity-shear rate plots in Fig. 6.8 (a)-(c). It could be observed from these figures that viscosities of the raw WCO are typically higher, and was found to be reduced when the WCO is treated with PPDs, where the PPDR-1%GO exhibited better performance than IL at all tested temperatures. Higher viscosities of the WCO are result of the higher shear force required to break the extensive network of wax crystals.

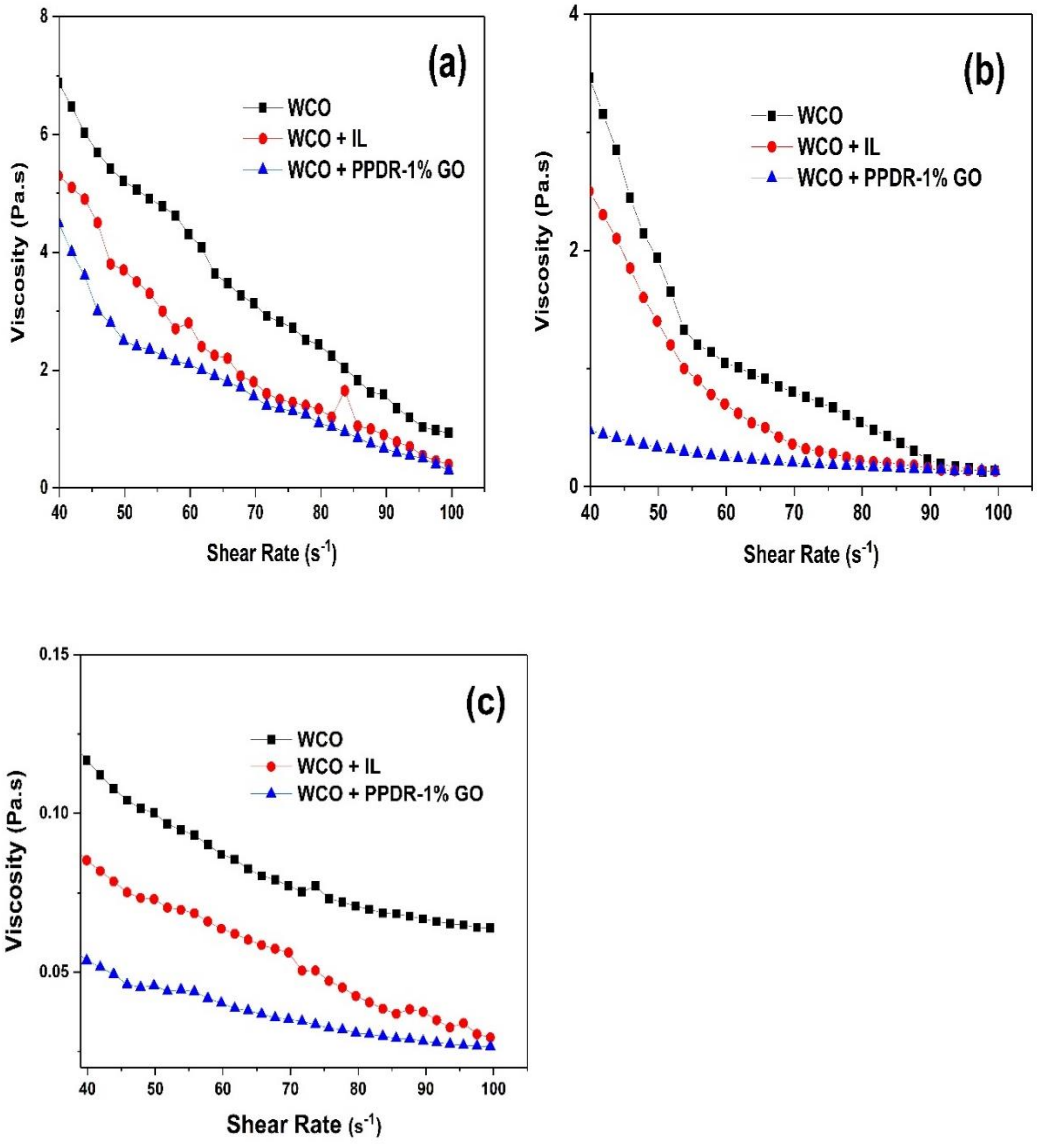

Figure 6.8. Variation of apparent viscosities of the raw crude oil (WCO), IL treated crude oil and the nanocomposite PPD (PPDR-1%GO) treated crude oil at shear rates 40-100 s^{-1} at (a) 30°C, (b) 40°C and (c) 50°C. IL and PPDR-1%GO were doped at optimized concentration (i.e. 500 and 250 ppm respectively) in the crude oil.

In order to understand the changes in the dynamic flow properties of the additive treated WCO, the viscosities are listed in Table 6 where decrease in the apparent viscosities of the WCO after treatment with IL and PPDR-1%GO PPDs was observed. Viscosities of the WCO recorded at 30°C is as high as 7 Pa.s, which seems substantially high to be transported through the pipeline network. Reduction in viscosities were observed when WCO was treated with IL additive and their viscosities reduces down to 0.6 Pa.s at 30°C. Further reduction in viscosities were recorded when treated with PPDR-

1%GO, which decreased down to 0.2 Pa.s at 30℃. At higher temperature (40℃), the viscosities of the WCO reduced to 0.17 – 3.5 Pa.s, while it reduced to 0.1 – 2.5 Pa.s when treated with the additive IL, and these viscosities diminished further to 0.09 – 0.5 Pa.s in the case of PPDR-1%GO treated oil. As the temperature rose to 50℃, a further reduction in viscosities occurred and were observed to 0.06 - 0.13 Pa.s (for WCO) and 0.04 - 0.08 Pa.s (for IL treated WCO) and 0.02 - 0.06 Pa.s (for PPDR-1%GO treated WCO). The improvement in the viscosities of additive-treated WCO samples was more profound at lower temperatures.

This reduction in the viscosities of the oil samples could be attributed to the role of PPDs allowing only limited networking of wax crystals, especially, the effect was profound with nanocomposite PPDR-GO, where the GO sheets effectively reduces the networking of wax clusters and assures easier flow. Thus, these results indicate that the developed PPDs has also acted as a viscosity reducer for the WCO.

Table 6.5. Reduction in the apparent viscosities of the virgin WCO, IL and the PPDR-1%GO treated WCO samples measured over shear rates 40-100 s^{-1}. The PPDs were doped at their optimum concentration: 500 ppm (IL) and 250 ppm (PPDR-1%GO)

Sample	Shear Rate (s^{-1})	Apparent viscosities of crude oil samples (Pa.s) at different temperatures		
		30℃	40℃	50℃
WCO	50	4.1	1.9	0.92
WCO + IL		3.6	1.6	0.6
WCO+PPDR-1%GO		2.5	1.4	0.2
WCO	70	1.9	0.84	0.17
WCO + IL		1.36	0.34	0.1
WCO+PPDR-1%GO		0.30	0.26	0.09
WCO	100	0.1	0.08	0.06
WCO + IL		0.08	0.05	0.04
WCO+PPDR-1%GO		0.05	0.03	0.02

6.5.3 Aging effect on crude oil samples

IL and PPDR-1%GO have shown significant beneficiation in the WCO upon being tested using different evaluation techniques, and therefore, it becomes important to understand the changes occurring in the properties of the PPD-treated oil samples with increase in time, and this was understood by performing pour point depression test after storing the samples for few days. The PPDs were doped in the WCO samples and were stored for 15 and 30 days, and pour points were tested subsequently. The PPDs were doped at their optimum concentrations for aging test. Table 6.6 exhibits the changes in the pour point of samples after specified days of storage.

Table 6.6 Changes in the pour point of the PPD-beneficiated oil samples with time (Aging)

PPD	Concentration (ppm)	Pour Point (°C)		
		Day 0	Day 15	Day 30
WCO + IL	500	21	24	27
WCO + PPDR-1%GO	250	9	12	12

An increase in the optimized pour point by 3°C and 6°C was observed in IL-treated WCO sample after 15 days and 30 days of storage respectively, while the increase was limited to 3°C (pour point reached 12 °C) in the case of PPDR-1%GO treated WCO sample after the same storage period. This indicates that PPDR-1%GO exercises better control over the aging tendency and there is limited depreciation in the crude oil properties. This also suggest that the PPDR-1%GO treated oil samples would not experience any major flow assurance issues in terms of longer transportation duration, including during pipeline shutdown and subsequent pipeline restart. Thus, both the additives showed remarkable improvement in the pour point of the Indian WCO and also controlled the aging effect of crude oil substantially, especially the nanocomposite PPDR-1%GO. This effective control over aging could be attributed to the synergistic influence of VGO sheets and IL on waxes, which indicates a better control on the gelation and deposition of waxes (on the pipe walls) with time. Thus, the synthesized PPDs would

produce great beneficiation upon their application in the waxy crude oils, even after long term storage of crude oil samples.

6.5.4 Effect of additives on viscoelastic development of crude oil

The gelation point determination of the WCO evaluates the performance of the additives under application of shear stress in comparison to the pour point evaluation where no shear is applied. This analysis provides valuable information about wax deposition process, since shear conditions are inclusive in wax deposition process during pipeline transportation (Venkatesan *et al.*, 2002). This experimental technique finds important application in the case of pipeline restart, where the wax-oil gelling occurs prominently and the additives would be tested for their efficacy in delaying the gelation phenomena in crude oils to lower temperatures, in order to ease the pipeline restart.

Fig. 6.9 (a)-(c) exhibits that the loss modulus is dominant at temperatures above gelation point, and with decrease in temperatures the storage modulus overcomes the loss modulus, and their intersection temperature is termed as the gelation point (Sharma *et al.*, 2019). At temperatures below the WAT, the wax precipitation starts and below the gelation point, wax-oil gelling develops completely.

The gelation point of the WCO was found to be 36.7℃, and upon treatment with the additive IL the gelation point reduces to 23.4℃. Best improvement is observed with PPDR-1% GO, which reduced the gelation point to 14.5℃. These results suggest that the viscoelastic development in the WCO is significant and starts from higher temperatures itself possibly due to the precipitation of waxes, indicating that liquid-like characteristics were dominant at temperatures higher than 36.7℃, which diminishes at lower temperatures, paving way to loss of fluidity and the gelling development i.e. elasticity in crude oil. The additives shift the transition in viscoelastic properties of WCO to lower temperatures, and pushes the gelation point down by 13.3℃ and 22.2℃ with IL and PPDR-1%GO respectively. It indicates that these additives have significant potential to possibly affect the wax networking tendency and their subsequent deposition. These results give major insights into the role of additives in improving the flow properties of the WCO.

The lowering in gelation tendency of the PPDR-GO treated crude oil may possibly be attributed to the role of VGO sheets in reducing the build-up of wax network and thus

would result in lesser entrapment of the crude oil in porous wax structures and would assure an easier flow.

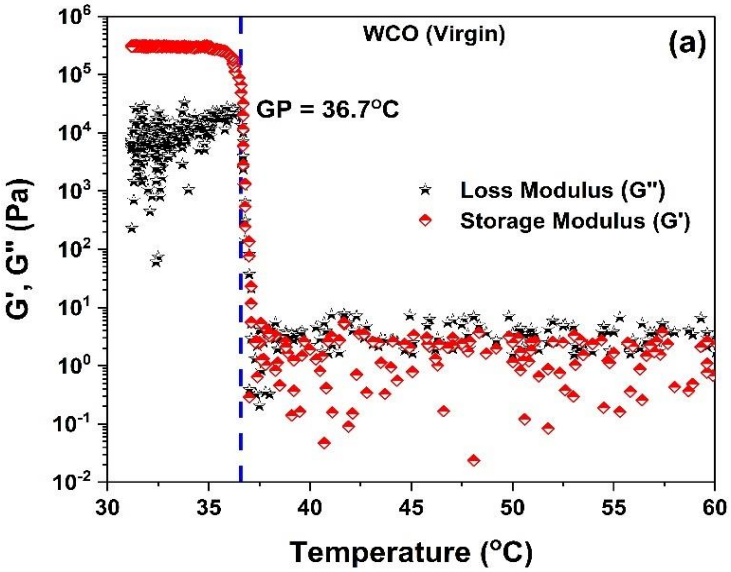

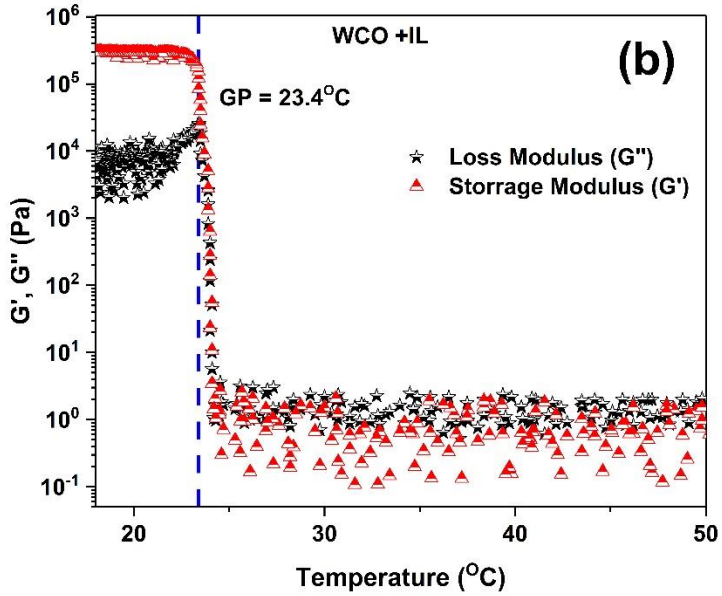

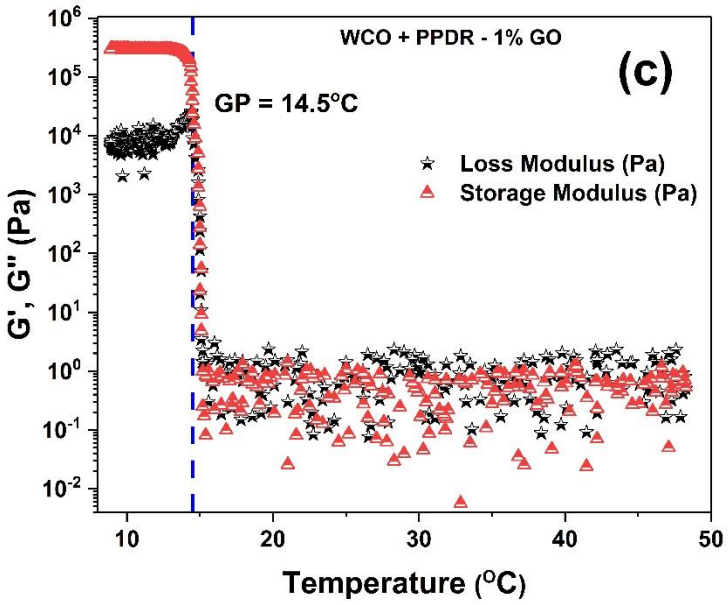

Figure 6.9. Gelation point (GP) determination of the crude oil samples (a) WCO (without additive), (b) WCO + IL and (c) WCO + PPDR-1% GO. Additives are mixed at their respective optimum concentrations.

6.5.5 Microscopic investigation of wax morphology

The microscopic imaging of the WCO samples treated with and without additives was conducted under a polarized microscope and the images are exhibited in Fig. 6.10 (a)-(e). Fig. 6.10 (a) exhibits the wax crystal morphology of the virgin WCO at ambient temperature 25°C, where it is clearly evident that wax crystals have formed interlocking clusters which would present hindrance in the flowability of WCO. The presence of extensive network of porous wax clusters would trap a significant fraction of oil inside and hinder its movement inside the pipeline, which would then require significant amount of shear force for continuous movement and thus, it also indicates that pipeline restart could be an issue in such a case if conditions such as temperature, flow rate etc. are not monitored regularly. The microscopic image of WCO treated with additive IL is shown in Fig. 6.10 (b), displays a substantially broken and disconnected wax network , indicating an improvement in the arrangement of wax network compared to WCO. The interconnectivity of wax clusters has reduced substantially and thus, would cause lesser

entrapment of oil molecules, which suggest an important development in improving the flowability of the crude oil.

Fig. 6.10 (d) exhibits the wax morphology of the PPDR-1%GO treated oil at 25℃, where it is observed that the network of wax crystals has been fragmented and disappeared significantly, and they appear in a very dispersed state and in scattered form, which is a highly improved configuration of wax crystals than with IL.

Since the PPDR-1%GO exhibited the best beneficiation in all the evaluation techniques, additional analysis was performed to understand the changes in wax structure at different temperatures. Therefore, the microscopic observations of the wax structures in the presence of PPDR-1%GO were taken at temperatures lower and above the ambient temperature (i.e. at 15℃ and 35℃) and they are displayed in Fig. 6.10 (c)-(e). The Fig. 6.10 (c) exhibits the modifications in the wax structure with additive PPDR-1%GO at 15℃, where highly dispersed and disconnected waxes are present. The wax structure is dense than at 25℃, still it appears that the additive controlled the networking of waxes appreciably. With an increase in temperature to 35℃, an associated increase in solubility and therefore, reduced dispersion density of wax crystals is observed (Fig. 6.10 (e)) and the wax crystals network disintegrates to higher extent. PPDR-1%GO exhibited that it alters the wax morphology and reduces wax networking significantly at all tested temperatures, even at low temperatures it acts upon the waxes and prevents their growth and networking. This microscopic study shows that upon application, the additives IL and PPDR-1%GO has altered the morphological structure of wax crystals significantly, thereby would result in an improvement in the flow of crude oil.

Although after the addition of IL PPD, amount of wax crystals is seen to be increased, but the reduction in wax crystal size and breaking of the large flocks will prevent their aggregation. This change in wax crystal morphology and reduction in size causes much better dispersion of wax in the base oil, which is very difficult in the case of large wax flocs. This result is also mentioned in previous literature (Deka et al. 2020), and is in accordance with the justification for wax dispersion. Similar observation was also reported in (Coto et al., 2014), mentioning better dispersion of smaller sized wax molecules in the base oil. Additionally, the presence of shear force in pipeline leads to an unhindered flow of dispersed smaller sized wax crystals and thus, prevents their interlocking tendency. Hence, the increased number of wax crystals would not cause flow

assurance problem as their sizes are much reduced. The observations made above are applicable for the wax morphological distribution in the case of additive IL treated crude oil. The morphology of waxes transitions to significantly smaller and dispersed structures, with lesser amount of waxes being visible in Fig 9(c)-9(e) in the crude oil when treated with nanocomposite additive PPDR-1%GO. This indicates that the graphenes have played an important part in reducing the wax amounts and their networking. This result agrees to the experimental findings from our previous works (Sharma et al., 2019b, 2019a) where the nanocomposite treated crude oils have shown similar wax morphologies i.e. dispersed and decreased waxes and reduced wax networking. Moreover, the research work (Hazrati et al., 2021) stated that the ionic liquid co-crystallizes with the wax chains and leads to deformation of the wax crystals, which cannot perform re-aggregation and thus leads to postponement of the pour point.

The microscopic analysis of the PPD-treated crude oil supports the findings of other techniques to evaluate flow improvers. This is because the modulation of the wax structures is in agreement to the efficacy shown by the additives during various evaluation techniques. Thus, IL and PPDR-1%GO proved to be excellent candidates for improving the flow properties of WCO.

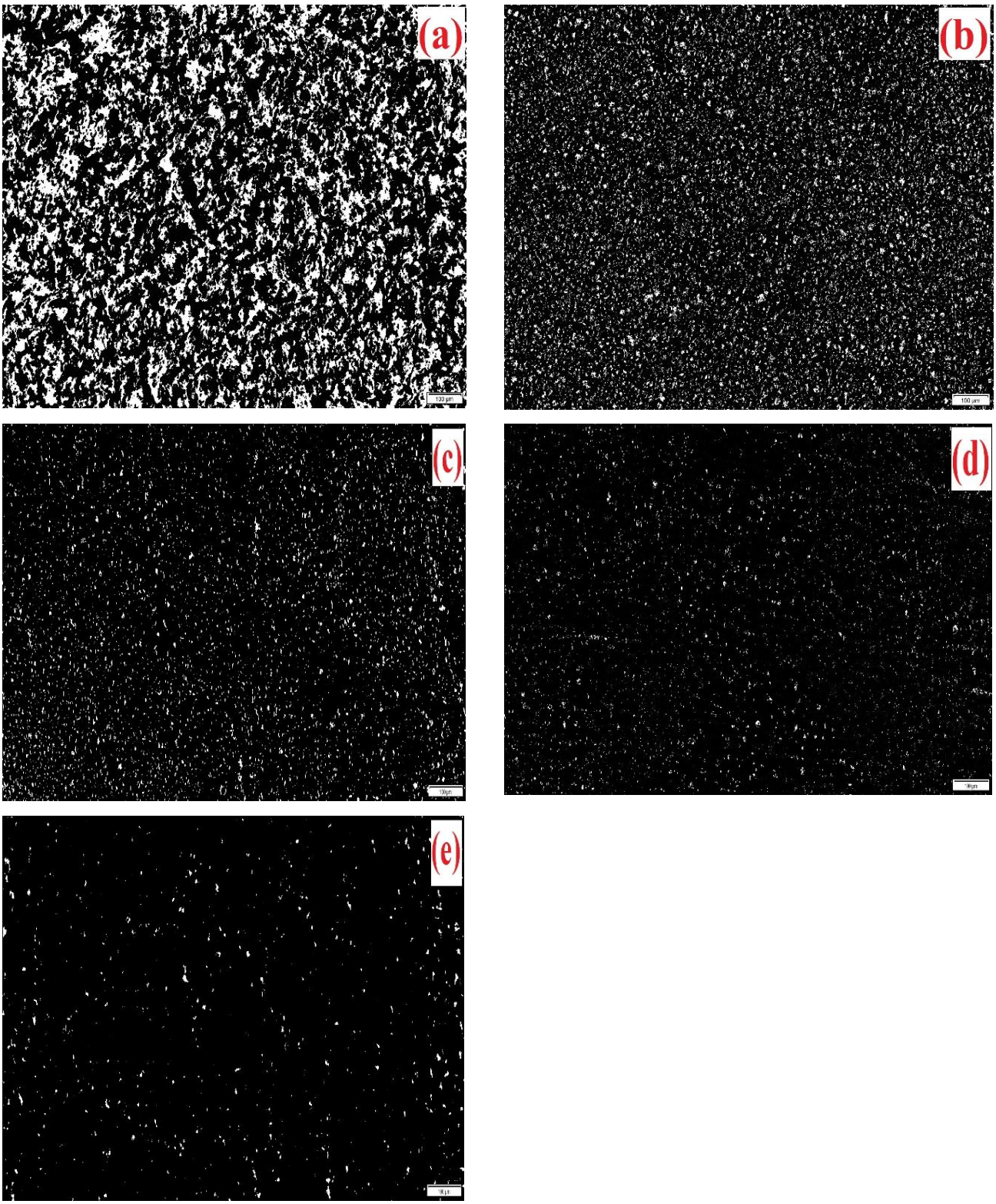

Figure 6.10. Polarized microscopic analysis of the samples (a) WCO, (b) WCO + IL, (c) WCO + PPDR-1%GO at 15°C, (d) WCO + PPDR-1%GO at 25°C and (e) WCO + PPDR-1%GO at 35°C. Scale in microscopic images is 100 micrometer.

6.5.6 Analysis of wax deposition with the cold finger test

In order to quantify the beneficiation brought by the PPDs IL and PPDR-1%GO in terms of wax deposition, cold finger test is important. The schematic of the cold finger setup used for this experimental study was illustrated earlier in the experimental section of this work, and its components were also described in detail. Tables 6.7, 6.8 and 6.9 lists the percentage inhibition of the wax deposition in additive-treated WCO samples at different surface temperatures (representing the temperatures of pipeline wall) and constant hot water bath temperature (pumping station temperature). The weight of unfilled copper tube was 260.5 g. The WCO samples were flowed through the cold finger setup, and the percentage of wax deposited and wax inhibition was calculated using equations (2) and (3) respectively (Deka, Sharma and Mahto, 2020). For this experiment, the additives were doped at their optimum concentrations in WCO samples.

$$\text{Percentage of wax deposited} = \frac{W_{wax}}{W_{co}} X\ 100$$

…….....……..(6.2)

Where,

W_{wax} : Weight of deposited wax, g

W_{CO} : Weight of crude oil flowed through pipeline, g

$$\text{Percentage of wax inhibition} = \frac{(W_{UT})-(W_T)}{(W_{UT})-W_{Cu}}\ X\ 100$$

…….(6.3)

Where,

W_{Cu} : Weight of empty copper tube, g

W_T : Weight of Copper tube with wax deposited in the treated crude oil, g

W_{UT} : Weight of Copper tube with wax deposited in the untreated crude oil, g

The wax deposition in the tubes can be calculated as the difference in the weight of the copper tubes observed prior and subsequent to circulation of crude oil samples. The Table 6.7 exhibits the percentage wax deposition for the oil samples at surface temperature of 20℃. The percentage wax deposition was found to be high around 6.08

% for the virgin WCO. While it reduced considerably down to 4.5 % in IL treated oil sample and the best reduction was 2 % in the case of PPDR-1%GO treated WCO sample. The efficacy of the additives were measured in terms of wax inhibition capacity. IL-treated WCO showed about 26 % inhibition in wax deposition capacity. While this wax inhibition improved remarkably in the case of PPDR-1%GO to 67.1 %, i.e. the wax inhibition efficacy of the PPDR-1%GO was found to be nearly 2.5 times of IL.

With the increase in surface temperature (cooling bath) to 25℃, changes were observed in the wax deposition tendency and wax inhibition capacities of the additives, details of which are mentioned in the Table 6.8. The percentage wax deposition in the WCO was found to be lesser compared to those at 20℃, with 4.47 % deposition recorded in WCO, which reduces to 2.9 % with IL and further falls to 1.3 % in the case of PPDR-1%GO. Similarly, the inhibition efficacy of the additives for the WCO was found to be 33.8 % with IL, which increases significantly to 70.6 % in the case of PPDR-1%GO.

With increasing surface temperatures, there was in general decrease in the deposition tendency of the wax crystals, possibly due to the lower temperature difference between temperatures of pumping station and pipelines. As shown in Table 6.9, at 30℃ surface temperature, the percentage wax deposition was observed to be 3.77 % (WCO), which reduces to 2.07 % (WCO + IL) and 0.94 % (WCO + PPDR-1%GO). The wax inhibition by the additives improved to 45 % with IL, and further increased to 75 % in the case of PPDR-1%GO.

These results indicate that both the additives were able to reduce the wax deposition and cause wax inhibition significantly, and the nanocomposite PPDR-1%GO showed higher efficacy than IL at all the surface temperatures tested (20 ℃, 25 ℃ and 30℃). These results might be attributed to the way in which the additives interact with the wax crystals under flowing conditions and prevent their deposition. The improved efficacy of the PPDR-1%GO may be possibly attributed to the synergistic effect of the VGO sheets and IL on reducing the wax crystal networking and deposition.

Table 6.7. Cold finger test of WCO samples at pumping station temperature 55 ℃ and surface temperature 20 ºC

Crude oil Sample	Weight of (copper tube + deposited wax) (g)	Weight of deposited wax (g)	Percentage of wax deposited (%)	Percentage of wax inhibition (%)
WCO	303.1	42.6	6.08	-
WCO + IL	292.0	31.5	4.5	26
WCO+ PPDR-1%GO	274.5	14	2	67.1

Table 6.8. Cold finger test of WCO samples at pumping station temperature 55 ℃ and surface temperature 25 ºC

Sample	Weight of (copper tube + deposited wax) (g)	Weight of wax deposited (g)	Percentage of wax deposited (%)	Percentage of wax inhibition (%)
WCO	291.8	31.3	4.47	-
WCO + IL	281.2	20.7	2.9	33.8
WCO+ PPDR-1%GO	269.7	9.2	1.3	70.6

Table 6.9. Cold finger test of WCO samples at pumping station temperature 55 ℃ and surface temperature 30 ºC

Sample	Weight of (copper tube + deposited wax) (g)	Weight of wax deposited (g)	Percentage of wax deposited (%)	Percentage of wax inhibition (%)
WCO	286.9	26.4	3.77	-
WCO + IL	275.0	14.5	2.07	45
WCO+ PPDR-1%GO	267.1	6.6	0.94	75

6.6. Conclusions

This is an introductory research where development and application of the graphene-based ionic liquid nanocomposite as pour point depressants opens a new door to utilize the beneficiation of graphene and ionic liquid structure in the field of flow assurance. This work provides a new class of nanocomposite PPDs: PPDR-GO and another novel PPD: IL.

PPDR-1%GO and IL showed tremendous beneficiation in the flow properties of the WCO. The beneficiation in the flow properties include reduction in the pour point, gelation point, apparent viscosities and also reduction was noticed in networking tendency of wax crystals and wax deposition. The optimum pour point reduction of WCO using additives about 18℃, 24℃ and 30℃ was observed at very low dosages about 500 ppm, 250 ppm and 250 ppm of IL, PIL-0.5 % GO and PPDR-1%GO respectively. The cold finger test revealed significant amount of wax inhibition caused by the additives, about 45 % with IL and 75 % with PPDR-1%GO. The additives exhibited great control over aging effect, where IL-treated WCO experienced up to 6℃ growth in the pour point of crude oil, while the increase was limited to 3℃ with PPDR-1%GO, after 30 days of sample storage. Microscopic investigation revealed that the wax crystal network was substantially broken in the presence of IL additive and further disassociation of wax

network was observed with PPDR-1%GO. Thus, highly effective and low dosage novel PPDs were developed in this work.

A new type of working mechanism of the nanocomposite PPD PPDR-GO is proposed, where the presence of VGO sheets in ionic liquid system provides nucleation sites for waxes, while the alkyl component of ionic liquid co-crystallizes with waxes, which further minimizes the wax crystal networking. Additional benefit is obtained from the interaction of polar part of PPD with asphaltenes, which prevents asphaltene aggregation and deposition. Thus, these asphaltenes aid in dispersion of waxes by co-crystallization. The synergism of the ionic liquid and the graphene oxide has significantly inhibited the networking of wax crystals.

Chapter 7

Analysis of the flow assurance of waxy oils in subsea pipelines through modelling and numerical simulation approach

7.1 Introduction

Computational Fluid Dynamics (CFD) is an important study for analyzing the fluid dynamics of any fluid flow. Very few works have reported primarily on the CFD aspect of the crude oil flow in pipelines, and the literatures emphasizing on the fundamentals of wax deposition through CFD approach are found to be scarce. Especially little efforts have been made to simulate the gelling phenomenon of the crude oils using enthalpy porosity technique, which has been used in this work. Therefore, in this research work focus is given to touch upon this area to highlight the importance of understanding the fluid dynamics of the flow assurance challenge caused from wax deposition.

In this work, focus would be mainly on the initial stage of wax deposition i.e. gelling phenomenon. The primary motive behind focusing on this stage of wax deposition, can be understood in a way that before proceeding to simulate the other stages of wax deposition, it is imperative to understand the gelling structure well. Simulating the remaining stages of wax deposition would be the objectives for our future work. This work would provide the understanding as to how the gelling phenomenon occurs and varies with changes in the operating flow conditions of crude oil in a sample pipeline. [4]

In this work, the authors tried to simulate the gelling phenomenon of the crude oil through CFD approach. In this work, a wax-oil mixture (representing the crude oil) was used as the flowing fluid in a pipeline of particular dimensions. The crude oil was pumped into the pipeline at higher temperatures and the pipe ambient temperatures were considered significantly lower in order to simulate the wax deposition phenomenon, and

---

[4] This chapter is a slightly modified version of my research publication titled "Predicting the Wax Deposition and Gelation Behavior of Waxy Oils in Subsea Pipelines through Modelling and Numerical Simulation Approach" SPE-202368-MS. In: Proceedings of SPE Asia Pacific Oil & Gas Conference and Exhibition," published (November 2020), 1-16; and it has been reproduced here with the permission of copyright holder.

the simulation was tested under laminar conditions to develop a preliminary idea of the gelling process.

Theory of wax precipitation, gelation and deposition in pipelines:

The effective pipeline transportation of crude oils is affected mainly due to the precipitation and deposition of components of crude oils known as waxes. These waxes are high molecular weight components of crude oil, usually comprising higher carbon compounds, anywhere between C18 up to C80 as reported in various literatures. Even 2 wt % waxes in crude oil are sufficient to initiate the dense networking of wax crystals in pipeline and seriously affect the flow characteristics and dynamics of crude oil**.** These paraffin waxes have a characteristic property of exhibiting variable solubilities at different temperatures. At higher temperatures, the waxes stay in dissolved state, such as those observed in reservoir conditions. When the temperature of the crude oil starts dropping below wax appearance temperature (WAT), the precipitation of these wax crystals initiates and it continues until the temperatures keeps dropping till the pour point temperature of the oil is attained, where the flow of oil completely stops (Sharma *et al.*, 2019; Sharma, Mahto and Vuthaluru, 2019; Deka *et al.*, 2020; Deka, Sharma and Mahto, 2020). WAT is termed as the temperature, above which the crude oil is in complete liquid state and the wax crystals are in highly dissolved state. WAT of the crude oils varies with the type of oil and the reservoir conditions. Pour point of the oil is termed as the lowest temperature below which the flow of the crude oil ceases completely under static conditions. But when the there are changes in the conditions such as increase in shear rates, the movement of oil could actually happen below the pour point (Deka *et al.*, 2018; Sharma *et al.*, 2018). Therefore, in order to better assess the dynamics of the crude oil under flowing state, there is a need for correctly assessing the gelation characteristics of crude oil. The correct estimation of gelation helps to identify the freezing characteristics of crude oils. Experimentally the gelation point could be determined rheologically using different methods such as viscosity temperature plots and variation of storage & loss modulus against temperature (Sharma et al. 2019c, Singh et al. 2002). Usually the changes in storage and loss modulus of the crude oil are tracked with temperature to identify the gelation tendencies, and as the temperature decreases, the storage modulus attempts to

overcomes loss modulus, indicating the dominating features of waxes in the rheology of the crude oil (Sharma *et al.*, 2019).

There is no universal agreement over the mechanism of wax deposition in crude oils, and there are few theories that have been proposed regarding it namely molecular diffusion, Brownian diffusion, gravity settling and shear dispersion. These mechanisms have been proposed after detailed experimental works carried out by several authors. The widely accepted methodology among them is the molecular diffusion of wax particles from the bulk crude oil. The current work would also consider the molecular diffusion as the primary mechanism for wax deposition. The molecular diffusion is initiated due to the development of a thermal gradient between the bulk fluid and the pipe-wall temperatures. Previous work on development of wax deposition models (Singh *et al.*, 2000) states that it is the initial formation of incipient thin wax-oil gel that is responsible for the subsequent wax precipitation and deposition phenomena. During pipeline transportation, when the ambient temperatures are low, wax precipitation could be observed near the pipewall region, leading to concentration gradient in the crude oils, and the wax molecules starts to flow from the bulk oil towards the pipewall. At this situation, the carbon numbers greater than the critical carbon number starts to precipitate and moves towards the pipewall. These wax crystals are porous structures having the capacity to hold a huge amount of oil, usually about 90-95 %. Due to this porous and liquid holding feature of wax crystals, a gel structure is created on the pipewalls as the initial stage of wax deposition, comprises a mixture of a broad distribution of carbon numbers. After this gel formation stage, there would probably be the diffusion of carbon compounds towards pipewall as we discussed above. This would lead to increase in the thickness of the deposited wax layer. But soon, this thickness would stop growing due to thermal resistance offered by the less conductive wax layers and thus decreasing temperature gradient, which would slow down the wax transfer from the bulk towards the wall. Still, there would be a thermal gradient present inside the deposited wax layer, which would lead to further internal diffusion of carbon compounds. This process would in general increase the content of wax in the wax deposit layer, and this stage is also referred to as aging phenomenon. This internal diffusion inside the wax layers is an important part of the aging process in crude oils, which leads to subsequent hard deposit on the pipewalls. Along with the internal diffusion process, where the reverse diffusion of oil molecules

occur that were trapped in wax-gel structure diffuses back towards the bulk oil, due to the similar type of concentration gradient being developed. The stages comprising of the internal diffusion up to reverse diffusion contributes to the aging effect in crude oils and thus completes the process of wax deposition (Venkatesan *et al.*, 2002).

7.2 Methodology

The procedure to simulate the crude oil flow in is described in brief in the following discussion. The geometry was created in Spaceclaim®2019, and the meshing was performed using ANSYS®2019 R2 meshing. After the meshing process was completed, the meshed geometry was then transferred to the Fluent® setup, where the appropriate models for the flow case were selected according to the requirements and the solution was then calculated using the solution component of the Fluent® 2019 R2, which was run in order to complete the simulation process. The results of this simulation were calculated using its post processing which, were either accessed in solution mode itself or the solution be transferred to the results section and then calculated. The methodology consists of the following sections: Geometry creation, meshing and setting up model.

7.2.1 Geometry creation

In this research work, a simple geometry of a cylindrical pipe was created and split into half symmetrically for carrying out further simulation process. This was done in order to reduce the computational expense as the number of cells are reduced and consequently the calculations, but the results would not be affected, as the geometry is sliced symmetrically. The 3D version of the geometry was used for the simulation purpose. The dimensions of the cylindrical pipe were 0.0072 m in radius and 2.44 m in length.

7.2.2 Meshing

Meshing is the most important feature of the simulation process and must be given the utmost care because the accuracy of the solution ultimately depends on the quality of meshing used in the simulation. Also, care should be given to optimizing the number of cells being used for a particular simulation, so that excess computational expense is not accrued in the simulation work for diminishing return. Meanwhile, care should be given to the minimum quantity of meshes to correctly simulate the features of the fluid dynamics into the simulation work.

In this work, the half cylindrical pipe geometry was meshed volumetrically, with the minimum element size of 0.001 m and the maximum cell size of 0.003 m, cell growth rate ratio of 1.15, no adaptive sizing curvature normal angle of 18°. The proximity and the curvature were captured. Now looking into the meshing methods, it consisted of two techniques; first one is using the sweep method in order to create a homogenous cell format throughout the flow length and the other one is creating inflation layers on the pipewall. Inflation layers were created in order to capture the fluid dynamics occurring near the pipewall, where the wall shear stresses are dominant and other important significant phenomena occur. The sweep method was used where the meshes were created with the all triangular cells. The number of inflation layers created were 8 with the first layer thickness of 0.0001 m, growth rate of 1.15 and transition ratio of 0.272. The total number of meshed cells created were 275184, and nodes being 1135479, target skewness of 0.9 and the smoothing was kept high. The mesh metrics are as follows: element quality-minimum of 0.18 and maximum of 0.996. The total volume of the cylinder was 4.967 cubic meters. The geometry walls were named as inlet, pipewall, symmetry and outlet, where symmetry represents the sliced portion of the cylinder.

7.2.3 Setting up the model

The characteristic property of the wax-oil mixture is listed in the Table 7.1.

Table 7.1. Characteristic properties of the wax-oil mixture

Property	Value
Density	838.5 kg/m^3
Specific heat	2259 J/Kg-K
Thermal conductivity	0.1466 w/m-k
Viscosity	0.0087 kg/m-s
Pure solvent melting heat	8000 J/kg
Solidus temperature (pour point)	277 K
Liquidus temperature (Wax appearance temperature)	286.9 K
Wax content of the mixture	0.67 wt.%

Some of the characteristic properties of the wax-oil mixture have been taken from (Singh *et al.*, 2000). Setting up appropriate models are essential for obtaining correct results of any type of simulation and to correctly describe the physics behind the simulation process. The model in this work was setup with some fundamental inputs such as the solver used was pressure based, velocity formulation was kept absolute, and the transient technique was used to perform the calculations. The reason for adopting the transient technique instead of steady state technique was mainly to calculate a number of parameters that were based on flow time, and the parameters usually change with flow time. The model used in this simulation work was the Viscous-laminar model to characterize the flow of the crude oil under laminar conditions. Gravitational body forces due to natural convection and buoyancy driven flows were neglected in this simulation, as density of wax-oil mixture is not considered as temperature-dependent in this work.

To simulate or model a fluid flow problem the conservation of mass and continuity should be established appropriately. Following are the conservation equations used in the simulation. The mass conservation or continuity equation used in the modelling work is mentioned below. It is applicable for both compressible and incompressible flows. In this work, crude oil flow is considered as an incompressible flow.

$$\frac{\partial \rho}{\partial t} + \nabla.(\rho\vec{v}) = 0 \quad \text{.....(7.1)}$$

In this equation, ρ is the density and $\vec{v}$ is the fluid flow velocity vector.

The conservation of the momentum in an inertial frame of reference is done by using the equation

$$\frac{\partial(\rho\vec{v})}{\partial t} + \nabla.(\rho\vec{v}\vec{v}) = -\nabla p + \nabla.(\boldsymbol{\tau}) \text{.....(7.2)}$$

where p refers to the static pressure and τ is average stress tensor which is defined as follows:

$$\boldsymbol{\tau} = \mu[\left(\nabla\vec{v} + \overline{\nabla}\vec{v}^{\overline{T}}\right) - \frac{2}{3}\nabla.\vec{v}\mathbf{I}] \text{.....(7.3)}$$

where μ refers to molecular viscosity, the second term on the right hand side is the effect of volume dilation and I refers to unit tensor, Gravitational forces and external body forces were neglected in the momentum conservation equations.

Heat transfer can occur via three modes, but the modes that are applicable in this case are conduction and convection only. The energy conservation, which is very important aspect of the modelling, the equation is as follows:

$$\frac{\partial(\rho E)}{\partial t} + \nabla \cdot (\vec{v} \quad ((\rho E) \quad + p)) = \nabla \cdot ((k \nabla T) + (\boldsymbol{\tau}. \vec{v})) \quad \ldots\ldots\ldots\ldots\ldots\ldots\ldots (7.4)$$

(*ANSYS Fluent 18.1 Theory Guide*, 2017)

The first term on the right side of the equation is for energy transfer by conduction and the second term is for viscous dissipation.

Now, for simulating the gelling of the wax crystals, solidification approach is adopted in this simulation. This approach is based on the enthalpy-porosity formulation proposed by (Voller and Prakash, 1987) related to the numerical solution of convection-diffusion dominated mushy region phase-transformation cases. In this approach, there is a liquid solid region mushy zone present in the fluid flow region which represents the gelling structure of the crude oil. This mushy zone is considered as the porous zone, and the porosity is equal to the liquid fraction i.e. the fraction of liquid present in the zone. Therefore, in order to incorporate solidification, appropriate sink terms are added to the momentum conservation equation owing to the presence of pseudo solid in the fluid flow region.

The energy of the material is calculated as the sum of sensible enthalpy, h and latent heat, ΔH:

$$H = h + \Delta H \ldots\ldots\ldots\ldots\ldots\ldots\ldots\ldots\ldots\ldots\ldots\ldots\ldots\ldots\ldots\ldots\ldots\ldots\ldots\ldots\ldots\ldots (7.5)$$

$$h = h_{ref} + \int_{T}^{Tref} C_p \, dt \ldots\ldots\ldots\ldots\ldots\ldots\ldots\ldots\ldots\ldots\ldots\ldots\ldots\ldots\ldots\ldots\ldots\ldots\ldots\ldots\ldots\ldots (7.6)$$

where h_{ref} = reference enthalpy, T_{ref} = reference temperature, and C_p = specific heat at constant pressure.

The liquid fraction Ƶ can be defined as,

$$Ƶ = 0 \qquad \text{if } T < T_{solidus}$$

$$Ƶ = 1 \qquad \text{if } T > T_{liquidus}$$

$$Ƶ = \frac{T - T_{solidus}}{T_{liquidus} - T_{solidus}} \quad \text{if } T_{solidus} < T < T_{liquidus} \ldots\ldots\ldots\ldots (7.7)$$

The latent heat content can be defined in the terms of Latent heat of material, L:

$$\Delta H = Ƶ L \ldots\ldots\ldots\ldots\ldots\ldots\ldots\ldots\ldots\ldots\ldots\ldots\ldots\ldots\ldots\ldots\ldots\ldots\ldots\ldots\ldots\ldots (7.8)$$

The latent heat content may lie between zero (in the case of solid) and L (in the case of a liquid).

For solidification/melting problems, the energy transfer equation could be written in an updated form as:

$$\frac{\partial(\rho H)}{\partial t} + \nabla \cdot (\rho \vec{v} H) = \nabla . (K \nabla T) \quad \text{.....(7.9)}$$ (*ANSYS Fluent 18.1 Theory Guide*, 2017)

where H = enthalpy

ρ = density

$\vec{v}$ = fluid velocity

The solution for temperature is essentially an iteration between the energy equation (Equation 7.9) and the liquid fraction equation (Equation 7.7).

Finite volume approach was used to calculate the solution in Fluent.

The material used in the simulation is a wax-oil mixture and the average properties of the mixture is used for the simulation. The wax proportion of the wax-oil mixture is about 0.67 wt% in the oil.

***Inputs for the Boundary conditions on the simulation for the wax-oil mixture*:**

The inlet boundary conditions were velocity at the pipe inlet of 0.38 m/s (1 GPM), gauge pressure at inlet of 0 Pa, temperature of the bulk wax oil mixture at inlet of 295.2 K. The pipewall boundary conditions were set as follows: The pipewall was considered to be stationary and no motion at wall was considered, and also no slip shear conditions were set at the wall and the temperature of the pipewall was set at 281.3 K. The shear conditions on the wall were set as no slip condition indicating the wax-oil mixture would adhere to the wall and with the same velocity as the wall, if in case the wall is moving. These conditions would help to develop a fully developed viscous laminar flow in the pipe. The outlet was set a gauge pressure of 0 Pa and conditions were set to prevent backflow, and in case of backflow fluid temperature was set at 295.2 K. Some of the initial boundary conditions for the fluid flow has been taken from a previous work (Singh *et al.*, 2000). The flow was maintained under laminar conditions.

Pressure based solver was used for the simulation. Appropriate methods were selected for solving the mass and momentum conservation equations, the energy balance equations and solidification equations. The methods that were used are described as

follows: SIMPLE scheme was selected for pressure velocity coupling. Spatial discretization of the meshed geometry was performed using the least square cell based methodology, while for pressure based calculations PRESTO scheme was used, for solving momentum and energy equations, the second order upwind scheme was chosen, while to calculate the transient formulation the first order implicit scheme was used. The under-relaxation factors were set at 0.3, 1, 0.7, 1, 1 and 0.9 for the pressure, body forces, density, liquid fraction update, energy and momentum respectively. The convergence history of the calculation was tracked by monitoring the residuals and the convergence criteria set for them was 10^{-6}, this was done in order to enhance the accuracy of the calculations. The problem was then initialized from the inlet and the calculation were then solved/run with the time step size of 0.5 and was run for 5 days, and the maximum iterations were set at 30 iterations per timestep. The reporting interval and the solution profile was updated after every 1 interval, i.e. the convergence report of the residuals would be plotted/updated after every iteration. The smaller interval chosen would help to monitor the convergence of the residuals appropriately.

The complete cylindrical pipe geometry was considered as the fluid domain. Doing this helps to simplify the simulation in terms of computational expense and time. Therefore, all the cell zone conditions would be considered as fluid domain and thus the calculations under this simulation work would be carried out on the fluid volume only.

7.3 Results and Discussion

The pipe geometry is displayed in the Fig. 7.1. It is a symmetrical half section of the cylindrical pipe created for the flow of wax-oil mixture. It consists of one inlet and outlet each, a pipewall and the pipe symmetry.

Figure 7.1. Geometry of the half section of the cylindrical pipe

Fig. 7.2 displays the meshed inlet face of the geometry, while Fig. 7.3 displays the meshed section of the pipewall. Figure 7.4 illustrates the meshed section of the pipe symmetry.

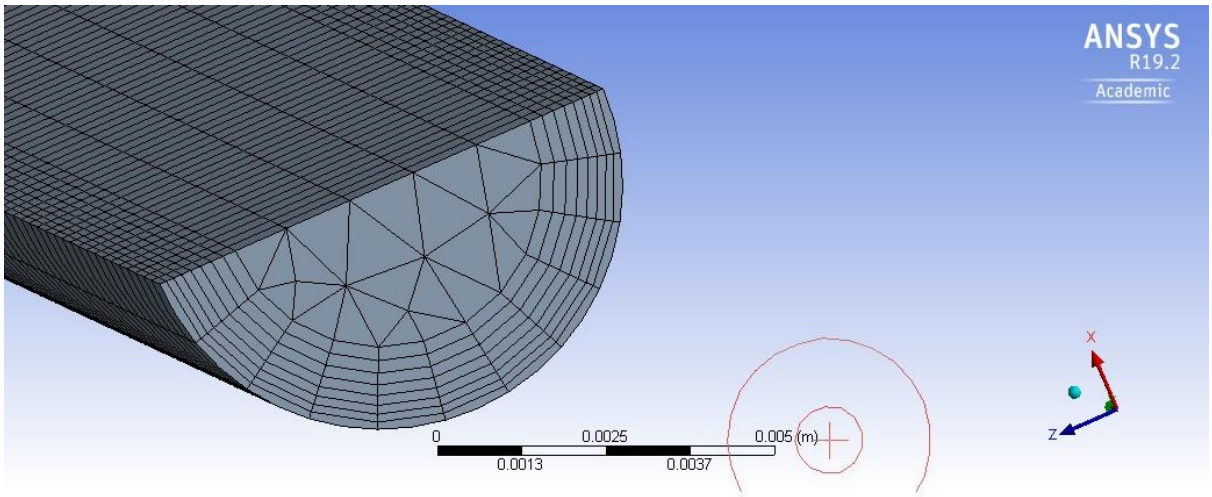

Figure 7.2. Illustration of the meshing at the pipe inlet with the presence of inflation layers on the wall

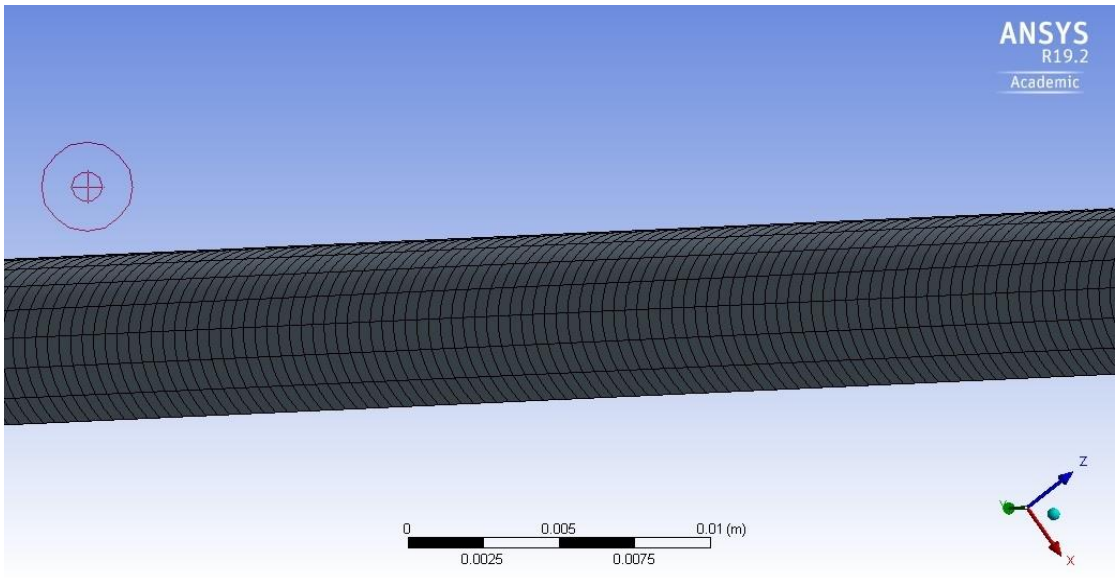

Figure 7.3. Illustration of the meshing at the pipewall. The scale bar illustrated in is 0.01 m, with major divisions of 0.0025.

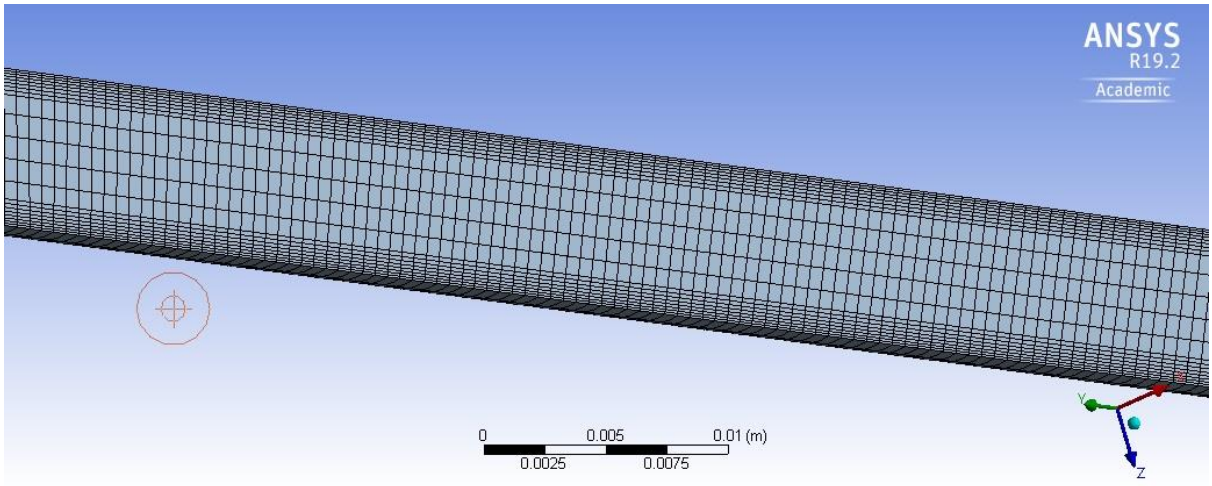

Figure 7.4. Illustration of the meshing at the pipe symmetry. The scale bar is 0.01 m, with major divisions of 0.0025.

The temperature profile of the pipewall is displayed in Fig. 7.5, where it can be observed that the heat transfer in the wax-oil mixture occurs at a fast rate and most of the heat transfer occurs near the inlet section of the pipewall. The temperature of the wax-oil mixture drops from 295.2 K down to 286 K within a short length of the pipewall. This observation could be correlated with the wax gelation process, where most of the wax precipitation and deposition occurs within only a few minutes of the crude oil flow due to convection processes dominating the heat transfer process. Subsequently as the flow progresses the diffusion process dominates, which would cause aging in the wax-oil deposit. The gelling would start at the very beginning of the fluid flow, due to rapid heat transfer from the bulk fluid to the pipewalls. Although, this simulation work would not exhibit the aging phenomenon usually observed in the crude oil flow, but this task would be performed in our future works. The temperature profile of the pipe symmetry is exhibited in Fig. 7.6, which indicates that the complete heat transfer has taken place, and the lowest temperatures of around 281 K were recorded at the pipewalls and temperature gradient was formed in the pipe. Fluid temperature keeps increasing as we proceed towards the centre of the pipewall. This temperature profile at the symmetry indicates the temperature profile at the middle of the pipe, which suggest that a temperature gradient exists, and the heat transfer occurs from bulk fluid (at the center) to the pipewall (cold). And in this process, wax deposition and gelling phenomena occurs.

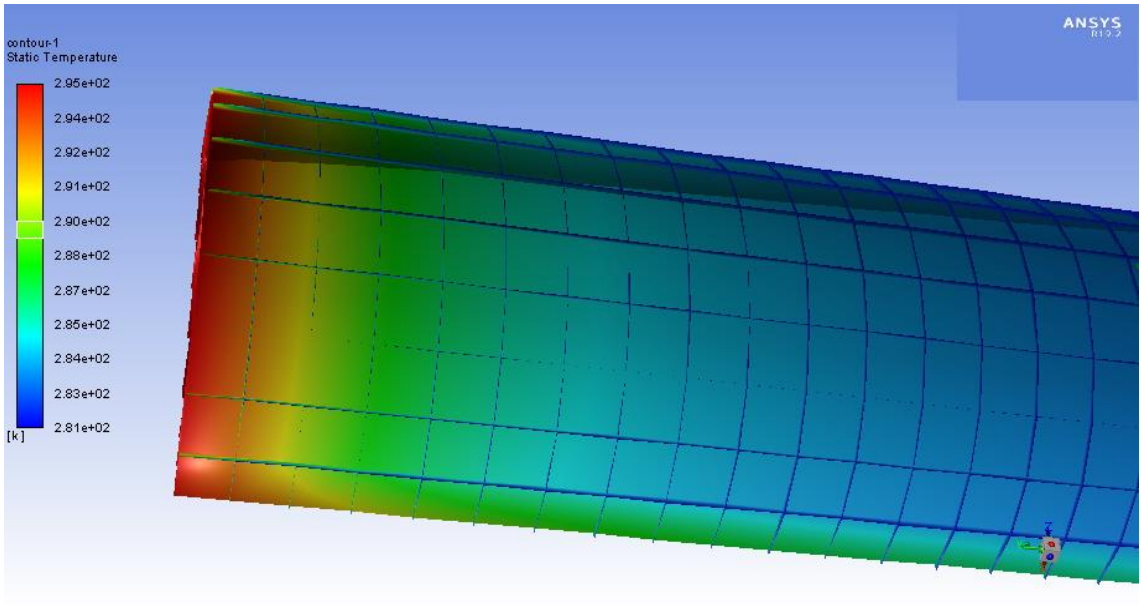

Figure 7.5. Illustration of the temperature variation along the pipewall (starting from the inlet section)

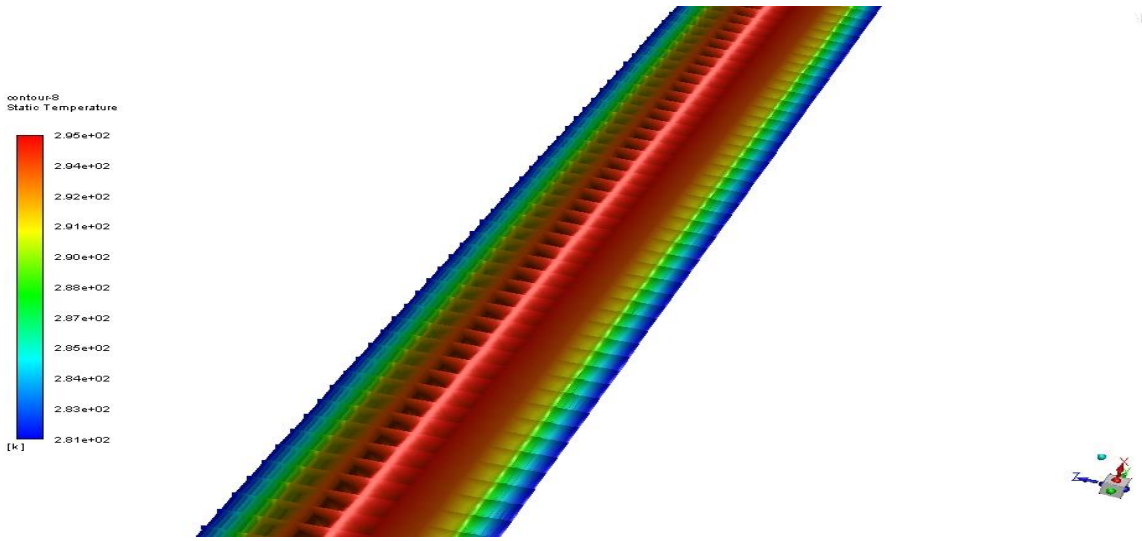

Figure 7.6. Illustration of the temperature profile at pipe symmetry

The velocity profiles at the inlet and the outlet are shown in Fig. 7.7. This figure illustrates that velocity gradient were not developed at the inlet section, while it developed fully during fluid flow and at the outlet. Lower velocities were observed at the pipewalls, while higher velocities were observed in bulk fluid. This is due to the lower temperatures and also the wax deposition and gelling phenomenon near the pipewalls, which obstructs the fluid flow and reduces the fluid velocity.

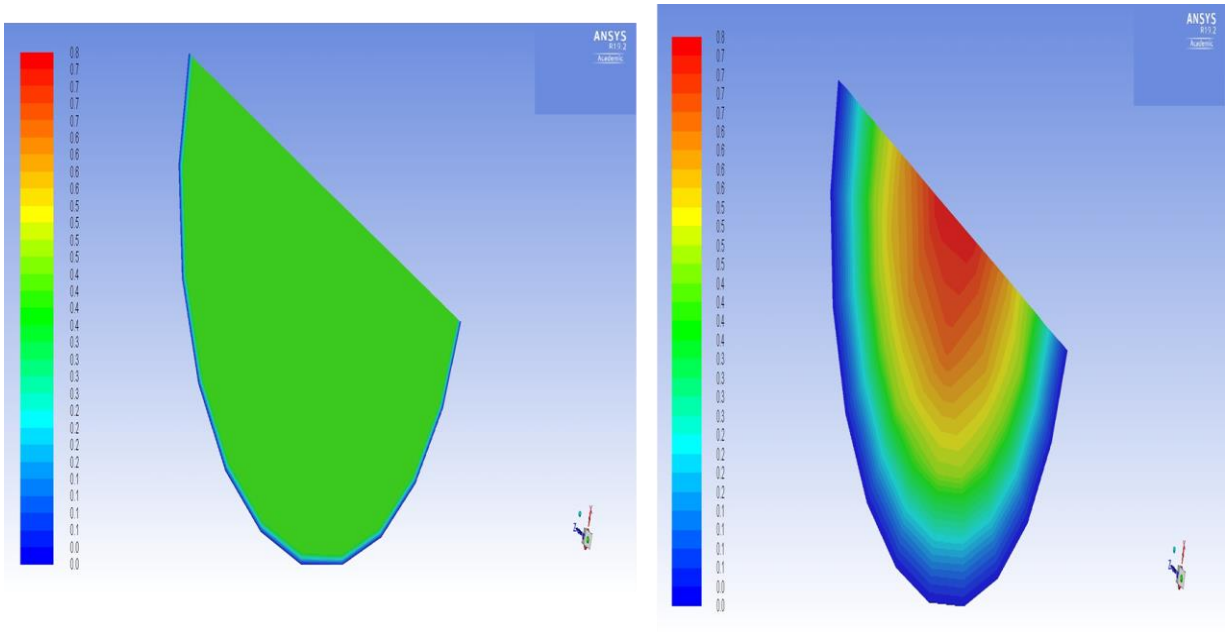

Figure 7.7. Velocity profile at the inlet (left illustration) and outlet (right illustration)

Fig.7.8 illustrates the velocity profile at the symmetry of the pipe, where the changing velocity contours indicate that the laminar flow has been fully developed and then there are very small changes in the velocity contours with increase in the flow time. The properties of the wax-oil mixture would become more consistent in the fully developed laminar region.

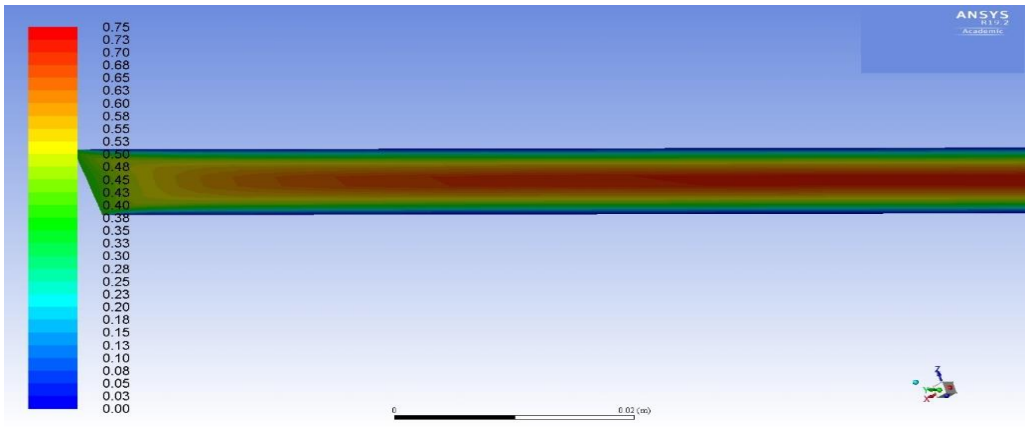

Figure 7.8. Illustration of velocity profile at the pipe symmetry and the fully developed laminar flow

Fig. 7.9 illustrates the velocity contours along the pipe symmetry, which indicates that the velocity is very low at the centre (near zero) and keeps increasing towards the centre and increases up to 0.75 m/s. Also, this figure indicates that almost no change occur in the velocity profile throughout the length of the pipe as most of the changes in the velocity has occurred near the inlet section.

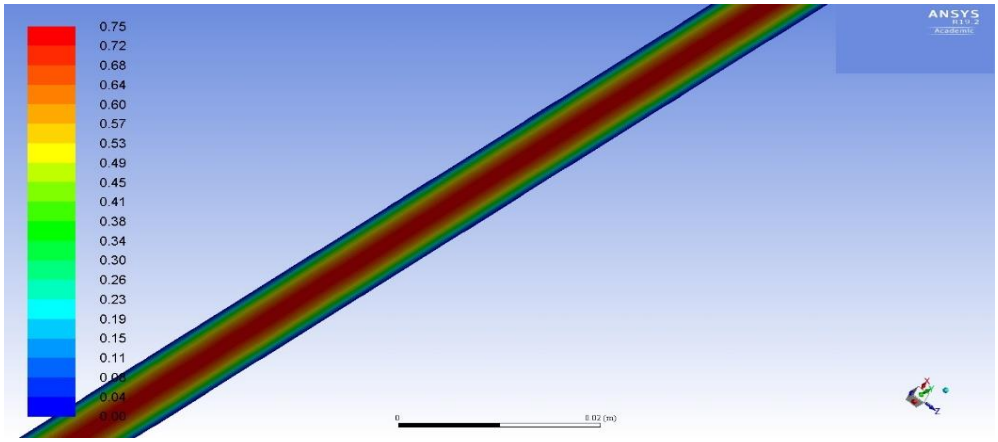

Figure 7.9. Illustration of the velocity contours at the pipe symmetry

Monitoring shear stresses on the pipewalls is very important aspect of pipeline monitoring, because sudden change in the shear stresses could indicate the presence of solid deposition near the pipewalls. Therefore, the shear stresses were monitored and exhibited in Fig. 7.10, where it could be observed that most of the changes in the shear stress occurs near the pipe inlet. This may be attributed to the rapid precipitation and deposition of the waxes near the inlet, which lead to higher shear stress, as the shear forces become dominant in this region.

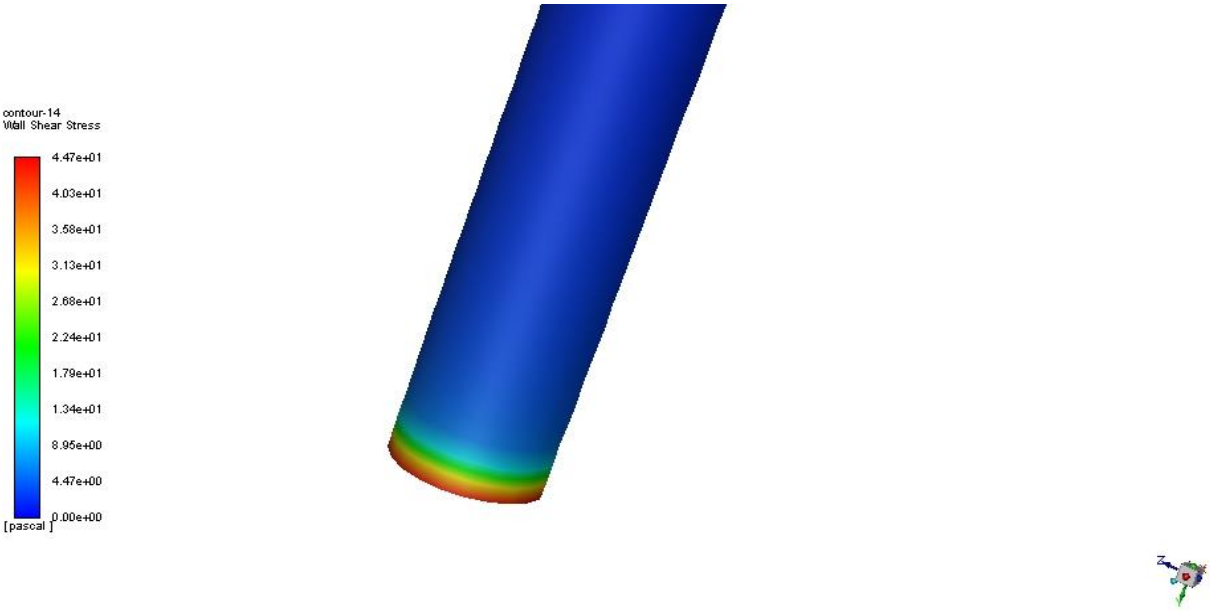

Figure 7.10. Illustration of the shear stress at the pipewalls

The wax gelling phenomenon on the pipewalls is displayed in Fig. 7.11. Wax gelling is monitored through the changes in the liquid fraction parameter of the simulation. As the wax starts to precipitate, the liquid fraction of the wax-oil mixture reduces, and it indicates the formation of the wax-oil gel. In this simulation process we observed a very clear phenomenon of wax gelling on the pipewalls due to the flow of crude oil on in the pipeline. The liquid fraction was observed to be higher near the inlet and keeps on decreasing as the flow progress. It increases with the increase in wax deposition and was found to decrease with the flow from 1 at the inlet (100% liquid) to 0.469 (46.9%) solidification at the outlet wall. This indicates that wax gelling occurs up to 53.31 % during the fluid flow.

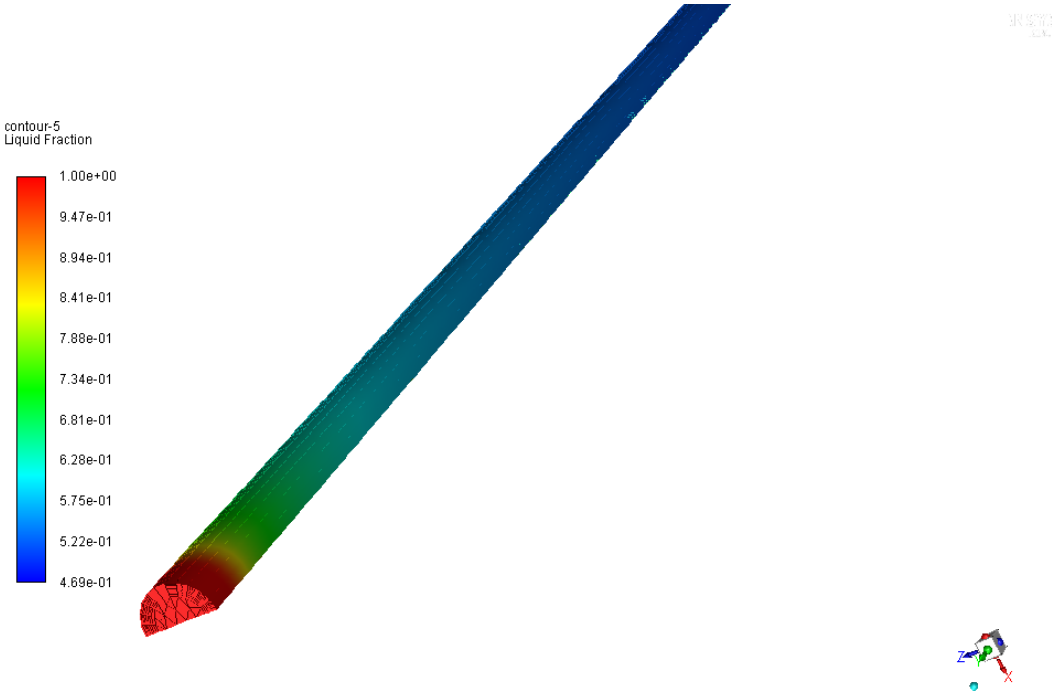

Figure 7.11. Illustration of the contours of liquid fraction on the pipewalls representing the solidification phenomenon

The solidification can also be observed through the pipe symmetry as observed in Fig. 7.12, where the contours of the liquid fraction changes rapidly near the wall region and becomes constant near the pipe central region.

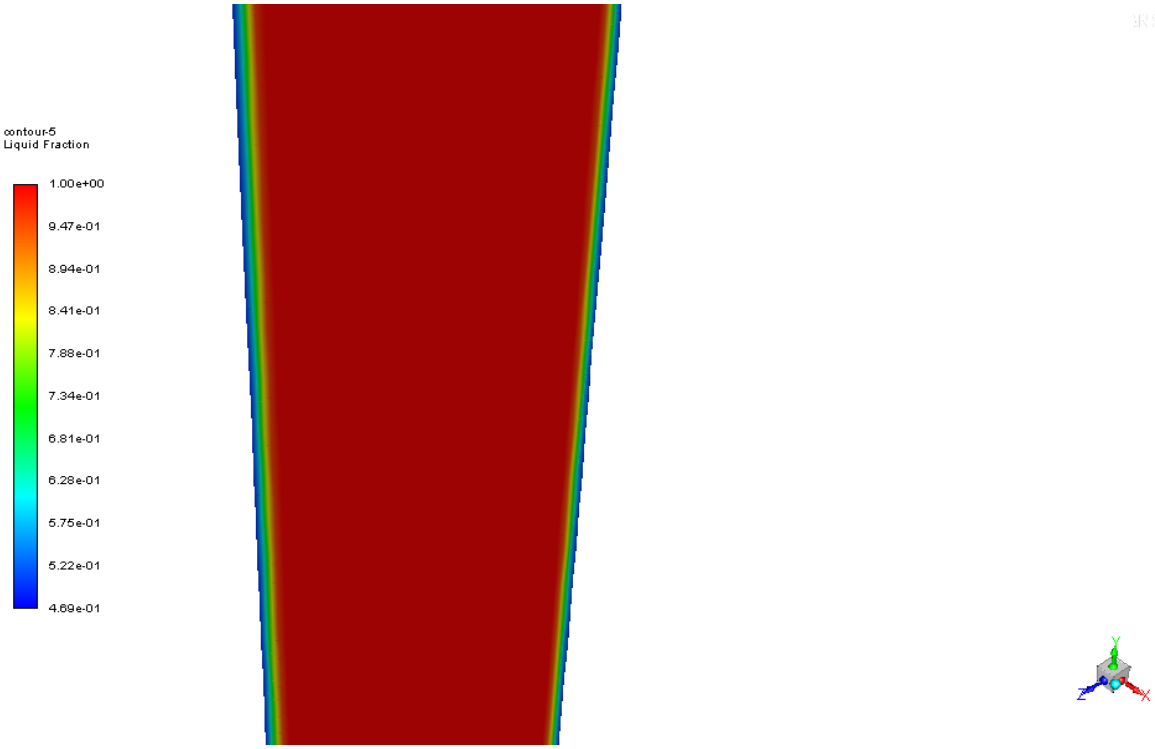

Figure 7.12. Illustration of the contours of liquid fraction representing the solidification at the boundaries of the pipe symmetry

More details of the wax gelling phenomenon were investigated at the inlets and the outlets. Fig. 7.13 illustrates the liquid fraction contour at the pipe inlet, where we can observe that no change in the liquid fraction was observed, indicating that the wax gelling phenomenon did not start at the inlet, and it may have developed during the fluid flow.

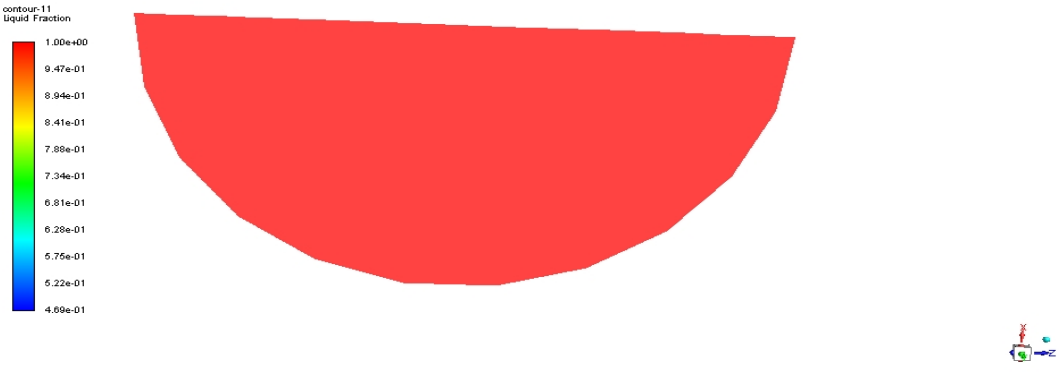

Figure 7.13. Illustration of liquid fraction contours exhibiting no solidification at the pipe inlet

Investigating the wax gelling at the outlet, clear contours of the solidification are observed at the pipe outlet (Fig. 7.14) and the liquid fraction changes from 1 to 0.469

from the wall towards the centre. This confirms that the wax gelation phenomenon occurs in the flow of the wax-oil mixture and it continues until the outlet.

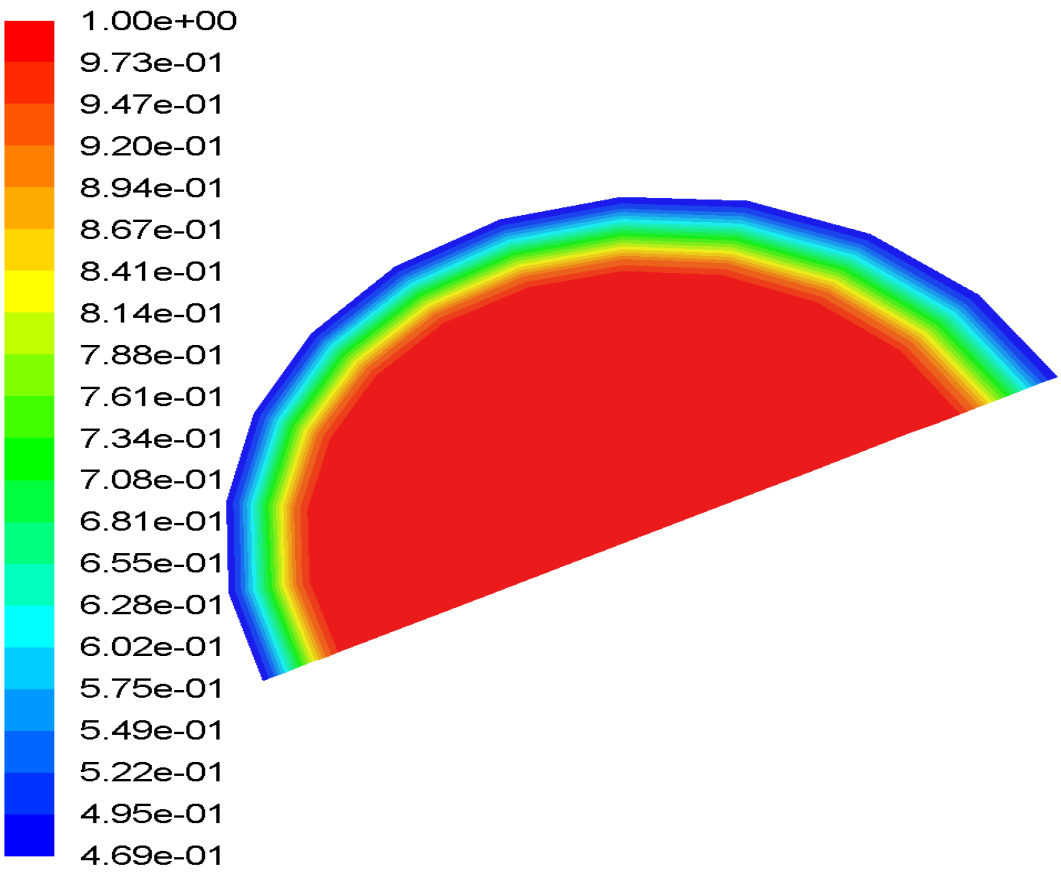

Figure 7.14. Illustration of the solidification at the pipe outlet

Effect of flow rate on the wax-oil gelling

The results obtained and discussed up to now were carried out at flow rate of 1 GPM, and it provided a good illustration of the occurrence of gelling phenomenon in the wax-oil mixture in flowing conditions. Additionally, in order to understand the effect of flow rates on the solidification phenomenon in crude oil, fluid flow rates were varied between 1-5 GPM.

The effect of fluid flow rates on the liquid fraction and solid fraction of the wax-oil mixture can be observed from Fig. 7.15 and Fig. 7.16 respectively, and it is seen that the liquid fraction increases with increasing flow rate, and therefore, the solid fraction

decreases, suggesting that the solidification of the wax crystals decreases at higher flow rates. Moreover, it can be seen from Table 7.2 that solidification decreases swiftly at small flow rates, and this reduction slows down gradually at higher flow rates. Higher flow rates are impeding the solidification process at the pipewalls, i.e., they reduce the tendency of wax deposition at pipewalls owing to the molecular diffusion process to small extent. This suggest that the flow rate has significant effect on the wax-oil gelling phenomenon.

Moreover, major solidification occurred in starting length of the pipeline, and the growth occurred slowly in subsequent pipe length. These results indicate that wax precipitation and gelation occur rapidly during initial flow and slows down subsequently.

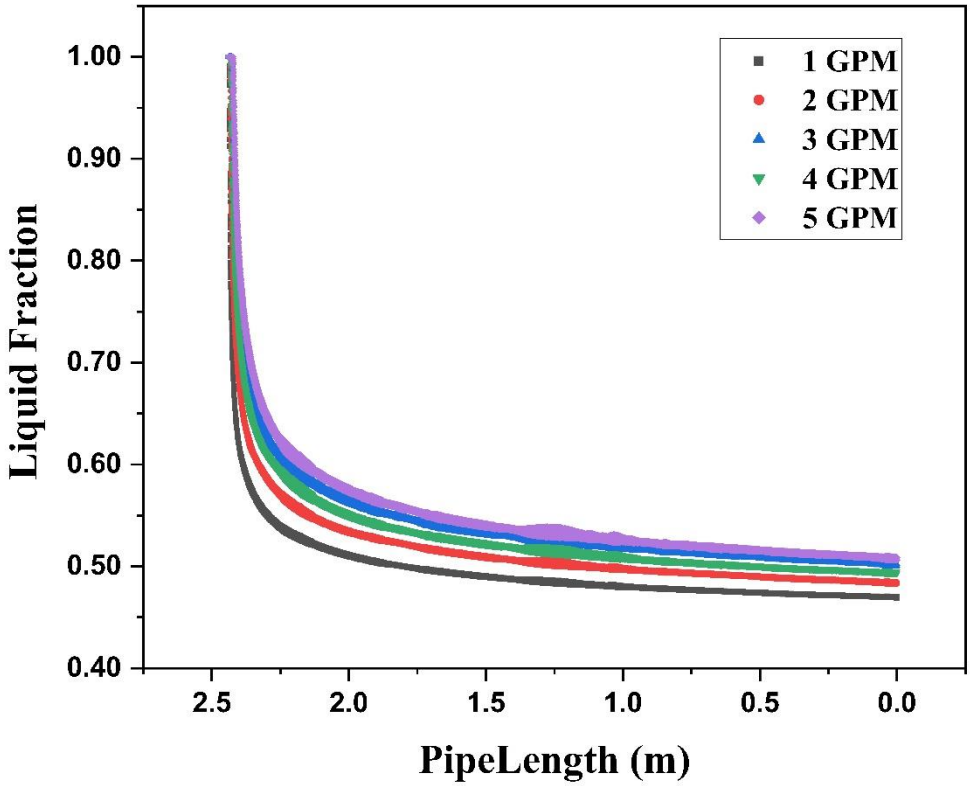

Figure 7.15. Illustration of the decrease in the liquid fraction with increase in flow rate (pipe length = 2.5 m) (pipe length Y axis coordinates lies between 2.5 m to 0 m, inlet and outlet lies at 2.5 m and 0 m respectively)

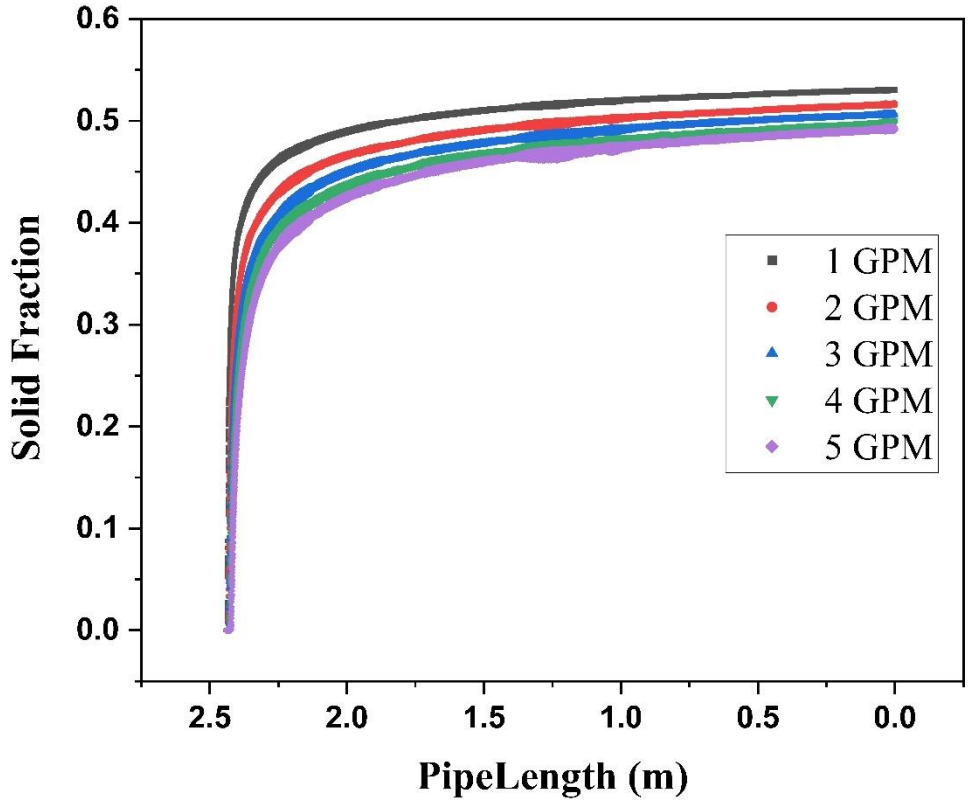

Figure 7.16. Illustration of the solid fraction at pipewall with pipelength (Pipelength Y-axis coordinates vary between 2.5 m and 0 m, inlet and outlet lies at 2.5 m and 0 m respectively)

Table 7.2. Variation in the solidification with different flow rates

Inlet Flow Rate (GPM)	Inlet Velocity (m/s)	Inlet Bulk Fluid Temperature (K)	Pipewall Temperature (K)	Solidification at Pipewalls, Area Wt. Avg.
1	0.38	295.2	281.3	0.531
2	0.773	295.2	281.3	0.482
3	1.1605	295.2	281.3	0.468
4	1.547	295.2	281.3	0.46
5	1.934	295.2	281.3	0.447

Grid Independence Test

A grid independence test was performed in order to test the efficiency of the numerical simulation performed in terms of optimization of computational resources and accuracy of the results. The model was simulated to calculate the solidification at the pipewalls at the flow of 2 GPM, for different set of mesh elements ranging from 1.5 X 10^5 to 5.4 X 10^5. From the Fig 7.17, it can be clearly seen that solidification was found to be lesser with mesh elements lesser than 2.75 X 10^5, while the solidification does not increase notably than mesh elements higher than 2.75 X 10^5 i.e upto 5.4 X 10^5. Thus, it can be concluded from the grid independence test, that the 2.75 X 10^5 is the optimized number of mesh elements for simulating the wax-oil gelation in pipeline flow. Thus, in this chapter 2.75 X 10^5 i.e. 275184 number of mesh elements were used in the model to calculate different output variables including liquid fraction and solidification at the pipewalls.

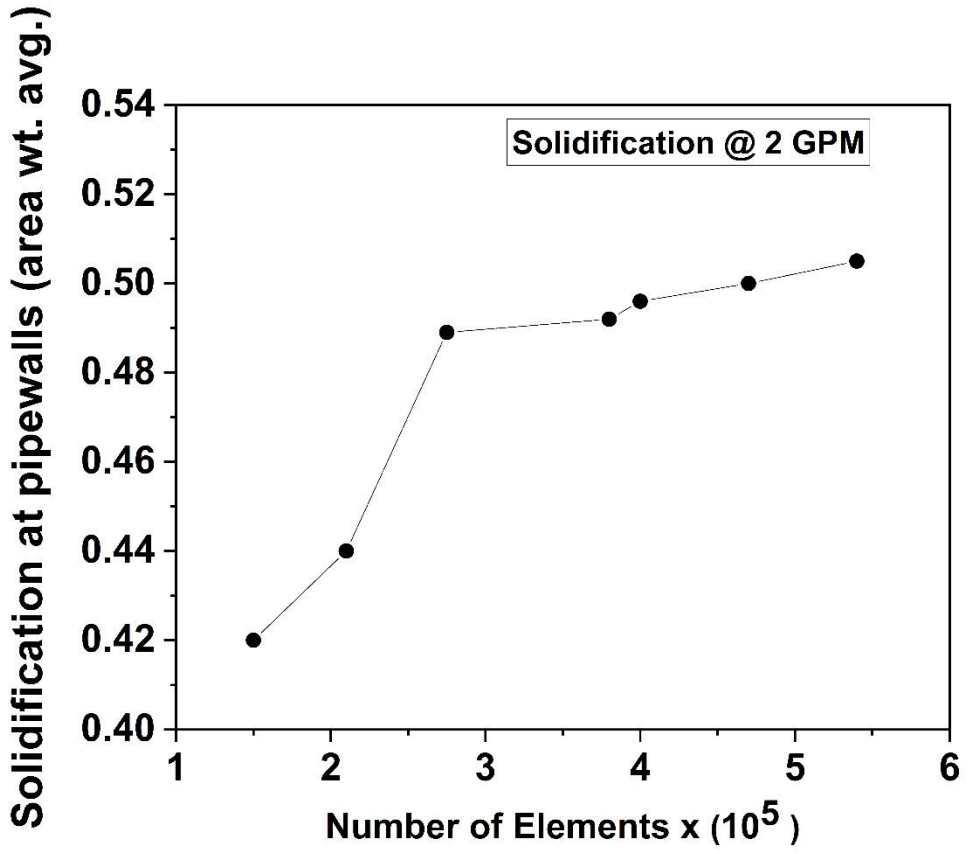

Fig 7.17 Grid Independence Test of the numerical solution

7.4 Conclusions

The modelling and simulation work performed in this research work, indicates clearly that the wax gelation phenomenon occurs during the flow of wax oil mixture under laminar flow conditions. The gelation phenomenon was observed in this simulation work through identifying the changes observed in the liquid fraction contours of the wax-oil mixture, and these liquid fraction contours were developed in this work based on theoretical approach of enthalpy-porosity technique, which is a unique way to simulate the wax gelling phenomenon and has not been tested much. The wax-oil mixture was taken as the representative sample for crude oil in simulation and the results demonstrated the occurrence of wax precipitation and gelation phenomenon in this mixture, primarily at the pipewalls, which affects the fluid velocities, wall shear stresses, fluid temperatures and near wall temperatures. The liquid fraction was found to be reduced to 46.9 % indicating that wax-oil mixture was solidified up to 53.1 % and trapped 46.9 % oil content

inside. This work presents a fundamental approach to understand the wax gelation process. The wax gelation phenomenon was exhibited in this simulation work using the computational fluid dynamics approach, which yielded important information about the effect of the wax gelation on the wax-oil mixture properties such as velocity, temperature, wall shear stress, heat transfer. Identification of wax gelation before performing experimental trials could save money and time for the petroleum companies. The findings of this work could be used to develop further simulations to understand more about the wax gelling process. The findings from this work could be used to observe the wax gelation in turbulent flow of the crude oils. The authors would further carry out wax gelation simulations in order to predict the aging phenomenon in their future works.

Chapter 8
Conclusions and Future Directions

8.1 Conclusions

- The thesis work was dedicated to understand the flow assurance of waxy crude oils. The extensive characterization of crude oils carried out provided information about the quality and other major characteristic of crude oil, and it gives an idea about the type of crude oil and helps in selecting the proper type of pour point depressants/flow improver for its flow beneficiation.
- The thesis work was able to successfully demonstrate the working of nanocomposite pour point depressants on the flow beneficiation of waxy crude oils. Their working mechanism on the wax crystals in the crude oil is explained in detail with substantial experimental investigation. The performances of the nanocomposite PPDs are compared with conventional PPDs through extensive experimental approach and detailed analyses of the results.
- The crude oils used in this study possess very higher pour points which may be attributed to presence of higher wax contents, and there is no possibility of emulsion formation issues owing to negligible water content in crude oils.
- The understanding of the problem statement and its chemical solution has increased with every thesis chapter, with working on the existing research gaps and satisfying them through development and application of novel chemical additives.
- The use of nanoparticles/nanosheets such as graphene oxide helped to huge extent in flow assurance of waxy crude oils. This thesis work is one of the earliest on utilizing graphene oxide into making successful pour point depressants and testing them extensively on crude oil. The work on graphene oxide to develop them into PPDs for crude oils on the industrial scale has not been reported sufficiently or at most the work may be in testing stage and not reported. Thus, the contents of thesis would be extremely beneficial for the researchers and equally for the industry personnel's in order to develop their understanding regarding possible usage of the science of nanocomposite PPDs. Graphene oxide are good alternative to other nanoparticles

such as silica to make the PPDs, as the science revolving around graphite and its derivatives has progressed tremendously in several applications, and the findings obtained from these studies could be easily utilized in petroleum industry, thus paving a way for multidisciplinary research domain.

- One of the findings of this work is understanding that the functionalization of graphene oxide is an essential step towards its further reaction with polymeric/non polymeric additives to develop nanocomposite. The non-functionalized graphene oxide did not yield a proper nanocomposite and might not solve flow assurance issues.
- Whatever, be the effectiveness of the nanocomposite PPDs on crude oil for an initial duration, their efficacy could be reduced with time owing to issues such as homogeneous dispersion and solubility of the nanocomposites into the crude oil. The long-term solubility of graphene oxide nanocomposite into hydrocarbon solvents such as xylene, toluene may become an issue which has to be taken into considerations carefully during addition of the nanocomposite additives (pre-dispersed into solvents) in the crude oils. This was one of the significant research gaps stated in this work, which was addressed through testing the dispersion of nanocomposites into several solvents and ultimately finding the solution in the form of a class of chemicals known as ionic liquids, which have tremendous physico-chemical properties itself including its properties to acts as an excellent solvent for dispersion of nanoparticles such as graphene oxide.
- The nanocomposite PPDR-GO proved to be an excellent PPD for the waxy crude oils, which produced exciting set of results mentioned in chapter 6, producing a 30°C reduction from the original pour point of the crude oil and a reduction in the gelation point of crude oil by 22.2°C. This amount of reduction is surely capable of addressing flow assurance to large extent in the petroleum industry. Further research on this class of novel nanocomposite would help the research community to reap additional benefits out of this class of additive and understand detailed fundamental interactions among waxes, asphaltenes, resins and ionic liquids.
- As the three PPDs PMMA-GO, P(2-EHA)-GO and IL-GO have reduced the pour point of the crude oils significantly down to 18℃, 15℃ and 9℃. Thus, they will definitely work on crude oils with pour points less than 18℃.

- This thesis work was able to highlight the extended efficiency of the PPDs through evaluating them through aging tests, where the synthesized PPDs performed well, while the best performance was observed in the case of nanocomposite PPDs. This indicates that the presence of nanoparticles has long lasting improvement in the effects of the PPDs on the wax crystals, and the results from this test suggest the potential importance of the nanocomposite PPDs among conventional PPDs present in the market.
- During unplanned shut in operations, the effectiveness of the chemicals can be determined from two aspects 1) aging tendency 2) duration of shut in operations. The developed additives have shown to impart excellent aging resistance to crude oils where they are able to maintain the lower pour points of crude oils up to 2-4 weeks. Hence, during any unplanned shut in operations, till this duration of aging resistance, the crude oil flow properties will be maintained without having flow assurance issues, and thus, the operations remain economical by avoiding flow assurance remedial operations.
- The Chapter 7 focused on simulation of the wax deposition phenomena and it helped to understand the computational fluid dynamics aspect of the wax deposition and gelation process using a new approach of enthalpy-porosity methodology.
- The thesis showed clearly how the benefits of graphene oxide can be utilized, through incorporating them into conventional polymeric PPDs or other new polymeric/non-polymeric structures. The thesis would serve as a fundamental document to understand the flow assurance of waxy crude oils, where significant focus is given to develop the chemical solutions and later efforts were given to solve multiple flow assurance issues simultaneously. The thesis would also provide an understanding about the simulation of wax gelation studies in pipeline flow of waxy crude oil.

8.2 Limitations

- Understanding of interactions among waxes and asphaltenes is still limited, although this has been researched for decades. This could impair the efficacy of the additives to solve multiple flow assurance issues simultaneously, or atleast the proper development of effective chemical additives for flow assurance of crude oils, owing to lack of information on their interactions with waxes and asphaltenes.

- The simulation of the wax gelation and deposition was carried out under laminar flow conditions and it needs to be further worked for turbulent flow conditions of crude oil flow. This work showed single phase studies, while there is a need to understand the CFD simulation of multiphase crude oil flow. Thus, future studies should extend the current work and test the simulation developed in this work for multiphase flow and turbulent flow conditions for providing more practical solutions to the petroleum industry.

8.3 Future Directions

- As it is already known that the composition of crude oil varies significantly through different geographical regions. Therefore, the PPDs developed are more or less crude oil specific and there is an important need to devise the formulation of PPDs with more generalized performance. To develop such PPDs there is a need to test it on bigger experimental facilities such as larger and more complex flow loop setup apart from one developed in our laboratory. Effect of operating conditions should be studied in detail and needs to be optimized in order to evaluate the efficacy of these synthesized additives under pipeline flowing conditions.
- The future research should focus on simulating the wax gelation phenomena in turbulent flow and multiphase oil-water flow or gas-oil-water flow occurring pipeline transportation of hydrocarbons. Additionally, the wax gelation simulations should be carried out in order to predict the aging phenomenon in the future works.
- CFD simulation in future should exhibit the effects of chemical additives in the gelation and deposition of wax crystals in crude oil pipeline.
- The simulation performed to model the wax-oil gelation in the pipeline flow in the Chapter 7 has been done with standard meshing procedure, incorporating sufficient to moderate number of computational cells capable to capture the extensive fluid dynamics of crude oil in the pipeline and at the walls. In future, using higher computational facilities, focus would be given to further refine the meshing of the body cells present in the pipe geometry in order to produce more accurate results, while simultaneously optimizing the number of elements.

References

Agaev, S. G. , *Kazakova, L.P and Gundyrev, A.A.* (1980) 'Electrokinetic studies of mechanism of pour point depressant action. *Chemisty and Technology of Fuels and Oils*, 16(9), pp. 605-08 . doi: 10.1007/BF00725807

ASTM D1480-15, A. (2010) 'Standard Test Method for Density and Relative Density (Specific Gravity) of Viscous Materials by Bingham Pycnometer', *ASTM International*, West Conshohocken, PA (C), pp. 1–7. doi: 110.1520/D0097-17A

ASTM D 95-13 'Standard Test Method for water in petroleum and bituminous materials by distillation', *ASTM International*, West Conshohocken, PA 2013:1–6. doi:10.1520/D0095-13E01

ASTM D97-17a Standard Test Method for Pour Point of Petroleum Products, *ASTM International*, West Conshohocken, PA, 2017, doi: 10.1520/D0097-17A

ASTM D97-17b Standard Test Method for Pour Point of Petroleum Products, *ASTM International*, West Conshohocken, PA, 2017, doi: 10.1520/D0097-17B

Al-Sabagh, A. M. et al. (2013) 'Preparation the Esters of Oleic Acid-Maleic Anhydride Copolymer and Their Evaluation as Flow Improvers for Waxy Crude Oil', *Journal of Dispersion Science and Technology*, 34(11), pp. 1585–1596. doi: 10.1080/01932691.2012.739857

Al-Sabagh, A. M. et al. (2016) 'Preparation and Evaluation of Poly(methyl methacrylate)-Graphene Oxide Nanohybrid Polymers as Pour Point Depressants and Flow Improvers for Waxy Crude Oil', *Energy and Fuels*, 30(9), pp. 7610–7621. doi: 10.1021/acs.energyfuels.6b01105

Al-Safran, E. M. and Brill, J. P. (2017) *Applied Multiphase Flow in Pipes and Flow Assurance : Oil and Gas Production*. Richardson, United States: SPE. Available at: http://ebookcentral.proquest.com/lib/curtin/detail.action?docID=5139929.

ANSYS Fluent 18.1 Theory Guide (2017).

Anto, R. *et al.* (2020) 'Nanoparticles as flow improver of petroleum crudes: Study on temperature-dependent steady-state and dynamic rheological behavior of crude oils', *Fuel*, 275(March), p. 117873. doi: 10.1016/j.fuel.2020.117873.

Ariza-Leon, E., Molina-Velasco, D.R and Chaves-Guerrero, A. (2014) 'Review of studies on asphaltene-wax interaction and the effect thereof on crystallization', *CT&F-Ciencia,*

Tecnología y Futuro, 5(5), pp. 39–53. http://www.scielo.org.co/scielo.php?script=sci_arttext&pid=S0122-53832014000200003#.YXBAZV13xVQ.google

Bala, K. (2007). Impact of chemical additives on flow behaviour of south gujarat oil. Ph.D. thesis, The Maharaja Sayaji Rao University of Baroda. Viewed 20 October 2021. http://hdl.handle.net/10603/59140

Banhart, F., Kotakoski, J. and Krasheninnikov, A. V. (2011) 'Structural defects in graphene', *ACS Nano*, 5(1), pp. 26–41. doi: 10.1021/nn102598m.

Bardon, C. *et al.* (1996) 'The colloidal structure of crude oils and suspensions of asphaltenes and resins', *Fuel Science and Technology International*, 14(1–2), pp. 203–242. doi: 10.1080/08843759608947569.

Becker, J. R. (1997). Crude Oil Waxes, Emulsions and Asphaltenes. *Pennwell Books*, Tulsa, OK

Brodie, B.C. (1859) 'On the atomic weight of graphite', *Philosphical transaction, The Royal Society*, 149, pp. 249–259. doi: 10.1098/rstl.1859.0013.

Betiha, M. A., Osman, D. I. and Mahmoud, T. (2019) 'Synthesis and characterization of nanohybrid of poly (octadecylacrylates derivatives)/ montmorillonite as pour point depressants and fl ow improver for waxy crude oil', 47333, pp. 1–15. doi: 10.1002/app.47333.

Bhawal, P. *et al.* (2016) 'Synthesis and characterization of graphene oxide filled ethylene methyl acrylate hybrid nanocomposites', *RSC Advances*, 6(25), pp. 20781–20790. doi: 10.1039/C5RA24914G.

Borthakur, A. *et al.* (1995) 'Synthesis and evaluation of alkyl fumarate–vinyl acetate copolymers in combination with alkyl acrylates as flow improvers for Borholla crude oil', *Journal of Chemical Technology & Biotechnology*, 62(1), pp. 75–80. doi: 10.1002/jctb.280620112.

Burger, E. D., Perkins, T. K. and Striegler, J. H. (1981) 'Studies of Wax Deposition in the Trans Alaska Pipeline', *Journal of Petroleum Technology*, 33(06), pp. 1075–1086. doi: 10.2118/8788-PA.

Carbognani, L. *et al.* (2000) 'Studies on large crude oil alkanes. II. Isolation and characterization of aromatic waxes and waxy asphaltenes', *Petroleum Science and Technology*, 18(5), pp. 607–634. doi: 10.1080/10916460008949863.

Coto, B., et al. (2014) 'Experimental study of the effect of inhibitors in wax precipitation by different techniques', *Energy Science and Engineering*. 2, 196–203. https://doi.org/10.1002/ese3.42

Chen, J. *et al.* (2013) 'An improved Hummers method for eco-friendly synthesis of graphene oxide', *Carbon*, 64(1), pp. 225–229. doi: 10.1016/j.carbon.2013.07.055.

Chen, J. *et al.* (2014) 'High-yield preparation of graphene oxide from small graphite flakes via an improved Hummers method with a simple purification process', *Carbon*, 81, pp. 826–834. doi: 10.1016/j.carbon.2014.10.033.

Chong, B. *et al.* (2006) 'Thermolysis of RAFT-Synthesized Poly(Methyl Methacrylate)', *Australian Journal of Chemistry*, 59(10), p. 755. doi: 10.1071/CH06229.

Coto, B. *et al.* (2008) 'A new method for the determination of wax precipitation from non-diluted crude oils by fractional precipitation', *Fuel*, 87(10–11), pp. 2090–2094. doi: 10.1016/j.fuel.2007.12.012.

Dantas de Oliveira, A. and Augusto Gonçalves Beatrice, C. (2018) 'Polymer Nanocomposites with Different Types of Nanofiller', in *Nanocomposites - Recent Evolutions*. IntechOpen, pp. 103–128. doi: 10.5772/intechopen.81329.

Deka, B. *et al.* (2018) 'Synthesis and evaluation of oleic acid based polymeric additive as pour point depressant to improve flow properties of Indian waxy crude oil', *Journal of Petroleum Science and Engineering*, 170, pp. 105–111. doi: 10.1016/j.petrol.2018.06.053.

Deka, B. *et al.* (2020) 'Quantum dots: Low-dosage hydrate inhibitors for deep water flow assurance', OTC-30654-MS, *Proceedings of the Annual Offshore Technology Conference*, 2020-May. doi: 10.4043/30654-MS

Deka, B., Sharma, R. and Mahto, V. (2020) 'Synthesis and performance evaluation of poly (fatty esters-co-succinic anhydride) as pour point depressants for waxy crude oils', *Journal of Petroleum Science and Engineering*, 191 , p. 107153. doi: 10.1016/j.petrol.2020.107153

Deshmukh, S. and Bharambe, D. P. (2008) 'Synthesis of polymeric pour point depressants for Nada crude oil (Gujarat, India) and its impact on oil rheology', *Fuel Processing Technology*, 89(3), pp. 227–233. doi: 10.1016/j.fuproc.2007.10.010

Dharaskar, S. A. *et al.* (2016) 'Synthesis, characterization and application of 1-butyl-3-methylimidazolium tetrafluoroborate for extractive desulfurization of liquid fuel',

Arabian Journal of Chemistry, 9(4), pp. 578–587. doi: 10.1016/j.arabjc.2013.09.034.

Du, Q. *et al.* (2010) 'Preparation of functionalized graphene sheets by a low-temperature thermal exfoliation approach and their electrochemical supercapacitive behaviors', *Electrochimica Acta*, 55(12), pp. 3897–3903. doi: 10.1016/j.electacta.2010.01.089

Dubey, A. (2016) *Investigation of the effects of operating conditions and inhibitors on paraffin deposition*, M.S. Thesis. The University of Tulsa. *ProQuest Dissertations and Theses*.

Viewed on 20 Oct 2021 from :

https://link.library.curtin.edu.au/gw?url=https://www.proquest.com/dissertations-theses/investigation-effects-operating-conditions/docview/1861178270/se-2?accountid=10382

Feng et al. (2012) 'Surface decoration of graphene by grafting polymerization using graphene oxide as the initiator †', J. Mater .Chem. 22 pp. 3982–3989. doi: 10.1039/c2jm13667h.

Ferriol, M., Gentilhomme, a and Cochez, M. (2003) '' Thermal degradation of poly (methyl methacrylate) (PMMA): modelling of DTG and TG curves.Polym Degrad Stab 2003, 79, pp. 271–281. doi: 10.1016/S0141-3910(02)00291-4

He, C. *et al.* (2016) 'Influence of the nano-hybrid pour point depressant on flow properties of waxy crude oil', *Fuel*, 167, pp. 40–48. doi: 10.1016/j.fuel.2015.11.031

Hou, D. *et al.* (2018) 'Facile synthesis of graphene via reduction of graphene oxide by artemisinin in ethanol', *Journal of Materiomics*, 4(3), pp. 256–265. doi: 10.1016/j.jmat.2018.01.002

Hu, J. *et al.* (2014) 'Effect of interfacial interaction between graphene oxide derivatives and poly(vinyl chloride) upon the mechanical properties of their nanocomposites', *Journal of Materials Science*, 49(7), pp. 2943–2951. doi: 10.1007/s10853-013-8006-1

Hu, Y. F. and Guo, T. M. (2005) 'Effect of the structures of ionic liquids and alkylbenzene-derived amphiphiles on the inhibition of asphaltene precipitation from CO 2-injected reservoir oils', *Langmuir*, 21(18), pp. 8168–8174. doi: 10.1021/la050212f

Huang, H. *et al.* (2018) 'The influence of nanocomposite pour point depressant on the crystallization of waxy oil', *Fuel*, 221, pp. 257–268. doi: 10.1016/j.fuel.2018.01.040

Jennings and Weisfenning (2006) Effects of shear and temperature on wax deposition : Coldfinger investigation with Gulf of Mexico crude oil', *Energy and Fuels*, 19(4), pp

1376-1386. doi: 10.1021/ef049784i

Jha, N. K. *et al.* (2014) 'Characterization of crude oil of upper assam field for flow assurance', *Society of Petroleum Engineers - SPE Saudi Arabia Section Technical Symposium and Exhibition*, pp. 1–9. doi: 10.2118/172226-ms

Jing, G. *et al.* (2017) 'Influence of Different Vinyl Acetate Contents on the Properties of the Copolymer of Ethylene and Vinyl Acetate/Modified Nano-SiO2Composite Pour-Point Depressant', *Energy and Fuels*, 31(6), pp. 5854–5859. doi: 10.1021/acs.energyfuels.7b00189

Jorio, A. (2012) 'Raman Spectroscopy in Graphene-Based Systems: Prototypes for Nanoscience and Nanometrology', *ISRN Nanotechnology*, 2012(2), pp. 1–16. doi: 10.5402/2012/234216

Kazantsev, O. A. *et al.* (2021) 'Dependence of efficiency of polyalkyl acrylate-based pour point depressants on composition of crude oil', *Egyptian Journal of Petroleum*, 30(3), pp. 21–26. doi: 10.1016/j.ejpe.2021.06.002

Khan, Mujeeb *et al.* (2015) 'Green Approach for the Effective Reduction of Graphene Oxide Using Salvadora persica L. Root (Miswak) Extract', *Nanoscale Research Letters*, 10(1), p. 281. doi: 10.1186/s11671-015-0987-z

Khan, W. S., Hamadneh, N. N. and Khan, W. A. (2016) 'Science and applications of Tailored Nanostructures 50 4 Polymer nanocomposites-synthesis techniques, classification and properties Outline', pp. 50–67

Khidr, T. T., Doheim, M. M. and El-Shamy, O. A. A. (2015) 'Effect of Ethoxylate on Pour Point Depressant of Fuel Oil', *Energy Sources, Part A: Recovery, Utilization and Environmental Effects*, 37(15), pp. 1697–1703. doi: 10.1080/15567036.2011.638970.

Kim, H., Abdala, A. A. and MacOsko, C. W. (2010) 'Graphene/polymer nanocomposites', *Macromolecules*, 43(16), pp. 6515–6530. doi: 10.1021/ma100572e.

Ko, S. and Huh, C. (2019) 'Use of nanoparticles for oil production applications', *Journal of Petroleum Science and Engineering*, 172(September 2018), pp. 97–114. doi: 10.1016/j.petrol.2018.09.051

Kuilla, T. *et al.* (2010) 'Recent advances in graphene based polymer composites', *Progress in Polymer Science*, 35(11), pp. 1350–1375. doi: 10.1016/j.progpolymsci.2010.07.005

Kumar, A. *et al.* (2016) 'Covalently Grafted Graphene Oxide/Poly(C n -acrylate)

Nanocomposites by Surface-Initiated ATRP: An Efficient Antifriction, Antiwear, and Pour-Point-Depressant Lubricating Additive in Oil Media', *Industrial & Engineering Chemistry Research*, 55(31), pp. 8491–8500. doi: 10.1021/acs.iecr.6b00848

Kumar, T. *et al.* (2016) 'Single step synthesis of sulfonic group bearing graphene oxide : A promising carbo-nano material for biodiesel production', *Journal of Environmental Chemical Engineering*, 4(3), pp. 2933–2940. doi: 10.1016/j.jece.2016.06.006

Lai, Q. *et al.* (2013) 'Ultraviolet-visible spectroscopy of graphene oxides Ultraviolet-visible spectroscopy of graphene oxides', 032146, pp. 3–8. doi: 10.1063/1.4747817

Lerf, A. *et al.* (1998) 'Structure of Graphite Oxide Revisited', *The Journal of Physical Chemistry B*, 102(23), pp. 4477–4482. doi: 10.1021/jp9731821

Li, N., *et al.* (2018) 'Advances in the research of polymeric pour point depressant for waxy crude oil', *Journal of Dispersion Science and Technology*, 39(8), pp. 1165–1171. doi: 10.1080/01932691.2017.1385484

Li, N., Mao, G. L., Wu, W., *et al.* (2018) 'Effect evaluation of ethylene vinyl acetate/nano-montmorillonite pour-point depressant on improving the flow properties of model oil', *Colloids and Surfaces A: Physicochemical and Engineering Aspects*, 555(April), pp. 296–303. doi: 10.1016/j.colsurfa.2018.06.065

Li, X., Hayashi, J-i. and Li, C.- Z. (2006) 'FT-Raman spectroscopic study of the evolution of char structure during the pyrolysis of a Victorian brown coal', *Fuel*, 85(12–13), pp. 1700–1707. doi: 10.1016/j.fuel.2006.03.008

Lyu, Q. *et al.* (2017) 'Imidazolium ionic liquid modified graphene oxide: As a reinforcing filler and catalyst in epoxy resin', *Polymers*, 9(9). doi: 10.3390/polym9090447

Mandal, A. *et al.* (2019) 'Synthesis, characterization and evaluation of a novel asphaltene inhibitor to control organic solid deposition in petroleum formation', *Petroleum Science and Technology*, 37(7), pp. 780–786. doi: 10.1080/10916466.2019.1566250

Marcano, D. C. *et al.* (2010) 'Improved Synthesis of Graphene Oxide', *ACS Nano* 4(8). pp 4806-4814. doi: 10.1021/cm5031409

Mcgrail, B. T., Rodier, B. J. and Pentzer, E. (2014) 'Rapid Functionalization of Graphene Oxide in Water', *Chemistry of Materials*. doi: 10.1021/cm5031409

Miller, R. (1982) 'Hydrocarbon Class Fractionation with Bonded-Phase Liquid Chromatography', *Analytical Chemistry*, 54(11), pp. 1742–1746. doi: 10.1021/ac00248a021

Misra, S., Baruah, S. and Singh, K. (1995) 'Paraffin problems in crude oil production and transportation: a review', *SPE Production and Facilities*, 10(1), pp. 50–54. doi: 10.2118/28181-pa.

Modesty Kelechukwu, E., Said Al-Salim, H. and Saadi, A. (2013) 'Prediction of wax deposition problems of hydrocarbon production system', *Journal of Petroleum Science and Engineering*, 108, pp. 128–136. doi: 10.1016/j.petrol.2012.11.008

Paredes, J. I. *et al.* (2008) 'Graphene Oxide Dispersions in Organic Solvents', Langmuir. 24(19) , pp. 10560–10564. doi: 10.1021/la801744a

Paso, K., Silset, A., Sørland, G., Gonçalves, M. de A. L., *et al.* (2009) 'Characterization of the Formation, Flowability, and Resolution of Brazilian Crude Oil Emulsions', *Energy & Fuels*, 23(1), pp. 471–480. doi: 10.1021/ef800585s

Paso, K., Silset, A., Sørland, G., Gonc, M. D. A. L., *et al.* (2009) 'Characterization of the Formation , Flowability , and Resolution of Brazilian Crude Oil Emulsions', (4), pp. 471–480. doi: 10.1021/ef800585s

Paso, K. G. (2014) 'Comprehensive Treatise on Shut-in and Restart of Waxy Oil Pipelines', *Journal of Dispersion Science and Technology*, 35(8), pp. 1060–1085. doi: 10.1080/01932691.2013.833105

Rajkumar, T. and Ranga Rao, G. (2008) 'Characterization of hybrid molecular material prepared by 1-butyl 3-methyl imidazolium bromide and phosphotungstic acid', *Materials Letters*, 62(25), pp. 4134–4136. doi: 10.1016/j.matlet.2008.06.029

Rogel, E. *et al.* (2016) 'Asphaltene characterization of paraffinic crude oils', *Fuel*, 178, pp. 71–76. doi: 10.1016/j.fuel.2016.03.030

Ronningsen, H. P. *et al.* (1991) 'Wax Precipitation from North Sea Crude Oils. 1. Crystallization and Dissolution Temperatures, and Newtonian and Non-Newtonian Flow Properties', *Energy and Fuels*, 5(6), pp. 895–908. doi: 10.1021/ef00030a019

Sharma, R et al. (November 2020) 'Effect of Thermal Shear Conditioning and Aging on the Effectiveness of Synthesized Nanocomposite PPD on Waxy Crude Oil.'OTC-30360-MS. In: Proceedings of Offshore Technology Conference Asia, Kuala Lumpur, Malaysia, pp. 1–9

Sharma, R. *et al.* (2018) 'Study the influence of sodium dodecyl sulfate on emulsification of heavy and waxy crude oils to improve their flow ability in low temperature conditions', *Asia-Pacific Journal of Chemical Engineering*, p. e2279. doi: 10.1002/apj.2279

Sharma, R. *et al.* (2019) 'Investigation into the Flow Assurance of Waxy Crude Oil by Application of Graphene-Based Novel Nanocomposite Pour Point Depressants', *Energy & Fuels*, 33(12), pp. 12330–12345. doi: 10.1021/acs.energyfuels.9b03124

Sharma, R., Deka, B. and Mahto, V. (2020) 'An additive for depressing the pour point of the waxy crude oils'. Indian Patent Application No. 202031039791 (Filed), Indian Patent Office 2020. Intellectual Property India (ipindiaservices.gov.in)

Sharma, R., Mahto, V. and Vuthaluru, H. (2019) 'Synthesis of PMMA/modified graphene oxide nanocomposite pour point depressant and its effect on the flow properties of Indian waxy crude oil', *Fuel*, 235, pp. 1245–1259. doi: 10.1016/j.fuel.2018.08.125

Sharma, R., Vuthaluru, H. and Mahto, V. (2020) 'Predicting the Wax Deposition and Gelation Behavior of Waxy Oils in Subsea Pipelines through Modelling and Numerical Simulation Approach'. SPE-202368-MS. In: Proceedings of Asia Pacific Oil and Gas Conference & Exhibition 2020, SPE International. doi: 10.2118/202368-ms

Sharma, R. et al. (2021) 'Experimental investigation into the development and evaluation of ionic liquid and its graphene oxide nanocomposite as novel pour point depressants for waxy crude oil'. *Journal of Petroleum Science and Engineering*. In press. doi: 10.1016/j.petrol.2021.109691

Silverstein (2014) 'Spectrometric identification of organic compounds, 8th edition', *John Wiley & Sons*.

Singh, M. *et al.* (2015) 'Annealing induced electrical conduction and band gap variation in thermally reduced graphene oxide films with different sp2/sp3 fraction', *Applied Surface Science*, 326, pp. 236–242. doi: 10.1016/j.apsusc.2014.11.121

Singh, P. *et al.* (2000) 'Formation and aging of incipient thin film wax-oil gels', *AIChE Journal*, 46(5), pp. 1059–1074. doi: 10.1002/aic.690460517

Soni, H. P. and Bharambe, D. P. (2006) 'Synthesis and evaluation of polymeric additives as flow improvers for Indian crude oil', *Iranian Polymer Journal (English Edition)*,15(12),pp.943–954. https://www.sid.ir/en/Journal/ViewPaper.aspx?ID=62307

Speight, J. G. (2006) 'The Chemistry and Technology of Petroleum (4th ed.)', *CRC Press*, Boca Raton e-ISBN: 9780429118494. Available at: https://doi.org/10.1201/9781420008388

Stankovich, S. *et al.* (2006) 'Synthesis and exfoliation of isocyanate-treated graphene oxide nanoplatelets', *Carbon*, 44(15), pp. 3342–3347. doi: 10.1016/j.carbon.2006.06.004

Staudenmaier, L. (1898) ‘Verfahren zur Darstellung der Graphitsäure’, *Ber. dtsch. chem. Ges.*, 31(2), pp. 1481–1487. doi: 10.1002/cber.18980310237

Sun, L. (2019) ‘Structure and synthesis of graphene oxide’, *Chinese Journal of Chemical Engineering*, 27(10), pp. 2251–2260. doi: 10.1016/j.cjche.2019.05.003

Sunil Kumar, M. N. (2015) *Studies on flow improvers*, Ph.D. thesis. Maharaja Sayajirao University of Baroda (India). *ProQuest Dissertations and Theses*. Viewed 20 October 2021from : https://link.library.curtin.edu.au/gw?url=https://www.proquest.com/dissertations-theses/studies-on-flow-improvers/docview/1755924395/se-2?accountid=10382

Šupová, M., Martynková, G. S. and Barabaszová, K. (2011) ‘Effect of Nanofillers Dispersion in Polymer Matrices: A Review’, *Science of Advanced Materials*, 3(1), pp. 1–25. doi: 10.1166/sam.2011.1136

Schuster, D. S. and Irani, C. A. (1984) ‘Reducing Energy Costs for Heated Uintah Basin Crude Oil Transport.’, Society of Petroleum Engineers of AIME, (Paper) SPE, pp. 165–176. doi: 10.2523/12910-ms.

Tang, H. *et al.* (2012) ‘Highly efficient synthesis of graphene nanocomposites’, *Nano Letters*, 12(1), pp. 84–90. doi: 10.1021/nl203023k

Taraneh, J. B. *et al.* (2008) ‘Effect of wax inhibitors on pour point and rheological properties of Iranian waxy crude oil’, *Fuel Processing Technology*, 89(10), pp. 973–977. doi: 10.1016/j.fuproc.2008.03.013

Tian, W. *et al.* (2017) ‘A review on lattice defects in graphene: Types generation effects and regulation’, *Micromachines*, 8(5). doi: 10.3390/mi8050163

Tinsley et al. (2007). ' Novel Laboratory Cell for Fundamental Studies of the Effect of Polymer Additives on Wax Deposition from Model Crude Oils', *Energy and Fuels*, 21(3), pp. 1301-1308. doi: 10.1021/ef060446m

Tiwari, S. K. *et al.* (2017) ‘Mixing sequence driven controlled dispersion of graphene oxide in PC/PMMA blend nanocomposite and its effect on thermo-mechanical properties’, *Current Applied Physics*, 17(9), pp. 1158–1168. doi: 10.1016/j.cap.2017.05.007

Veerapandian, M. *et al.* (2012) ‘Synthesis, characterization and electrochemical properties of functionalized graphene oxide’, *Carbon*, 50(11), pp. 4228–4238. doi:

10.1016/j.carbon.2012.05.004

Venkatesan, R. *et al.* (2002) 'Delineating the Pour Point and Gelation Temperature of Waxy Crude Oils', *SPE Journal*, pp. 349–352. doi: 10.2118/72237-PA

Venkatesan, R. *et al.* (2003) 'The effect of Asphaltenes on the Gelation of Waxy Oils', *Energy and Fuels*, 17(6), pp. 1630–1640. doi: 10.1021/ef034013k

Venugopal, G. *et al.* (2012) 'An investigation of the electrical transport properties of graphene-oxide thin films', *Materials Chemistry and Physics*, 132(1), pp. 29–33. doi: 10.1016/j.matchemphys.2011.10.040

Voller, V. R. and Prakash, C. (1987) 'A fixed grid numerical modelling methodology for convection-diffusion mushy region phase-change problems', *International Journal of Heat and Mass Transfer*. doi: 10.1016/0017-9310(87)90317-6

Wang, F. *et al.* (2011) 'The effect of nanohybrid materials on the pour-point and viscosity depressing of waxy crude oil', *Chinese Science Bulletin*, 56(1), pp. 14–17. doi: 10.1007/s11434-010-4174-4

Wei, B. (2015) 'Recent advances on mitigating wax problem using polymeric wax crystal modifier', *Journal of Petroleum Exploration and Production Technology*, pp. 391–401. doi: 10.1007/s13202-014-0146-6

Wilt, B. K., Welch, W. T. and Rankin, J. G. (1998) 'Determination of Asphaltenes in Petroleum Crude Oils by Fourier Transform Infrared Spectroscopy', *Energy & Fuels*, 12(5), pp. 1008–1012. doi: 10.1021/ef980078p

Wright, W. (2014) *Simple Equations to Approximate Changes to the Properties of Crude Oil with Changing Temperature*, Petroskills. Available at: https://www.petroskills.com/blog/entry/crude-oil-and-changing-temperature#YV7P7tpBzIW (Accessed 20 October 2021)

Xu, L. and Cheng, L. (2013) 'Graphite Oxide under High Pressure: A Raman Spectroscopic Study', *Journal of Nanomaterials*, 2013, pp. 1–5. doi: 10.1155/2013/731875

Yang, D. *et al.* (2009) 'Chemical analysis of graphene oxide films after heat and chemical treatments by X-ray photoelectron and Micro-Raman spectroscopy', *Carbon*, 47(1), pp. 145–152. doi: 10.1016/j.carbon.2008.09.045

Yang, F., Paso, K., *et al.* (2015) 'Hydrophilic nanoparticles facilitate wax inhibition', *Energy and Fuels*, 29(3), pp. 1368–1374. doi: 10.1021/ef502392g

Yang, F., Zhao, Y., *et al.* (2015) 'Polymeric Wax Inhibitors and Pour Point Depressants for Waxy Crude Oils: A Critical Review', *Journal of Dispersion Science and Technology*, 36(2), pp. 213–225. doi: 10.1080/01932691.2014.901917

Yang, F. *et al.* (2017) 'Performance improvement of the ethylene-vinyl acetate copolymer (EVA) pour point depressant by small dosages of the polymethylsilsesquioxane (PMSQ) microsphere: An experimental study', *Fuel*, 207, pp. 204–213. doi: 10.1016/j.fuel.2017.06.083

Yang, F. *et al.* (2018) 'Comb-like Polyoctadecyl Acrylate (POA) Wax Inhibitor Triggers the Formation of Heterogeneous Waxy Oil Gel Deposits in a Cylindrical Couette Device', *Energy and Fuels*, 32(1), pp. 373–383. doi: 10.1021/acs.energyfuels.7b03416

Yang, F., Li, C. and Wang, D. (2013) 'Studies on the structural characteristics of gelled waxy crude oils based on scaling model', *Energy and Fuels*, 27(3), pp. 1307–1313. doi: 10.1021/ef301921b

Yao, B., Li, C., Yang, F., Sjöblom, J., *et al.* (2016) 'Organically modified nano-clay facilitates pour point depressing activity of polyoctadecylacrylate', *Fuel*, 166, pp. 96–105. doi: 10.1016/j.fuel.2015.10.114

Yao, B., Li, C., Yang, F., Zhang, Y., *et al.* (2016) 'Structural properties of gelled Changqing waxy crude oil benefitted with nanocomposite pour point depressant', *Fuel*, 184, pp. 544–554. doi: 10.1016/j.fuel.2016.07.056

Yao, B. *et al.* (2017) 'Effective flow improving agents for waxy crude oil', *Petroleum Science and Technology*, 35(17), pp. 1775–1783. doi: 10.1080/10916466.2017.1375947

Yao, B. *et al.* (2018) 'Performance improvement of the ethylene-vinyl acetate copolymer (EVA) pour point depressant by small dosage of the amino-functionalized polymethylsilsesquioxane (PAMSQ) microsphere', *Fuel*, 220, pp. 167–176. doi: 10.1016/j.fuel.2018.01.032

Young, R. J. *et al.* (2012) 'The mechanics of graphene nanocomposites: A review', *Composites Science and Technology*, 72(12), pp. 1459–1476. doi: 10.1016/j.compscitech.2012.05.005

Zhang, L. *et al.* (2009) 'Size-controlled synthesis of graphene oxide sheets on a large scale using chemical exfoliation', *Carbon*, 47(14), pp. 3365–3368. doi: 10.1016/j.carbon.2009.07.045

Appendix

Techno-economic evaluation of nanocomposite PPDs

The costing of the nanocomposite PPDs have been detailed below in order to gain the practical aspect of the possible application of nanocomposite PPDs into crude oil. Following is the list of the chemicals and their cost involved used for the synthesis of nanocomposite with their costing.

Table A1. Expenditure for the laboratory development of P[(OMIM) Cl]-1% GO

Chemicals	Quantity	Amount (Rupees)	Amount required per synthesis	Costing (Rupees)
1-chlorooctane	500 mL	2150	13.6 mL	58.48
1- methylimidazole	500 g	4500	8.2 g	73.8
Graphite	500 g	340	1 g	0.68
Ethyl actetae	2.5 L	1200	200 mL	96
Acrylonitrile	2.5 L	2700	50 mL	54
1,4 dioxan	2.5 L	2200	50 mL	44
Sulphuric Acid	2.5 L	580	23 mL	5.3
Hydrochloric Acid	1 L	230	10 mL	2.3
Potassium Permanganate	500 g	680	3 g	4.08
Sodium Chloride	500 g	135	20 g	5.4
Hydrogen peroxide	500 mL	320	5 mL	3.2
Toluene	2.5 L	1270	50 mL	25.4
Benzoyl peroxide	500 mL	750	0.03 g	1.5
Methanol	2.5 L	270	50 mL	5.4
Distilled water	Readily available in the laboratory.			

Total costing to develop 15 mL of nanocomposite	**379.54 Rupees**

The following is the table detailing the amount of PPD required to treat the waxy crude oil

Table A2. Consumption of PPD to treat Indian waxy crude oil

Amount of PPD consumed	**Amount of crude oil that can be treated**
250 ppm = 0.25 mL	1 L
15 mL	**60 L**

The additives were doped in ppm quantities in crude oils. 250 ppm additive is the optimum amount of the additive IL-GO and it is equivalent to 0.25 mL of additive liquid, this amount can treat/beneficiate a total of 1 L of crude oil. 15 mL of the PPD is synthesized from the mentioned synthesis procedure at a time. Thus, it can be observed from the tables that it would cost about 380 rupees to develop 15 mL of the nanocomposite PPD, which is quite cheap considering the amount of improvement is it is causing in the flow properties of the crude oil.

The amount of PPD required to treat 1L of the crude oil is very minimal i.e. 0.25 mL, and the synthesized amount of the nanocomposite PPD (15 mL) can treat up to 60 L of crude oil. This data indicates that the PPD P[(OMIM)]-1% GO is a very effective PPD for the flow improvement of the waxy crude oils. Therefore, considering cost economics and the flow improvement caused, the current invention is a potential applicant for the industrial purpose to solve the flow assurance issues of waxy crude oils.

The above costing of the synthesized PPD was performed based on the prices of the laboratory fine chemicals provided by the suppliers. Further, when the PPD will be produced in bulk quantities, its price would be reduced significantly.

Similarly, the chemical costing for the nanocomposite PMMA-GO was calculated as shown below.

Table A3. Expenditure for the laboratory synthesis of PMMA-GO

Chemicals	**Quantity**	**Amount (Rupees)**	**Amount required per synthesis**	**Costing (Rupees)**
MMA	2.5L	3000	15 mL	18
Graphite	500 g	340	1 g	0.68
Acrylonitrile	2.5 L	2700	50 mL	54
1,4 dioxan	2.5 L	2200	50 mL	44
Sulphuric Acid	2.5 L	580	23 mL	5.3
Hydrochloric Acid	1 L	230	10 mL	2.3
Potassium Permanganate	500 g	680	3 g	4.08
Sodium Chloride	500 g	135	20 g	5.4
Hydrogen peroxide	500 mL	320	5 mL	3.2
Toluene	2.5 L	1270	50 mL	25.4
Benzoyl peroxide	500 mL	750	0.03 g	1.5
Methanol	2.5 L	270	50 mL	5.4
Distilled water	Readily available in the laboratory.			
Total costing to develop 15 mL of nanocomposite	**169.26 Rupees**			

Similarly, the chemical costing for the nanocomposite P(2-EHA)-GO was calculated as shown below.

Table A4. Expenditure for the laboratory synthesis of P(2-EHA)-GO

Chemicals	Quantity	Amount (Rupees)	Amount required per synthesis	Costing (Rupees)
2-EHA	2.5 L	2300	15 mL	13.8
Graphite	500 g	340	1 g	0.68
Acrylonitrile	2.5 L	2700	50 mL	54
1,4 dioxan	2.5 L	2200	50 mL	44
Sulphuric Acid	2.5 L	580	23 mL	5.3
Hydrochloric Acid	1 L	230	10 mL	2.3
$KMnO_4$	500 g	680	3 g	4.08
Sodium Chloride	500 g	135	20 g	5.4
Hydrogen peroxide	500 mL	320	5 mL	3.2
Toluene	2.5 L	600	50 mL	25.4
Benzoyl peroxide	500 mL	750	0.03 g	1.5
Methanol	2.5 L	270	50 mL	5.4
Distilled water	Readily available in the laboratory.			
Total costing to develop 15 mL of nanocomposite	**165.06 Rupees**			

Although, the costing involved to develop the nanocomposite PPDs may be high initially due to purchasing analytical grade chemicals in very small amount, the prices are expected to reduce substantially once its mass production begins in industry. The benefits brought by the nanocomposites are highly beneficial compared to conventional PPDs, owing to its extremely superior performance, which may also be a deciding factor to choose a particular type of PPD. Additionally, to understand the beneficiation by thee nanocomposite PPDs in terms of energy savings due to maintaining low pour point temperatures are detailed in the below section comprehensively

Calculations for economic evaluation using PPDs in heated pipeline transport

The following derivation was used to calculate the net savings if PPDs were used in the crude oil transportation in terms of pour point temperatures. Similar calculations were performed in previous work (Schuster and Irani, 1984).

Let $Q_1 = UA \triangle T_1$……..(1)

$Q_2 = UA \triangle T_2$……..(2)

Where,

Q_1 = heat input required for pipeline transport of untreated crude oil

Q_2 = heat input required for crude oil transport of PPD treated crude oil

T_1= minimum temperature for flow of untreated crude oil (pour point)

T_2= minimum temperature for flow of PPD treated crude oil (pour point)

T_A= ambient temperature

$\triangle T_1 = T_1 - T_A$

$\triangle T_2 = T_2 - T_A$

U= Overall heat transfer coefficient

A= area of pipeline available for heat transfer

The energy savings in terms of heat input to the pipeline could be measured in the form of ratio $(Q_1-Q_2)/Q_1$, in the case where the minimum flowing temperatures gets reduced from T_1 to T_2.

From equations (1) and (2),

$$ESF = \frac{Q_1 - Q_2}{Q_1} = \frac{UA \triangle T_1 - UA \triangle T_2}{UA \triangle T_1} = \frac{\triangle T_1 - \triangle T_2}{\triangle T_1} = \frac{T_1 - T_2}{T_1 - T_A}$$

…..……..(3)

The ratio of the decrease in energy requirement has been calculated based on the function of temperatures only. The ratio is termed as ESF.

The energy savings were calculated for all the additives developed in this work at two different ambient temperatures (15℃ and 25℃). The temperature 15℃ was chosen in order to understand the improvement in crude oil flow properties at low temperatures (winters), while a higher temperature (25℃) was selected to understand the PPD beneficiation in summer season. The Table 1 illustrates the energy saving factor (ESF) for all the PPD-treated crude oils, which suggest the reduction in the energy required to transport the crude oil in pipelines based on the pour point temperatures. It can be concluded from the Table 1 that the nanocomposite PPDs were mostly able to reduce the pumping energy requirement by 100% at both scenarios of summers and winters, and especially nanocomposites could be highly preferable in reducing the energy requirements in winters. All the PPDs were able to cut down the energy requirements for transportation , but the nanocomposites caused the highest reduction in Energy savings factor with creating efficiency as high as 176% (PMMA-1%GO), 123% (PMMA-0.5%GO), 164 % (P-2-EHA)-1%GO, 137% (P-2EHA)-0.5%GO, 214 % (PPDR-1%GO) and 171 %(PPDR-0.5%GO). The other non-nanocomposite additives were also effective and among them the PPD IL showed the best ESF of 129% compared to other conventional additives such as PMMA, P(2-EHA) and a commercial PPD Phoenix. Thus, from this discussion we can conclude the techno-economic analysis of the PPDs for their potential application in oilfields.

Table A5. Energy savings for pipeline transportation of crude oil treated with different PPDs

	Crude oil Pour point (℃)	PPD treated Pour point (℃)	PPD concentration (ppm)	Pour point reduction (℃)	Ambient Temperature (℃)	ESF*100 (%)
Study 1						
PMMA-1%GO	38	15	1500	23	25	176
					15	100
PMMA-0.5%GO	38	22	1500	16	25	123
					15	70
PMMA	38	27	1250	11	25	85
					15	48
Phoenix	38	24	1250	14	25	108
					15	61
Study 2						
P(2-EHA)-1%GO	36	18	750	18	25	164
					15	86
P(2-EHA)-0.5%GO)	36	21	750	15	25	137
					15	71
P(2-EHA)	36	24	750	12	25	109
					15	57
Study 3						
PPDR-1%GO	39	9	250	30	25	214
					15	125
PPDR-0.5% GO	39	15	250	24	25	171
					15	100
IL	39	21	500	18	25	129
					15	75

List of Publications

❖ Refereed Journal Publications

1) **Sharma, R.**, Mahto, V., & Vuthaluru, H. (2019). Synthesis of PMMA/modified graphene oxide nanocomposite pour point depressant and its effect on the flow properties of Indian waxy crude oil. *Fuel*, *235*, 1245-1259.

2) **Sharma, R.**, Deka, B., Mahto, V., Vuthaluru, H., & Li, C. Z. (2019). Investigation into the Flow Assurance of Waxy Crude Oil by Application of Graphene-Based Novel Nanocomposite Pour Point Depressants. *Energy & Fuels*, *33*(12), 12330-12345.

3) Sharma, R., Deka, B., Mahto, V., Barifcani, A., Vuthaluru, H. (2022). Experimental investigation into the development and evaluation of ionic liquid and its graphene oxide nanocomposite as novel pour point depressants for waxy crude oil. *Journal of Petroleum Science and Engineering*, *208*, 109691

❖ Refereed Conference Publications

1) **Sharma, R.**, Vuthaluru, H., & Mahto, V. (2020, November). Predicting the Wax Deposition and Gelation Behavior of Waxy Oils in Subsea Pipelines through Modelling and Numerical Simulation Approach. In *SPE Asia Pacific Oil & Gas Conference and Exhibition*. Society of Petroleum Engineers.

2) **Sharma, R.**, Mahto, V., Vuthaluru, H., & Li, C. Z. (2020, October). Effect of Thermal/Shear Conditioning and Aging on the Effectiveness of Synthesized Nanocomposite PPD on Waxy Crude Oil. In *Offshore Technology Conference Asia*. Offshore Technology Conference.

❖ Conference Presentations & Attending

1) **Sharma, R**., Deka B**.**, Mahto V. Flow improvement of waxy crude oil using nanocomposite / nanohybrid pour point depressants: a review. *Oilfield Chemical and Treatment Conference & Exhibition*, Mumbai, India, 18-19 July 2019.

2) Sharma, R., Mahto, V. and Deka, B. Synthesis, Characterization and Evaluation of A Nanocomposite Based Novel Pour Point Depressant for Improving the Flow Properties of Waxy Crude Oil. *XVII International Seminar on Mineral Processing Technology (MPT), IIT (ISM), Dhanbad, India*, 10 – 12 October 2018

Copies of Publications

Fuel 235 (2019) 1245–1259

Contents lists available at ScienceDirect

Fuel

journal homepage: www.elsevier.com/locate/fuel

Full Length Article

Synthesis of PMMA/modified graphene oxide nanocomposite pour point depressant and its effect on the flow properties of Indian waxy crude oil

Rohit Sharma[a], Vikas Mahto[a,*], Hari Vuthaluru[b]

[a] Department of Petroleum Engineering, Indian Institute of Technology (Indian School of Mines), Dhanbad 826004, India
[b] Australia – India Joint Research Centre for Coal and Energy Technology, WA School of Mines – Minerals, Energy & Chemical Engineering, Curtin University, GPO Box U 1987, Perth, WA 6845, Australia

ARTICLE INFO

Keywords:
Graphene oxide
Polymerization
Nanocomposite
Wax
Pour point

ABSTRACT

Application of Polymeric nanocomposites as pour point depressant (PPD) for crude oil has opened the doors for a new area of research in the petroleum industry. In this research work, a polymer nanocomposite Poly(methyl methacrylate)-Graphene Oxide (PMMA-GO) was synthesized in the laboratory using in-situ free radical polymerization with varying concentrations of Graphene Oxide (0.5%, 1% PMMA), where Graphene Oxide was synthesized using Improved Hummers method and the effect of the nanocomposite on the pour point depression and rheological properties of a Indian waxy crude oil sample is observed. The synthesized nanocomposite is evaluated as pour point depressant considering the improvement in the flow properties of the crude oil. Analysis of the synthesized nanocomposites using techniques such as FTIR, Raman and UV-visible spectroscopy, Field Emission Scanning Electron Microscopy (FESEM), Gel Permeation Chromatography (GPC) revealed the formation of PMMA-Graphene Oxide and the intermediate products. Thermogravimetric analysis indicated improved thermal stability of the synthesized nanocomposite than polymer PMMA. XRD analysis confirmed the formation of graphene oxide and the resultant nanocomposite. Efficiency of the synthesized nanocomposite on the flow properties of treated crude oil is compared with the performance of a commercial PPD. Rheological properties of the crude oil treated with synthesized and commercial PPD's are compared at temperatures 30, 40 and 50 °C and better performance of the synthesized PPD is observed in terms of reduction in apparent viscosity and yield stress. Crude oil treated with PMMA-Graphene Oxide shows up to 23 °C reduction in pour point and 99.8% reduction in apparent viscosity compared with that of virgin crude oil. Reduction of gelation point of nanocomposite treated crude oil by 24 °C from virgin crude oil shows improvement in pipeline restart flow of the studied crude oil. Moreover, yield stress of the crude oil drops from 60 Pa (virgin crude oil) to 0.1 Pa for PMMA-1% Graphene Oxide treated crude oil at 1500 ppm. The reduction in gel strength of crude oil was substantiated by the microscopic analysis of virgin and PPD beneficiated crude oil. The wax crystals take more compact shape and the wax interlocking was reduced significantly in case of PMMA-1% Graphene Oxide treated crude oil. Further, the long term stability of the nanocomposite treated crude oils revealed that its rheological properties undergo lesser degradation with time, as evident by the least increase in apparent viscosity between 16.5% and 32.9% (PMMA-1% Graphene Oxide) and 28%–37.7% (PMMA-0.5% Graphene Oxide) compared to an increase of 40.175%–44.93% observed in case of commercial PPD treated crude oil. These findings show the suitability of nanocomposite PMMA-GO as pour point depressant for Indian waxy crude oil.

1. Introduction

Waxy crude oil comprises of considerable amount of paraffin wax (typically ≥ 5 wt%) which creates difficulty in oilfield operations and pipeline transportation. Paraffin wax has characteristics of dissolution at higher temperatures, while precipitating out at lower temperatures, specifically below wax appearance temperature (WAT). These precipitated wax crystals are of platelet or needle shape in appearance and have tendency to agglomerate which leads to development of three dimensional networks in pipelines, causing reduction in flow ability of crude oil. Wax deposition phenomena reduces the effective pipeline diameter and may also cause full scale pipeline blockage under severe low temperature conditions, stalling the pipeline operations [1]. Improvement in pipeline transportation and rheological properties of

* Corresponding author.
E-mail address: vikas@iitism.ac.in (V. Mahto).

https://doi.org/10.1016/j.fuel.2018.08.125
Received 28 March 2018; Received in revised form 24 August 2018; Accepted 28 August 2018
Available online 04 September 2018
0016-2361/

energy&fuels

Article

Cite This: Energy Fuels 2019, 33, 12330−12345

pubs.acs.org/EF

Investigation into the Flow Assurance of Waxy Crude Oil by Application of Graphene-Based Novel Nanocomposite Pour Point Depressants

Rohit Sharma,[†,‡] Barasha Deka,[†,‡] Vikas Mahto,*[†] Hari Vuthaluru,[‡] and Chun-Zhu Li[‡]

[†]Department of Petroleum Engineering, Indian Institute of Technology (Indian School of Mines), Dhanbad, Jharkhand 826004, India

[‡]Fuels and Energy Technology Institute, Curtin University, GPO Box U 1987, Perth, Western Australia 6845, Australia

Supporting Information

ABSTRACT: In this research article, novel polymer nanocomposites poly(2-ethylhexyl acrylate)−graphene oxide [P(2-EHA)−GO] were developed (with 0.5−2 wt % GO concentrations) by in situ free-radical polymerization and were characterized using several analytical techniques to confirm the formation of nanocomposites. Subsequently, when doped in crude oil, beneficiation was observed in pour point and rheological parameters of a selected waxy crude oil, thus evaluating them as potential pour point depressants (PPDs). An optimized amount of GO (1 wt %) in nanocomposite results in improved flow characteristics of crude oil, providing a notable 18 °C depression in the pour point and upto 99% reduction in its apparent viscosity (down to 0.01 Pa s). Comparison of its beneficiation effect with P(2-EHA), the base polymeric PPD, indicated a superior performance using nanocomposite PPDs which was mainly attributed to a proposed pour point depression mechanism, according to which the GO sheets act as nucleation sites upon which wax crystal precipitates, helping polymeric chains to cocrystallize with these wax molecules and thereby avoiding the formation of a wax interlocking network. Additionally, the nanocomposite PPDs improved the restart flowability of crude oil, causing upto a substantial 17.8 °C reduction in its gelation point. Moreover, they exhibited better control over the aging effect in crude oils than P(2-EHA) and even better than the previously synthesized nanocomposite poly(methyl methacrylate)−GO upto 15 and 30 days. Overall, this study provides new insights into the physical nature of graphene−wax interactions and illustrates the resultant wax morphology modifications, which would help in the development and application of numerous graphene-based products for the flow assurance community of the researchers and the petroleum industry.

1. INTRODUCTION

Waxy crude oils are produced from several different oilfields consisting of substantial proportions of paraffin wax. When the temperature of crude oil reduces below the wax appearance temperature (WAT), paraffin waxes precipitate out and deposit alongside pipe walls, thereby reducing the effective pipeline diameter and leading to technical and economic challenges in pipeline crude oil transportation.[1] Therefore, steps must be taken to avoid wax deposition. The transportation of waxy crude oil through pipelines can be improved by employing physical or chemical technologies. Heating up pipeline is one of the options; but it can be a costly process due to the high consumption of electricity. Chemical technologies can be applied for the transportation of waxy crude oil such as emulsification and addition of pour point depressants (PPDs). Emulsification has a drawback that it requires a plenty of water source and also the crude oil needs to be dehydrated after transportation. The wastewater thus produced also requires expensive treatment. However, the dosage of PPDs in crude oils is small quantitatively and does not require treatment post transportation. Therefore, a PPD technology is considered as a time-saving, cost-effective and simple technique for improving the pipeline transportation of crude oil. PPD possesses ability to change the wax crystal morphology of waxy crude oil and helps to reduce wax deposition in pipelines.[2−4] Traditional PPDs can be produced using techniques of homopolymerization or copolymerization of several monomeric units. They can modify the wax crystal morphology in crude oil with interaction processes such as nucleation, adsorption, and cocrystallization. To improve the beneficiation effects of conventional PPDs, inorganic particles such as graphene or clay can be introduced into the polymer matrix.[5] Previous studies have highlighted the improvement in the thermal properties of the polymer, the changes in crystallization tendency, and wax crystal structures upon introducing the inorganic particles.[6,7]

Recently, significant attention is focused on the development of polymeric nanocomposite/nanohybrid as PPDs. The works performed for the development of polymer nanohybrid/nanocomposite and its evaluation as flow improvers is mentioned in detail in Table 1.

It can be observed from the literature studies that most of the development of nanocomposite/nanohybrid PPDs involved the usage of silicon as an inorganic nanoparticle in the polymeric matrix to improve its beneficiation effect. Very few works reported the usage of graphenes in the development of

Received: September 12, 2019
Revised: November 7, 2019
Published: November 8, 2019

DOI: 10.1021/acs.energyfuels.9b03124
Energy Fuels 2019, 33, 12330−12345

Journal of Petroleum Science and Engineering 208 (2022) 109691

Contents lists available at ScienceDirect

Journal of Petroleum Science and Engineering

journal homepage: www.elsevier.com/locate/petrol

Experimental investigation into the development and evaluation of ionic liquid and its graphene oxide nanocomposite as novel pour point depressants for waxy crude oil

Rohit Sharma [a,b], Barasha Deka [a,b], Vikas Mahto [a,*], Ahmed Barifcani [c], Hari Vuthaluru [b]

[a] Department of Petroleum Engineering, Indian Institute of Technology (Indian School of Mines), Dhanbad, 826004, India
[b] Fuels and Energy Technology Institute, WA School of Mines: Minerals, Energy and Chemical Engineering, Curtin University, Perth, WA, 6845, Australia
[c] Department of Petroleum Engineering, WA School of Mines: Minerals, Energy and Chemical Engineering, Curtin University, Perth, WA, 6845, Australia

ARTICLE INFO

Keywords:
Pour point depressant
Nanocomposite
Ionic liquid
Graphene oxide
Wax
Asphaltenes

ABSTRACT

Wax deposition in pipelines transporting crude oil is a serious problem as wax tends to precipitate under low temperature conditions observed during pipeline flow. The current research work embarks on the development of novel nanocomposite pour point depressant (PPD) for waxy crude oils. Two additives were synthesized in the laboratory: 1-octyl 3-methylimidazolium chloride [(OMIM)Cl], and a novel class of nanocomposite PPD: PPDR-GO. These additives were tested on an Indian waxy crude oil and proved to be acting as PPDs and flow improvers. Pour point reduction occurred from 39 °C to 21 °C with [(OMIM)Cl], while the depression occurred from 39 °C up to 9 °C with nanocomposite PPDR-1%GO, suggesting significant improvement in the flow ability of the crude oil. The PPDs also induced reduction in the apparent viscosities of crude oil significantly from 7 Pa s down to 0.04 Pa s by (OMIM)Cl and 0.02 Pa s (at higher shear rates and temperatures) by PPDR-1%GO respectively. Apart from the pour point and viscosity tests, the effectiveness of the additives were tested by cold finger, gelation point and aging tests and they produced encouraging set of results. The characterization of the two PPDs performed using spectroscopic analytical techniques FTIR, Proton NMR, XRD and Raman helped identifying the presence of different components and confirm their structure. The purpose of this work is to develop new pour point depressants which are highly effective for providing flow assurance of waxy crude oils. This research also aimed at improving the synthesized PPDs in important areas such as improving dispersion of VGO nanosheets in nanocomposite matrix, enhanced pour point depression ability, low dosage requirement of PPDs, eliminating the need of solvent for PPDs. The action mechanism of the PPDs develops theoretical insights on interactions of ionic liquids, graphene oxide sheets and asphaltenes with the wax structures, which would be highly beneficial for future research.

1. Introduction

Crude oil is a complex mixture consisting of paraffins (waxes), asphaltenes, resin, aromatics and naphthenes (Alcazar-Vara et al., 2012). Among these components, the precipitation and deposition of waxes and asphaltenes are known to primarily cause significant curtailment in the flowability of the crude oil in pipelines. The precipitation of waxes from the crude oil occurs at low temperatures due to loss of heat to the surroundings, it is a serious flow assurance problem in crude oil transportation (Sharma et al., 2020a,b,c). This wax precipitation leads to pipeline handling difficulties, and reduces the pipeline diameter available for crude oil to flow, and if it is not controlled timely, may lead to complete pipeline blockage and even abandonment of producing wells (Coto et al., 2014). With temperatures lower than wax appearance temperature (WAT), solubility of the high molecular weight wax component in crude oil significantly decreases, and they form stable crystals at low temperatures. This phenomena results in depreciation of the crude oil flow properties and an increase in its pour point, viscosities and yield stresses (Singh et al., 1999; Yang et al., 2015b). These wax crystals are porous structures which entraps crude oil and subsequently develops a gel structure of complex morphology, and this gelation obstructs an efficient pipeline flow (Sharma et al., 2020b).

The understanding of wax deposition studies becomes challenging when it is associated with asphaltene deposition. Asphaltenes are

* Corresponding author.
E-mail address: vikas.ismpe@hotmail.com (V. Mahto).

https://doi.org/10.1016/j.petrol.2021.109691
Received 14 June 2021; Received in revised form 27 September 2021; Accepted 15 October 2021
Available online 19 October 2021
0920-4105/

Society of Petroleum Engineers

SPE-202368-MS

Predicting the Wax Deposition and Gelation Behavior of Waxy Oils in Subsea Pipelines through Modelling and Numerical Simulation Approach

Rohit Sharma, IIT, ISM Dhanbad and Curtin University, Australia; Hari Vuthaluru, Curtin University, Australia; Vikas Mahto, IIT, ISM Dhanbad

This paper was prepared for presentation at the SPE Asia Pacific Oil & Gas Conference and Exhibition originally scheduled to be held in Perth, Australia, 20 - 22 October 2020. Due to COVID-19 the physical event was postponed until 17 - 19 November 2020 and was changed to a virtual event. The official proceedings were published online on 12 November 2020.

Abstract

Wax deposition during pipeline transportation of crude oil is one of the serious flow assurance problems faced in the petroleum industry (Deka et al., 2020b) and wax gelation phenomenon is an inherent characteristic of the wax deposition process and it must be investigated to understand the deposition process. Wax-gelation formation was simulated during flow of waxy oils by numerically simulating its gelling behavior during transportation under different operating conditions by developing a computational fluid dynamics (CFD) model. The modelling technique and the obtained results from this work would help to predict the wax deposition and gel formation tendency in different waxy oils. Wax deposition phenomenon was modelled for a model wax-oil mixture (representing a waxy oil). A numerical model was developed to predict the wax gelation with time and length of pipeline. It involves heat and mass transfer calculations and molecular diffusion mechanism is considered as the primary mechanism for wax deposition, with the calculations being performed for 5 days. The CFD model uses enthalpy porosity technique where wax-oil gel is treated as the solid-liquid region with porosity equal to the liquid fraction. Fluid flow was considered laminar with flow rates being 1-5 GPM and ambient temperature was maintained at 281.3 K. The developed numerical model predicts that the wax gelation increases with time initially and then slowed down subsequently and less increment is observed upon 5 days of fluid flow. These results indicate the wax gelation is fast initially and slows down subsequently, showing strong dependence on time. Wall temperature of wax-oil mixture and the gel deposit decreases from bulk fluid temperature (295.2 K) to the ambient temperature (281.3 K). Increase in the temperature difference between wall and ambient temperature leads to higher wax deposition and gelling formation. Wax gelation was observed to be function of time. The CFD model numerically-simulates the wax-oil gelling formation in terms of liquid fraction (gel formation), where the liquid fraction gets reduced up to 44.7 % upon crude oil flow in the pipeline, being highest at the centre and lowest at pipe-walls, indicating the possible gel formation regions on pipewall. The gel formation was strongly affected by the wall temperatures, duration and length. This work would be one of its kind to report CFD-simulations of wax-oil gel formation in pipelines, where interdependency of fluid flow parameters would be assessed. Therefore, in this work, an attempt was made to simulate the gelling behaviour of the wax crystals in pipeline using an enthalpy porosity technique which has been not been tested much before.

OTC-30360-MS

Effect of Thermal/Shear Conditioning and Aging on the Effectiveness of Synthesized Nanocomposite PPD on Waxy Crude Oil

Rohit Sharma, IIT, ISM, Dhanbad and Curtin University, Australia; Vikas Mahto, IIT, ISM, Dhanbad; Hari Vuthaluru and Chun-Zhu Li, Curtin University, Australia

This paper was prepared for presentation at the Offshore Technology Conference Asia originally scheduled to be held in Kuala Lumpur, Malaysia, 17 - 19 August 2020. Due to COVID-19 the physical event was postponed until 2 – 6 November 2020 and was changed to a virtual event. The official proceedings were published online on 27 October 2020.

Abstract

Wax deposition is a serious issue during the pipeline transportation of crude oil. This research work has investigated the effects of some important parameters on the flow characteristic of crude oil during the pipeline transportation in offshore and onshore field environments i.e. effects of thermal/shear conditioning and aging on the flow properties of virgin crude oil and additive-treated crude oil. Polymeric nanocomposites are a new and improved family of pour point depressants that can enhance the performance of polymeric additives. This work is in continuation of our previous work of Sharma et al. 2019c, where polymeric nanocomposites based on graphene oxide were synthesized, namely poly (methyl methacrylate)-graphene oxide [PMMA-GO] with different concentrations of graphene oxide (0.5, 1 wt. %), and were subsequently evaluated as potential pour point depressants for a waxy Indian crude oil possessing substantial wax deposition and gelation issues. The effectiveness of the PMMA-GO was examined in this work based on its pour point depression, flow performance, and enduring thermal conditioning, shear conditioning and aging phenomenon in the PMMA-GO treated crude oil. Its performance was compared to that of polymer PMMA-treated crude oil, and a PPD-wax interaction mechanism was proposed. The effects of thermal conditioning on the performance of PPDs were evaluated by determining the gelation points at cooling rates of 0.5, 1 and 1.5°C/min. Also, the pour points of additive-treated crude samples were calculated after repetitive heating at temperatures 60°C, 55°C, 50°C and 45°C. The effects of aging on the flow behaviour of crude oil were determined by obtaining the rheological properties and pour point values on the 1st and 15th day of its storage. For evaluation under shear conditioning, apparent viscosities were measured over shear rates of 0.1-500 s^{-1} at temperatures 30°C, 40°C and 50°C below and near wax appearance temperature (WAT). This study complements the benefits of the PMMA-GO as a flow improver obtained in our previous study and details its effectiveness under more practical applications.

Introduction

The pipeline transportation of waxy crude oil has always faced issues due to wax deposition on pipe walls under offshore and onshore field conditions. The deposition may be attributed to the nature of paraffin wax,

Copyrights

All the chapters contain a portion or full content of these copyrighted materials.

The places in thesis where the copyrighted material have been used is listed here.

Figure 1.1, Chapter 1

SPRINGER NATURE LICENSE
TERMS AND CONDITIONS

Aug 23, 2021

This Agreement between Mr. Rohit Sharma ("You") and Springer Nature ("Springer Nature") consists of your license details and the terms and conditions provided by Springer Nature and Copyright Clearance Center.

License Number	5087811362152
License date	Jun 14, 2021
Licensed Content Publisher	Springer Nature
Licensed Content Publication	Springer eBook
Licensed Content Title	Petroleomics and Structure–Function Relations of Crude Oils and Asphaltenes
Licensed Content Author	Oliver C. Mullins
Licensed Content Date	Jan 1, 2007
Type of Use	Thesis/Dissertation
Requestor type	academic/university or research institute
Format	print and electronic
Portion	figures/tables/illustrations
Number of figures/tables/illustrations	1
Will you be translating?	no
Circulation/distribution	1 - 29
Author of this Springer Nature content	no
Title	Study the effects of nanohybrid polymers/polymer nanocomposites on the flow behaviour of Indian waxy crude oil
Institution name	IIT (ISM) Dhanbad
Expected presentation date	Sep 2021
Order reference number	15 June 2021
Portions	Figure 1.1. Various solids that obstruct oil pipelines. , Chapter 1, page 6
Requestor Location	Mr. Rohit Sharma Department of Petroleum Engineering IIT (ISM), Dhanbad Dhanbad, 826004 India Attn: Mr. Rohit Sharma
Total	**0.00 USD**

Figure 1.2, Chapter 1

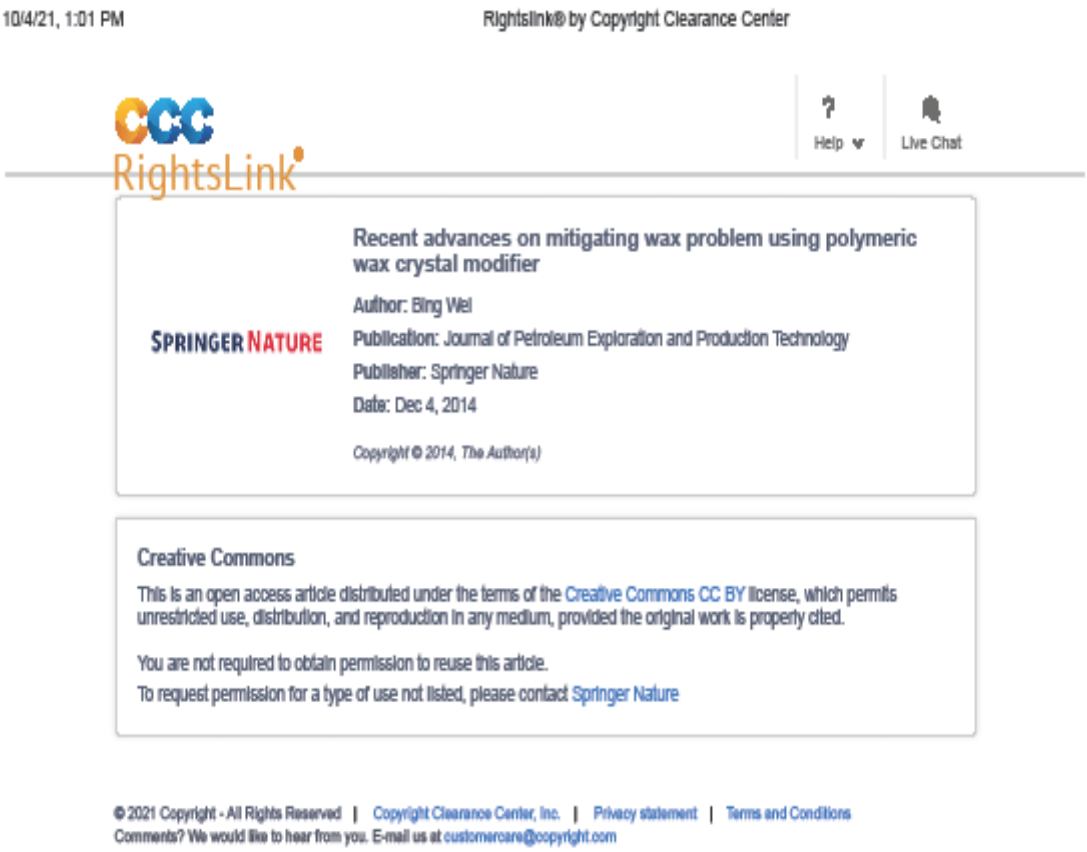

Figure 2.1, Chapter 2

ELSEVIER LICENSE
TERMS AND CONDITIONS

Aug 23, 2021

This Agreement between Mr. Rohit Sharma ("You") and Elsevier ("Elsevier") consists of your license details and the terms and conditions provided by Elsevier and Copyright Clearance Center.

License Number	5087580321520
License date	Jun 14, 2021
Licensed Content Publisher	Elsevier
Licensed Content Publication	Chinese Journal of Chemical Engineering
Licensed Content Title	Structure and synthesis of graphene oxide
Licensed Content Author	Ling Sun
Licensed Content Date	Oct 1, 2019
Licensed Content Volume	27
Licensed Content Issue	10
Licensed Content Pages	10
Start Page	2251
End Page	2260
Type of Use	reuse in a thesis/dissertation
Portion	figures/tables/illustrations
Number of figures/tables/illustrations	1
Format	both print and electronic
Are you the author of this Elsevier article?	No
Will you be translating?	No
Title	Study the effects of nanohybrid polymers/polymer nanocomposites on the flow behaviour of Indian waxy crude oil
Institution name	IIT (ISM) Dhanbad
Expected presentation date	Sep 2021
Order reference number	14 June 2021
Portions	Figure 1
Requestor Location	Mr. Rohit Sharma Department of Petroleum Engineering IIT (ISM), Dhanbad Dhanbad, 826004 India Attn: Mr. Rohit Sharma
Publisher Tax ID	GB 494 6272 12
Total	**0.00 USD**

Chapter 3 & 4

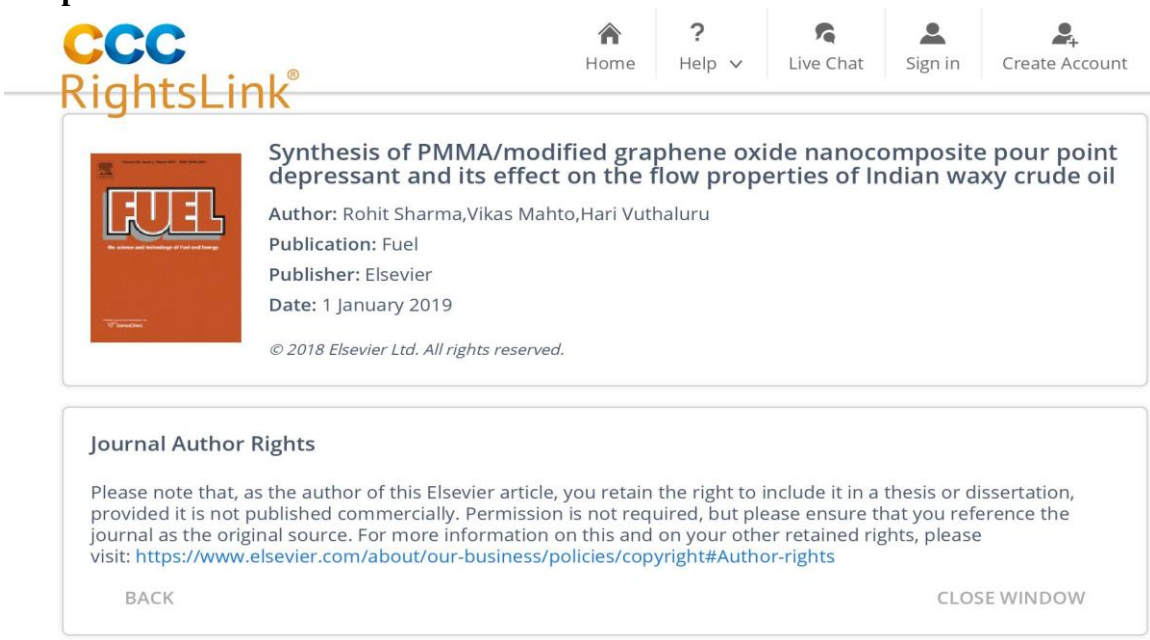

Chapter 3 & 5

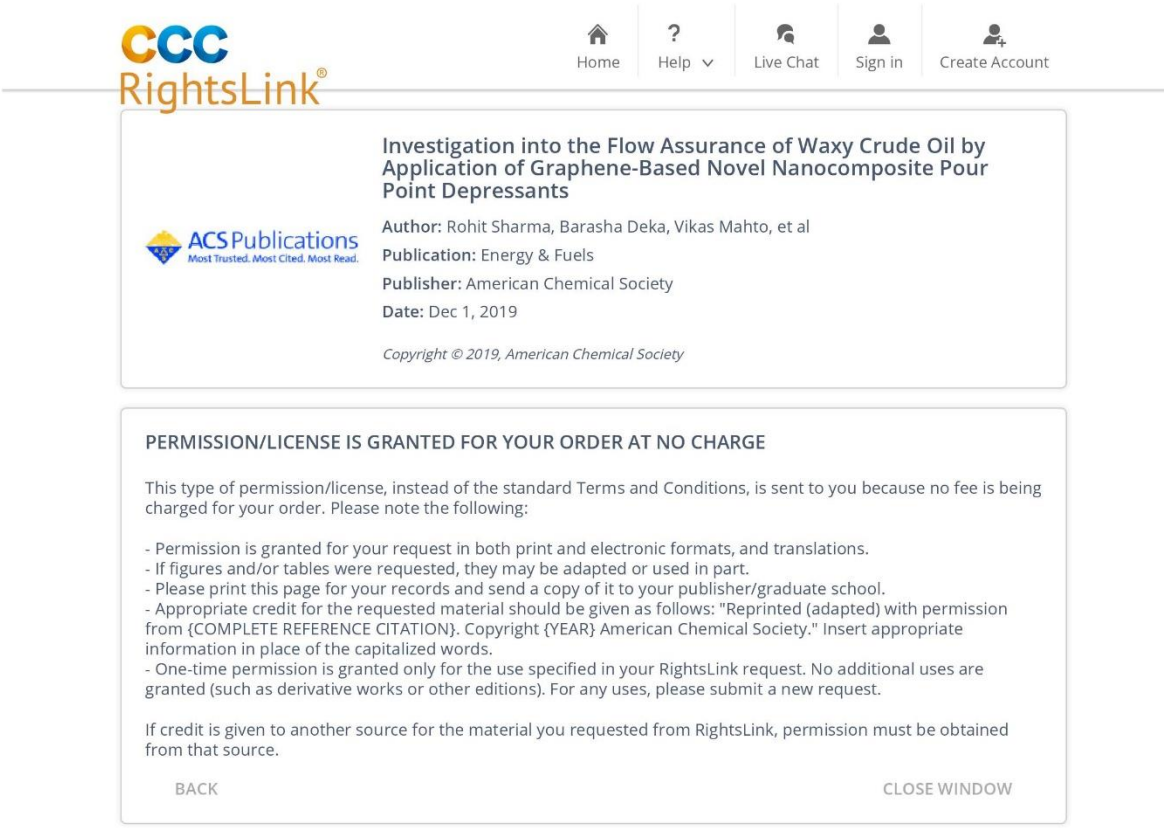

Chapter 3 & 6

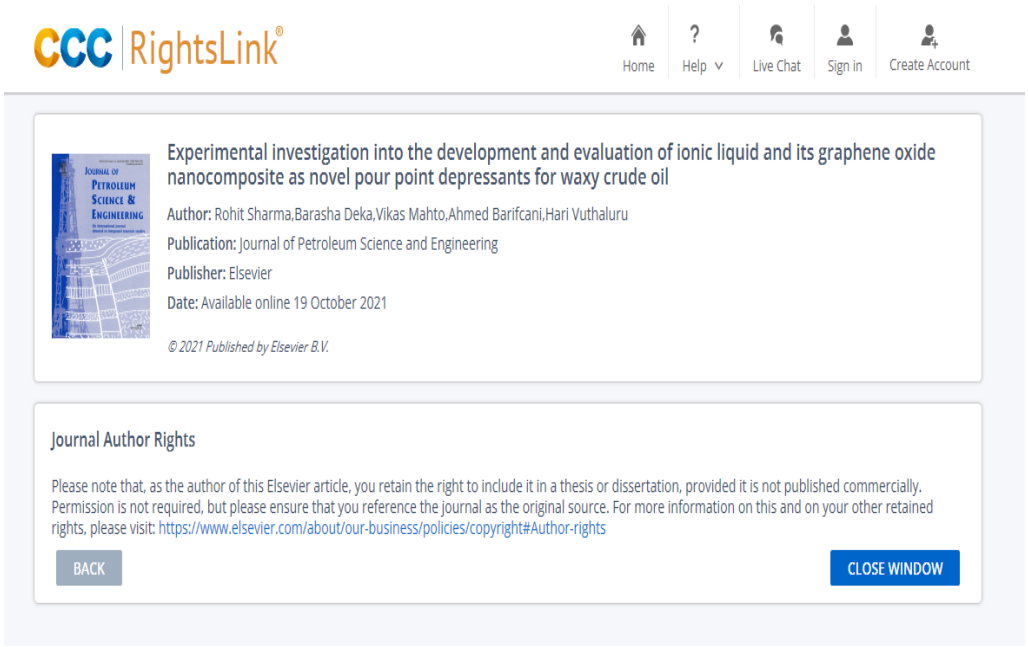
RightsLink
Home
Help
Live Chat
Sign in
Create Account
Experimental investigation into the development and evaluation of ionic liquid and its graphene oxide nanocomposite as novel pour point depressants for waxy crude oil
Author: Rohit Sharma,Barasha Deka,Vikas Mahto,Ahmed Barifcani,Hari Vuthaluru
Publication: Journal of Petroleum Science and Engineering
Publisher: Elsevier
Date: Available online 19 October 2021
© 2021 Published by Elsevier B.V.
Journal Author Rights
Please note that, as the author of this Elsevier article, you retain the right to include it in a thesis or dissertation, provided it is not published commercially. Permission is not required, but please ensure that you reference the journal as the original source. For more information on this and on your other retained rights, please visit: https://www.elsevier.com/about/our-business/policies/copyright#Author-rights
BACK
CLOSE WINDOW

Chapter 3 & 7

CCC Marketplace™

This is a License Agreement between Rohit Sharma / IIT (ISM), Dhanbad & Curtin University, Australia ("User") and Copyright Clearance Center, Inc. ("CCC") on behalf of the Rightsholder identified in the order details below. The license consists of the order details, the CCC Terms and Conditions below, and any Rightsholder Terms and Conditions which are included below.

All payments must be made in full to CCC in accordance with the CCC Terms and Conditions below.

Order Date	15-Aug-2021	**Type of Use**	Republish in a thesis/dissertation
Order License ID	1140617-1		
ISBN-13	9781613997093	**Publisher**	Society of Petroleum Engineers
		Portion	Chapter/article

LICENSED CONTENT

Publication Title	Asia Pacific Oil & Gas Conference and Exhibition (20APOG)	**Country**	United States of America
		Rightsholder	Society of Petroleum Engineers (SPE)
Date	01/01/2020	**Publication Type**	e-Book
Language	English		

REQUEST DETAILS

Portion Type	Chapter/article	**Rights Requested**	Main product
Page range(s)	1-16	**Distribution**	Worldwide
Total number of pages	16	**Translation**	Original language of publication
Format (select all that apply)	Print, Electronic	**Copies for the disabled?**	No
Who will republish the content?	Author of requested content	**Minor editing privileges?**	No
Duration of Use	Life of current edition	**Incidental promotional use?**	No
Lifetime Unit Quantity	Up to 499	**Currency**	USD

NEW WORK DETAILS

Title	Study the effects of nanohybrid polymers/polymer nanocomposites on the flow behaviour of Indian waxy crude oil	**Institution name**	IIT (ISM), Dhanbad & Curtin University, Australia
		Expected presentation date	2021-11-05
Instructor name	Prof. Vikas Mahto, A/Prof. Hari Vuthaluru and A/Prof. Ahmed Barifcani		

ADDITIONAL DETAILS

Order reference number	11 August 2021	**The requesting person / organization to appear on the license**	Rohit Sharma / IIT (ISM), Dhanbad & Curtin University, Australia

REUSE CONTENT DETAILS

Title, description or numeric reference of the portion(s)	Predicting the Wax Deposition and Gelation Behavior of Waxy Oils in Subsea Pipelines through Modelling and Numerical Simulation Approach	**Title of the article/chapter the portion is from**	Predicting the Wax Deposition and Gelation Behavior of Waxy Oils in Subsea Pipelines through Modelling and Numerical Simulation Approach
Editor of portion(s)	N/A	**Author of portion(s)**	Rohit Sharma, Hari Vuthaluru and Vikas Mahto
Volume of serial or monograph	978-1-61399-709-3		
Page or page range of portion	1-16	**Issue, if republishing an article from a serial**	N/A
		Publication date of portion	2020-11-12